Charles University

First Faculty of Medicine

Institute of Inherited Metabolic Disorders

Prague, Czech Republic

NOVEL ASPECTS OF MOLECULAR BIOLOGY AND PATHOLOGY OF LYSOSOMAL STORAGE DISORDERS. STUDIES WITH PARTIAL USE OF *Caenorhabditis elegans*

Ph.D. thesis

Jakub Sikora

Supervisor: Prof. MUDr. Milan Elleder, DrSc.
Consultant: MUDr. Martin Hřebíček

Prague 2007

Acknowledgements

I would like to thank my supervisor Prof. MUDr. Milan Elleder, DrSc. and MUDr. Martin Hřebíček for their scientific approach, critical guidance and understanding during the years of my postgraduate studies. The truly academic atmosphere of respect and freedom of scientific opinion that they managed to create was an unforgettable experience. I must express my gratitude for the opportunity to work in the ever inspiring environment of the Institute of Inherited Metabolic Disorders.

I must also thank all my colleagues at the Institute of Inherited Metabolic Disorders, namely ing. Jana Uřinovská, RNDr. Robert Dobrovolný, PhD., ing. Hana Pavlů-Perreira, RNDr. Jana Ledvinová, CSc., ing. Helena Poupětová, RNDr. Lenka Dvořáková, CSc., MUDr. Marta Kostrouchová, CSc., Jana Sovová, Marie Kolářová, and Eva Horáková for their interest in my work, and for creating pleasant working atmosphere.

Last but not least, I would like to thank my family for their love, understanding and permanent support.

This thesis was elaborated within the postgraduate program for Biology and Pathology of the Cell at the Institute of Inherited Metabolic Disorders, 1st Faculty of Medicine, Charles University, Prague.

The work was funded by the grants 301/93/01854, 303/02/1324 provided by the Czech Scientific Agency (Grant Agency of the Czech Republic); and by the grant 8351-3 of the Ministry of Health of the Czech Republic. The institutional financial support was provided by the research projects 111100003 and 0021620806 of the Ministry of Education, Youth and Sports of the Czech Republic.

Note:

Authorship of all the appended publications is in compliance with the criteria for authorship as accepted by the International Committee of Medical Journal Editors (ICMJE)[1]. Individual contributions can be provided on request if not listed in the appended publications.

In order to avoid any ambiguities, word mutation was omitted in the following text, if not stated otherwise, and was replaced by the term pathogenic variation in accordance with the valid recommendations[2].

... By 1955, our results were sufficiently advanced to allow us to propose with a certain measure of assurance the existence of a new group of particles with lytic properties, the lysosomes ...

Prof. Christian de Duve
Nobel lecture – Exploring Cells with a Centrifuge
December 12, 1974

... Nevertheless, the identification of the lysosomal N-acetyltransferase gene marks the end of the gene-discovery phase for lysosomal genetic enzymopathies.

Hřebíček et al. - Am J Hum Genet, 79, 2006

Contents

1 Introduction

Christian de Duve and his colleagues proposed the existence of a novel type of membrane endowed intracellular granules rich in hydrolytic enzymes, and designated them as lysosomes, in the year 1955[3]. Information about this cellular compartment, present in every eukaryotic cell, has increased immensely since that year. Despite the prevailing perception of lysosomes as degradative cellular compartment, lysosomal functions should be considered as complex in cellular biology.

1.1 Lysosomes - 2007, overview

Lysosomes represent an integral part of membranous endosomal – lysosomal system that is defined by progressive intraluminal pH decrease realized by the action of vacuolar H^+ ATPase. Functional and spatial stratification of endosomal – lysosomal compartment is very complex. The tendency to subdivide the system, whose inherent function is continuous multidirectional flow of membranous constituents and luminal cargo molecules, sometimes results in unwanted simplifications. Generally accepted concept of distinct vesicular populations (early, recycling, late endosomes and lysosomes) with their specified molecular markers should be considered cautiously. The intimate functional connection between late endosomes (mannose-6-phosphate receptor – M-6-PR positive) and lysosomes (M-6-PR negative) resulted in compound designation: late endosomal-lysosomal (term also used in this thesis)[4].

As stated above, endosomal - lysosomal system represents extremely dynamic compartment with widespread contacts in the cell. Spatial coordination of membrane and luminal contents shuttling is vast and in majority of aspects not fully understood. The proper cellular targeting and homeostasis of either endocytosed or redistributed material (protein, carbohydrate or lipidic moieties) is essential for proper cellular functioning. Many of these processes require complex molecular interactions of protein-protein or protein-lipid phases (some of them are described in more detail in sections *1.2* and *3*). Late endosomal-lysosomal compartment exerts extensive contacts with other cellular compartments (Golgi apparatus, endoplasmic reticulum, mitochondria or cytoplasmic membrane). The system is further functionally and spatially stratified. NPC1 positive compartment[5] (see *3.2.8.3.1*) or chaperon mediated autophagy (CMA, see below or *1.2*) competent lysosomal sub-compartments[6,7] are

just two examples. To further demonstrate lysosomal diversity, it should be noted that certain cellular types have lysosomes with exocytic potential (lysosome related organelles)[6].

Christian de Duve defined lysosomes on the basis of the association of their flotation properties with five different hydrolytic enzymatic activities[3]. Current knowledge about lysosomal proteomics assigns nearly ten (or more) times more proteins to reside and function in this cellular compartment. The original criterion of hydrolytic activity is not valid anymore; although hydrolases predominate in the lysosomal proteome. Lysosomal proteins, in the most general sense, are either luminal or integral membrane proteins. As many substrate molecules are hydrophobic by nature and are distributed in layered membrane sheets, considerable proportion of luminal proteins functions in intimate membrane association and displays membrane perturbation potential (for further details see section *3*). Common denominator of the two protein groups (lysosomal hydrolases and structural non-enzymatic proteins) is their acidic pH functional optimum. Substrate characteristics of otherwise selectively functioning hydrolases are diverse, and their list exceeds this text.

Lysosomal membrane and its proteome are intensively studied at the present time[9,10]. Historical paradigm claiming that lysosomal membrane serves only as a passive barrier protecting cytosolic contents against aggressive lysosomal hydrolases, has been rejected. Growing number of lysosomal membrane proteins as well as diversity of their functions are striking. Latest advances including characterization of the gene coding for lysosomal membrane protein acetyl-coenzyme A:α-glucosaminide N-acetyltransferase[11,12] (HGSNAT, section *4*) or the issue of detergent-resistant microdomains (DRMs)[7,13] and their participation in chaperon mediated autophagy are discussed later (sections *1.2* and *4*). Lipid properties and constitution of the lysosomal membrane are as important as the proteomic context of the membrane. The composition, homeostasis, recycling and remodelling of the lysosomal membrane bilayer is a cornerstone of lysosomal function with implications for human pathology states[14].

The fundamental quality of lysosomal apparatus as ordered intracellular system is, besides others, maintained by energy dependent selective delivery of lysosomal proteins. There are at least five different protein targeting mechanisms serving this purpose. Mannose-6-phosphate (M-6-P) recognition targeting of luminal hydrolases is probably the most thoroughly explored pathway[15,16]. In addition to this direct (Golgi apparatus > late endosome > lysosome) compartmental succession, indirect mannose receptor (MR) dependent cytoplasmic membrane recycling pathway is used by some proteins (e.g. β-glucocerebrosidase)[17,18]. Recent reports suggested additional sorting mechanism for saposin-

like lysosomal proteins employing sortillin protein as a receptor and carrier[19] (see *3.1.1* and *3.2.1.1*). These three receptor mediated pathways depend on the potential of the carrier molecules to recognize 3D signal patches on the secondary structure of the transported proteins. Two additional mechanisms of selective protein delivery to lysosomes employ conserved targeting sequences in the primary protein structure. Lysosomal membrane proteins are delivered on the basis of the presence of either tyrosin or dileucin motifs[20]. Recently described mechanism of direct selective import of certain cytosolic proteins into the lysosomal lumen is the basis of CMA mediated by LAMP 2a (lysosomal associated membrane protein) isoform and hsc-73 co-chaperon[21-23].

Substrate entry into the late endosomal-lysosomal compartment is principally realized by three distinct pathways: endocytosis, phagocytosis and autophagy[4]. Proportional contribution of each of these delivery pathways is substrate, cell and tissue type specific, and is difficult to estimate, universally. Each of these three mechanisms, on its own, is an extensive topic to discuss. With respect to the following text only autophagy will be briefly discussed, as it represents very dynamic subject with immense implications for lysosomal biology and pathology. Autophagy is an evolutionary conserved mechanism used for degradation of inherent cellular contents and lysosomal compartment is a key player in this complex pathway. Current concept of autophagy recognizes three basic variants: macroautophagy (degradation of complete cytosolic regions with prior generation of autophagosomal membrane), microautophagy (degradation of cytosolic regions with direct engulfment by lysosomal membrane) and chaperon mediated autophagy (CMA, selective protein degradation pathway employing protein sequence tags)[24,25]. Latest advances have especially disclosed molecular background of macroautophagy and CMA. In case of macroautophagy, it was the delineation of autophagosomal membrane constituting machinery of ubiquitin-like proteins including critical LC3 component[26,27]. For CMA, it was the characterization of the selectivity of lysosomal targeting of certain cytosolic proteins with KFERQ-like signal sequences, description of the critical protein recognition and trans-lysosomal membrane transfer and roles of DRMs in the whole process[7,21,23]. Autophagy represents one of the three basic mechanisms of protein elimination in eukaryotic cell (other two are cytosolic proteases and ubiquitin – proteasomal pathways). Latest reports have directly demonstrated concerted action of these pathways and their partial functional overlap and substitutability[28-30]. It was shown that autophagy (both macro- and CMA variants) represents a constitutively active and continuous process, which is absolutely indispensable for proper cellular protein clearance[31-35]. The issues of cellular protein elimination or

autophagy related programmed cell death (PCD II) should thus be considered integral part of lysosomal function[36]. Molecular defects in these pathways represent fundamental part of cell pathology in protein folding-clearance disorders but also in some lysosomal storage disorders (sections *1.2* and *3.1*).

1.2 Lysosomal storage disorders - 2007, overview

The history of lysosomal storage disorders (LSDs)[37] dates back to the original clinical observations by Tay, Sachs or Gaucher in the second half of 19th century. The identification of acid α-glucosidase enzymatic deficiency in Pompe disease in the year 1963 by Hers et al.[38] and sulfatase deficiency in metachromatic leukodystrophy by Austin et al.[39,40], one year later, virtually starts the molecular defect characterization phase in LSDs. At the present time (year 2007) LSDs represent a group of 48 entities[41] that are defined on the molecular level (DNA) and are inherited as recessive Mendelian monogenic traits (overall incidence of 1:6000 newborns)[42]. Common denominator in this heterogenous group of molecular defects is the expansion of lysosomal compartment of affected cell types with foamy transformation of the cytoplasm.

Majority of LSDs (30 out of 48 entitities) are single lysosomal enzymatic deficiencies (29 hydrolases and 1 acetyl-transferase). Summarizing list provides the following: ten mucopolysaccharidoses (MPS), seven glycoproteinoses, nine lipidoses, one glycogen storage disease, and three neuronal ceroid lipofuscinoses (NCLs) due to enzymatic deficiency. It must be noted that the gene discovery period of biochemically defined LSDs was closed by the characterization of the critical gene in the pathogenesis of MPS type IIIc (heparin acetyl-coenzyme A:α-glucosaminide N-acetyltransferase deficiency). This lysosomal membrane protein resides most probably in DRMs of a sub-population of lysosomes[13]. MPS IIIc thus represents the only deficiency of synthetic lysosomal enzyme (for details see section *4*) in the group of otherwise hydrolytic deficiencies[12].

Another eight LSDs result from enzymatic deficiency due to either malfunction of co- or post-translation protein processing (multi sulphatase deficiency, mucolipidosis II/III), lack of enzymatic protection by protective protein/cathepsin A (PPCA, galactosialidosis), or from enzyme activator deficiency (GM_1 activator deficiency, saposin and prosaposin deficiencies, extensively discussed in section *3.1*). Overall, all these thirty eight entities are directly or

indirectly related to enzymatic deficiency, and as such, changes on the cellular level are due to the accumulation of undigested substrate molecules in the lysosomes.

Rest of lysosomal storage disorders (ten) result from molecular defects in lysosomal membrane proteins. Two of these are trans-membrane transporter defects (cystinosis, sialic acid storage disease), and the cellular phenotype thus originates from deficient lysosomal export of the critical moiety. Remaining eight disorders are difficult to characterize on the basis of their common molecular pathogenesis. These defects (NCL 3, 5, 6 and 8, mucolipidosis type IV, Danon disease, Niemann-Pick disease type C1) are caused by affection of lysosomal membrane proteins with diverse functions (e.g. Ca^{2+} sensing, cholesterol homeostasis, autophagosome formation or autophagosome-lysosome fusion). Some of these issues are discussed later (sections *1.2.1, 3.1.3, 3.1.4* and *3.2.8.3.1*). Cellular phenotype of these last eight disorders (i.e. lysosomal storage), in a very simplified way, originates from defective membrane content handling (shuttling, targeting or redistribution) or from inability of lysosomal compartment to perform some of its principal goals, such as participation in autophagy.

As was demonstrated above, all of the historical LSDs were defined on the molecular level during the last 40 years. This period of discovery of LSDs can be considered as devoted to biochemical and genetic (in the monogenic sense of the word) description of these pathology states with immense impact especially on diagnostics. It is tempting to speculate whether other, so far, unrecognized defects with "lysosomal" phenotype will be characterized in the future. With respect to the complexity of the endosomal-lysosomal proteome, the probability that such entities will appear is high, especially in this post-genomic millennium with its not hypothesis- but curiosity driven approaches. Primary causes in the known LSDs were defined; present and near future time must represent a renaissance of intensified cell biological studies in order to generate integrative data about cellular and tissue pathogenesis of LSDs.

1.2.1 Cellular consequences of lysosomal storage – complex mosaic

Data about functional cellular consequences, in other words about cellular pathophysiology and pathology, of lysosomal storage are voluminous, but unfortunately predominantly descriptive. LSDs represent heterogenous group of disorders, each of them described in different depth. The characteristics (morphological, biochemical) of cellular and tissue storage patterns differ considerably among individual disorders. Complex and

summarizing review of current atomized data in the field of LSD cellular pathology exceeds the format of this text, so only brief overview of recently released data will be provided.

The process of lysosomal storage due to accumulation of whatever material remains substantially enigmatic in the following areas: (i) functionality and turnover of the storage lysosomes; (ii) compensatory mechanisms in lysosomal biogenesis and lysosomal proteomics; (iii) recycling and redistribution of accumulated material; (iv) impact of storage process on partner cellular compartments and fundamental cellular regulations including protein clearance and cell death induction; (v) cell and tissue specific consequences of lysosomal storage; (vi) extralysosomal roles of both deficient proteins and accumulated moieties. Following paragraphs represent just few pieces from the incomplete mosaic of LSD pathogenesis.

Impacts of lysosomal storage on the lysosomal biogenesis might be quite diverse, sometimes very pronounced, and were demonstrated on RNA and protein levels[43]. Available data support connection between transcriptional regulation of certain lysomal (both luminal and membrane) proteins and storage induction. In addition to overall up regulation of lysosomal related protein machinery due to lysosomal storage, cellular protein mistargeting was also observed. The molecular machinery involved and mechanisms of some of these phenomena are hypothetical, common transcription regulation of GC rich TAATA less promoters of lysosomal related genes included. Spatial coordination of distribution of lysosomal storage compartment and functionality of both ordered membrane structures and lysosomal matrix is also more or less unknown. Heterogeneity of late endosomal – lysosomal sub-compartmental spatial distribution may play important roles especially in polarized cells (e.g. axonal dystrophy in Niemann-Pick disease type C, see *3.2.8.3.1*).

Redistribution of undegraded substrate molecules in the affected cells and their extralysosomal effects might be also very important in the pathogenesis of lysosomal storage. It is especially the issue of glycolipid recycling and genesis of toxic moieties that is currently in focus. It seems that this mechanism of extralysosomal shuttling into membrane sheets may provide clues for many diverse and so far not understood observations. Gaucher but also Krabbe or Niemann-Pick disease types A and B may serve as examples[14].

Direct involvement in fundamental cellular regulatory pathways and non-lysosomal functions of proteins deficient in LSDs and their target molecules represent further contributory factors to LSD pathogenesis. Prosaposin or acid sphingomyelinase that are discussed in detail in sections *3.1* and *3.2* may serve as prototypic examples.

Last but not least, the issue of induced cell death must be mentioned in the context of LSDs. Lysosomal roles in programmed cell death (PCD) of either caspase mediated (type I) or autophagic (type II) are a subject of numerous review articles[24,35]. Participation of these processes under the conditions of lysosomal storage was announced just lately. Direct involvement of certain glycolipids or ceramide in apoptosis regulation or induction is generally accepted fact of immense importance (for details see section *3.2*). Nevertheless, it seems more and more probable that combination of these phenomena (PCD type I and II) is the reality in LSDs. Just to demonstrate autophagy patricipation in LSD pathogenesis several examples are given. Lysosomal accumulation of subunit C of mitochondrial ATP synthase (SCMAS) is a phenomenon attributable to autophagy deregulation in NCLs, especially when battenin (variant in NCL3) has been shown to directly mediate autophagosomal-lysosomal fusions in mice[44-47]. Malfunction of lysosomal system and associated build-up of autophagosomal compartment is the basis of Pompe disease due acid α-glucosidase deficiency in skeletal muscle[48]. In addition, it has been postulated that α-glucosidase deficient cells suffer from endocytosis sorting defects further aggravating autophagy defects[49]. Similar mechanisms of autophagy deregulation are involved in LAMP 2 deficiency (Danon disease)[50,51]. Protective protein/Cathepsine A deficiency (galactosialidosis) is also most probably going to attain some of its pathology from increased rates of CMA, due to its upregulation[52]. If one considers the extent of regulation of CMA (see *1.1*) and extensive consequences of its deficiency, protein clearance in LSDs is another issue contributing to cellular pathology[7].

As mentioned at the beginning the mosaic is still incomplete, with many data not mentioned. Cellular pathology in LSDs should definitely be the primary objective of present research.

2 Summarized aims of the studies

The exact aims of the studies are listed and defined in the particular sections of the following text and in the appended publications. This part of the thesis serves as an overview and a general concept of the studies.

Saposin-like proteins in lysosomal biology and pathology: prosaposin, saposins and acid sphingomyelinase

- To evaluate neuropathologic changes in the available cases of pSap deficiency with special emphasis on the differences between neurolysosomal and non-neurolysosomal populations
- To evaluate roles of protein clearance mechanisms (ubiquitin-proteasome) in the pSap pathology and compare the findings with other selected LSDs
- To evaluate origins of massive postnatal loss of cortical neurons with respect to potential roles PCD type II in this process

- To perform genotype-phenotype correlation studies in the selected populations of acid sphingomyelinase deficient patients (Niemann-Pick disease type A and B) with emphasis on the phenotypic diversity

Bioinformatic study of HGSNAT protein, critical protein in MPSIIIc pathogenesis

- To perform detailed predictive study of the evolutionary and functional traits of the newly defined HGSNAT protein involved in MPSIIIc pathogenesis. Special emphasis given to interspecies synteny conservation, transmembrane protein domains and potential sites of posttranslation modifications

Caenorhabditis elegans as a model organism for selected lysosomal storage disorders

- To perform bioinformatic, biochemical and cell biological characterization of the single *C.elegans* ortholog of mammalian acid α-galactosidase and α-N-acetylgalactosaminidase with special emphasis on evolutionary clustering and diversification of these catalytic functions

3 Saposin-like proteins in lysosomai biology and pathology – prosaposin, saposins and acid sphingomyelinase

Saposin like proteins (SAPLIPs) are membrane interacting proteins of diverse biochemical and cellular functions. The unifying and characterizing feature of these proteins is the presence of either confirmed or predicted saposin-like domain in their secondary protein structure[53,54]. The definition of this type of protein domain is complicated by the fact that the conservation of the primary sequence is usually low and can be missed by generally employed algorithms using sequence similarity thresholds. The secondary structure of saposin-like domain includes hydrophobic protein core with six invariable cysteine residues forming three disulphide bridges and a common position of four to five α-helices. Another common feature of SAPLIPs, true at least for saposins (Sap), is their overall negative surface charge without considerable presence of positively charged surface patches, feature accounting for the acidic pH dependence of the activator function (see *3.1*). Some experimental structural data are available for SAPLIPs (Sap A and C included)[55-57].

The phylogenetic origins of SAPLIPs are diverse and include proteins from eukaryotic and prokaryotic organisms and even from plants[54]. SAPLIPs secondary structure organization might comprise small single saposin-like domain proteins (e.g. Saps) or multidomain proteins in which the saposin-like domain represents a part of the protein. There are at least seven different genes in the human genome coding for eleven different proteins that can be included among SAPLIPs. Human SAPLIPs are, for example, prosaposin (pSap) and deriving Saps (see *3.1*), acid sphingomyelinase (ASM, see *3.2.1.1*), acyloxy acylase, surfactant protein B or granulysin, for overview see Bruhn (2005)[54].

SAPLIP properties related to membrane (lipid) interactions can be clustered into three general areas sharing specific common features: (i) membrane association with local disordering of the bilayer structure (e.g. ASM[58,59]); (ii) fundamental membrane perturbation without direct permeabilization for the purposes of antigen presentation or enzymatic activity (e.g. Saps); and (iii) membrane permeabilization for defensive mechanisms (e.g. granulysin). It should be noted that SAPLIPs are directly involved in other cellular signaling pathways besides the direct membrane (lipid) interactions (see *3.1.2* and *3.1.4.1*). Certain SAPLIPs (e.g. pSap or J3 crystallin) were documented to function as molecular scaffold proteins in multi protein complexes[60]. The topic of SAPLIP biology is very broad and this text will concentrate on the issues directly related to lysosomal biology. Primarily, pSap (Saps) and ASM will be discussed.

3.1 Prosaposin deficiency – enzyme activator precursor versus neurotrophic factor

3.1.1 Prosaposin - gene, cellular trafficking and posttranslational modifications

Human prosaposin gene (*PSAP*) is located on the chromosome 10 (10q22.1)[61]. *PSAP* gene mRNA encodes for a polypeptide (~53 kDa, pSap) that contains signal peptide and four distinct but homologous sphingolipid (sphingolipidhydrolase) activating proteins (Sap A-D)[62]. Human *PSAP* gene structure was determined to result from two rounds of tandem duplication events[63]. Such a structure of the gene is conserved in several higher organisms including mice. The promoter of *PSAP* gene has been thoroughly defined including core regulatory promoter sequence and tissue specific (neuronal and visceral) regulatory elements[64-66]. Complex ontogenetic temporo-spatial expression patterns were determined for *PSAP* gene[67]. Exon 8 (3 amino acid residues in Sap C domain) of *PSAP* gene is a subject of alternative splicing resulting in three different pSap mRNA variants (524, 526, and 527 amino acids) with specific ratios of tissue and ontogenetic stage abundance[68]. The intracellular transport of pSap was determined to depend on the specific splicing variant. No substantial impact of the mRNA splicing on the pSap functionality was reported for *PSAP* gene[69]. Studies undertaken to evaluate phylogenetic conservation of splicing patterns including their tissue distribution showed evolutionary conservation of this phenomenon and demonstrated dispensability of exon 8 sequence for developmental, secretory and lysosomal roles of pSap[70].

Translated pSap (53 kDa) is posttranslationally processed by a succession of modifications. pSap is modified to 65 kDa form which is further glycosylated to 70 kDa secretory molecule. The 65 kDa molecule is associated with Golgi apparatus membranes and is destined to lysosomes for further proteolytic processing. The sorting step discriminating the secretory and lysosomal forms is only partially elucidated[62]. It was demonstrated that Golgi/lysosomal sorting mechanism does not employ mannose-6-phosphate (M6P) receptor but is dependent on pSap's interaction with sphingolipids (i.e. sphingomyelin)[71] and sortilin receptor protein. pSap sortilin interaction is mediated via an adaptor protein GGA and requires a specific stretch of C-terminal pSap sequence that includes α-helix stabilized by disulfide bridges (a general property of saposin-like domain)[19,72]. Similar mechanism of Golgi/lysosomal targeting was documented for acid sphingomyelinase[73] (see *3.2.1.1*) and

GM_2 activator protein[72], the molecular basics of these protein interactions with sortilin are very similar to those employed by pSap/sortilin protein pair.

Proteolytic processing of pSap to four Saps in the late endosome-lysosome occurs via cleavage by hydrolytic proteases, especially by cathepsin D[74]. The lysosomal targeting of procathepsin D was documented, under certain conditions, to be directly linked to pSap lysosomal transport. Sap-like domain in this case functions as a molecular scaffold for procathepsin D that in autocatalytic manner cleaves 10,5-11,5 kDa Saps from the precursor pSap molecule in the acidic environment of lysosomes[60,75-77].

Secretory targeting of pSap is present in a number of cell types and pSap was detected in numerous body fluids (e.g. milk, semen, cerebro-spinal fluid, pancreatic juice or bile). Functions of secreted pSap are diverse in different tissues[78] (some of them are discussed in sections *3.1.2* and *3.1.4.1*). The endocytosis of pSap was demonstrated to be mediated by lipoprotein like receptor (LRP)[79]. Uptake of pSap by M6P receptor or mannose receptor from cellular surface is also possible[77]. Some of the downstream cellular signaling exerted by pSap is mediated by its interaction with incompletely defined G0-protein associated receptor[80] (see *3.1.2*).

3.1.2 Saposins and prosaposin, versatile proteins with diverse functions

Human Saps (A-D) function as membrane glycosphingolipid mobilizing agents[53]. The unique quality of Saps to interact with membranes is related to their secondary protein structure (conserved hydrophobic protein core, with three conserved disulfide bridges and conserved α-helices), which has been evaluated by several NMR structural analyses[57]. Tertiary and quartenary protein structure has not been unequivocally solved yet, but Sap B, for example, most probably functions as homodimer[81]. Sap interaction with glycosphingolipid or phospholipid membrane sheets intensifies with lower pH and is directly related to overall negative surface charge of Sap molecules[53,54]. Atomic force microscopy and high resolution optical microscopy rendered data documenting direct interaction of Sap molecules with membrane lipids resulting in extensive bilayer remodeling[82]. Critical amino acid residues mediating the protein-lipid interactions were suggested in Sap C[81]. Overall, Saps mediate intermembrane transport of gangliosides and glycosphingolipids, reorganization and destabilization of phopholipid membrane sheets, and fusion of acidic phospholipid vesicles.

One additional biological function of Saps is their role in trimming and presenting of CD1-related lipid antigens[83].

Four homologous human Saps (A-D) are substantially different from each other in many aspects. Their substrate specificities as lysosomal hydrolase activators may overlap, the majority of these data originating from *in vitro* studies[78]. The following overview is in many aspects simplified for the purposes of further understanding of pSap and Sap deficiencies. Sap activator potential is directly linked to their membrane perturbation potential. Saposins A-D act as activators of the following lysosomal hydrolases – galactocebrosidase, arylsulphatase A, glucocerebrosidase and ceramidase, respectively. Sap B, in addition, functions as lysosomal acid α-galactosidase activator in degradation of globotriaosylceramide. Lactosyl ceramide hydrolysis by β-galactosylceramidase and β-galactosidase is associated with Sap A and B activation, respectively[84,85]. Controversy prevails over the issue of Sap activation of another SAPLIP protein – lysosomal acid sphingomyelinase. As described in more detail in section *3.2.1.1*, SAP-like domain of acid sphingomyelinase most probably substitutes utilization of Sap activator for sphingomyelin hydrolysis.

Prosaposin precursor molecule has diverse functions that are, similarly to Saps, linked to its lipid interaction characteristics[86,87]. Its glycosphingolipid and phospholipid binding affinity underlies pSap roles in transport of these moieties; it may also facilitate membrane fusions and remodeling. In addition, pSap was lately defined as important extracellular regulator with anti-apoptotic and cell cycle promoting functions[88,89]. pSap was demonstrated to interact with G0 protein coupled receptor in different tissues and trigger MAP kinase and other signaling pathways directly associated with S phase promotion and apoptosis down regulation[80,90]. Trophic effects of secreted pSap on male reproductive system have been demonstrated in pSap deficient mice[91-93]. Direct connection was established between pSap anti-apoptotic effect and prostate cancer progression[88,94,95], similar pSap mediated anti-apoptotic regulation was documented in monocytic cell lines[96]. Prosaposin's neurotrophic and neuroprotective effects that are exerted by similar mechanisms of signalling, are discussed in section *3.1.4.1*.

It should be stressed out that this janusian-like duality of pSap function has direct consequences in the molecular pathology of pSap deficiency (see *3.1.4*).

3.1.3 Prosaposin deficiency and isolated deficiencies of saposins, overview

Prosaposin deficiency is a rapidly progressive fatal infantile neurovisceral lysosomal storage disorder. Molecular a biochemical pathogenesis of pSap deficiency reflects both the absence of pSap as well as its four deriving Saps. The consequences must be attributed to the biochemical enzymatic deficiencies due to the lack of activator functions of Saps and its other inherent functions of pSap (see *3.1.2*). pSap deficiency represents very complex biological and pathogenic problem with many different aspects to consider[78,84,85,97,98], this text provides only a brief overview.

Up to now, six patients with pSap deficiency from five different families were reported worldwide, the seventh patient is under evaluation. The original assumption that pSap deficiency is an extremely rare lysosomal storage disorder had to be reconsidered with the growing number of diagnosed patients. Molecular basis of pSap deficiency lies in the complete absence of pSap and all four deriving Saps (A-D) in the cells and tissues[78] due to specific pathogenic variations in *PSAP* gene that interfere either with functional mRNA transcription (degraded by nuclear non-sense mediated decay) or with pSap protein translation initiation[84,85,98]. Survival of pSap deficient patients ranges from weeks to months. The morphological (optical and electron microscopic) and biochemical (accumulated lipid spectra, cellular lipid turnover) alterations can be assigned to the enzymatic deficiency of 5 different lysosomal hydrolases associated with activator functions of Saps. In a very simplified manner, morphological and biochemical consequences of pSap deficiency can be attributed to a combination of changes found in five different and defined single lysosomal hydrolase deficiencies (metachromatic leukodystrophy, Farber, Fabry, Krabbe and Gaucher diseases). At this point it must be noted that a substantial difference exists between the lysosomal storage in non-neuronal cells and neurons (see *3.1.4*)[84,85,99]. This difference is related to predominant functionality of pSap protein in the particular cell type – neuronal (neurotrophic effect of pSap) or non-neuronal (enzyme activation by Saps).

General morphological changes in non-neuronal cells (various types of epithelia or histiocytes) represent foamy cytoplasmic transformation by lysosomal storage. Storage macrophages may include Gaucher-like bodies. Electron microscopic findings include mixture of pleomorphic, sometimes oligolamellar lysosomal deposits, which might display some typical ultrastructural characteristics of the above mentioned isolated deficiencies. The lysosomal storage compartment in pSap deficiency is devoid of lipopigment. Biochemical spectra of accumulated lipids are complex and some display tissue specific characteristics. Lysosomal accumulation of multiple sphingolipids without contribution of either sphingomyelin or cholesterol is the predominant feature; lactosyl-ceramide is universally

stored. Ceramide, glucosylceramide, galactosylceramide, globotriaosylceramide, sulphatide and G_{M1-3} gangliosides are accumulated in tissue dependent manner. Some of these moieties also display reduced turnover in cultured pSap deficient fibroblasts. The glycosphingolipid/ sphingomyelin ratio or certain tissue specific storage patterns (e.g. adrenal cortex storage) might serve as very efficient tools to discriminate pSap deficiency from acid sphingomyelinase deficiency (Niemann-Pick disease type A and B) or Niemann-Pick type C or Wolman diseases[84,85].

In addition to pSap deficiency, isolated Sap deficiencies (A, B, C)[78] were reported and described. The molecular pathogenesis of these fatal lysosomal storage disorders, mimicking the particular activated hydrolase deficiency – Krabbe disease, metachromatic leukodystrophy and Gaucher disease type 3, is a result of pathogenic variations in the critical Sap domain of *PSAP* gene. Not a single case of isolated Sap D deficiency has been described yet. Single report describes a compound-heterozygous patient with Sap C and Sap D variations, but with Gaucher disease phenotype[100].

Important clues for pSap and isolated Sap deficiencies can be deduced from the studies of murine knockout models (pSap deficiency and Sap A and D deficiencies)[101-104].

3.1.4 Comments and discussion to the appended publication #1 - Sikora et al. (2007)

Publication by Sikora et al. (2007) documents neuronal specific characteristics of pSap deficiency which are substantially different from the lysosomal storage process in non-neuronal tissues and cells. This work demonstrates different (additional) roles of pSap in human neurons and suggests extensive lysosomal sequestration of ubiquitin-tagged proteins most probably due to massive autophagy. In addition, it describes immense sensitivity of cortical neurons to pSap deficiency resulting in their death in the relatively short postnatal time period.

The work utilizes formaldehyde fixed paraffin embedded (FFPE) biological material from three previously described pSap-deficient infants[84,85,97]. The fact that the three affected children deceased at different postnatal time points (day 27, day 89, and day 119) allowed evaluation of the temporal course of the neuropathologic process.

Our study represents detailed analysis of neural tissues in pSap deficiency employing optical and electron microscopic approaches. The optical microscopic analyses use extensive

set of antibodies with either histochemical or fluorescence secondary detection including multiple fluorescence labeling (for methodological details see appended publication #1).

A general comment (also given in the publication) must be made at this point to prevent any conceptual ambiguities. The term neurolysosomal describes lysosomal compartment in the neurons.

3.1.4.1 Specific features of neuronal affection in pSap deficiency

This commentary will concentrate on the previously unreported features of neurolysosomal storage process in pSap deficiency, for the overall description of neuropathologic findings in the analyzed patients the reader should refer to appropriate publications[84,85,97].

Neurons in all analyzed cases of pSap deficiency displayed cytoplasmic distension by fine eosinofilic granules, the changes attained granulovacuolar appearance in the oldest deceased patient (day 119). The granular/granulovacuolar appearance contrasted with foamy cytoplasmic transformation in the non-neuronal cells. The granules were not autofluorescent and were not stainable by any routine histological technique. There was no evidence of birefringent moieties, nor significant presence of glycolipids or sphingolipids. Glial elements (astrocytes and oligodendrocytes) displayed considerably milder morphological changes, microglial phagocytes are discussed later. Neuronal ultrastructural changes were featured by numerous vacuoles (0.5-1 μm in diameter, depending on the particular case) containing variably dense material with amorphous or coarse membranous substructure. This degraded material was reminiscent of degraded organelles (especially mitochondria), some of the vacuoles seemed to be endowed by double membrane. These changes were found both in the neuronal perikarya and in dystrophic axons, and there was no substantial difference between central and peripheral neurons either on the optical or electron microscopic levels of observation.

When summarized, observed changes were fundamentally different from the changes seen in non-neuronal cells in pSap deficiency or from changes observed in other lysosomal storage disorders characterized by membranous lipid deposits. The true origin of the granular transformation of neurons in pSap deficiency must have been addressed, if directly related to the lipid lysosomal storage due to enzymatic activator deficiency of Saps.

Immunophenotype of the neuronal granules was determined as late endosomal-lysosomal (LAMP 1, 2 and cathepsin D positive). Neurons in pSap deficiency displayed variable, but significant, immunohistochemical positivity of subunit C of mitochondrial ATP synthase (SCMAS). SCMAS represents an epitope that can be considered a marker of mitochondrial intralysosomal degradation[45-47].

A completely novel and suprising finding in pSap deficiency was the uniform and strong granular immunopositivity of ubiquitin in the whole neuronal population including axonal spheroids. Such an extent of ubiquitination was not observed in non-neuronal cells affected by pSap deficiency. Noteworthy is the fact that we evaluated not only the overall cellular ubiquitin (free and bound) but also ubiquitin protein conjugates (mono- and polyubiquitinated)[105], which were also considerably enhanced in presence. In order to exclude hypothetical dominant contribution of aggresomal protein sequestration, p62[106] (aggresomal protein component) immunohistochemical detection was performed, and was negative. Unfortunately, ubiquitin+1 forms[107-109] were not evaluated at the time of publication, and thus contribution of molecular mRNA misreading in pSap deficiency was not addressed. Critically addressing other findings and available data on mRNA misreading in neuropathology, massive involvement of ubiquitin+1 is, in our opinion, not probable in pSap deficiency. Because data regarding ubiquitination in lysosomal storage disorders are limited[110], comparative immunistochemical study in other (selected) lysosomal storage disorders was performed and results were included into the publication. We were not able to demonstrate comparably extensive and neuronally selective ubiquitination in any other lysosomal storage disease besides some very specific situations (neurofibrillary tangles in Niemann-Pick disease type C or axonal spheroids).

Because the immunohistochemical staining patterns of ubiquitin were suggestive of its association with the lysosomal compartment and electron microscopy observations displayed changes reminiscent of autophagy, we resorted to immunoflurescence multiple labeling in order to address these issues. The experimental setup employed laser scanning confocal microscopy (LSCM) with additional image restoration based on deconvolution algorithms to improve the effective image resolution[111,112]. The successive colocalization analysis was based on Pearson's coefficient cross-correlation function (CCF) analysis of dual channel images[113,114], which will be discussed briefly in this commentary.

Evaluation of signal colocalization patterns in fluorescence microcopy represents very valuable source of data in cell biology. Unfortunately, it also represents one of the most controversial issues in the optical microscopy, as considerable amount of published data are

biased by methodological mistakes. It should be noted that no universally accepted colocalization evaluation method is available at the moment[115]. We resorted to the use of CCF method because of the following reasons[114]: (i) it provides an overall estimate of signal correlation evaluated by defined statistical coefficient; (ii) it does not implement image segmentation based on subjective estimate; (iii) it possesses the unique advantage of internal control; (iv) it clearly discriminates between colocalizing, randomly distributed and non-colocalizing (excluding) signals; (v) our staining patterns fulfilled the criteria necessary for CCF analysis. Details about the CCF methodology and interpretation as well as combinations of antibodies used for the colocalization studies are listed in the appended publication #1.

CCF analysis showed unambiguous colocalization (positive correlation) of ubiquitin signal with late endosomal-lysosomal markers. Unfortunately, we were not able to distinguish the prevalence of either of the two phenomena - ubiquitination of membranes or contents of the late endosomal-lysosomal compartment, most probably due to sub-resolution size of the evaluated objects. The issue of direct demonstration of autophagy events by observing the organellar entrapment in lysosomal lumen, which would clearly complement electron miscroscopy, remained unaswered, most probably due to advanced stage of the intralysosomal epitope degradation.

Other important finding in pSap deficiency was the massive loss of cortical neuronal population in the early postnatal life as was demonstrated by comparison of the findings in the youngest deceased patient (day 27) and two other cases (days 89 and 119). This phenomenon does not seem to be related to improper functioning of subependymal germinal zone, neuronal migration or cortex remodeling, and it does not seem to be mediated via caspase dependent (apoptotic) cell death. As a consequence of such an extensive cellular loss, replacement of the neuronal cortical population by dense population of microglial phagocytes (CD 68 positive) and GFAP positive astrocytes occurred.

This massive, ontogenetic stage dependent neuronal loss, most probably caused by the absence of pSap, occurs within a time period of 60-80 days in the early postnatal period. There is virtually no comparable phenomenon in the human neuropathology; the only other process resembling such an immense neuronal loss can be attributed to hereditary cathepsin D deficiency and consequent congenital neuronal ceroid lipofuscinosis[116]. Neuronal loss in case of cathepsin D deficiency is gradual, most probably starting in utero and continuing in the postnatal period. With respect to the extent and relative abruptness of the neuronal loss in pSap deficiency, and in order to express the limited potential of normally evolving neurons to survive, we designated it cortical neuronal survival crisis. This phenomenon of massive cell

death represents an important difference to otherwise very similar neuropathological changes observed in murine model of pSap deficiency[104].

As mentioned above, neuronal affection in pSap deficiency displayed several fundamental characteristics that cannot be directly assigned to biochemical consequences of combined Saps activator deficiency despite increased levels of certain lipid moieties in the brain tissue. The true origin of these changes (massive ubiquitination, signs of autophagy and cortical neuronal survival crisis) is, in our opinion, reflection of the absence of pSap's trophic and neuroprotective functions. These activities of secreted pSap, which have been documented both in *in vivo* and *in vitro* studies[117-126], represent a platform for the growing number of reports on pSap trophic and cell-cycle promoting functions (for details see section *3.1.2*). Molecular basis of these properties of pSap molecule has been assigned to N-terminal sequence stretch in Sap C domain of pSap[127-129]. It has been further documented that the neurotrophic signal patch (9 amino acid residues) is spatially segregated from activator properties of Sap C[130].

The true sequel of changes, as observed in pSap deficient neurons, is a matter of hypothetical deduction comparable to jigsaw puzzle. The massive segregation of ubiquitin tagged proteins and observed ultrastructural changes can be compared to other processes previously described to result from macroautophagy[131-133]. SCMAS detectability and ubiquitin-lysosomal colocalization further support autophagic origin of the changes[47]. In addition, massive ubiquitination has been suggested to trigger autophagy under specific conditions[31]. Despite the existence of respectable data about the link of pSap to apoptosis down regulation we were not able to assign the neuronal cortical crisis to caspase mediated cell death. We thus speculate that the impact of pSap deficiency and depletion of neuronal postnatal stimulation triggers massive protein ubiquitination and sequential enhanced autophagy, while lipid storage is of minor importance at this time point. Cortical neurons, probably the most vulnerable neuronal population to pSap deficiency, abruptly and systematically succumb to cell death that displays characteristics of autophagy executed process (programmed cell death type II)[35]. These processes (protein clearance by ubiquitin-proteasome system and constitutive autophagy) are tightly linked[32,33] and regulated (for more details see section *1.1*) and according to the presented data they seem to converge in pathology of pSap deficiency.

Acta Neuropathol (2007) 113:163–175
DOI 10.1007/s00401-006-0148-7

Neurolysosomal pathology in human prosaposin deficiency suggests essential neurotrophic function of prosaposin

Jakub Sikora · Klaus Harzer · Milan Elleder

Received: 28 June 2006 / Revised: 15 August 2006 / Accepted: 29 August 2006 / Published online: 6 October 2006

Abstract A neuropathologic study of three cases of prosaposin (pSap) deficiency (ages at death 27, 89 and 119 days), carried out in the standard autopsy tissues, revealed a neurolysosomal pathology different from that in the non-neuronal cells. Non-neuronal storage is represented by massive lysosomal accumulation of glycosphingolipids (glucosyl-, galactosyl-, lactosyl-, globotriaosylceramides, sulphatide, and ceramide). The lysosomes in the central and peripheral neurons were distended by pleomorphic non-lipid aggregates lacking specific staining and autofluorescence. Lipid storage was borderline in case 1, and at a low level in the other cases. Neurolysosomal storage was associated with massive ubiquitination, which was absent in the non-neuronal cells and which did not display any immunohistochemical aggresomal properties. Confocal microscopy and cross-correlation function analyses revealed a positive correlation between the ubiquitin signal and the late endosomal/lysosomal markers. We suppose that the neuropathology most probably reflects excessive influx of non-lipid material (either in bulk or as individual molecules) into the neurolysosomes. The cortical neurons appeared to be uniquely vulnerable to pSap deficiency. Whereas in case 1 they populated the cortex, in cases 2 and 3 they had been replaced by dense populations of both phagocytic microglia and astrocytes. We suggest that this massive neuronal loss reflects a cortical neuronal survival crisis precipitated by the lack of pSap. The results of our study may extend the knowledge of the neurotrophic function of pSap, which should be considered essential for the survival and maintenance of human cortical neurons.

Keywords Prosaposin deficiency · Neurolysosomal disorder · Ubiquitination · Cross-correlation function · Cortical neuronal survival crisis

J. Sikora · M. Elleder (✉)
Institute of Inherited Metabolic Disorders,
1st Faculty of Medicine, Charles University and
General Teaching Hospital, Ke Karlovu 2,
Prague 2, 12808, Czech Republic
e-mail: melleder@beba.cesnet.cz

K. Harzer
Neurometabolic Laboratory,
Department of Pediatrics and Child Development
(Universitäts-Kinderklinik), University of Tübingen,
Tübingen, 72076, Germany

Introduction

Prosaposin (pSap) deficiency is a rapidly progressive fatal neurovisceral lysosomal storage disorder caused by mutations in the *PSAP* gene which leads to the blockage of pSap protein translation or to the premature (intranuclear) nonsense-mediated decay of pSap mRNA [13, 25, 43, 54]. The proven genotypes result in the absence of pSap and the products of pSap proteolytic processing. These polypeptide products, called saposins (Saps, sphingolipidhydrolase activating proteins), are essential for activating a set of lysosomal sphingolipid hydrolases [54]. In the absence of Saps, the sphingolipid substrates remain undegraded. The accumulated substrates, in visceral cell types, cause the lysosomes to become distended, giving them a foamy appearance and the process ultimately ends in organ failure, similar to full blown classic lipid storage disorders [3, 13, 25]. In this study, we show that in pSap deficiency the neurolysosomes of both the peripheral and

3.2 *Acid sphingomyelinase - Niemann-Pick disease type A/B – acid sphingomyelinase deficiency – model lysosomal enzymopathy – molecular studies*

Niemann-Pick disease type A and B (NPD A/B, acid sphingomyelinase deficiency) represents a classical, prototypic lysosomal storage disorder caused by the deficiency of a single lysosomal hydrolase with SAPLIP characteristics - acid sphingomyelinase (ASM, MIM 257200 and 607616) [134]. The history of the study of this disorder is more than 90 years old, starting with the initial description of the first case by Niemann[135]. The milestones of studies of NPD A/B (identification of stored material, biochemical description and isolation of the deficient enzyme, identification of the critical coding gene, description of pathogenic sequence variations, genotype-phenotype correlation studies, biochemical and cellular consequences of the storage process, and search for causal therapeutic agents)[134] are logical and could be, with minor differences, applied to all other lysosomal storage disorders resulting from a single lysosomal hydrolase deficiency.

With respect to the recently opened debate on the issue of ASM deficiency classification, the use of abbreviations NPD A/B should be understood as referring to ASM deficiency in the most general sense of cellular pathology or phenotypic presentation, if not stated otherwise. Abbreviations NPD A/B and ASM deficiency should be considered equivalent in meaning.

3.2.1 Sphingomyelin and sphingomyelinases

Sphingomyelin is a phospholipid composed of sphingenine, long chain fatty acid (together ceramide) and phosphorylcholine. The composition of the sphingomyelin molecule varies between different tissues and organs, the most variable part being the long chain fatty acid residue. Sphingomyelin comprises 5-20 % of the cellular phospholipids and is the essential constituent of the biological membranes, predominantly located in the outer bilayer leaflet. Its main synthetic pathway includes direct condensation of ceramide and phosphocholine catalyzed by phosphocholin-ceramide transferase[134].

Sphingomyelinases catalyze the hydrolysis of sphingomyelin into ceramide and phosphorylcholine[134]. The classification proposed by Samet and Barenholz[136] includes following mammalian enzymes: acid sphingomyelinase (ASM, E.C. 3.1.4.12) and its secretory Zn^{2+} activated variant (products of a single gene), neutral Mg^{2+} dependent

sphingomyelinase, Mg^{2+} independent neutral sphingomyelinase and alkaline sphingomyelinase from the intestinal tract. In addition to this classification, at least two other enzymes related to sphingomyelin degradation should be mentioned - α toxin of *C. perfringens*[137] and product of the *plcB* gene from *L. monocytogenes*[138], both functioning as sphingomyelinase- phospholipase C.

Sphingomyelinases, in general, act as soluble membrane associated proteins[139], with the exception of mammalian neutral Mg^{2+} dependent sphingomyelinase, which is an integral membrane protein[140]. The ezyme protein-lipid bilayer interaction is essential for the proper sphingomyelinase function[54,139,141]. Sphingomyelinases carry out the catalysis on the surface of the lipid membrane bilayer and therefore, only the head group of sphingomyelin is predicted to be available for the substrate recognition (see *3.2.1.1*). It has been demonstrated, that not only the spectrum of membrane lipids, but also physical membrane curvature directly influences sphingomyelinase function. On the other hand, ceramide release by sphingomyelinase might exert substantial influence on either membrane permeability or membrane aggregation/fusion potential due to regulation of membrane bending. Membrane permeability can be influenced by symmetric lateral segregation of ceramide residues into ordered ceramide rich platforms. Membrane bending, in the opposite fashion, results from asymmetric lateral segregation of ceramide. It is especially the formation of ceramide enriched membrane phases that seems to play crucial role in regulated receptor clustering or other forms of internal membrane organization and successive downstream signaling[139,142,143].

Despite the fact that sphingomyelinases have been known for a long time, recent renewed interest in these enzymes and sphingomyelin/ceramide biology is related to the discoveries of much broader biological roles of these moieties. Sphingomyelinases play crucial roles in the pathogenesis of some bacterial and viral infections (*N. gonorrhoae, P. aeruginosa*) and have substantial implications to the apoptosis triggering by some natural or artificial cytotoxic agents or ionizing radiation[142]. Ceramide, a product of sphingomyelin hydrolysis, functions as a secondary messenger in a number of regulatory pathways including apoptosis, cell differentiation or proliferation. Therapeutic influence of ceramide release represents a very challenging field of anticancer drug research[143]. The unraveling of sphingomyelinase and ceramide related regulation of complex cellular processes represents a task for additional and extensive investigation and should supplement already available data, mostly centered around the issue of ASM deficiency and related NPD A/B pathology.

3.2.1.1 Human ASM (E.C. 3.1.4.12)

ASM is a soluble metal ion (Zn^{2+}) dependent, membrane associated SAPLIP glycoprotein with a pH optimum of ~ 4.5–5.5. Two forms of ASM have been described, one intracellular (lysosomal) and the other extracellular (secreted). Both protein forms are products of a single gene (*SMPD1*, see *3.2.2*) differing by intracellular trafficking and pH optimum[144]. The first (intracellular) form is targeted to lysosomes by means of sortilin receptor patway or mannose-6-phosphate receptor mediated transport and possesses acidic pH optimum of 4.5-5.0[73]. The proportional contribution of these two transport mechanisms is undetermined, but sortilin pathway seems to prevail (see *1.1* and *3.1.1*). The extracellular (secreted) form bypasses N-acetylglucosamine-1-phosphotransferase step in the mannose-6-phosphate lysosomal targeting pathway and is secreted from the cell via Golgi apparatus and cytoplasmic membrane (default secretory pathway), its pH optimum is broader as it may also function at neutral pH. Both forms of ASM are Zn^{2+} dependent, despite the differences in temporo-spatial coordination of the enzyme's Zn^{2+} activation[144].

Molecular weight of the mature, active monomeric ASM protein is predicted to be 72-74 kD, and is based on the cDNA expression experiments performed in prokaryotic and eukaryotic systems[134,145]. The initial translated protein encoded by *SMPD1* gene has 629 amino acid residues and consists of a signal peptide, predicted saposin domain, phosphoesterase domain containing predicted dimetal center, and carboxy terminal part.

Crystallographic or other experimental structural data on ASM protein are not available at the present time. Fortunately, bioinformatic methods employing homology modeling based on structurally related mammalian purple acid phosphatase rendered a representative model of phosphoesterase domain of ASM. This model, whose root mean square deviation (RMSD) from the template molecule is 0.78 Å, comprises residues 201-472 of ASM and thus may provide valuable insights into the structure of this key ASM domain[141]. It is suggested to have dimetal-containing phosphoesterase properties with twofold symmetry axis, each half containing βαβαβ structural motif (see Figure 1). The model, prepared with Zn^{2+} in the dimetal center, identifies five potential metal coordinating sequence motifs with RMSD of 0.5 Å for the critical residues Asp 206, Asp 278, Asn318, His 425 and His 457. It further suggests structural model of phosphorylcholine head group recognition site and establishes sound basis for the catalytic mechanism of ASM mediated sphingomyelin hydrolysis, assigning the critical function of proton donation to His319 residue. Despite the fact that the structural data are based on homology modeling and not on direct experimental

data, they might be employed for relevant predictions of the impact of *SMPD1* gene (see sections *3.2.5, 3.2.8.1* and *3.2.8.2*) pathogenic variations on the ASM structure and function.

ASM, unlike some other acid lysosomal hydrolases, has no clearly defined activator needed for its enzymatic function. The substantial necessity of saposins (see *3.1.2*) for sphingomyelin hydrolysis by ASM has not, so far, been unequivocally demonstrated. Considering the potential role of saposin related activation of ASM, the role of the saposin-like domain (see section *3*) present in the ASM protein sequence (amino acid residues 89-165), must be mentioned[58]. Based on the available data, this domain might function in the mobilization of the substrate by disturbing the target membrane structure, as well as, by maintaining the folding stability of the whole enzyme[59]. Impaired function of this domain could not be fully supplemented by the presence of saposins, suggesting its critical importance in the protein structure.

3.2.1.2 Sphingomyelinases with neutral pH optimum

Neutral sphingomyelinases (see *3.2.1*) represent, in all aspects, less characterized group of proteins, compared to ASM[140]. The most important of the mammalian (human) enzymes is Mg^{2+} dependent neutral sphingomyelinase. Unfortunately, the data regarding the biochemical properties of the protein, its cellular localization, function and especially the critical genomic background are still contradictory. For the purpose of this overview, it must be noted that considerable care must be taken for the presence of contaminating activity while performing and evaluating ASM activity assays (see *3.2.6*).

3.2.2 Molecular genetics of ASM (*SMPD1* gene)

ASM is coded by *SMPD1* (sphingomyelin phosphodiesterase) gene, which is located on the short arm of chromosome 11 (11p15.1-p15.4)[146-148]. *SMPD1* gene is considered to be expressed in a housekeeping manner (constitutively). The overall size of the *SMPD1* gene is ~5kb including 5′ and 3′ untranslated regions, it has six exons (sized 77-773 bp) and five introns (sized 153-1059 bp). There is one Alu I repetitive element in reverse orientation located in intron 2. Three distinct *SMPD1* transcripts resulting from alternative splicing were isolated and expressed in eukaryotic cells. Only the full length (2347bp) mRNA encodes

catalytically active enzyme. The open reading frame of this full length mRNA is 1890 bp long and codes for 629 amino acids-long protein.

There are several polymorphisms present in the primary sequence of *SMPD1* gene – Thr322Ile, Gly506Arg and variable number (3-5) of hexanucleotide repeats in exon 1[149] (see *3.2.8.1*).

SMPD1 gene proximal promoter region is GC rich and lacks TAATA and CAAT elements. The closest TAATA and CAAT elements relative to the translation initiation site of *SMPD1* gene are located between -704 bp to -898 bp, their functionality has never been demonstrated. The functional analysis of *SMPD1* promoter defined the core promoter spanning the sequence of -219 to +119, with several predicted Sp1 transcription factor binding sites. Additional experimental findings showed active role of Sp-1 and Ap-2 transcription factors in the basal and regulated promoter activity of *SMPD1* gene[150]. These data are in agreement with general concepts of the function of TATA-less promoters.

Only recently, results of the studies on Beckwith-Wiedemann syndrome (BWS), in 20% of cases caused by uniparental disomy of paternal chromosomal region 11p15 (over 5 Mb in length), suggested a possibility of genomic imprinting of the *SMPD1* locus[151]. Detailed analysis of the *SMPD1* promoter region confirmed this hypothesis. These recent findings shed new light onto the previously described phenotypic variability of otherwise genotypically identical heteroallelic individuals with NPD A/B or possible phenotypic affection of NPD A/B carriers[152] (see also *3.2.8.2.1*).

3.2.3 Cellular and organ pathology of ASM deficiency, consequences of the storage process

Basic morphological change characterizing the lysosomal storage process on the optical and electron microscopic levels is gradual and three dimensional distension of the cellular lysosomal compartment[134,145,153]. In other words, every cell affected by considerable lysosomal storage becomes vacuolated. The final stage of this process could be described as foamy transformation of the cell. This kind of morphological change is most evident in cell types that are naturally spiny in shape (e.g. neurons or macrophages). Historically, such morphological changes were considered as specific for NPD, and as such, the storage cell was designated - Niemann-Pick (NP) cell. Current state of knowledge considers this kind of morphological transformation completely unspecific, in comparison to the presence of diagnostically specific sphingomyelin liquid crystals in the cells affected by storage. The

overall microscopic appearance might be modified by the presence of autofluorescent lipopigments, again without any diagnostic significance.

Lysosomal storage caused by ASM deficiency (NPD A/B) is generalized, multi cellular type affection. ASM deficiency is, in other words, generalized sphingomyelinosis. Total sphingomyelin content in the tissues of individuals affected by ASM deficiency can be increased 50 fold. The cholesterol content is also increased (3-10 fold). Monoacylglycerobisphophates, glucocerebroside, G_{M2} and G_{M3} gangliosides, lactosylceramide, Gb3 and Gb4 ceramides are increased comparably less.

The massive and generalized accumulation of sphingomyelin distinguishes NPD A/B from NPD type C (disorder with a completely different molecular basis, see *3.2.8.3.1*), that is characterized by sphingomyelin accumulation in histiocytic elements; all other cell types in NPD type C accumulate a mixture of lipids, predominantly glycosphingolipids and cholesterol[154].

The consequences of the lysosomal storage process on the normal cellular functions are still controversial (see section *1.2.1*). Lysosomal storage process due to ASM deficiency might, in some cell types, even result in cell death. Unfortunately, the fundamental questions regarding the dynamics and turnover of the storage compartment and accumulated substrate remain unanswered.

Tissue and organ distribution of the lysosomal storage process in NPD A/B can be perceived from different angles (historical, ontogenetic, clinical, and pharmacokinetic). Whatever point of view taken, the cardinal quality is the presence of the sphingomyelin lysosomal storage either in neuronal or visceral (non-neuronal) tissues. The evaluation of tissue distribution of lysosomal storage in a particular affected individual poses a general problem of bioptic sample inaccessibility, thus the bulk of information originates from post-mortem autoptic studies. A reliable and easily detectable intravital indicator of the neuronal storage process in NPD A/B has not yet been found, event though repetitive attempts were made.

3.2.3.1 Neuronal storage compartment

The extent of neuropathological affection can be quite variable and includes both central and peripheral nervous system. Affected neurons have distended foamy cytoplasm

with detectable sphingomyelin birefringent crystals. The general tendency to atrophy and gliosis is a result of neuronal depopulation due to lysosomal storage and parallel proliferation of astroglia. Cerebellum is usually the most affected part of the brain, with extensive involvement of Purkinje cells and their dendrites in molecular zone. Similar changes might be detected in the spinal cord, sympathetic ganglion cells or in adrenal medulla. There is sometimes detectable peripheral demyelinization with lysosomal storage in Schwann cells.

3.2.3.1.1 Retina - a window into the brain?

Retina is a complex histological structure with extensive neuronal population. It is easily accessible to noninvasive fundoscopic evaluation, and as such, retinal changes are considered important[155,156] for the evaluation of neuronal lysosomal storage, not only in ASM deficiency. The cellular types affected by lysosomal storage in retina, however, have not yet been clearly defined. Ganglion cells are expected to be highly susceptible to lysosomal storage; besides that, some authors suggest affection of sessile retinal macrophagic cells[157]. The concentration of ganglion cells is highest in the perifoveolar region, fovea is free of this cell type. Grey-yellowish haze of retina appears when lipid deposits accumulate in the somata of ganglion cells. Fovea, under the conditions of lysosomal storage, contrasts in red with the surrounding yellowish retina.

Two descriptive terms are used for these fundoscopic findings - macular halo or cherry red macula. Macular halo is used to describe fundi in which the total diameter of the ring of pale, opaque retinal tissue is no more than 3 times the diameter of fovea. Macular halo is defined by sharp demarcation of its borders and granular interior. Larger zones of retinal whitening than those of macular halo, are considered cherry red maculae[158].

3.2.3.2 Visceral storage compartment

Spleen is the most affected organ in ASM deficiency. Splenomegaly may be very variable, but 10 fold increases in overall size is not exceptional. Splenic architecture is considerably abnormal with the storage present especially in the histiocytes of both pulps, if white pulp is preserved[159]. The storage process is always present in the lining cells of sinusoids.

The hepatic lobule, with all its constituents, is a dynamic structure and its affection by the lysosomal storage process in ASM deficiency may be very variable. Generally, the intensity

of the storage process in the hepatic lobule exhibits porto-central vectorial increase. In some very mild cases lysosomal distension in the hepatocytes can be hardly discernible on the optical microscopy level. Sessile liver histiocytes (Kupffer cells) are always affected, even though to variable extent, suggesting their higher sphingomyelin turnover. Protracted storage process might also result in deposition of autofluorescent ceroid. Correlation between the extent of enzymatic ASM deficiency and histological tissue affection exists, but only to a limited extent[160]. There is always some degree of hepatomegaly present, and there are reports showing reactive fibrosis and cirrhosis due to lysosomal storage[161].

Bone marrow and lymphatic nodes display variable admixture of foamy macrophages, sometimes with considerable amount of ceroid (sea-blue histiocytes) in protracted cases. Pulmonary parenchyma (alveolar septa, alveolar space) can be infiltrated by foamy cells of macrophagic origin, especially in visceral storage limited cases. Adrenal glands (especially cortex – epithelial cells and infiltrating macrophages) and thymus are enlarged. Other organs i.e. gonads, thyroid gland, hypophysis, pancreas or salivary glands may exhibit mild storage changes but usually no substantial functional impairment. Foamy histiocytes can be found in the wall of all portions of gastrointestinal tract.

3.2.4 Clinical classification of ASM deficiency, phenotypic heterogeneity versus historical perspective

The history of classification of Niemann-Pick disease reflects the general problems of disease initially described by morphological measures without the knowledge of the pathogenic basis of the process[134]. The initial classification scheme of Niemann-Pick disease included unrelated entities that shared similar morphological qualities. The first step in re-classification was taken, when type C of NPD was declared a separate pathogenic entity, not related to ASM deficiency[162] (see *3.2.8.3.1*). Ever since, NPD due to ASM deficiency is described as having two distinct phenotypic variants – types A and B.

The neurovisceral storage associated form, type A, is characterized as rapid and fatal clinical phenotype with progressive neurodegeneration and death within the first three years of life[163]. Type B is, on the other hand, characterized by visceral-only (non-neuronal) affection with mild, slowly progressive clinical course and survival till adulthood[164]. Sphingomyelin lysosomal storage is, so far, the only accepted cause of clinical symptomatology, neuronal lysosomal storage resulting in neurological affection and non-neuronal storage resulting in visceral symptomatology. The principal difference of these two

phenotypic variants (lack of neuronal affection by lysosomal storage) was demonstrated in several typical NPD type B patients by post mortem evaluation of brain sphingomyelin content[165].

During the last thirty years a number of reports accumulated, including larger cohorts of patients affected by intermediate phenotypic variants of ASM deficiency (especially slowly progressive neurological affection associated with longer survival), which did not fulfill the accepted classification criteria[160,166-169]. It became apparent that ASM deficiency displays wide phenotypic variability both in the neurological and visceral symptomatology, and typically affected patients (A or B phenotypes as defined) might represent a minor fraction of all ASM deficient patients.

Neurological affection ranges from overt perinatal crises, severe psychomotor retardation, severe muscle dysfunction or irritability to milder presentations such as peripheral neuropathy, mild mental retardation with learning disabilities, or only macular halo syndrome without additional abnormal neurological findings. Extensive effort is made to elucidate the issue of affection of retina in ASM deficiency. Fundoscopic changes (cherry red macula or macular halo) might serve, to a limited extent, as direct and easily accessible indicators of neurolysosomal storage (see *3.2.3.1.1*)[158,160,167]. Special care must be taken to differentiate neurological or psychiatric epiphenomena that are not directly related to the lysosomal storage, but that were reported in several ASM deficient patients[160].

Visceral affection was also repeatedly demonstrated as very variable. Liver failure due to massive hepatocellular storage in early years of life, or extensive pulmonary infiltration by storage laden macrophages contrast with cases featured by minute lysosomal storage in sessile tissue histiocytes and minimal organ dysfunction[160,161].

Another factor complicating the ambiguity of the current classification is the absence of clearly defined and easily assessable classification criteria, other than clinical phenotype. It is obvious that residual enzymatic activity or genotype information will not, universally, serve this purpose, especially when prediction of neurological affection and thus neuronal storage is so critically needed. Under certain circumstances, sphingomyelin loading test might have predictive value of the protracted neurovisceral course or accelerated visceral storage[160] (for discussion see *3.2.6* and *3.2.8.2*).

It seems to be clear that clinical course (temporal and tissue related) and storage intensity are definitely not classical type (A or B) specific, and as such, the accepted classification scheme oversimplifies the biological problem of ASM deficiency. It is a task for near future to reconsider this issue, because it might soon result in indicative controversies

over the newly introduced enzyme replacement therapy (see also *3.2.7* and *3.2.8.2*). Several proposals of ASM deficiency reclassification have appeared but none of them received general acceptance in the medical community[160,168]. Whatever modification of the current classification scheme is going to be achieved, it must reflect the immense variability of the clinical phenotype, and should result in increased alert about sub-clinical neurological affection in a considerable fraction of patients.

3.2.5 Molecular pathology of the *SMPD1* gene, population genetics, genotype-phenotype correlations, implications of *SMPD1* gene variations for ASM protein malfunction

NPD A/B is inherited as an autosomal recessive trait[134]. The first pathogenic variation in the *SMPD1* gene was reported in the year 1991[170]. There are, at least, 99 different pathogenic sequence variations reported in the *SMPD1* gene[171]. These variations comprise 81 missense or nonsense variations, 1 splicing intronic variation and 17 small deletions or insertions. The pathogenic variations are distributed over the whole *SMPD1* gene, the highest number of them is in exon 2 (44% of the *SMPD1* protein coding sequence). There are no reports demonstrating large scale rearrangements in the *SMPD1* gene, but it should be repeated that the chromosomal region 11p15 can be a subject of imprinting[151].

ASM deficiency, in all its phenotypic variants, should be regarded as a truly panethnic disorder with global distribution. Despite that, it must be noted, that certain ethnic groups with tendency to socio-economic clustering and higher rates of consanguineous marriages show higher incidence of ASM deficiency (Ashkenazi Jews[172], Israeli Arabs[173] or Arabic population of North African region of Maghreb[174]) compared to "general" population. With respect to historical aspects of NPD A/B description, the best studied ethnic group are Ashkenazi Jews, with the estimated incidence of classical NPD type A 1:40 000 and classical NPD type B 1:80 000[175]. The panethnic (global) population frequency of NPD A/B including heterozygote carriers is not available despite the existence of demographically very heterogeneous series of genotyped patients[164]. Correct estimates of the incidence values (applicable to all LSDs) are hampered by ethnically selective patient collection, which is directly related to the diagnostic potential of each single national health system (usually favoring less affected patients for proper diagnosis). Caucasian patients predominate in all the reported cohorts.

Last fifteen years represent time of intensive genotype-phenotype correlation studies in the field of lysosomal storage disorders. General limitations of these studies (compound

heterozygosity, heterogeneous phenotype and phenotypic overlaps, quality and relevance of evaluated phenotypic traits) can also be applied to NPD A/B.

Despite these drawbacks several pathogenic variations were clearly correlated with certain phenotypic variants of ASM deficiency (R496L, L302P and fsP330 are classical NPD type A[170,172,176] pathogenic variations with prevalence in Ashkenazi Jewish population, delR608 is panethnic classical type B associated variation even in compound heterozygotes[164,174,177]). Less affected patients (NPD type B), are predominantly diagnosed in global scale, and as such numerous pathogenic variations were declared as classical type B variations in different ethnic and national populations. With respect to the above mentioned ongoing discussion on the matter of ASM deficiency phenotypic classification and relative paucity of classical NPD phenotypes (A and B) among affected patients, pathogenic variation Q292K[160,166,168] associated with slowly progressive neurovisceral affection must be noted (for detailed discussion see *3.2.8.2*).

Majority of reported *SMPD1* variations are private, thus resulting in the necessity of individualized molecular genetic diagnostics and counseling in the affected families.
The impact of *SMPD1* pathogenic variations on the ASM protein structure and function, evaluated by means of its residual activity, is variable. In certain aspects, residual ASM degradation capacity attained by loading the cells with labeled sphingomyelin substrate may be more informative than the expressed or natural residual activity measurements (see section *3.2.8.2*). The values of residual enzymatic activity are still considered as very important for phenotypic correlations; nevertheless, these values should not be overestimated without complex and critical assessment. Historical concept associating massive visceral storage with severe neuronal damage and low residual ASM activity does not seem to be universally valid (for details see *3.2.8.2*).

Limited information is available about the impact of *SMPD1* gene nonsense pathogenic variations and subsequent nonsense mRNA mediated decay or physical instability of the truncated ASM protein molecules. No report has ever clearly demonstrated protein misfolding or enhanced proteasome degradation as a consequence of any of *SMPD1* pathogenic variations, even though this mechanism of protein degradation can be expected. The impact of *SMPD1* pathogenic variations has been, so far, evaluated by their expression in ASM deficient eukaryotic cell lines and by subsequent residual enzymatic activity measurements[160,172,178]. This approach of single allelic expression overcomes the influence of second interacting allelic product, as happens in compound heterozygotes. It must be noted

that information about tertiary ASM protein interactions is limited and thus purely speculative.

As mentioned in section *3.2.1.1*, the structural model of ASM protein based on experimental data is not available; nevertheless, model of ASM phosphoesterase domain based on homology modeling provides very interesting platform to hypothesize about the impact of pathogenic variations on the ASM protein structure and function[141]. Based on this premise, pathogenic variations M382I and N383S interfere with substrate recognition, L302P might result in kinking of one of the α helices and thus decrease protein stability, and W391G variation may destabilize the protein by disrupting important hydrophobic interactions. It should be noted that only one of *SMPD1* gene variations (D278A, see also *3.2.8.2*) occurs in the predicted metal coordinating residues. It is highly probable that a homozygous presence of alteration of any of these residues (Asp 206, Asp 278, Asn318, His 425 and His 457) would result in a prenatal death or very severe phenotype. The impact of pathogenic variations Q292K, H319Y and P371S on the predicted protein structure as well as consequences of variations in the saposin-like domain is discussed in sections *3.2.8.1.1* and *3.2.8.1.2*.

3.2.6 NPD A/B diagnostics – histopathoiogy, enzyme biochemistry, molecular genetics, differential diagnosis

The diagnostics of lysosomal storage disorders, and NPD A/B is not an exception, are a complex and multilevel process which should be performed and evaluated in specialized centers, as lysosomal storage disorders represent more than a biomedical problem. Efficient diagnostic process can be achieved only by the coordinated action of trained specialists.

The identification of the lysosomal storage of sphingomyelin can be usually performed by histochemical detection of sphingomyelin liquid crystals or additional ceroid admixture in the foamy cells. The bioptic tissue used is most usually bone marrow aspirate or skin biopsy.

The measurement of activity of ASM is very efficient method to detect ASM deficiency; it also serves as a potent differential diagnostic tool to exclude other lysosomal storage disorders. Residual ASM activity is measured in the cell homogenate (either leukocyte or fibroblast pellet). There are several methods for ASM estimation, differing in the substrate used for the analysis. It is possible to employ natural radiolabeled N-methyl-^{14}C sphingomyelin[179], which must be handled according to the limitations of radioactive material use, thus making this assay less convenient for general practice. Other possibility is the use of

artificial substrates with conjugated chromogenic or fluorogenic labels. There are at least two substrates of this type available at the moment: 2-N-(hexadecanoyl)-amino-4-nitrophenyl phosphorylcholine (HNP-PC)[168] or 6-hexadecanoylamino-4-methylumbelliferyl-phosphorylcholine (HMU-PC)[180]. Unfortunately, ASM assay employing HNP-PC substrate rendered pseudo-normal ASM activities in NPD A/B patients with one of the pathogenic variations (Q292K)[168]. This phenomenon most probably results from abnormal affinity of the variant protein to the artificial substrate as compared to the natural substrate (see also *3.2.8.2*). The use of HMU-PC with parallel addition of natural substrate as competitor overcame the limitations of HNP-PC in detection of pseudo-normal ASM values for Q292K variation, and as such, this assay setup was recently demonstrated as reliable for diagnostic use[180].

The values of residual ASM activity in affected individuals, heterozygotes or healthy individuals are not strictly separated. Classical NPD type A patients do not express more than 2 % of normal ASM activity. Classical NPD type B patients usually exhibit values of 5-10 % of normal ASM activity[134]. It must be noted that values reaching 20 % of normal were measured in some very mild NPD type B patients. Strictly defined, values for heterozygotes are missing. Inconclusive grey-zone values of ASM residual activity must be interpreted very cautiously and with regard to additional findings, including molecular genetic testing. Additional method of evaluation of ASM degradative capacity is the use of LDL or liposome mediated sphingomyelin loading test in the cell culture with consecutive sphingomyelin degradation products determination[160]. This type of assay setup might, in certain aspects, characterize the residual sphingomyelin degradative capacity of the lysosomal apparatus in a more "biological" way than the values of residual ASM activity obtained from cell homogenates. Potential drawback of this assay is the cellular type evaluated (fibroblast). Cultured skin fibroblasts are not prototypic cells affected by lysosomal storage in NPD A/B.

The ultimate diagnostic tool of NPD A/B is the molecular genetic evaluation of the *SMPD1* DNA sequence. Methods of pathogenic variation detection are variable, ranging from PCR/RFLP detection of prevalent variations to global *SMPD1* coding sequence analyses. Analysis of RNA may be useful in certain special cases (i.e. nonsense variations, intronic variations affecting consensus splicing factors binding sites etc.). Epigenetic modifications (i.e. imprinting of the *SMPD1* locus) should not be ignored. Molecular genetic counseling in individual affected families should always result in complete disclosure of the molecular pathology on the level of genotype. Molecular genetic examination must be perceived as integral and standard part of the diagnostic considerations.

The differential diagnostics of NPD A/B require broad clinical, histopathological and laboratory considerations. The complexity of the problem is demonstrated in the appended publication #4, which deals with description of atypical case of NPD type C, initially misdiagnosed as Gaucher disease.

3.2.7 NPD A/B therapy (bone marrow transplantation, enzyme replacement therapy, gene therapy)

Therapeutic interventions available for lysosomal storage disorders, albeit limited are intensively studied. There is no causal, efficient therapy available for NPD A/B at the moment. The goal of principal correction of the enzymatic deficiency has not yet been achieved. Therapeutic modalities being considered are: enzyme replacement therapy (ERT) or substrate reduction therapy, bone marrow transplantation or other means of stem cells therapy in conjunction with gene therapy. Other types of therapeutic interventions (e.g. splenectomy) must be perceived as supplementary.

Each of the above mentioned therapeutic approaches to ASM deficiency is facing multiple biological obstacles – generalized character of affection, relative pharmacokinetic inaccessibility of certain tissue compartments (especially central nervous system), phenotypic variability hampering efficient indication protocols, and economic demands for health care systems.

Bone marrow transplantation[134] was performed in several patients with classical NPD type A phenotype, unfortunately without any significant success. Neurological deficits in the patients did not improve and the transplanted children succumbed shortly after the intervention. One transplanted NPD type B patient showed decrease of the sphingomyelin content in the liver, bone marrow and lungs, but also this patient died within months after the transplantation.

ASM deficiency is one of the candidates for enzyme replacement therapy. Recombinant acid sphingomyelinase has already entered advanced stages of clinical testing and should be available to NPD type B patients in a short time. ERT, as an established therapeutical approach, is successfully used in therapy of Gaucher, Fabry , Pompe and Hurler (muccopolysaccharodisos - MPS type I) diseases, and is planned in near future for MPS type II and MPS type VI[181]. Despite very respectable results of ERT on the level of clinical trials and other clinical evaluation studies, data on the direct impact of ERT on the lysosomal storage compartment on the cellular level are still limited. Cell biological and treatment

related bioptic and autoptic evaluation studies are under way, and some important results have already been published[182]. Unfortunately, the volume of ERT related samples (bioptic and autoptic) available to the academic community is limited, as ERT clinical applications tend to be very closely coordinated by commercial suppliers.

The impressive results of ERT have not resulted in loss of interest in gene therapy of NPD A/B, because it represents the fundamental approach to deal with the molecular defect. General limitations of gene transfer therapy (i.e. transgenic vector selection, transgene expression regulation, transgene tissue targeting, immune reactions, etc.) can be applied to ASM deficiency. Research in this field focuses on ASM knock-out murine model. For recent summarizing review on gene therapy of LSDs see Hodges and Cheng (2006)[183].

Several retroviral adeno-associated viruses (AAV) were tested for their efficiency in the ASM transgene transfer[184]. Non-neuronal (visceral) storage was significantly reduced in ASM knock-out mice when transplanted with ASM overexpressing haematopoietic stem cells. Nevertehless, neuronal lysosomal storage was influenced in this therapeutic setup to a comparably lesser extent[185]. Stereotactic intracerebral application of the ASM bearing vector (either directly or via transformed neural progenitory or mesenchymal stem cells) rendered very promising results in reduction of lysosomal storage process and successful propagation of the transgene in the brains of the experimental animals[186,187].

3.2.8 Comments and discussion to the appended publications #2 – 4

3.2.8.1 Sikora et al. (2003)

Publication by Sikora et al. (2003, appended publication #2) describes a molecular study of *SMPD1* pathogenic variations in a cohort of 7 NPD A/B patients provided by a cooperating Dutch center involved in diagnostics of inherited metabolic disorders. The goal of the study was to evaluate genotype-phenotype correlations in this patient group, which represented, at that time, the first molecular study performed among the Dutch residents affected by ASM deficiency.

We analyzed seven non-related NPD A/B patients (out of 27 diagnosed in the Netherlands in the years 1970-1999), whose diagnosis of ASM deficiency was based on previous ASM activity measurements using N-methyl-^{14}C sphingomyelin substrate. Three of the patients were of Dutch ethnic origin, the remaining four patients, even though Dutch

residents were of Turkish origin. The clinical phenotype corresponded with the classical type A of NPD in three patients, one patient was described as slower but progressive type A patient (died at 5 years of age), and the remaining three patients were affected by typical type B phenotype of NPD. Detailed clinical description of the studied subjects is provided in the appended publication #2.

The overall evaluation of the coding region (including previously described polymorphisms) of *SMPD1* gene was performed by direct sequencing of the PCR products and rendered quite surprising results. The analysis of fourteen alleles disclosed eight different pathogenic variations, seven (G29fsX74, S248R, H319Y, P371S, F463S, P475L, and Y537H) of these variations were novel, at that time. In addition, we found one synonymous heterozygous variation in one of the patients. All of the found sequence variations were confirmed by an independent method, in this case either by PCR/RFLP or ARMS (amplification refractory mutation system). Novel pathogenic variations were assessed in additional 100 wild type *SMPD1* alleles to exclude the possibility that they represent common genetic polymorphisms. None of these seven variations was found on any of the evaluated wild type alleles. All the novel pathogenic variations were submitted to the public sequence variations databases[171]. Unfortunately, no conclusion regarding prevalent pathogenic variation in Dutch NPD A/B population could have been drawn, both due to the ethnic heterogeneity of the patient group and relatively small number of evaluated subjects.

The fundamental question regarding the pathogenic potential of the novel variations was based on the following premises: (i) no other nucleotide change, besides the common polymophisms, was found in the *SMPD1* coding sequence; (ii) all of the variations result in a non-conservative amino-acid exchange, except for P475L; (iii) one of the variations (G29fsX74) is a micro deletion with a reading frame shift resulting in a premature stop codon in the ASM ORF (open reading frame); (iv) all of the affected amino acid residues display broader evolutionary conservation; (v) found variations are not common polymorphisms; (vi) extensive searches in EST (expressed sequence tags) databases did not render a single positive hit when searched for these variant sequences.

Out of seven evaluated individuals five were homozygotes (all four Turkish patients and one Dutch patient) for respective pathogenic variations - H319Y, P371S, Y537H and delR608. This finding was rather unexpected, with respect to high proportion of compound heterozygotes among NPD A/B patients worldwide, and suggested possible contribution of socio-economic clustering in the affected families. On the other hand, this higher proportion of homozygotes allowed more representative estimates of genotype-phenotype correlations

because of the equal allelic contribution to the phenotypic presentation. H319Y and Y537H associated with NPD type A and P371S associated with NPD type B (see below). Variation delR608 represents the most frequently occurring *SMPD1* variation worldwide among NPD type B patients[164,174,177]. It is an in-frame single codon deletion in the C-terminal portion of ASM protein. It is usually this position of the deletion in the ASM protein that is given as a molecular basis of the high residual activity of the variant ASM. delR608 was always associated with very mild type B phenotype without any neurological affection, including any detectable retinal lesions. At the time of publication (year 2003), delR608 was considered to be prevalent pathogenic variation among the Arabic NPD type B population of North African region of Maghreb. The appended publication was one of the first suggesting that delR608 occurrence is panethnic, this suggestion was later confirmed by additional studies in the ethnically heterogeneous NPD type B patient cohorts[164]. The genotype-phenotype correlation between delR608 and mild NPD type B phenotype without any neurological affection is an accepted fact of immense significance. With respect to the planned introduction of ERT into the therapy of ASM deficiency, genotype-based indication criterion (delR608 positivity) seems to be valid for inclusion of the affected pathogenic variation carrier into the therapeutic protocol.

One of the pathogenic variations among the evaluated patients was a microdeletion with additional shift of predicted mRNA reading frame (G29fsX74) and premature novel stop codon occurring on the residue 74. Several mechanisms might be expected in the process of elimination of such a truncated RNA or protein molecule. One of these is non-sense mediated decay of the compromised mRNA molecule; the other would be efficient elimination of the truncated protein, most probably by misfolded protein degradation pathways. In general, mechanisms of incompetent RNA or protein molecules elimination are accepted as extensively employed and represent an important contribution to molecular pathogenesis of monogenic disorders. RNA and protein instability in ASM deficiency are objectives for near future and are directly dependent on the release of the ASM crystallographic data.

As was mentioned in the introductory part, no experimentally based structural data on ASM protein are available at the moment. Fortunately, this gap in the knowledge about sphingomyelin metabolism related to ASM function was partly filled by the release of the structural model of phosphoesterase domain of ASM constructed using homology modeling approaches (see 3.2.1.1)[141]. This model suggested a molecular mechanism for shingomyelin hydrolysis including the following consecutive steps: (i) substrate recognition and binding; (ii) phosphorus atom of the substrate molecule is attacked by a hydroxide ion bound to the

dimetal center forming a pentacoordinate phosphate transition state; (iii) proton is donated by the enzyme protein to the oxygen atom bridging the phosphorus atom and alcohol, which results in the hydrolysis of the phosphorus/oxygen bond; (iv) release of ceramide and phosphorylcholine. The critical residue donating the proton for the hydrolytic step of the reaction was suggested to be H319. One of the supportive arguments provided for this hypothesis of ASM catalytic site composition is the homozygous occurrence of H319Y in one of the above described NPD type A patients. On the contrary, P371S variation found in one of the NPD type B patients is predicted to be situated at the end of a β-strand between the two central β-sheets, but is not in the close vicinity of the catalytic center. Variant serine at this position might result in the slight change of the two sub-domains spatial orientation and thereby affect the enzyme's catalytic activity. Topology of the global phosphoesterase domain of ASM with the discussed residues is depicted on Figure 1.

The expanding data on the protein structure and function start to efficiently complement the genomic data in many monogenic disorders, and ASM deficiency is a very nice example of this genomic-proteomic conjunction. The knowledge, if only of a bioinformatic, but highly representative protein structural prediction, remarkably extends the potential to reasonably hypothesize about the pathogenic variation impact on the protein structure and function. In the same logic, the information about pathogenic variation primarily generated for medical purposes might provide important clues for protein catalytic function.

Appended publication

Seven Novel Acid Sphingomyelinase Gene Mutations in Niemann-Pick Type A and B Patients

J. Sikora[1]*, H. Pavlu-Pereira[1], M. Elleder[1], H. Roelofs[2] and R. A. Wevers[2]

[1] *Institute of Inherited Metabolic Disorders, Charles University, 1st Faculty of Medicine, Prague, Czech Republic*

[2] *Laboratory of Pediatrics and Neurology, University Medical Center Nijmegen, Nijmegen, The Netherlands*

Summary

We have analyzed acid sphingomyelinase (*SMPD1*; E.C. 3.1.4.12) gene mutations in four Niemann-Pick disease (NPD) type A and B patients of Turkish ancestry and in three patients of Dutch origin.

Among four NPD type A patients we found two homozygotes for the g.1421C > T (H319Y) and g.3714T > C (Y537H) mutations and two compound heterozygotes, one for the g.3337T > C (F463S) and g.3373C > T (P475L) mutations and the other for the g.84delC (G29fsX74) and g.1208A > C (S248R) mutations.

One of the type B patients was homozygous for the g.2629C>T (P371S) mutation. The last two type B patients were homozygotes for the common g.3927_3929delCGC (R608del) mutation.

The G29fsX74, S248R, H319Y, P371S, F463S, P475L and Y537H *SMPD1* mutations are all novel and were verified by PCR/RFLP and/or ARMS. All of the identified mutations are likely to be rare or private, with the exception of R608del which is prevalent among NPD type B patients from the North-African Maghreb region. Geographical and/or social isolation of the affected families are likely contributing factors for the high number of homozygotes in our group.

Introduction

Niemann-Pick disease is an autosomal recessive sphingolipidosis caused by the deficiency of lysosomal acid sphingomyelinase (ASM, E.C. 3.1.4.12) resulting in lysosomal accumulation of sphingomyelin. At the extremes of the phenotype spectrum lie two common presentations: infantile neurovisceral fatal type A, and type B, characterized by purely visceral involvement and by survival till adulthood (Elleder, 1989; Kolodny, 2000; Schuchman & Desnick, 2001; Vanier & Suzuki, 1996). Patients with intermediate phenotypes have been reported (Elleder & Cihula, 1983; Elleder *et al.* 1986; Sperl *et al.* 1994; Takada *et al.* 1987). Both type A and B variants have higher prevalence in the Ashkenazi Jewish population, reaching 1:40 000 for NPD type A (Goodman, 1979); NPD type B incidence is estimated to be significantly less than that of NPD type A (Schuchman & Desnick, 2001) in this population. Little is known about the frequency of NPD types A and B in non-Jewish populations. Individual reports on the number of NPD type A and B patients and estimated birth prevalence data are available from several European countries, and Australia (Czartoryska *et al.* 1994; Krasnopolskaya *et al.* 1993; Meikle *et al.* 1999; Ozand *et al.* 1990; Poorthuis *et al.* 1999).

The *SMPD1* gene is 5kb long, consists of six exons (Schuchman *et al.* 1992; Schuchman *et al.* 1991), and is located on chromosome 11p15.1–11p15.4 (Da Veiga Pereira *et al.* 1991). More than 20 mutations associated with both types of NPD in Ashkenazi and non-Ashkenazi patients have been published. Most of the mutations are single base substitutions and small deletions with or without a frameshift. Three mutations, g.3592G > T (R496L) (Levran *et al.* 1991a), g.1372T > C (L302P) (Levran *et al.* 1992) and a single nucleotide

*Correspondence: Dr. Jakub Sikora, Institute of Inherited Metabolic Disorders, Div. B, Ke Karlovu 2, 128 08, Praha 2, Czech Republic. Fax: + 420/2/2491 9392. E-mail: jakub.sikora@lf1.cuni.cz

3.2.8.2 Pavlů-Perreira et al. (2005)

Publication by Pavlů-Perreira et al. (2005, appended publication #3) represents an extensive multi parameter study of 25 NPD A/B patients from the region of former Czechoslovakia. This respectable cohort of patients was evaluated from different perspectives (clinical with special emphasis on the neurological and ophthalmologic affections, histopathological concentrating on the neuropathology and liver presentation of ASM deficiency, biochemical including sphingomyelin degradation capacity in cell-loading assays, and molecular genetic analysis of *SMPD1* gene sequence). The complexity of the gathered data allowed extensive conclusions towards the genotype-phenotype correlations. The robustness of the studied patient cohort also provided sound basis to critically address the current classification of ASM deficiency[134]. It can be stated that this publication together with a similar patient cohort from Germany [168](published in parallel) renewed debate about the phenotypic heterogeneity of ASM deficiency that was previously limited to several isolated case observations of, so called, intermediate phenotype[169]. This discussion, more or less fruitfully, continues to the present time, and at a certain time point will definitely result in some classification scheme change of ASM deficiency. Only several of the topics raised in this publication are discussed in this text (for further details refer to the appended publication #3).

3.2.8.2.1 ASM deficiency phenotypic variability and related implications

Cardinal observation in this work is related to the fact that classical NPD phenotypes comprised minor proportion of all evaluated patients (9 of 25 cases, 36%); rest of the patients (16 of 25 cases, 64%) displayed clinically variable phenotype that could not have been classified according to the currently accepted criteria. This phenotypic variability can be perceived as continuous spectra of severity of neurological or visceral symptomatology (or their overlaps) due to sphingomyelin lysosomal storage. The fundamental necessity to discriminate between neuronal and non-neuronal cell pools and their affection by lysosomal storage was mentioned in section *3.2.3*.

It is especially the high proportion of patients with variable protracted but progressive neurological affection and associated visceral storage that makes this cohort unique. It must be noted that not only the neurological affection, but also the visceral affection displayed variant phenotypes among the evaluated patients. The publication describes three patients

with accelerated visceral course with rudimentary neurological lesions, who suffered from progressive visceral storage and organ failure, liver and/or lungs in particular.
The conclusion that can be drawn in relation to such an extent of clinical variability is that a considerable care must be taken during neurological evaluation of ASM deficient patients. Neurological affection can be protracted, sub-clinical and easily missed. A battery of tests, including EEG, evoked potentials and nerve conductance tests, should be performed to exclude such minute clinical lesions. Neurological examinations should also be repetitive to disclose slow progression.

Separate note must be given to ophthalmologic findings (for introductory note see *3.2.3.1.1*), an area that represents a truly controversial issue. According to the point taken in the paper, retinal lesions without any additional neurological affection may be considered as the most benign feature of neuronal lysosomal storage in ASM deficiency. Even though most benign feature, it is still a sign of neuronal lysosomal storage. On the contrary, several recent publications evaluating larger cohorts of NPD type B patients treat retinal lesions in a rather ambiguous manner, arguing in favor of sensitivity but not specificity of these lesions for neurological affection[158,167]. This controversy clearly demonstrates that phenotypic features cannot overcome biological basis of the disease entity and strict adherence to the current classification scheme might result in questionable conclusions.

In addition to general phenotypic variability of ASM deficiency in the studied patients, we were able to demonstrate a situation of substantial phenotypic variability in three, otherwise genotypically identical, siblings. Such a phenomenon has been previously reported, together with rare cases of affection of heterozygote carriers[151,152]. The hypothesis of epigenetic factors (methylation mediated promoter inactivation) is tested at the present time. Results suggesting role of such a modifying epigenetic influence would supplement already available data, and would most probably result in a necessity to reevaluate genetic counseling strategies in the affected families and to accept the possibility of pseudo dominance in *SMPD1* heterozygote carriers.

3.2.8.2.2 *SMPD1* genotype in central Europe, implications for ASM enzymatic activity assays

In comparison to the publication by Sikora et al. (2003), genotype evaluation of the ASM deficient patients from former Czechoslovakia revealed one prevalent pathogenic variation - Q292K. This variation was demonstrated to clearly associate with slowly

progressive neuronopathic phenotype of ASM deficiency when present on both *SMPD1* alleles in one patient. Phenotypic presentation of Q292 K compound heterozygotes relies on the second contributing allelic variant. Data from Germany[168], released nearly in parallel with the Czech-Slovak patient series, suggested central European prevalence of Q292K pathogenic variation. But as with other variations, the geographic distribution of Q292K variation was later demonstrated to be broader[164]. Additional six pathogenic variations in our cohort of patients were reported as novel at the time of publication.

Evaluation of the position of Q292 residue in the proposed structural model of phosphoesterase ASM domain demonstrates its location in one of the peripheral α-helices. The impact of the substitution can be assumed in a very limited way. The Q292 variation is not in close vicinity of the proposed catalytic site or substrate recognition loop (Figure 1). The role of the critical α-helix is not easily predictable, and consequences of its kinking by introduction of Lys residue are unclear. The issue of Q292 impact on the protein structure and function becomes even more enigmatic, when one considers the above mentioned "pseudo-normal" ASM activity values of the Q292K variant enzyme when measured with one of the artificial substrates (HNP-PC)[168]. The hypothesis of higher affinity of the substrate molecule to the variant ASM molecule becomes less probable due to the mentioned structural position of Q292 residue. Whatever is the explanation, care must be taken during substrate selection in ASM activity assays. Preferential use of HMU-PC or natural substrate is advantageous[180].

3.2.8.2.3 Proposals to the classification of ASM deficiency

Considering the phenotypic variability in the evaluated group of patients, the current classification of ASM deficiency is biologically restrictive. Other authors share this opinion, and based on very similar findings, proposed their own modifications of classification scheme[168]. Dramatic change in the phenotypic perception of the ASM deficiency cannot be expected, especially when considerable number of authors in the field tends to adhere to historical connotations[167].

The proposal raised in the paper suggests inclusion of all variant phenotypes of ASM deficiency (neuronopathic and non-neuronopathic) into a category of "intermediate phenotype". This is definitely a formal association. More importantly, the publication tried to express the necessity to perceive the existence of broad phenotypic variability of ASM deficiency by declaring that both the speed of the clinical course and storage intensity are not classic type specific. Importance of concise ASM classification for ERT therapy has been

stressed out repeatedly throughout this text. In addition, it was demonstrated that sphingomyelin degradation capacity, when evaluated by cell-loading assays may discriminate between the classical types (A and B) and "intermediate" type of affection, especially in Q292K homozygotes.

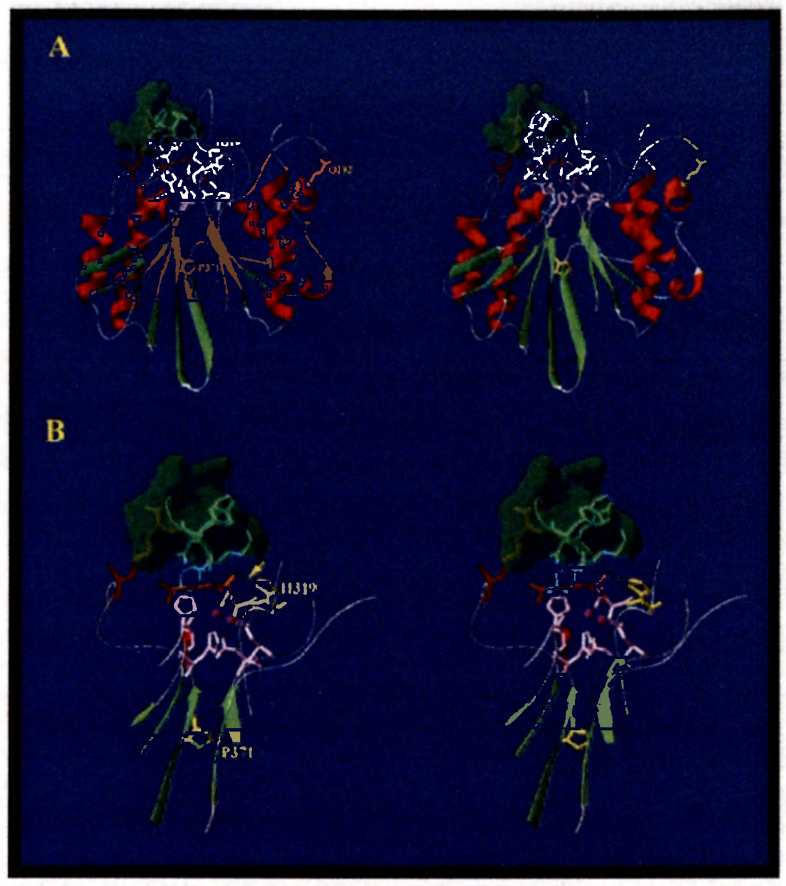

Figure 1

Structural model of ASM phosphoesterase domain

A – Global representation of the predicted crystal structure of ASM phosphoesterase domain with twofold symmetry, each half containing βαβαβ structural motif (α-helices in red, β-sheets in green, loops in grey). Two Zn^{++} ions are shown in violet; phosphorylcholine (substrate) is superposed into the protein model in orange. Dimetal coordinating residues (206, 278, 318, 425, and 457) are displayed in light pink. Predicted disulfide bond formed by Cys 385 and 431 (deep red) is in direct contact with the substrate recognition loop. Calculated molecular surface of the residues (382-390, light blue) involved in substrate recognition was rendered in transparent green color. Three discussed variant residues (Q292, H319, and P371) are presented in yellow. Residue Q292 lies outside of the predicted catalytic site of ASM phosphoesterase domain in one of the predicted short peripheral α-helices. Residue P371 is located at the C-terminal end of one of the central β-sheets; the potential impact to the protein structure is discussed in the text.

B – Detailed view of the catalytic site and substrate recognition loop. Coloring is identical to part A of this Figure. Arrow signifies the calculated H-bond between the proton donating H319 (yellow) and phosphorylcholine substrate (orange). Residue H319 is the predicted active residue in the catalytic site of ASM.

The presented structure was downloaded from (PDB protein crystal structure database[188]) and corresponds to the original 1X9O .pdb file[141]. The images were rendered in DeepView/Swiss PDB Viewer software. Image pairs represent stereo views with rotation angle of +/- 2° from the central axis.

J. Inherit. Metab. Dis. 28 (2005) 203–227

Acid sphingomyelinase deficiency. Phenotype variability with prevalence of intermediate phenotype in a series of twenty-five Czech and Slovak patients. A multi-approach study

H. PAVLŮ-PEREIRA[1], B. ASFAW[1], H. POUPĚTOVÁ[1], J. LEDVINOVÁ[1], J. SIKORA[1], M. T. VANIER[3], K. SANDHOFF[4], J. ZEMAN[2], Z. NOVOTNÁ[1], D. CHUDOBA[5] and M. ELLEDER[1*]

[1]*Institute of Inherited Metabolic Disorders;* [2]*Department of Pediatrics, Charles University I[st] Faculty of Medicine and University Hospital, Prague, Czech Republic;* [3]*INSERM U189, Lyon-Sud Medical School, and Laboratoire Fondation Gillet Mérieux, Lyon-Sud Hospital, Pierre-Bénite, France;* [4]*Institute of Organic Chemistry and Biochemistry, University of Bonn, Germany;* [5]*Institute of Biology and Medical Genetics, Charles University 2[nd] Faculty of Medicine and University Hospital Motol, Prague, Czech Republic*

[*]*Correspondence: Institute of Inherited Metabolic Disorders, Division B, Bldg. D, Ke Karlovu 2, 128 08 Prague 2, Czech Republic. E-mail: melleder@beba.cesnet.cz*

Summary: A multi-approach study in a series of 25 Czech and Slovak patients with acid sphingomyelinase deficiency revealed a broad phenotypic variability within Niemann–Pick disease types A and B. The clinical manifestation of only 9 patients fulfilled the historical classification: 5 with the rapidly progressive neurovisceral infantile type A and 4 with a slowly progressive visceral type B. Sixteen patients (64%) represented a hitherto scarcely documented 'intermediate type' (IT). Twelve patients showed a protracted neurovisceral course with overt or mild neurological symptoms, three a rapidly progressing fatal visceral affection with rudimentary neurological lesion. One patient died early from a severe visceral disease. The genotype in our patients was represented by 4 frameshift and 14 missense mutations. Six were novel (G166R, R228H, A241V, D251E, D278A, A595fsX601). The Q292K mutation (homoallelic, heteroallelic) was strongly associated with a protracted neurovisceral phenotype (10 of 12 cases). The sphingomyelin loading test in living fibroblasts resulted in total degradation from less than 2% in classical type A to 70–80% in classical type B. In the IT group it ranged from 5% to 49% in a 24 h chase. The liver storage showed three patterns: diffuse, zonal (centrolobular), and discrete submicroscopic. Our series showed a notable variability in both the neurological and visceral lesions as well as in their proportionality and synchrony, and demonstrates a continuum between the historical 'A' and 'B' phenotypes of ASM deficiency. This points to a broad

3.2.8.3 Dvořáková et al. (2006)

Differential diagnostic pitfalls of a slowly progressive lysosomal storage disorder with minute histological changes are demonstrated in the publication by Dvořáková et al. (2006, appended publication #4). This report shows crucial role of implementation of molecular methods into the diagnostic work-up. It also provides new insights into the phenotypic variability of Niemann-Pick disease type C. The discussion related to this article deals primarily with variant adult Niemann-Pick disease type C and its differentiation from ASM deficiency.

The report describes a 53-year-old female patient without significant medical history, who succumbed to cardio-respiratory failure after encountering an attack of pulmonary embolism. The autopsy disclosed previously asymptomatic hepatosplenomegaly and lymphadenopathy. The initial diagnosis proposed by histopathologist was Gaucher disease, and as such, was the case consulted with the Institute of Inherited Metabolic Disorders. The available formaldehyde fixed paraffin embedded (FFPE) tissues were also submitted for further analysis.

The microscopic affection was dominated by the presence of histiocytic foam cells, containing considerable amount of ceroid pigment. Maximum of these cells was found in the lymph nodes and in the liver. The lysosomal system seemed to be morphologically activated (distended) in hepatocytes and neurons, but lysosomal storage was on the verge of detection resolution by means of optical microscopy. The initial diagnostic suggestion of Gaucher disease was rejected on the basis of histopathological changes, i.e. on the basis of absence of Gaucher cells (storage histiocytes with typical cytology). The described changes seemed to correlate with the findings in slowly progressive ASM deficiency (classical NPD type B, see section *3.2*). Unfortunately, FFPE tissues available for analysis hampered in-situ detection of sphingomyelin liquid crystals.

Additional diagnostic step to confirm ASM deficiency would have been the residual activity measurements in the affected proband, but again, no suitable material (leukocyte or fibroblast pellet) was available. ASM activity values assessed in obligate heterozygotes (mother and two children of the proband) were inconclusive. At this point, the only possibility to exclude or confirm ASM deficiency in the proband was to perform DNA analysis of the sequence of the *SMPD1* gene. The sequence analyses were started with high quality DNA obtained from expected obligatory heterozygotes, but rendered wild type *SMPD1* coding

sequence. The analysis of the proband's DNA isolated from FFPE tissues was not undertaken. At this stage, diagnostic considerations shifted into the category of wishful thinking and to previously rejected explanation of the findings by assigning them to extremely rare variant of adult onset visceral form of Niemann-Pick disease type C (NPC).

3.2.8.3.1 Niemann-Pick disease type C (lysosomal storage disorder due to defective intracellular lipid trafficking)

Niemann-Pick disease type C was delineated in the moment when it became obvious that despite phenotypic similarity, complex of changes characterizing this entity does not result from ASM deficiency[162]. In other words, it was demonstrated that lysosomal storage in NPC does not represent generalized sphingomyelinosis (ASM deficiency) even though sphingomyelin is partly accumulated. The lysosomal storage in NPC has specific characteristics in different tissues and cell types, the most extensively affected cell types are monocytes/macrophages and neurons. Spleen and liver (mostly macrophages) accumulate predominantly unesterified cholesterol and sphingomyelin, and a comparably smaller proportion of bis(monoacylglycero) phosphate, and glycolipids (glucosylceramide, lactosylceamide, and GM_3 ganliosides). In neurons, the ratio is reversed with predominance of glycolipids and minute accumulation of unesterified cholesterol and sphingomyelin[154].

The molecular basis for the accumulation of such a mixture of lipid moieties in the late endosomal-lysosomal system represented for a long time a disturbing enigma, especially, when no enzymatic activity deficiency associated with the phenotype. The search for the fundamental molecular defect in NPC culminated in its causative association with one particular gene (*NPC1*)[189]. Soon after the discovery of *NPC1* gene, it became clear that there exists another complementation group in NPC phenotype, resulting in discovery of the second critical gene (*NPC2*)[190]. Despite minor phenotypic differences that surpass the extent of this text, NPC phenotype can be assigned to two functionally complementing critical genes (*NPC1* and *NPC2*) and the deriving proteins[154,191]. The overall ratio of these two complementation groups, perceived by the percentage of variant alleles in NPC patient population, is 95% (*NPC1*) and 5% (*NPC2*). *NPC1* genetic defects thus overwhelmingly predominate.

The discovery of critical genes involved in the pathogenesis of NPC accelerated the understanding of molecular mechanisms involved in pathogenesis of NPC storage phenotype. Findings that both protein products (NPC1 and NPC2) are directly involved in intracellular lipid (especially cholesterol) trafficking and homeostasis provided sound basis for the

previous hypotheses proposed at time of NPC exclusion from ASM deficiency phenotype[192,193]. NPC1 is a multi-transmembrane protein residing in the membranes of a specialized subset of late endosomal-lysosomal compartment (NPC1+/LAMP2+/M6PR-)[5,194]. This specific membrane endowed subcompartment represents extremely dynamic intracellular structure that lively communicates with its cellular partners (especially Golgi apparatus and other constituents of endosomal-lysosomal compartment). NPC1 protein possesses a predicted sterol sensing domain on one of its extra membranous loops[193]. Oversimplified interpretation of the current understanding of the functions of NPC1 protein and NPC1 positive cellular compartment is the regulation of intracellular lipid sorting, trafficking, and targeting. It is not only cholesterol, but also other lipid moieties (e.g. glycolipids) that are regulated by NPC1[194]. NPC1 positive tubulo-vesicular compartment seems to be internally organized in a very complex manner, both temporally and spatially. Neurons, as highly polarized cells, might be given as a good example. Intra axonal NPC1+ system is most probably functioning differently than perinuclear NPC1+ compartment[195-198].

NPC2 protein is, unlike *NPC1* gene, soluble late endosomal-lysosomal luminal protein, functioning in cholesterol binding[192]. The fundamental principle of its function, similar to NPC1 protein, has not yet been fully elucidated. Despite that, it can be postulated that NPC1 and NPC2 proteins function in a non-redundant functional coordination, whether by direct interaction or successive action[199] is not known.

Phenotypic presentation of Niemann-Pick disease type C is very variable. The phenotype almost always includes hepatosplenomegaly and neurological impairment[154,200]. Both these affections vary in intensity. Phenotypic presentations can be subdivided into perinatal (dominated by overt hepatal failure with cholestasis), infantile, classical juvenile and adult forms. For simplification, it is especially the nearly omnipresent neurological affection that adopts extreme phenotypic variability from severe psychomotor retardation in infantile forms to presentation by psychiatric symptoms (e.g. bipolar psychosis) in adult NPC variants. Up to date, only two patients with visceral only NPC without neurological affection, presenting by isolated hepatosplenomegaly in their fourth and sixth decades, were reported[201,202].

The diagnostics of NPC are, in principal, similar to ASM deficiency. Histopathological evaluation might provide initial suspicion by affection of bone marrow macrophages; special emphasis should always be given to the non-generalized sphingomyelin storage and about the histological distribution of accumulated cholesterol. The basis of NPC diagnostics is filipin staining test (increased in NPC) in cultured fibroblasts, and evaluation of

the rate of LDL-derived cholesterol esterification (decreased in NPC)[154]. Delineation of the variant genotype on the DNA sequence level is the final step in the diagnostics. The fact that NPC represents two complementation groups should not be overlooked, despite increased methodological demands. Since the discovery of *NPC1* and *NPC2* genes, considerable amount of data accumulated about different pathogenic variations and genotype-phenotype associations. Genetic counseling and prenatal molecular diagnostics are as important in NPC as in the rest of lysosomal storage diseases.

In order to test the hypothesis that our patient represented third case of the extremely rare visceral only NPC affection in adult age, we resorted to DNA sequence evaluation in the obligate heterozygote relatives. Both *NPC1* and *NPC2* genes were evaluated. Unfortunately, we were not able to perform filipin staining test or characterize the storage pattern in the affected cells. All three evaluated relatives were found to be heterozygous for either previously reported *NPC1* pathogenic variation (S666N) or novel pathogenic variation (N961S). The pathogenity of the novel variation was based on similar premises as described for *SMPD1* variations (see section *3.2.8.1*). Both variations were also found in the proband's *NPC1* DNA sequence isolated from FFPE tissues. Methodological details are described in the appended publication #4.

These results allowed us to conclude that this patient suffered from visceral only NPC without manifest neurological affection at the age of 53 years. Neuropathologic evaluation demonstrated neither the lysosomal storage changes nor other neuropathologic epiphenomena characteristic for NPC (neurofibrillary tangles, neuroaxonal dystrophy)[154]. We can only hypothesize about the possibility of later appearance of neurological affection in this patient. The report points to the fact that such minute NPC affection in adults might be easily missed and similar cases may be under- or misdiagnosed. As new therapeutic approaches (e.g. glycolipid deprivation by N-butyldeoxynojirimycin)[203] are entering therapeutic practice, improper diagnosis might result in patient maltreatment.

JIMD Short Report #009 (2006) Online
DOI 10.1007/s10545-006-0330-z

SHORT REPORT

Subclinical course of adult visceral Niemann–Pick type C1 disease. A rare or underdiagnosed disorder?

L. Dvorakova · J. Sikora · M. Hrebicek · H. Hulkova · M. Bouckova · L. Stolnaja · M. Elleder

Received: 13 January 2006 / Accepted: 8 May 2006

Summary We present the third case of Niemann–Pick disease type C without neurological symptoms. The patient was a 53-year-old woman without significant prior health problems who died of acute pulmonary embolism. Autopsy findings of hepatosplenomegaly, lymphadenopathy and ceroid-rich foam cells raised the suspicion of the visceral form of acid sphingomyelinase deficiency (Niemann–Pick disease type B; NPB) or a much rarer disorder, variant adult visceral form of Niemann–Pick disease type C (NPC). To verify the histopathological findings, *SMPD1*, *NPC1* and *NPC2* genes were analysed. Two novel sequence variants, c.1997G > A (S666N) and c.2882A > G (N961S) were detected in the *NPC1* gene. No pathogenic sequence variants were found either in the *SMPD1* gene mutated in NPB or in *NPC2* gene. The pathogenicity of both *NPC1* variants was supported by their location in regions important for the protein function. Both variations were not found in more than 300 control alleles. Identified sequence variations confirm the diagnosis of the extremely rare adult visceral form of Niemann–Pick disease type C, which is otherwise dominated by neurovisceral symptoms. Although only three patients have been reported, this (most probably underdiagnosed) form of NPC should be considered in differential diagnosis of isolated hepatosplenomegaly with foam cells in adulthood.

Communicating Editor: Robert Steiner

Competing interests: None declared

References to electronic databases: OMIM (http://www.ncbi.nlm.nih.gov/): Niemann–Pick disease, type C1 #257220; Niemann–Pick disease, type C2 #607625; Niemann Pick disease type A/B #257200, #607616; Gaucher disease, type I #230800. GenBank reference sequences (http://www.ncbi.nlm.nih.gov/), accession numbers: *SMPD1*, NC_000011.8 REGION: 6368302..6372783; *NPC1*, NC_000018.8, REGION: complement (19365461..19420426); *NPC2 (HE1)*, NC_000014.7, REGION: complement(74016397..74029837). Uniprot database (http://www.expasy.uniprot.org/). The National Center for Biotechnology Information (http://www.ncbi.nlm.nih.gov/). Databases used for SNP analysis: GenBank (http://www.ncbi.nlm.nih.gov/), Ensembl (http://www.ensembl.org/), HGVD (http://hgvbase.cgb.ki.se/).

Enzymes: SMPD1 (EC 3.1.4.12), HMG CoA reductase (EC 1.1.1.88)

L. Dvorakova · J. Sikora · M. Hrebicek · H. Hulkova · M. Bouckova · L. Stolnaja · M. Elleder (✉)
Institute of Inherited Metabolic Disorders, Charles University, First Faculty of Medicine and University Hospital, Prague, Czech Republic.
e-mail: melleder@beba.cesnet.cz

Abbreviations

FFPE	formalin fixed paraffin-embedded
LDL	low-density lipoprotein
NP A/B	Niemann–Pick disease type A/B
NPB	Niemann–Pick disease type B
NPC	Niemann–Pick disease type C
PCR	polymerase chain reaction
RFLP	restriction fragment length polymorphism
SSD	sterol sensing domain

Introduction

Niemann–Pick disease type C (NPC; OMIM 257220, 607625) is an autosomal recessive lysosomal disorder caused by deregulation of the cellular lipid trafficking due to the molecular defects in either of the two late endosomal/lysosomal proteins (NPC1 and NPC2). NPC1, a transmembrane protein localized in a subset of late endosomes, is endowed with a sterol sensing domain exerting control of cholesterol content of late endosomal membranes (Liscum and Sturley [illegible]ss cholesterol is translocated for

4 Bioinformatic predictive study of acetyl-coenzyme A:α-glucosaminide N-acetyltransferase - appended publication #5 – Hřebíček et al. (2006)

Publication by Hřebíček et al. (2006, appended publication #5) describes a genetic linkage analysis performed in several families affected by mucopolysacccharidosis type IIIc (Sanfilippo type C syndrome, MPS IIIc, for introductory notes see sections *1.1* and *1.2*). The main conclusion of the study is that MPS IIIc results from pathogenic variations in the gene designated *TMEM.76*, located in the pericentric region of chromosome 8. The study employed genetic linkage disequilibrium estimate employing LOD scores for the critical chromosomal regions assignments (for details see appended publication #5). Noteworthy is the fact that in parallel with the release of these results another group published identical data, which were achieved by completely different methods based on proteomic analysis[11]. This publication denoted the critical *TMEM.76* gene as *HGSNAT* (heparin acetyl-coenzyme A:α-glucosaminide N-acetyltransferase), this designation is an official gene name. Assignment of a coding gene to the previously described enzymatic deficiency in case of MPSIIIc finished the gene discovery phase among defined lysosomal enzymopathies.

The HGSNAT protein (663 amino acids, 73 kD), which displays considerable degree of instability under *in-vitro* conditions, was previously demonstrated to reside in the DRMs of lysosomal membranes[13]. HGSNAT primary function is to transfer acetyl moiety to heparan sulfate and render it available for consecutive intralysosomal degradation by α-N-acetyl glucosaminidase. Deficiency in this, otherwise synthetic, step (acetylation) results in the accumulation of heparan sulfate in the lysosomal compartment. The molecular mechanisms of HGSNAT catalytic function are still not understood, as their explanation was hampered by the absence of knowledge of HGSNAT primary structure. Two different hypotheses exist about the issue of transmembrane transfer of acetyl-CoA with additional acetylation of heparan sulfate inside the lysosomes. One of the hypotheses suggests a *ping-pong* mechanism[204], by which the acetylation of the HGSNAT protein results in the conformation change and transmembrane transfer of acetyl-CoA intralysosomally with consecutive transfer to heparan sulfate. The other hypothesis suggests a formation of a transient tertiary complex formed by the HGSNAT protein, acetyl-CoA and heparan sulfate[205].

The immense growth of the genomic information in the last decades due to availability of efficient and high throughput methods of nucleic acids analyses, which was not paralleled

by a comparable rate of acquisition of proteomic or cell biological data, resulted in the expansion of bioinformatic tools employing the "sequence domain" to predict protein properties and their cellular functions[206]. Some of these methods were used for HGSNAT protein in the mentioned publication and shall be discussed in this text.

Computational algorithms generally used to disclose evolutionary relations among sequences (e.g. BLASTN or BLASTP) provided very surprising results. The only confirmed protein (both by genomic and proteomic means) present in the available public databases was murine ortholog of human HGSNAT. No other confirmed othologous protein or cDNA sequence is available at the moment, although HGSNAT is predicted in nearly all available animal genomes. The only other proteins homologous to HGSNAT belong to COG4299 bacterial protein family (uncharacterized), a cohort of protein predictions from a broad range of bacteria. Functions of these proteins are only inferred, but their roles in transmembrane acetylation and glycosaminoglycans metabolism cannot be excluded. The issue of complex polysaccharide acetylation of prokaryotic cell walls is tempting and will definitely be further studied.

The extent of evolutionary conservation can be demonstrated by comparative sequence alignments (as presented in the appended publication #5). With respect to the above mentioned absence of available experimentally confirmed sequences, the presented alignment utilized sequence predictions, even though reliable. Additional approach that is capable to document evolutionary conservation is based on the use of available genomic DNA data that are fully experimental and thus not based on prediction. These methods allow alignments of long (in order of tens of kb to Mbs) DNA sequences to evaluate the extent of similarity among them. Several computational algorithms are available at the moment; the two most widely used are VISTA and PIPMaker functioning as www interfaces[207,208]. The results of multiple VISTA alignment of chromosomal regions syntenic to human chromosome 8, carrying *HGSNAT* gene, are shown on Figure 2. The major advantage of this kind of sequence comparison lies in its capability to efficiently predict conserved non-coding sequence stretches (functionally important, CNS) in the syntenic DNA sequences. Figure 2 depicts considerable evolutionary conservation of the coding (exonic) sequence in the *HGSNAT* locus, besides that, it shows CNS regions that might be involved in either expression, RNA splicing or other regulations. The information on CNS gathered in this alignment is going to be further tested experimentally.

In order to evaluate previously proposed transmembrane (TM) nature of HGSNAT protein, its primary sequence was searched for membrane spanning domains using TMMOD algorithm[209]. The resultant prediction suggests 11 TM domains. The critical issue of TM orientation (cytosolic vs. non-cytosolic) was addressed, and assigned the C-terminal end of the protein to face the cytosol. For the orientation of the TM domains refer to Figure 3.
In addition, an attempt was made to predict posttranslational modifications (PTM) using an integrated www interface[210]. HGSNAT primary sequence was evaluated for the presence of potential signal peptide (SignalIP, see Figure 3) and N-linked glycosylation sites (NetNGlyc). As demonstated on Figure 3, there are at least four potential N-glycosylation sites present in the protein sequence, all four sites are predicted to face lysosomal lumen, which is a finding in accordance with the concepts of lysosomal membrane protein properties. N-terminal acetylation was not predicted as probable by NetAcet, which is definitely a result to reconsider. Predictions of O-linked glycosylation patterns or phosphorylation sites did not provide results that would allow their further use.

The presented results demonstrate advantageous use of bioinformatic approaches to predict protein structure, PTMs and function, even though the only available data is the primary protein sequence and the number of homologous genes is small, and there are no structural data available for homology modeling. The implementation of these methods prior to "wet" experimental work allows establishing more focused and concise hypotheses (i.e. design of immunizing peptides for antibody production, etc.).

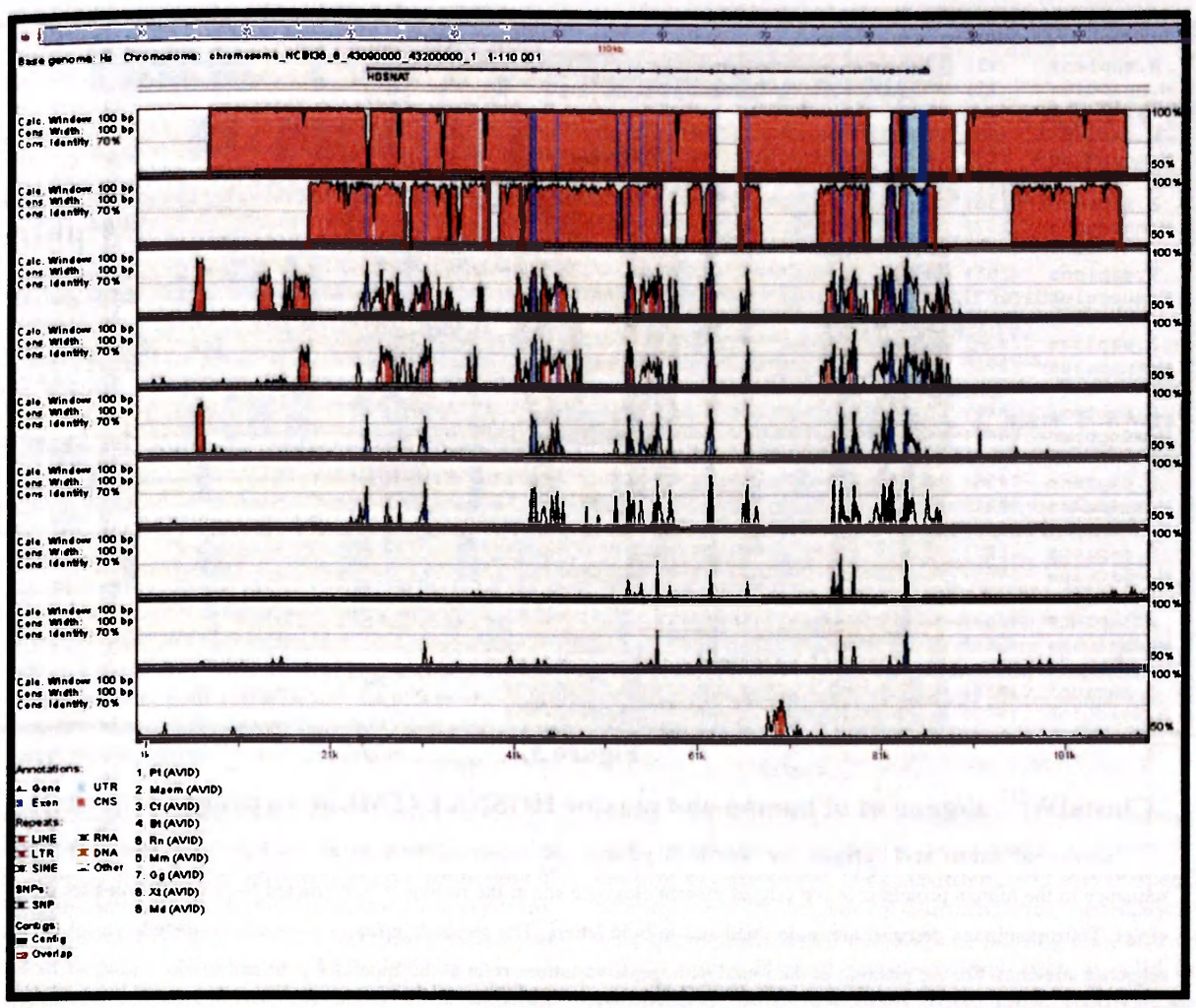

Figure 2

Syntenic alignment of appropriate *HGSNAT* chromosomal regions

Alignment of multiple syntenic sequences of the critical pericentric region of chromosome 8, annotation based on Ensemble database[211]. The alignment was performed using mVISTA algorithm provided by Berkeley genome pipeline[208]. The aligned sequences are listed below the image and follow the order given (top line represents human *HGSNAT* gene with annotated 5′- 3′ orientation, Pt - *Pan troglodytes*, Macm - *Macaca mulatta*, Cf - *Canis familiaris*, Bt - *Bos taurus*, Rn - *Ratus norvegicus*, Mm – *Mus musculus*, Gg - *Gallus gallus*, Xt - *Xenopus tropicalis*, Md – *Monodelphis domestica*). The length of the aligned sequences ranged from 27 to 97 kb.

The conserved exonic sequences are depicted in light blue, coding non-conserved sequences (CNS) are shown in pink. Exon sequences are generally conserved from humans to frog (*Xenopus tropicalis*). Regions of CNS are located in the promoter regions, of note are CNS sequences in the vicinity of alternatively spliced exons 9 and 10 (for details see appended publication #5). For the details about the alignment construction see text.

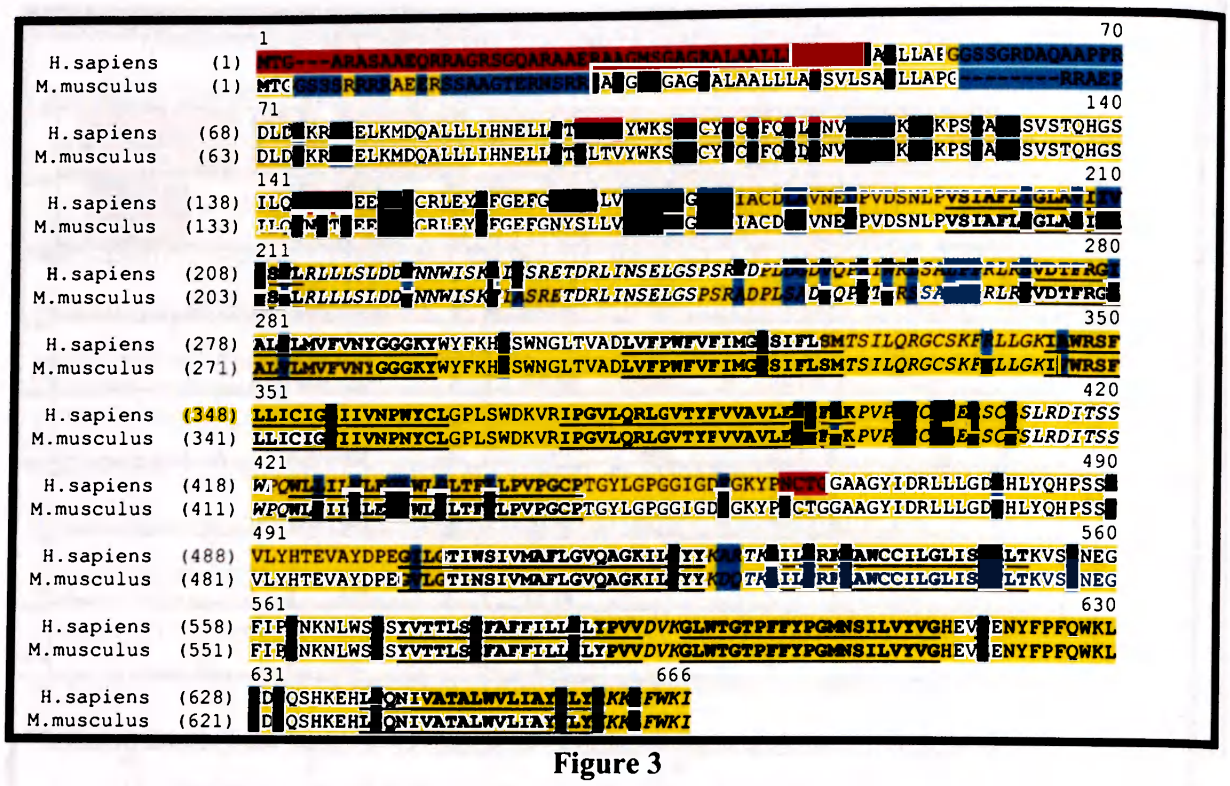

Figure 3

ClustalW[212] alignment of human and murine HGSNAT (TMEM76) protein sequences.

Conserved amino acid residues are shown in yellow, non-conserved residues are in light blue. Predicted signal sequence in the human protein is in red (signal protein cleavage site at the residue 47). Predicted N-glycosylation sites are in violet. Transmembrane domains are underlined and in bold letters. The residues in *italics* represent predicted cytosol facing sequence stretches. For the position of the found pathogenic variations refer to the appended publication #5.

Appended publication

ARTICLE

Mutations in *TMEM76** Cause Mucopolysaccharidosis IIIC (Sanfilippo C Syndrome)

Martin Hřebíček, Lenka Mrázová, Volkan Seyrantepe, Stéphanie Durand, Nicole M. Roslin, Lenka Nosková, Hana Hartmannová, Robert Ivánek, Alena Čížková, Helena Poupětová, Jakub Sikora, Jana Uřinovská, Viktor Stránecký, Jiří Zeman, Pierre Lepage, David Roquis, Andrei Verner, Jérôme Ausseil, Clare E. Beesley, Irène Maire, Ben J. H. M. Poorthuis, Jiddeke van de Kamp, Otto P. van Diggelen, Ron A. Wevers, Thomas J. Hudson, T. Mary Fujiwara, Jacek Majewski, Kenneth Morgan, Stanislav Kmoch,† and Alexey V. Pshezhetsky

Mucopolysaccharidosis IIIC (MPS IIIC, or Sanfilippo C syndrome) is a lysosomal storage disorder caused by the inherited deficiency of the lysosomal membrane enzyme acetyl–coenzyme A:α-glucosaminide *N*-acetyltransferase (*N*-acetyltransferase), which leads to impaired degradation of heparan sulfate. We report the narrowing of the candidate region to a 2.6-cM interval between *D8S1051* and *D8S1831* and the identification of the transmembrane protein 76 gene (*TMEM76*), which encodes a 73-kDa protein with predicted multiple transmembrane domains and glycosylation sites, as the gene that causes MPS IIIC when it is mutated. Four nonsense mutations, 3 frameshift mutations due to deletions or a duplication, 6 splice-site mutations, and 14 missense mutations were identified among 30 probands with MPS IIIC. Functional expression of human *TMEM76* and the mouse ortholog demonstrates that it is the gene that encodes the lysosomal *N*-acetyltransferase and suggests that this enzyme belongs to a new structural class of proteins that transport the activated acetyl residues across the cell membrane.

Heparan sulfate is a polysaccharide found in proteoglycans associated with the cell membrane in nearly all cells. The lysosomal membrane enzyme, acetyl–coenzyme A (CoA):α-glucosaminide *N*-acetyltransferase (*N*-acetyltransferase) is required to *N*-acetylate the terminal glucosamine residues of heparan sulfate before hydrolysis by the α-*N*-acetyl glucosaminidase. Since the acetyl-CoA substrate would be rapidly degraded in the lysosome,[1] *N*-acetyltransferase employs a unique mechanism, acting both as an enzyme and a membrane channel, and catalyzes the transmembrane acetylation of heparan sulfate.[2] The mechanism by which this is achieved has been the topic of considerable investigation, but, for many years, the isolation and cloning of *N*-acetyltransferase has been hampered by its low tissue content, instability, and hydrophobic nature.[3–5]

Genetic deficiency of *N*-acetyltransferase causes mucopolysaccharidosis IIIC (MPS IIIC [MIM 252930], or Sanfilippo syndrome C), a rare autosomal recessive lysosomal disorder of mucopolysaccharide catabolism.[6–8] MPS IIIC is clinically similar to other subtypes of Sanfilippo syndrome.[9] Patients manifest symptoms during childhood with progressive and severe neurological deterioration causing hyperactivity, sleep disorders, and loss of speech accompanied by behavioral abnormalities, neuropsychiatric problems, mental retardation, hearing loss, and relatively minor visceral manifestations, such as mild hepatomegaly, mild dwarfism with joint stiffness and biconvex dorsolumbar vertebral bodies, mild coarse faces, and hypertrichosis.[7] Most patients die before adulthood, but some survive to the 4th decade and show progressive dementia and retinitis pigmentosa. Soon after the first 3 patients with MPS IIIC were described by Kresse et al.,[6] Klein et al.[8,10] reported a similar deficiency in 11 patients who had received the diagnosis of Sanfilippo syndrome, therefore suggesting that the disease is a relatively frequent subtype. The birth prevalence of MPS IIIC in Australia,[11] Portugal,[12] and the Netherlands[13] has been estimated to be 0.07, 0.12, and 0.21 per 100,000, respectively.

The putative chromosomal locus of the MPS IIIC gene was first reported in 1992. By studying two siblings who received the diagnosis of MPS IIIC and had an apparently

From the Institute for Inherited Metabolic Disorders (M.H.; L.M.; L.N.; H.H.; R.I.; A.Č.; H.P.; J.S.; J.U.; V. Stránecký; J.Z.; S.K.) and Center for Applied Genomics (R.I.; A.Č.; V. Stránecký; J.Z.; S.K.), Charles University 1st School of Medicine, and Institute of Molecular Genetics, Academy of Sciences of the Czech Republic (R.I.), Prague; Hôpital Sainte-Justine and Départements de Pédiatrie (V. Seyrantepe; S.D.; J.A.; A.V.P) and Biochimie (A.V.P), Université de Montréal, and Research Institute of the McGill University Health Centre (N.M.R.; T.J.H.; T.M.F.; K.M.), McGill University and Genome Quebec Innovation Centre (P.L.; D.R.; A.V.; T.J.H.; J.M.), and Departments of Human Genetics (T.J.H.; T.M.F.; J.M.; K.M.), Medicine (T.J.H.; T.M.F.; K.M.), and Anatomy and Cell Biology (A.V.P.), McGill University, Montreal; Biochemistry, Endocrinology & Metabolism Unit, UCL Institute of Child Health, London (C.E.B.); Hôpital Debrousse, Lyon, France (I.M.); Department of Medical Biochemistry, Academic Medical Center UVA (B.J.H.M.P.), and Department of Clinical Genetics, VU University Medical Center (J v.d.K.), Amsterdam; Department of Clinical Genetics, Erasmus University Medical Center, Rotterdam, The Netherlands (O.P.v.D.); and Laboratory of Pediatrics and Neurology, University Medical Center, Nijmegen, The Netherlands (R.A.W.)

Received June 8, 2006; accepted for publication August 8, 2006; electronically published September 8, 2006.

Address for correspondence and reprints: Dr. Alexey V. Pshezhetsky, Service de Génétique Médicale, Hôpital Sainte-Justine, 3175 Côte Sainte-Catherine, Montreal, Quebec H3T 1CS, Canada. E-mail: alexei.pchejetski@umontreal.ca

* Footnote added in proof: the gene name has been changed to *HGSNAT*.

† S.K. has led the Prague team.

Am. J. Hum. Genet. 2006;79:000–000. 0002-9297/2006/7905-00XX$15.00

5 *Caenorhabditis elegans* as a model organism for selected lysosomal storage diseases

There are numerous animal models available for the lysosomal storage disorders. Some of them are naturally occurring variants, but a considerable number of them were prepared *in-vitro* by different genetic manipulations. In general, mammalian species are advantageous for the study of human pathology states, but there are several well established non-mammalian model organisms available as well. Nematode *Caenorhabditis elegans* (*C. elegans*) is one of these. The most general criterion evaluating the quality of the animal model is the extent and complexity by which the model reflects the studied biological phenomenon. Fundamental genetic background similarity between the model and the subject should be achieved. More extensive the evolutionary-genomic-proteomic conservation, more representative the model is. Unfortunately, the criterion of biological-evolutionary similarity has its limits with respect to laboratory utilization. Some of the limiting factors are related to the ease of genetic manipulation, life or reproductive cycle duration, genetic variation transmissibility, physical ease of animal maintenance, ethical issues of study protocols or related financial costs.

C. elegans is a respected model organism for concerted genetic, ultrastructural and behavioral studies[213]. *C.elegans* was the first of complex multicellular eukaryotic organisms for which the complete genomic sequence became known. About thirty-six percent of the genes are homologous to human genes, including those implicated in human pathology[214,215]. *C. elegans* is easily maintained in the laboratory and enables straightforward genetic manipulation. RNA-mediated interference (RNAi) technique allows inhibition of *C. elegans* genes expression at the level of the whole organism with the ease unavailable in any other eukaryotic organism[216,217]. The immense contribution of the use of *C. elegans* to biomedical research is a generally accepted fact which has already been twice reflected by awarding the Nobel Prize for Physiology and Medicine to five key *C. elegans* investigators in the years 2002 and 2006.

5.1 C. elegans, general characteristics

C. elegans is a small (~1 mm long), translucent, soil nematode feeding primarily on bacteria and reproducing with a life cycle of about 3 days. The mature hermaphrodite adult is

fertile for about 4 days and has a life span of about 17 days after reaching adulthood. *C. elegans* has five holocentric autosomes and a sex chromosome (X). Sex is determined chromosomally, depending on the X/autosomal ratio. Hermaphrodites are diploid for both autosomes and the X chromosome (XX), while the males have only one copy of the X chromosome. Males arise spontaneously by non-disjunction during meiosis in hermaphrodites with frequency of about 1:500 worms[213,218]. The fundamentals of *C. elegans* genetics were established by Sydney Brenner in the 1970s and are valid up to now[219]. Very efficient transgenic techniques have been developed for *C. elegans*. It is fairly easy to follow the expression of transgenes (GFP or X-Gal linked), single cell ablations can be performed very efficiently[220] and the laboratory maintenance of the nematode cultures is also easy and does not require any substantial financial investment. The complete cellular anatomy of *C. elegans* was characterized in the last two decades, including complex cellular systems such as the whole neural network[213]. *C. elegans* has invariant number of cells (adult hermaphrodite has 959 somatic cells; the adult male has 1031 cells). The lineage of each single cell during development was precisely characterized. Detailed ultrastructural data, including 3D electron microscopic atlases are available to the *C. elegans* research community.

It is for these reasons that *C. elegans* can be considered a valuable model for higher organisms despite its evolutionary position.

5.1.1 *C. elegans* genome, tool for biomedical research

The sequence of the complete *C. elegans* genome, including 15kb of mitochondrial DNA, was determined and assembled by the concerted efforts of the *C. elegans* sequencing consortium[215]. Since the year of its release (1998) genomic data have been continuously updated. The 97 Mb genome is very compact with an average density of one gene per 5kb. It is predicted to contain only 27% of intronic sequences. *C. elegans* genome includes, at the present time (January 2007) 7821 confirmed genes, 10741 partially confirmed genes, and 4650 predicted ORFs. Complete annotated genomic sequence of *C. elegans* is freely available via www database[221] (Wormbase, curated by European Bioinformatic Institute in Hinxton, UK). This database integrates genomic data with available EST (expressed sequence tags), OST (ORF sequence tag), micro array and RNA expression data, pangenomic RNAi experimental data, and available deletion mutants created by *C.elegans* gene knock-out consortium[222]. It also allows the use of additional bioinformatic tools including phylogenetic

homology searches and others. It is definitely an ultimate bioinformatic resource for *C. elegans* related research.

There are more protein similarities between *C. elegans* and *H. sapiens* than with any other multicellular organism (with the exception of other nematodes, typically *Caenorhabditis brigssae*), with the average predicted protein similarity of 36%. Many conserved genes, exhibit immense conservation, in some proteins as high as 97 %[215,223].

The identification and comparison of orthologs of human proteins in the nematode shows interesting clues as to the respective functions of proteins in the two species. The surprising conservation of core cell biological processes thus permits to work on different organisms in parallel and to transfer the results from the model organism to the subject organism. This approach employing simplified models has gained respect especially as the hypothesis driven research in the higher organisms has, in certain aspects, reached its limits.

5.1.2 RNA-mediated interference

In *C. elegans*, the introduction of double-stranded RNA (dsRNA) results in the specific and potent inactivation of genes containing homologous sequences[216,217]. Gene-specific loss-of-function results from the degradation of endogenous mRNA by a set of consecutive molecular steps. RNAi molecular machinery is evolutionary conserved pathway, and as such can be also experimentally used in higher organisms[224]. DsRNA-mediated interference in *C. elegans* is transmitted to the progeny of F1 generation and possibly even to further generations[225]. DsRNA shows a surprising ability to cross cellular boundaries. Studies involving RNAi have shown that it is possible to initiate RNAi by injection of dsRNA, however, as the RNA can be absorbed through the nematode's gut, the effect was also observed in animals soaked in dsRNA solution and also in worms fed with Escherichia coli expressing double-stranded RNA[226]. *C. elegans* is unique in comparison to mammalian cells by the capacity to be affected by long dsRNA, increasing RNAi capacity. Not surprisingly, RNAi was quickly embraced as a tool for determining the functions of specific genes not only in *C. elegans*, despite minor contribution of "off target" effects[227]. Fundamental findings involving the mechanisms of RNAi were awarded by Nobel Prize in the year 2006 (see above).

5.1.3 Endosomal - lysosomal system in *C. elegans*

The protein constituents of the cellular system involved in endocytosis, sorting, transport, substrate degradation and redistribution are well conserved in *C. elegans* in comparison to higher organisms, including man. The basic concept that every eukaryotic cell is capable of endocytosis and exocytosis is also valid in *C.elegans*. The extent of conservation of proteins participating in the constitution of the endosomal-lysosomal system is broad; some of the structural proteins such as clathrin subunits or coatomer proteins are virtually identical with their mammalian orthologs. Table 1 lists selected proteins participating in the function of endosomal-lysosomal system and their potential orthologs found by BLASTP algorithm in the *C. elegans* genome, the evaluated parameter being the expectancy value (*e- value*). The selected proteins are sorted into two groups: (i) proteins with a defined lysosomal storage phenotype and their potential *C. elegans* orthologs; (ii) basic structural constituents of the endosomal-lysosomal system. As can be seen, the degree of conservation is variable for different proteins, most probably reflecting the nematode's metabolic demands. The conclusion that can be drawn from this simple bioinformatic experiment is that *C. elegans* may serve as a good model organism for this particular cell biological field because the protein machinery is well conserved. The answer that cannot be concluded by these methods is, for example, the spectrum of utilized substrates or differences in preferred metabolic pathways.

C. elegans has already been utilized in numerous works dealing with issues regarding basic endosomal-lysosomal system functioning[220-232]. *C. elegans* has also been repetitively used as a good model organism for different human pathology states, metabolic disorders and lysosomal storage disorders included[214,233]. The main advantage of C. elegans in comparison to cell cultures is the possibility to evaluate complex organismal regulations, not only isolated cellular processes.

C. elegans was used in modeling of Niemann-Pick disease type C[234] or neuronal ceroid lipofuscinosis type 3[235]. *C. elegans* was demonstrated to have two types of acid sphingomyelinase[236], and it to possess defined cathepsin D[237] or LAMP/CD68[238] like proteins. Pioneering character can be assigned to the works on *cup-5*[239-243], *C. elegans* ortholog of mucolipin-1, a protein that is defective in mucolipidosis type IV (see *1.2*). The knowledge attained in *C. elegans* directly influenced biological considerations for the function of the human ortholog. It should be stressed that all the listed publications evaluated non-catalytic late endosomal or lysosomal proteins, and thus the experimental pathology was not

attributable to enzyme activity deficiency. In other words, no classical lysosomal enzymopathy was modeled in *C. elegans* besides Fabry and Schindler diseases as is described in the appended publication #6.

LSD	**Variant human protein**	***e-value*** **(expectancy)**	***C. elegans*** **ORF**	***C. elegans*** **gene**
Fabry disease	alpha galactosidase	2,3e -87	R07B7.11	*gana-1*
Farber disease	acid ceramidase	2,1e -84	HK11D2.2	
Gaucher disease	beta glucocerebrosidase	1,2e -106	Y4C6B.6	
GM1 gangliosiosis	beta galactosidase	5,6e -116	T19B10.3	
Tay-Sachs disease	alpha hexosaminidase	2,6e -95	T14F9.3	
Sandhoff disease	beta hexosaminidase	9,1e -84	T14F9.3	
Krabbe disease	galactosylceramidase	2,1e -47	C29E4.10	
Metachromatic leukodystrophy	arylsulfatase A	1,5e -43	D1014.1	
Mucolipidosis IV	mucolipin	1,2e -79	R13A5.1	*cup-5*
Niemann-Pick disease A,B	acid sphingomyelinase	2,0e -86	B0252.2	*asm-1, asm-2*
Schindler disease	N-acetylgalactosaminidase	3,7e -87	R07B7.11	*gana-1*
Aspartylglycosaminuria	aspartylglycosaminidase	1,7e -68	R04B3.2	
Fucosidosis	alpha fucosidase	2,9e -96	W03G11.3	
Galctosialidosis	cathepsin A	8,1e -92	F41C3.5	
alfa- mannosidosis	alpha mannosidase	1,1e -157	F55G10.1	
beta-mannosidosis	beta mannosidase	5,8e -150	C33G3.4	
MPSII	iduronate 2 sulfatase	2,7e -07	D1014.1	
MPSVI	arylsulfatase B	4,6e -18	D1014.1	
MPSIVA	galactosamin sulfate sulfatase	5,9e -26	D1014.1	
MPSIIIA	sulfamidase	2,5e -07	D1014.1	
MPSIIIB	alpha N-acetyl glucosaminidase	4,5e -98	K09E4.4	
MPSIIID	N-acetylglucosamin sulfatase	2,3e -91	K09C4.8	
MPSVII	beta glucuronidase	6,1e -114	Y105E8B.TT	
Pompe disease	alpha glucosidase	2,7e -134	D2096.3	
Wolman disease	acid lipase	3,2e -81	Y57E12B.B	
cystinosis	solute carrier family 3 member 1	2,0e -36	F2D10.9	
sialic acid storage disease	solute carrier family 17 member 5	2,1e -100	C38C10.2	
NCL1	palmitoyl-thioesterase 1	1,2E -81	F44C4.5	
NCL3	CLN3 protein	7,6e -80	F07B10.1	*cln-3.1, cln-3.2, cln-3.3*
congenital NCL	cathepsin D	1.5e -108	R12H7.2	*cad-1*
Niemann-Pick C1	NPC1 protein	8,7e -87	F02E8.6	*lmp-1*
prosaposin deficiency	prosaposin	3,2e -09	C28C12.7	
Structural protein	**subunit**	***e-value*** **(expectancy)**	***C. elegans*** **ORF**	
rab4 A		7,2e - 59	K09A9.2	
rab4B		1,8e - 60	K09A9.2	
rab5A		3,1e - 83	F26H9.5	
rab7		3,3e - 78	W03C9.3	
rab9		3,1e - 51	W03C9.3	
rab5B		2,4e - 83	F26H9.5	
LAMP1		7,8e - 08	C05D9.2	
LAMP2		7,2e - 06	C05D9.2	
coatomer proteins	A	0	Y71F9AL.17	
	B	0	F38E11.5	
	E	3,8e - 46	F45G2.4	
	D	4,e - 128	C13B9.3	
	Z	5,2e - 49	F59E10.3	
	G2	8,e - 262	T14G10.5	
	B2	0	F38E11.5	
	G	8,9e - 260	T14G10.5	
clathrin protein	CLTA	1,9e - 09	T05B11.3	
	CLTB	1,2e -06	T05B11.3	
	CLH1	0	T20G5.1	
	CLH2	0	T20G5.1	

Table 1

List of selected human proteins involved in pathogenesis of lysosomal storage diseases or functioning in endosomal-lysosomal system.

C. elegans orthologs found by BLASTP algorithm in the nematode's ORF database. The value of expectancy (*e-value*) in principle represents the probability that BLASTP result represents a random positive hit directly related to the size of the database. In other words, smaller the *e-value* (closer to zero) higher the probability that the two sequences are non-randomly related. Expectancy values are given in the order of 10 to the minus value given in the table.

Note near identity of certain structural proteins and near random relation for others (prosaposin, sulfamidase or iduronate–2-sulfatase). The example of prosaposin demonstrates the potential drawback of similarity thresholding algorithms, *C. elegans* most probably possesses pSap ortholog, but it must be disclosed on the level of secondary protein structure.

5.2 *Comments and discussion to the appended publication #6 - Hujová, Sikora, Dobrovolný et al. (2005)*

The appended publication by Hujová, Sikora, Dobrovolný et al. (2005, equal contributors) describes the use of *C.elegans* in delineation of biochemical and molecular aspects of evolution of human lysosomal enzymes degrading moieties with terminal α-galactose and α-N- acetylgalactosamine. The respective enzymes are lysosomal α-galactosidase (α-GAL) and α-N-acetylgalactosaminidase (α-NAGA). Both α-GAL and α-NAGA belong to the melibiase protein family (glycoside hydrolase family 27, clan D), and they represent true paralogs (genes evolving from a common ancestral gene by multiplication, paralogs often posses similar, but distinct functions)[244]. The overall similarity between α-GAL and α-NAGA is extensive. The evolutionary concept of protein duplication and additional functional divergence has been previously proposed, but never unambiguously demonstrated[245,246].

Enzymatic properties of both proteins, including substrate specificities, further support the theory of common evolutionary origin. α-GAL is active against substrates containing terminal α-galactose, while α-NAGA is participating in intralysosomal degradation of glycoconjugates containing terminal α-N- acetylgalactosaminoyl(α-galNAc) but partially also against moieties with terminal α-galactose[247].

Both enzymes are soluble lysosomal hydrolases with acid pH optima targeted to lysosomes by mannose-6-phosphate receptor mediated pathway. Hereditary deficiency of either α-GAL or α-NAGA activity results in Fabry or Schindler (or Kanzaki) diseases, respectively[245,246]. Both these disorders represent distinct lysosomal storage entities with

different phenotypic presentation. Whereas Fabry disease can be designated as the only lysosomal storage disorder with adult onset, Schindler disease is defined as typically infant-age onset lysosomal storage disorder. Hypotheses addressing this intriguing phenotypic discrepancy suggest partial contribution of α-NAGA activity to degradation of α-galactose conjugates. Biological material accumulating in α-GAL deficiency is almost exclusively GB_3 ceramide in comparison to α-NAGA deficiency which results in the predominant storage of α-galNAc bearing glycoproteins.

Simple preliminary BLAST search[248] for *C. elegans* orthologs of human α-GAL and α-NAGA, revealed only a single ORF with comparable *e-values* (for details see appended publication #6 or Table 1).This ORF (R0B7.11), later designated as *gana-1* (α-GAL and α-NAGA ortholog) is the only ortholog of these two genes in the nematode's genome.

The goal of the study was to evaluate and characterize *gana-1* evolutionary relations to α-GAL and α-NAGA as well as its functional properties in order to demonstrate that this single *C. elegans* ortholog adopts functions of both human (vertebrate) proteins. Following discussion briefly comments the appended publication.

5.2.1 *gana-1* evolutionary context

Prior to all experimental work *gana-1* gene structure was evaluated, both on the level of genomic DNA and cDNA (RNA), the *in-silico* prediction was confirmed by experimental data. Further bioinformatic studies (multiple alignments, evolutionary tree construction, or homology modeling) were thus based on validated data.

Multiple protein sequence alignment with other members of melibiase protein family disclosed extensive similarity among the aligned sequences and clearly delineated plant sequences from their animal counterparts. The alignment similarity evaluated by sequence position conservation was not restricted to the predicted active site but was present throughout the whole sequence alignment. The successive evolutionary tree construction based on the multiple protein alignment was performed by three different algorithms based on maximum parsimony, nearest neighbor estimate or maximum likelihood statistical approaches[249] (for details see the appended publication #6). We used multiple bootstrapped tree analysis to construct the final evolutionary trees. These three different methods rendered very similar results: (i) gana-1 protein was always positioned between animal and plant sequences; (ii) it was located very close (closest) to primary tree node (animal vs. plant), suggesting its lowest

evolutionary position among the evaluated animal sequences; (iii) when it was included into one of the sequence clusters (GALs vs. NAGAs), it was always among α-NAGAs, a fact that corresponded well with its further defined characteristics. It is necessary to note, that the algorithms used did not employ molecular clock estimate. So, the length of the cladogram branches does not correspond with the time axis evolution difference. The constructed evolutionary models suggest that *gana-1* represents an ancestor of vertebrate GALs and NAGAs.

Following bioinformatic step was the construction of a structural model of gana-1 protein based on the on the crystal structures of rice and human α-GAL using homology modeling approaches. Our predicted structure suggests two-domain organization with homodimeric tertiary organization. The active site and the N-acetyl recognition loop of gana-1, as it was modeled, adopted a structure more similar to α-NAGA, suggesting its capability to utilize substrates of both types. For the details about the protein model see the appended publication #6.

5.2.2 gana-1 enzymatic activity, RNAi induced compound enzymatic deficiency, cellular localization of gana-1

α-GAL and α-NAGA activity measurements in the mixed culture *C. elegans* homogenates showed presence of both activities, α-NAGA activity predominated over α-GAL. The addition of N-acetyl-D-galactosamine (α-NAGA inhibitor) resulted in the considerable activity drop of both (α-GAL and α-NAGA) enzymatic activities, which is a phenomenon undetectable in vertebrate (human) proteins. N-acetyl-D-galactosamine selectively inhibits α-NAGA but does not influence α-GAL activity. In comparison, the addition of D-galactose (α-GAL inhibitor) also resulted in the drop of both activities. Based on these results that supported the hypothesis of dual substrate specificity of gana-1 RNAi experiments selectively targeting *gana-1* mRNA were performed. Parallel and proportional drops of both enzymatic activities were observed in repetitive experiments after RNAi treatment. The induced activity decreases were in the order of tens of per cents in comparison to controls.

Despite RNAi mediated introduction of considerable enzymatic deficiency in the nematodes, we were not able to document specific morphological changes (lysosomal storage) associated with either of the phenotypes. This could be explained by relatively high

residual enzymatic activity after RNAi. This situation is reminiscent of LSD heterozygotes status, when despite having enzymatic activities as low as 10% of controls these individuals do not suffer from lysosomal storage.

In order to elucidate the cellular functions of gana-1 we performed C terminal EGFP (enhanced green fluorescent protein) tagging of gana-1. *gana-1*::GFP transgene was introduced into the standard Bristol N2 *C. elegans* strain and the expression pattern was studied *in vivo*. We were able to document GFP presence in the vacuolar compartment of subset of six *C. elegans* cells with high endocytic turnover called coelomocytes. Special treatment of transgenic worms, employing phenomenon pH dependence of GFP[250,251] molecules, allowed associating of gana-1::GFP transgene with the acidic pH cellular compartment.

The results and conclusions of this publication clearly demonstrated usefulness of *C. elegans* for the study of human pathology states. Despite relative evolutionary distance between the subject species (*Homo sapiens*) and the model organism our publication tried to answer some fundamental questions that are most imminent to biology of α-GAL and α-NAGA function in eukaryotic cells. Suggested evolutionary scheme of the two paralogous genes/proteins may represent important premise for future design of either enzymatic assays setups or drugs. The integrative conjunction of bioinformatic methods and experiments in easily genetically modifiable animal model generated results that would not be obtainable in other (mammalian) species in the same time.[252] The fact that we were not able to replicate the morphological storage phenotype does not lower the results; it just demonstrates the limits of RNAi. It can also be deduced that any further study of lysosomal enzyme orthologs in *C. elegans* should be aware of the obstacle of residual enzymatic activity and employ preferentially deletion mutants with low residual activity. As can be demonstrated on some other studies using *C. elegans* as a model for human diseases, lack of comparable phenotypic presentation does not necessarily mean lack of important and applicable biological message[253-255].

Appended publication #6

BioMed Central

BMC Cell Biology

Research article

Open Access

Characterization of *gana-1*, a Caenorhabditis elegans gene encoding a single ortholog of vertebrate α-galactosidase and α-N-acetylgalactosaminidase

Jana Hujová†, Jakub Sikora†, Robert Dobrovolný†, Helena Poupětová, Jana Ledvinová, Marta Kostrouchová and Martin Hřebíček*

Address: Institute of Inherited Metabolic Disorders, Charles University, 1st Medical Faculty, Prague, Czech Republic

Email: Jana Hujová - jhujo@lf1.cuni.cz; Jakub Sikora - jakub.sikora@lf1.cuni.cz; Robert Dobrovolný - rdobr@lf1.cuni.cz; Helena Poupětová - helena.poupetova@lf1.cuni.cz; Jana Ledvinová - jledvin@beba.cesnet.cz; Marta Kostrouchová - marta.kostrouchova@lf1.cuni.cz; Martin Hřebíček* - mhreb@lf1.cuni.cz

* Corresponding author †Equal contributors

Published: 27 January 2005

BMC Cell Biology 2005, 6:5 doi:10.1186/1471-2121-6-5

Received: 13 September 2004

Accepted: 27 January 2005

This article is available from: http://www.biomedcentral.com/1471-2121/6/5

Abstract

Background: Human α-galactosidase A (α-GAL) and α-N-acetylgalactosaminidase (α-NAGA) are presumed to share a common ancestor. Deficiencies of these enzymes cause two well-characterized human lysosomal storage disorders (LSD) – Fabry (α-GAL deficiency) and Schindler (α-NAGA deficiency) diseases. *Caenorhabditis elegans* was previously shown to be a relevant model organism for several late endosomal/lysosomal membrane proteins associated with LSDs. The aim of this study was to identify and characterize *C. elegans* orthologs to both human lysosomal luminal proteins α-GAL and α-NAGA.

Results: BlastP searches for orthologs of human α-GAL and α-NAGA revealed a single *C. elegans* gene (R07B7.11) with homology to both human genes (α-galactosidase and α-N-acetylgalactosaminidase) – *gana-1*. We cloned and sequenced the complete *gana-1* cDNA and elucidated the gene organization.

Phylogenetic analyses and homology modeling of GANA-1 based on the 3D structure of chicken α-NAGA, rice α-GAL and human α-GAL suggest a close evolutionary relationship of GANA-1 to both human α-GAL and α-NAGA.

Both α-GAL and α-NAGA enzymatic activities were detected in *C. elegans* mixed culture homogenates. However, α-GAL activity on an artificial substrate was completely inhibited by the α-NAGA inhibitor, N-acetyl-D-galactosamine.

A GANA-1::GFP fusion protein expressed from a transgene, containing the complete *gana-1* coding region and 3 kb of its hypothetical promoter, was not detectable under the standard laboratory conditions. The GFP signal was observed solely in a vesicular compartment of coelomocytes of the animals treated with Concanamycin A (CON A) or NH_4Cl, agents that increase the pH of the cellular acidic compartment.

Immunofluorescence detection of the fusion protein using polyclonal anti-GFP antibody showed a broader and coarsely granular cytoplasmic expression pattern in body wall muscle cells, intestinal cells, and a vesicular compartment of coelomocytes.

Inhibition of *gana-1* by RNA interference resulted in a decrease of both α-GAL and α-NAGA activities measured in mixed stage culture homogenates but did not cause any obvious phenotype.

Conclusions: GANA-1 is a single *C. elegans* ortholog of both human α-GAL and α-NAGA proteins. Phylogenetic, homology modeling, biochemical and GFP expression analyses support the hypothesis that GANA-1 has dual enzymatic activity and is localized in an acidic cellular compartment.

6 Concluding notes

As was mentioned in the Introduction (section *1*), the last 40 years were dedicated to the studies on substantial monogenic bases of lysosomal storage disorders. Present time in the LSD research represents a transitory step between the hypothesis-driven and curiosity-driven experimental approaches, which are gaining more and more attention. Today's LSD research thus could be characterized by intensive demand for integration of the available data with outcomes towards pathogenic mechanisms, novel diagnostic approaches or therapeutic modalities.

Purpose of this section of the thesis is to provide final summarizing overview of the perfomed and published findings. Reader is refered to the previous detailed discussions on the presented topics. The appended publications represent novel findings in the area of saposin-like proteins related lysosomal storage disorders. The reported "non-enzymatic" functions of pSap are integral part of pSap deficiency pathogenesis and are in complete accordance with the recently opened topics of protein clearance and autophagy related cell impairment in LSDs. In a closely related manner, HGSNAT protein (deficient in MPS IIIc), which resides in lysosomal DRMs, is most probably directly or indirectly involved in chaperon mediated autophagy and implications of its function might be relevant to a broader spectrum of LSDs.

Presented genotype-phenotype correlations in ASM (another Sap-like protein) deficiency rendered important data towards ASM catalytic functions and re-opened debate on phenotypic diversity and Niemann-Pick disease type A and B classification. These data should not be perceived as mere pathogenic variation reports as they contain broad pathogenic considerations and implications.

Last but not least, *C. elegans* was demonstrated as relevant model organism for lysosomal enzymopathies. The data demonstrating evolution of two related lysosomal hydrolases could have never been achieved with such an ease in mammalian model. These findings also point to sometimes overlooked neccesity to study the evolutionary relations in order to answer questions of human pathology.

All the appended publications were a subject of peer-review assesment and some have already been further cited (see sections *9* and *10*).

7 Abbreviations

AAV	adeno associated virus
3D	three dimensional
α-GAL	alpha-galactosidase
α-NAGA	alpha-N-acetylgalactosaminidase
ARMS	amplification refractory mutation systém
ASM	acid sphingomyelinase
BLASTN/P	basic local alignment seach tool nucleotide/protein
bp	base pair
BWS	Beckwith-Wiedemann syndrome
C.elegans	*Caenorhabditis elegans*
CCF	cross-correlation function
cDNA	complementary deoxyribonucleic acid
CMA	chaperon mediated autophagy
CNS	conserved non-coding sequence
DNA	deoxyribonucleic acid
DRM	detergent resistant microdomain
EST	expressed sequence tag
e-value	expectancy value
FFPE	formaldehyde fixed paraffin embedded
gana-1	α-GAL and α-NAGA ortholog
GFAP	glial fibrillary acidic protein
HGSNAT	heparin acetyl-coenzyme A:α-glucosaminide N-acetyltransferase
HMU-PC	6-hexadecanoylamino-4-methylumbelliferyl-phosphorylcholine
HNP-PC	2-N-(hexadecanoyl)-amino-4-nitrophenyl phosphorylcholine
kb	kilo base
kDa	kiloDalton
LAMP	lysosome associated membrane protein
LC3	microtubule-associated protein 1 light chain 3
LRP	lipoprotein receptor-related protein
LSCM	laser scanning confocal microscopy
LSD	lysosomal storage disorder
M-6-P	mannose-6-phosphate
M-6-PR	mannose-6-phosphate receptor
Mb	mega base
MIM	mendelian inheritance in man
MPS	mucopolysaccharidosis
MR	mannose receptor
mRNA	messenger ribonucleic acid
NCL	neuronal ceroid lipofuscinosis
NPC	Niemann-Pick disease type C
NPD	Niemann-Pick disease
NPD A/B	Niemann-Pick disease type A/B
ORF	open reading frame
OST	ORF sequence tag
PCD	programmed cell death
PCR	polymerase chain reaction
PPCA	protective protein / Cathepsin A
pSap	prosaposin
PTM	post-translational modification
RFLP	restriction fragment length polymorphism
RMSD	root mean square deviation

RNAi	RNA mediated interference
Sap	saposin
SAPLIP	saposin-like protein
SCMAS	subunit c of mitochondrial ATP synthase
SMPD	sphingomyelin phosphodiesterase
TM	transmembrane
TMMOD	improved transmembrane hidden Markov model

8 References

1. Uniform Requirements for Manuscripts Submitted to Biomedical Journals: Writing and Editing for Biomedical Publication - http://www.icmje.org/
2. den Dunnen, J.T. & Antonarakis, S.E. Nomenclature for the description of human sequence variations. *Hum Genet* **109**, 121-124 (2001).
3. De Duve, C., Pressman, B.C., Gianetto, R., Wattiaux, R. & Appelmans, F. Tissue fractionation studies. 6. Intracellular distribution patterns of enzymes in rat-liver tissue. *Biochem J* **60**, 604-617 (1955).
4. Alberts, B., *et al.* Intracellular vesicular traffic. in *Molecular biology of the cell* (ed. Gibbs, S.) 711-765 (Garland Science, New York, 2002).
5. Neufeld, E.B., *et al.* The Niemann-Pick C1 protein resides in a vesicular compartment linked to retrograde transport of multiple lysosomal cargo. *J Biol Chem* **274**, 9627-9635. (1999).
6. Cuervo, A.M., Dice, J.F. & Knecht, E. A population of rat liver lysosomes responsible for the selective uptake and degradation of cytosolic proteins. *J Biol Chem* **272**, 5606-5615 (1997).
7. Kaushik, S., Massey, A.C. & Cuervo, A.M. Lysosome membrane lipid microdomains: novel regulators of chaperone-mediated autophagy. *Embo J* **25**, 3921-3933 (2006).
8. Dell'Angelica, E.C., Mullins, C., Caplan, S. & Bonifacino, J.S. Lysosome-related organelles. *Faseb J* **14**, 1265-1278 (2000).
9. Bagshaw, R.D., Mahuran, D.J. & Callahan, J.W. Lysosomal membrane proteomics and biogenesis of lysosomes. *Mol Neurobiol* **32**, 27-41 (2005).
10. Bagshaw, R.D., Mahuran, D.J. & Callahan, J.W. A proteomic analysis of lysosomal integral membrane proteins reveals the diverse composition of the organelle. *Mol Cell Proteomics* 4, 133-143 (2005).
11. Fan, X., *et al.* Identification of the gene encoding the enzyme deficient in mucopolysaccharidosis IIIC (Sanfilippo disease type C). *Am J Hum Genet* 79, 738-744 (2006).
12. Hrebicek, M., *et al.* Mutations in TMEM76 Cause Mucopolysaccharidosis IIIC (Sanfilippo C Syndrome). *Am J Hum Genet* 79, 807-819 (2006).
13. Taute, A., *et al.* Presence of detergent-resistant microdomains in lysosomal membranes. *Biochem Biophys Res Commun* **298**, 5-9 (2002).
14. Elleder, M. Glucosylceramide transfer from lysosomes-the missing link in molecular pathology of glucosylceramidase deficiency: A hypothesis based on existing data. *J Inherit Metab Dis* (2006).
15. Alvarez, V., Parodi, A.J. & Couso, R. Characterization of the mannose 6-phosphate-dependent pathway of lysosomal enzyme routing in an invertebrate. *Biochem J* **310**, 589-595. (1995).
16. Le Borgne, R. & Hoflack, B. Mannose 6-phosphate receptors regulate the formation of clathrin-coated vesicles in the TGN. *J Cell Biol* **137**, 335-345 (1997).
17. Van Patten, S.M., *et al.* Effect of mannose chain length on targeting of glucocerebrosidase for enzyme replacement therapy of Gaucher disease. *Glycobiology* (2007).
18. Bijsterbosch, M.K., *et al.* Quantitative analysis of the targeting of mannose-terminal glucocerebrosidase. Predominant uptake by liver endothelial cells. *Eur J Biochem* **237**, 344-349 (1996).
19. Lefrancois, S., Zeng, J., Hassan, A.J., Canuel, M. & Morales, C.R. The lysosomal trafficking of sphingolipid activator proteins (SAPs) is mediated by sortilin. *Embo J* **22**, 6430-6437 (2003).
20. Bonifacino, J.S. & Traub, L.M. Signals for sorting of transmembrane proteins to endosomes and lysosomes. *Annu Rev Biochem* **72**, 395-447 (2003).
21. Cuervo, A.M. & Dice, J.F. Lysosomes, a meeting point of proteins, chaperones, and proteases. *J Mol Med* 76, 6-12 (1998).
22. Cuervo, A.M. & Dice, J.F. Unique properties of lamp2a compared to other lamp2 isoforms. *J Cell Sci* **113 Pt 24**, 4441-4450 (2000).
23. Cuervo, A.M., Gomes, A.V., Barnes, J.A. & Dice, J.F. Selective degradation of annexins by chaperone-mediated autophagy. *J Biol Chem* **275**, 33329-33335 (2000).
24. Cuervo, A.M. Autophagy: in sickness and in health. *Trends Cell Biol* **14**, 70-77 (2004).
25. Cuervo, A.M. Autophagy: many paths to the same end. *Mol Cell Biochem* **263**, 55-72 (2004).
26. Kabeya, Y., *et al.* LC3, a mammalian homologue of yeast Apg8p, is localized in autophagosome membranes after processing. *Embo J* **19**, 5720-5728 (2000).
27. Tanida, I., Ueno, T. & Kominami, E. LC3 conjugation system in mammalian autophagy. *Int J Biochem Cell Biol* **36**, 2503-2518 (2004).
28. Cuervo, A.M., Stefanis, L., Fredenburg, R., Lansbury, P.T. & Sulzer, D. Impaired degradation of mutant alpha-synuclein by chaperone-mediated autophagy. *Science* **305**, 1292-1295 (2004).
29. Lenk, S.E., Susan, P.P., Hickson, I., Jasionowski, T. & Dunn, W.A., Jr. Ubiquitinated aldolase B accumulates during starvation-induced lysosomal proteolysis. *J Cell Physiol* **178**, 17-27 (1999).
30. Webb, J.L., Ravikumar, B., Atkins, J., Skepper, J.N. & Rubinsztein, D.C. Alpha-Synuclein is degraded by both autophagy and the proteasome. *J Biol Chem* **278**, 25009-25013 (2003).
31. Komatsu, M., *et al.* Impairment of starvation-induced and constitutive autophagy in Atg7-deficient mice. *J Cell Biol* **169**, 425-434 (2005).
32. Hara, T., *et al.* Suppression of basal autophagy in neural cells causes neurodegenerative disease in mice. *Nature* **441**, 885-889 (2006).

33. Komatsu, M., *et al.* Loss of autophagy in the central nervous system causes neurodegeneration in mice. *Nature* **441**, 880-884 (2006).
34. Massey, A.C., Kaushik, S., Sovak, G., Kiffin, R. & Cuervo, A.M. Consequences of the selective blockage of chaperone-mediated autophagy. *Proc Natl Acad Sci U S A* **103**, 5805-5810 (2006).
35. Cuervo, A.M. Autophagy in neurons: it is not all about food. *Trends Mol Med* **12**, 461-464 (2006).
36. Bursch, W. The autophagosomal-lysosomal compartment in programmed cell death. *Cell Death Differ* **8**, 569-581 (2001).
37. *The Metabolic & Molecular Bases of Inherited Disease*, (The McGraw-Hill Companies, Inc., New York, 2001).
38. Hers, H.G. alpha-Glucosidase deficiency in generalized glycogenstorage disease (Pompe's disease). *Biochem J* **86**, 11-16 (1963).
39. Austin, J., *et al.* Low sulfatase activities in metachromatic leukodystrophy (MLD). A controlled study of enzymes in 9 living and 4 autopsied patients with MLD. *Trans Am Neurol Assoc* **89**, 147-150 (1964).
40. Austin, J., *et al.* Abnormal sulphatase activities in two human diseases (metachromatic leucodystrophy and gargoylism). *Biochem J* **93**, 15C-17C (1964).
41. Online Mendelian Inheritance in Man - http://www.ncbi.nlm.nih.gov/entrez/query.fcgi?db=OMIM
42. Meikle, P.J., Hopwood, J.J., Clague, A.E. & Carey, W.F. Prevalence of lysosomal storage disorders. *Jama* **281**, 249-254 (1999).
43. Karageorgos, L.E., *et al.* Lysosomal biogenesis in lysosomal storage disorders. *Exp Cell Res* **234**, 85-97 (1997).
44. Mitchison, H.M., Lim, M.J. & Cooper, J.D. Selectivity and types of cell death in the neuronal ceroid lipofuscinoses. *Brain Pathol* **14**, 86-96 (2004).
45. Koike, M., *et al.* Participation of autophagy in storage of lysosomes in neurons from mouse models of neuronal ceroid-lipofuscinoses (Batten disease). *Am J Pathol* **167**, 1713-1728 (2005).
46. Elleder, M., Sokolova, J. & Hrebicek, M. Follow-up study of subunit c of mitochondrial ATP synthase (SCMAS) in Batten disease and in unrelated lysosomal disorders. *Acta Neuropathol (Berl)* **93**, 379-390 (1997).
47. Cao, Y., *et al.* Autophagy is disrupted in a knock-in mouse model of juvenile neuronal ceroid lipofuscinosis. *J Biol Chem* **281**, 20483-20493 (2006).
48. Fukuda, T., *et al.* Dysfunction of endocytic and autophagic pathways in a lysosomal storage disease. *Ann Neurol* **59**, 700-708 (2006).
49. Fukuda, T., *et al.* Autophagy and mistargeting of therapeutic enzyme in skeletal muscle in Pompe disease. *Mol Ther* **14**, 831-839 (2006).
50. Tanaka, Y., *et al.* Accumulation of autophagic vacuoles and cardiomyopathy in LAMP-2- deficient mice. *Nature* **406**, 902-906 (2000).
51. Fanin, M., *et al.* Generalized lysosome-associated membrane protein-2 defect explains multisystem clinical involvement and allows leukocyte diagnostic screening in Danon disease. *Am J Pathol* **168**, 1309-1320 (2006).
52. Cuervo, A.M., Mann, L., Bonten, E.J., d'Azzo, A. & Dice, J.F. Cathepsin A regulates chaperone-mediated autophagy through cleavage of the lysosomal receptor. *Embo J* **22**, 47-59 (2003).
53. Vaccaro, A.M., Salvioli, R., Tatti, M. & Ciaffoni, F. Saposins and their interaction with lipids. *Neurochem Res* **24**, 307-314 (1999).
54. Bruhn, H. A short guided tour through functional and structural features of saposin-like proteins. *Biochem J* **389**, 249-257 (2005).
55. Ahn, V.E., Leyko, P., Alattia, J.R., Chen, L. & Prive, G.G. Crystal structures of saposins A and C. *Protein Sci* **15**, 1849-1857 (2006).
56. Vaccaro, A.M., *et al.* Structural analysis of saposin C and B. Complete localization of disulfide bridges. *J Biol Chem* **270**, 9953-9960 (1995).
57. John, M., Wendeler, M., Heller, M., Sandhoff, K. & Kessler, H. Characterization of human saposins by NMR spectroscopy. *Biochemistry* **45**, 5206-5216 (2006).
58. Ponting, C.P. Acid sphingomyelinase possesses a domain homologous to its activator proteins: saposins B and D. *Protein Sci* **3**, 359-361 (1994).
59. Kolzer, M., *et al.* Functional characterization of the postulated intramolecular sphingolipid activator protein domain of human acid sphingomyelinase. *Biol Chem* **385**, 1193-1195 (2004).
60. Gopalakrishnan, M.M., *et al.* Purified recombinant human prosaposin forms oligomers that bind procathepsin D and affect its autoactivation. *Biochem J* **383**, 507-515 (2004).
61. Rorman, E.G., Scheinker, V. & Grabowski, G.A. Structure and evolution of the human prosaposin chromosomal gene. *Genomics* **13**, 312-318 (1992).
62. Zhao, Q. & Morales, C.R. Identification of a novel sequence involved in lysosomal sorting of the sphingolipid activator protein prosaposin. *J Biol Chem* **275**, 24829-24839 (2000).
63. Hazkani-Covo, E., Altman, N., Horowitz, M. & Graur, D. The evolutionary history of prosaposin: two successive tandem-duplication events gave rise to the four saposin domains in vertebrates. *J Mol Evol* **54**, 30-34 (2002).
64. Sun, Y., Jin, P. & Grabowski, G.A. The mouse prosaposin locus: promoter organization. *DNA Cell Biol* **16**, 23-34 (1997).
65. Sun, Y., Jin, P., Witte, D.P. & Grabowski, G.A. Isolation and characterization of the human prosaposin promoter. *Gene* **218**, 37-47 (1998).
66. Sun, Y., Jin, P., Witte, D.P. & Grabowski, G.A. Prosaposin: promoter analysis and central-nervous-system-preferential elements for expression in vivo. *Biochem J* **352** Pt **2**, 549-556 (2000).
67. Sun, Y., Witte, D.P., Jin, P. & Grabowski, G.A. Analyses of temporal regulatory elements of the prosaposin gene in transgenic mice. *Biochem J* **370**, 557-566 (2003).

68. Cohen, T., *et al.* Conservation of expression and alternative splicing in the prosaposin gene. *Brain Res Mol Brain Res* **129**, 8-19 (2004).
69. Madar-Shapiro, L., *et al.* Importance of splicing for prosaposin sorting. *Biochem J* **337 (Pt 3)**, 433-443 (1999).
70. Cohen, T., *et al.* The exon 8-containing prosaposin gene splice variant is dispensable for mouse development, lysosomal function, and secretion. *Mol Cell Biol* **25**, 2431-2440 (2005).
71. Lefrancois, S., Michaud, L., Potier, M., Igdoura, S. & Morales, C.R. Role of sphingolipids in the transport of prosaposin to the lysosomes. *J Lipid Res* **40**, 1593-1603 (1999).
72. Hassan, A.J., Zeng, J., Ni, X. & Morales, C.R. The trafficking of prosaposin (SGP-1) and GM2AP to the lysosomes of TM4 Sertoli cells is mediated by sortilin and monomeric adaptor proteins. *Mol Reprod Dev* **68**, 476-483 (2004).
73. Ni, X. & Morales, C.R. The lysosomal trafficking of acid sphingomyelinase is mediated by sortilin and mannose 6-phosphate receptor. *Traffic* 7, 889-902 (2006).
74. Hiraiwa, M., *et al.* Lysosomal proteolysis of prosaposin, the precursor of saposins (sphingolipid activator proteins): its mechanism and inhibition by ganglioside. *Arch Biochem Biophys* **341**, 17-24 (1997).
75. Zhu, Y. & Conner, G.E. Intermolecular association of lysosomal protein precursors during biosynthesis. *J Biol Chem* **269**, 3846-3851 (1994).
76. Lefrancois, S., May, T., Knight, C., Bourbeau, D. & Morales, C.R. The lysosomal transport of prosaposin requires the conditional interaction of its highly conserved d domain with sphingomyelin. *J Biol Chem* **277**, 17188-17199 (2002).
77. Laurent-Matha, V., *et al.* Procathepsin D interacts with prosaposin in cancer cells but its internalization is not mediated by LDL receptor-related protein. *Exp Cell Res* **277**, 210-219 (2002).
78. Sandhoff, K., Harzer, K. & Furst, W. Sphinglipid activator proteins. in *The Metabolic & Molecular Bases of Inherited Disease*, Vol. 3 (eds. Scriver, C.R., *et al.*) 3375-3388 (The McGraw-Hill Companies, Inc., New York, 2001).
79. Hiesberger, T., *et al.* Cellular uptake of saposin (SAP) precursor and lysosomal delivery by the low density lipoprotein receptor-related protein (LRP). *Embo J* **17**, 4617-4625 (1998).
80. Hiraiwa, M., Campana, W.M., Martin, B.M. & O'Brien, J.S. Prosaposin receptor: evidence for a G-protein-associated receptor. *Biochem Biophys Res Commun* **240**, 415-418 (1997).
81. Hawkins, C.A., de Alba, E. & Tjandra, N. Solution structure of human saposin C in a detergent environment. *J Mol Biol* **346**, 1381-1392 (2005).
82. Alattia, J.R., Shaw, J.E., Yip, C.M. & Prive, G.G. Direct visualization of saposin remodelling of lipid bilayers. *J Mol Biol* **362**, 943-953 (2006).
83. Winau, F., *et al.* Saposin C is required for lipid presentation by human CD1b. *Nat Immunol* **5**, 169-174 (2004).
84. Hulkova, H., *et al.* A novel mutation in the coding region of the prosaposin gene leads to a complete deficiency of prosaposin and saposins, and is associated with a complex sphingolipidosis dominated by lactosylceramide accumulation. *Hum Mol Genet* **10**, 927-940 (2001).
85. Elleder, M., *et al.* Prosaposin deficiency -- a rarely diagnosed, rapidly progressing, neonatal neurovisceral lipid storage disease. Report of a further patient. *Neuropediatrics* **36**, 171-180 (2005).
86. Hiraiwa, M., Soeda, S., Kishimoto, Y. & O'Brien, J.S. Binding and transport of gangliosides by prosaposin. *Proc Natl Acad Sci U S A* **89**, 11254-11258 (1992).
87. Fu, Q., *et al.* Occurrence of prosaposin as a neuronal surface membrane component. *J Mol Neurosci* **5**, 59-67 (1994).
88. Lee, T.J., Sartor, O., Luftig, R.B. & Koochekpour, S. Saposin C promotes survival and prevents apoptosis via PI3K/Akt-dependent pathway in prostate cancer cells. *Mol Cancer* **3**, 31 (2004).
89. Misasi, R., *et al.* Prosaposin treatment induces PC12 entry in the S phase of the cell cycle and prevents apoptosis: activation of ERKs and sphingosine kinase. *Faseb J* **15**, 467-474 (2001).
90. Koochekpour, S., *et al.* Saposin C stimulates growth and invasion, activates p42/44 and SAPK/JNK signaling pathways of MAPK and upregulates uPA/uPAR expression in prostate cancer and stromal cells. *Asian J Androl* 7, 147-158 (2005).
91. Morales, C.R., Fuska, J., Zhao, Q. & Lefrancois, S. Biogenesis of lysosomes in marshall cells and in cells of the male reproductive system. *Mol Reprod Dev* **59**, 54-66 (2001).
92. Morales, C.R. & Badran, H. Prosaposin ablation inactivates the MAPK and Akt signaling pathways and interferes with the development of the prostate gland. *Asian J Androl* **5**, 57-63 (2003).
93. Morales, C.R., Zhao, Q., Lefrancois, S. & Ham, D. Role of prosaposin in the male reproductive system: effect of prosaposin inactivation on the testis, epididymis, prostate, and seminal vesicles. *Arch Androl* 44, 173-186 (2000).
94. Koochekpour, S., *et al.* Amplification and overexpression of prosaposin in prostate cancer. *Genes Chromosomes Cancer* 44, 351-364 (2005).
95. Campana, W.M., O'Brien, J.S., Hiraiwa, M. & Patton, S. Secretion of prosaposin, a multifunctional protein, by breast cancer cells. *Biochim Biophys Acta* **1427**, 392-400 (1999).
96. Misasi, R., *et al.* Prosaposin: a new player in cell death prevention of U937 monocytic cells. *Exp Cell Res* **298**, 38-47 (2004).
97. Elleder, M., *et al.* Niemann-Pick disease type C with enhanced glycolipid storage. Report on further case of so-called lactosylceramidosis. *Virchows Arch A Pathol Anat Histopathol* **402**, 307-317 (1984).
98. Bradova, V., *et al.* Prosaposin deficiency: further characterization of the sphingolipid activator protein-deficient sibs. Multiple glycolipid elevations (including lactosylceramidosis), partial enzyme deficiencies and ultrastructure of the skin in this generalized sphingolipid storage disease. *Hum Genet* **92**, 143-152 (1993).
99. Sikora, J., Harzer, K. & Elleder, M. Neurolysosomal pathology in human prosaposin deficiency suggests essential neurotrophic function of prosaposin. *Acta Neuropathol (Berl)* **113**, 163-175 (2007).

100. Diaz-Font, A., *et al.* A mutation within the saposin D domain in a Gaucher disease patient with normal glucocerebrosidase activity. *Hum Genet* **117**, 275-277 (2005).
101. Matsuda, J., Vanier, M.T., Saito, Y., Tohyama, J. & Suzuki, K. A mutation in the saposin A domain of the sphingolipid activator protein (prosaposin) gene results in a late-onset, chronic form of globoid cell leukodystrophy in the mouse. *Hum Mol Genet* **10**, 1191-1199 (2001).
102. Matsuda, J., *et al.* Mutation in saposin D domain of sphingolipid activator protein gene causes urinary system defects and cerebellar Purkinje cell degeneration with accumulation of hydroxy fatty acid-containing ceramide in mouse. *Hum Mol Genet* **13**, 2709-2723 (2004).
103. Fujita, N., *et al.* Targeted disruption of the mouse sphingolipid activator protein gene: a complex phenotype, including severe leukodystrophy and wide-spread storage of multiple sphingolipids. *Hum Mol Genet* **5**, 711-725 (1996).
104. Oya, Y., Nakayasu, H., Fujita, N. & Suzuki, K. Pathological study of mice with total deficiency of sphingolipid activator proteins (SAP knockout mice). *Acta Neuropathol (Berl)* **96**, 29-40 (1998).
105. Fujimuro, M., Sawada, H. & Yokosawa, H. Production and characterization of monoclonal antibodies specific to multi-ubiquitin chains of polyubiquitinated proteins. *FEBS Lett* **349**, 173-180 (1994).
106. Zatloukal, K., *et al.* p62 Is a common component of cytoplasmic inclusions in protein aggregation diseases. *Am J Pathol* **160**, 255-263 (2002).
107. van Leeuwen, F.W., Gerez, L., Benne, R. & Hol, E.M. +1 Proteins and aging. *Int J Biochem Cell Biol* **34**, 1502-1505 (2002).
108. van Leeuwen, F.W., Burbach, J.P. & Hol, E.M. Mutations in RNA: a first example of molecular misreading in Alzheimer's disease. *Trends Neurosci* **21**, 331-335 (1998).
109. de Pril, R., *et al.* Accumulation of aberrant ubiquitin induces aggregate formation and cell death in polyglutamine diseases. *Hum Mol Genet* **13**, 1803-1813 (2004).
110. Zhan, S.S., Beyreuther, K. & Schmitt, H.P. Neuronal ubiquitin and neurofilament expression in different lysosomal storage disorders. *Clin Neuropathol* **11**, 251-255 (1992).
111. Boutet de Monvel, J., Le Calvez, S. & Ulfendahl, M. Image restoration for confocal microscopy: improving the limits of deconvolution, with application to the visualization of the mammalian hearing organ. *Biophys J* **80**, 2455-2470 (2001).
112. Landmann, L. Deconvolution improves colocalization analysis of multiple fluorochromes in 3D confocal data sets more than filtering techniques. *J Microsc* **208**, 134-147 (2002).
113. Masata, M., Malinsky, J., Fidlerova, H., Smirnov, E. & Raska, I. Dynamics of replication foci in early S phase as visualized by cross-correlation function. *J Struct Biol* **151**, 61-68 (2005).
114. van Steensel, B., *et al.* Partial colocalization of glucocorticoid and mineralocorticoid receptors in discrete compartments in nuclei of rat hippocampus neurons. *J Cell Sci* **109** (**Pt 4**), 787-792 (1996).
115. Bolte, S. & Cordelieres, F.P. A guided tour into subcellular colocalization analysis in light microscopy. *J Microscopy* **224**, 213-232 (2006).
116. Siintola, E., *et al.* Cathepsin D deficiency underlies congenital human neuronal ceroid-lipofuscinosis. *Brain* **129**, 1438-1445 (2006).
117. Patton, S., Carson, G.S., Hiraiwa, M., O'Brien, J.S. & Sano, A. Prosaposin, a neurotrophic factor: presence and properties in milk. *J Dairy Sci* **80**, 264-272 (1997).
118. Tsuboi, K., Hiraiwa, M. & O'Brien, J.S. Prosaposin prevents programmed cell death of rat cerebellar granule neurons in culture. *Brain Res Dev Brain Res* **110**, 249-255 (1998).
119. Kotani, Y., *et al.* Prosaposin facilitates sciatic nerve regeneration in vivo. *J Neurochem* **66**, 2019-2025 (1996).
120. Hozumi, I., *et al.* Administration of prosaposin ameliorates spatial learning disturbance and reduces cavity formation following stab wounds in rat brain. *Neurosci Lett* **267**, 73-76 (1999).
121. Campana, W.M., Mohiuddin, L., Misasi, R., O'Brien, J.S. & Calcutt, N.A. Prosaposin-derived peptides enhanced sprouting of sensory neurons in vitro and induced sprouting at motor endplates in vivo. *J Peripher Nerv Syst* **5**, 126-130 (2000).
122. Hiraiwa, M., Campana, W.M., Mizisin, A.P., Mohiuddin, L. & O'Brien, J.S. Prosaposin: a myelinotrophic protein that promotes expression of myelin constituents and is secreted after nerve injury. *Glia* **26**, 353-360 (1999).
123. Calcutt, N.A., Freshwater, J.D. & O'Brien, J.S. Protection of sensory function and antihyperalgesic properties of a prosaposin-derived peptide in diabetic rats. *Anesthesiology* **93**, 1271-1278 (2000).
124. Lapchak, P.A., Araujo, D.M., Shackelford, D.A. & Zivin, J.A. Prosaptide exacerbates ischemia-induced behavioral deficits in vivo; an effect that does not involve mitogen-activated protein kinase activation. *Neuroscience* **101**, 811-814 (2000).
125. Sun, Y., *et al.* Prosaposin: threshold rescue and analysis of the "neuritogenic" region in transgenic mice. *Mol Genet Metab* **76**, 271-286 (2002).
126. Chu, Z., Sun, Y., Kuan, C.Y., Grabowski, G.A. & Qi, X. Saposin C: neuronal effect and CNS delivery by liposomes. *Ann N Y Acad Sci* **1053**, 237-246 (2005).
127. O'Brien, J.S., Carson, G.S., Seo, H.C., Hiraiwa, M. & Kishimoto, Y. Identification of prosaposin as a neurotrophic factor. *Proc Natl Acad Sci U S A* **91**, 9593-9596 (1994).
128. O'Brien, J.S., *et al.* Identification of the neurotrophic factor sequence of prosaposin. *Faseb J* **9**, 681-685 (1995).
129. Kotani, Y., *et al.* A hydrophilic peptide comprising 18 amino acid residues of the prosaposin sequence has neurotrophic activity in vitro and in vivo. *J Neurochem* **66**, 2197-2200 (1996).
130. Qi, X., Qin, W., Sun, Y., Kondoh, K. & Grabowski, G.A. Functional organization of saposin C. Definition of the neurotrophic and acid beta-glucosidase activation regions. *J Biol Chem* **271**, 6874-6880 (1996).

131. Nixon, R.A., *et al.* Extensive involvement of autophagy in Alzheimer disease: an immuno-electron microscopy study. *J Neuropathol Exp Neurol* **64**, 113-122 (2005).
132. Migheli, A., *et al.* Age-related ubiquitin deposits in dystrophic neurites: an immunoelectron microscopic study. *Neuropathol Appl Neurobiol* **18**, 3-11 (1992).
133. Lowe, J., *et al.* Ubiquitin conjugate immunoreactivity in the brains of scrapie infected mice. *J Pathol* **162**. 61-66 (1990).
134. Schuchman, E.H. & Desnick, R.J. Niemann-Pick Disease Types A and B: Acid Sphingomyelinase Deficiencies. in *The Metabolic & Molecular Bases of Inherited Disease*, Vol. 3 (eds. Scriver, C.R., *et al.*) 3589-3610 (The McGraw-Hill Companies, Inc., New York, 2001).
135. Niemann, A. Ein unbekantes Krankheitsbild. *Jahrb. Kinderheilkd.* **79**, 1-10 (1914).
136. Samet, D. & Barenholz, Y. Characterization of acidic and neutral sphingomyelinase activities in crude extracts of HL-60 cells. *Chem Phys Lipids* **102**, 65-77 (1999).
137. Titball, R.W. Bacterial phospholipases C. *Microbiol Rev* **57**, 347-366 (1993).
138. Zuckert, W.R., Marquis, H. & Goldfme, H. Modulation of enzymatic activity and biological function of Listeria monocytogenes broad-range phospholipase C by amino acid substitutions and by replacement with the Bacillus cereus ortholog. *Infect Immun* **66**, 4823-4831 (1998).
139. Goni, F.M. & Alonso, A. Sphingomyelinases: enzymology and membrane activity. *FEBS Lett* **531**, 38-46 (2002).
140. Chatterjee, S. Neutral sphingomyelinase: past, present and future. *Chem Phys Lipids* **102**, 79-96 (1999).
141. Seto, M., *et al.* A model of the acid sphingomyelinase phosphoesterase domain based on its remote structural homolog purple acid phosphatase. *Prot Sci* **13**, 3172-3186 (2004).
142. Gulbins, E. & Kolesnick, R. Raft ceramide in molecular medicine. *Oncogene* **22**, 7070-7077 (2003).
143. Jaffrezou, J.P. & Laurent, G. Ceramide : A New Target in Anticancer Research? *Bull Cancer* **91**, E133-161 (2004).
144. Schissel, S.L., Keesler, G.A., Schuchman, E.H., Williams, K.J. & Tabas, I. The cellular trafficking and zinc dependence of secretory and lysosomal sphingomyelinase, two products of the acid sphingomyelinase gene. *J Biol Chem* **273**, 18250-18259 (1998).
145. Vanier, M.T. & Suzuki, K. Niemann-Pick diseases. in *Neurodystrophies and Neurolipidoses*, Vol. 66(22) (ed. Moser, H.W.) 133-162 (Elsevier Science, Amsterdam, 1996).
146. Schuchman, E.H., Levran, O., Pereira, L.V. & Desnick, R.J. Structural organization and complete nucleotide sequence of the gene encoding human acid sphingomyelinase (SMPD1). *Genomics* **12**, 197-205 (1992).
147. Schuchman, E.H., Suchi, M., Takahashi, T., Sandhoff, K. & Desnick, R.J. Human acid sphingomyelinase. Isolation, nucleotide sequence and expression of the full-length and alternatively spliced cDNAs. *J Biol Chem* **266**, 8531-8539 (1991).
148. da Veiga Pereira, L., Desnick, R.J., Adler, D.A., Disteche, C.M. & Schuchman, E.H. Regional assignment of the human acid sphingomyelinase gene (SMPD1) by PCR analysis of somatic cell hybrids and in situ hybridization to 11p15.1----p15.4. *Genomics* **9**, 229-234 (1991).
149. Wan, Q. & Schuchman, E.H. A novel polymorphism in the human acid sphingomyelinase gene due to size variation of the signal peptide region. *Biochim Biophys Acta* **1270**, 207-210 (1995).
150. Langmann, T., *et al.* Transcription factors Sp1 and AP-2 mediate induction of acid sphingomyelinase during monocytic differentiation. *J Lipid Res* **40**, 870-880 (1999).
151. Simonaro, C.M., *et al.* Imprinting at the SMPD1 locus: Implications for Acid Sphingomyelinase-Deficient Niemann-Pick Disease. *Am J Hum Genet* **78**, 865-870 (2006).
152. Lee, C.Y., *et al.* Compound heterozygosity at the sphingomyelin phosphodiesterase-1 (SMPD1) gene is associated with low HDL cholesterol. *Hum Genet* **112**, 552-562 (2003).
153. Elleder, M. Niemann-Pick disease. *Pathol Res Pract* **185**, 293-328 (1989).
154. Vanier, M.T. & Millat, G. Niemann-Pick disease type C. *Clin Genet* **64**, 269-281 (2003).
155. Walton, D.S., Robb, R.M. & Crocker, A.C. Ocular manifestations of group A Niemann-Pick disease. *Am J Ophthalmol* **85**, 174-180 (1978).
156. Matthews, J.D., Weiter, J.J. & Kolodny, E.H. Macular halos associated with Niemann-Pick type B disease. *Ophthalmology* **93**, 933-937 (1986).
157. Lowe, D., Martin, F. & Sarks, J. Ocular manifestations of adult Niemann-Pick disease: a case report. *Aust N Z J Ophthalmol* **14**, 41-47 (1986).
158. McGovern, M.M., *et al.* Ocular manifestations of Niemann-Pick disease type B. *Ophthalmology* **111**, 1424-1427 (2004).
159. Elleder, M. The spleen in and storage disorders. in *Disorders of the spleen* (eds. Cuschieri, A. & Forbes, C.D.) 151-191 (Blackwell Scientific Publications, 1994).
160. Pavlu-Pereira, H., *et al.* Acid sphingomyelinase deficiency. Phenotype variability with prevalence of intermediate phenotype in a series of twenty-five Czech and Slovak patients. A multi-approach study. *J Inherit Metab Dis* **28**, 203-227 (2005).
161. Takahashi, T., *et al.* Heterogeneity of liver disorder in type B Niemann-Pick disease. *Hum Pathol* **28**, 385-388 (1997).
162. Elleder, M. & Jirasek, A. Niemann-Pick disease. *Acta Universitatis Carolinae Medica* **3-4**, 409-412 (1983).
163. McGovern, M.M., Aron, A., Brodie, S.E., Desnick, R.J. & Wasserstein, M.P. Natural history of Type A Niemann-Pick disease: possible endpoints for therapeutic trials. *Neurology* **66**, 228-232 (2006).
164. Simonaro, C.M., Desnick, R.J., McGovern, M.M., Wasserstein, M.P. & Schuchman, E.H. The demographics and distribution of type B Niemann-Pick disease: novel mutations lead to new genotype/phenotype correlations. *Am J Hum Genet* **71**, 1413-1419 (2002).

165. Rodriguez-Lafrasse, C. & Vanier, M.T. Sphingosylphosphorylcholine in Niemann-Pick disease brain: accumulation in type A but not in type B. *Neurochem Res* **24**, 199-205 (1999).
166. Pavlu, H. & Elleder, M. Two novel mutations in patients with atypical phenotypes of acid sphingomyelinase deficiency. *J Inherit Metab Dis* **20**, 615-616 (1997).
167. Wasserstein, M.P., *et al.* Acid sphingomyelinase deficiency: prevalence and characterization of an intermediate phenotype of Niemann-Pick disease. *J Pediatr* **149**, 554-559 (2006).
168. Harzer, K., *et al.* Niemann-Pick disease type A and B are clinically but also enzymatically heterogeneous: pitfall in the laboratory diagnosis of sphingomyelinase deficiency associated with the mutation Q292 K. *Neuropediatrics* **34**, 301-306 (2003).
169. Ferlinz, K., *et al.* Molecular analysis of the acid sphingomyelinase deficiency in a family with an intermediate form of Niemann-Pick disease. *Am J Hum Genet* **56**, 1343-1349 (1995).
170. Levran, O., Desnick, R.J. & Schuchman, E.H. Niemann-Pick type B disease. Identification of a single codon deletion in the acid sphingomyelinase gene and genotype/phenotype correlations in type A and B patients. *J Clin Invest* **88**, 806-810 (1991).
171. The Human Gene Mutation Database - http://www.hgmd.cf.ac.uk/
172. Levran, O., Desnick, R.J. & Schuchman, E.H. Identification and expression of a common missense mutation (L302P) in the acid sphingomyelinase gene of Ashkenazi Jewish type A Niemann-Pick disease patients. *Blood* **80**, 2081-2087 (1992).
173. Gluck, I., Zeigler, M., Bargal, R., Schiff, E. & Bach, G. Niemann Pick Disease type A in Israeli Arabs: 677delT, a common novel single mutation. Mutations in brief no. 161. Online. *Hum Mutat* **12**, 136 (1998).
174. Vanier, M.T., *et al.* Deletion of arginine (608) in acid sphingomyelinase is the prevalent mutation among Niemann-Pick disease type B patients from northern Africa. *Hum Genet* **92**, 325-330 (1993).
175. Goodman, R.M. *Genetic disorders among the Jewish people* (Johns Hopkins University Press, Baltimore, 1979).
176. Levran, O., Desnick, R.J. & Schuchman, E.H. Type A Niemann-Pick disease: a frameshift mutation in the acid sphingomyelinase gene (fsP330) occurs in Ashkenazi Jewish patients. *Hum Mutat* **2**, 317-319 (1993).
177. Fernandez-Burriel, M., *et al.* The R608del mutation in the acid sphingomyelinase gene (SMPD1) is the most prevalent among patients from Gran Canaria Island with Niemann-Pick disease type B. *Clin Genet* **63**, 235-236 (2003).
178. Dardis, A., *et al.* Functional in vitro characterization of 14 SMPD1 mutations identified in Italian patients affected by Niemann Pick Type B disease. *Hum Mutat* **26**, 164 (2005).
179. Vanier, M.T., Revol, A. & Fichet, M. Sphingomyelinase activities of various human tissues in control subjects and in Niemann-Pick disease - development and evaluation of a microprocedure. *Clin Chim Acta* **106**, 257-267 (1980).
180. van Diggelen, O.P., *et al.* A new fluorimetric enzyme assay for the diagnosis of Niemann-Pick A/B, with specificity of natural sphingomyelinase substrate. *J Inherit Metab Dis* **28**, 733-741 (2005).
181. Genzyme Corp - http://www.genzyme.com/
182. Thurberg, B.L., *et al.* Characterization of pre- and post-treatment pathology after enzyme replacement therapy for pompe disease. *Lab Invest* **86**, 1208-1220 (2006).
183. Hodges, B.L. & Cheng, S.H. Cell and gene-based therapies for the lysosomal storage diseases. *Curr Gene Ther* **6**, 227-241 (2006).
184. Passini, M.A., *et al.* AAV vector-mediated correction of brain pathology in a mouse model of Niemann-Pick A disease. *Mol Ther* **11**, 754-762 (2005).
185. Miranda, S.R., Erlich, S., Friedrich, V.L., Jr., Gatt, S. & Schuchman, E.H. Hematopoietic stem cell gene therapy leads to marked visceral organ improvements and a delayed onset of neurological abnormalities in the acid sphingomyelinase deficient mouse model of Niemann-Pick disease. *Gene Ther* **7**, 1768-1776 (2000).
186. Dodge, J.C., *et al.* Gene transfer of human acid sphingomyelinase corrects neuropathology and motor deficits in a mouse model of Niemann-Pick type A disease. *Proc Natl Acad Sci U S A* **102**, 17822-17827 (2005).
187. Shihabuddin, L.S., *et al.* Intracerebral transplantation of adult mouse neural progenitor cells into the Niemann-Pick-A mouse leads to a marked decrease in lysosomal storage pathology. *J Neurosci* **24**, 10642-10651 (2004).
188. PDB - Protein Data Bank - http://www.rcsb.org/pdb/
189. Davies, J.P., Levy, B. & Ioannou, Y.A. Evidence for a Niemann-pick C (NPC) gene family: identification and characterization of NPC1L1. *Genomics* **65**, 137-145 (2000).
190. Naureckiene, S., *et al.* Identification of HE1 as the second gene of niemann-pick C disease. *Science* **290**, 2298-2301. (2000).
191. Vanier, M.T. & Suzuki, K. Recent advances in elucidating Niemann-Pick C disease. *Brain Pathol* **8**, 163-174 (1998).
192. Vanier, M.T. & Millat, G. Structure and function of the NPC2 protein. *Biochim Biophys Acta* **1685**, 14-21 (2004).
193. Watari, H., *et al.* Determinants of NPC1 expression and action: key promoter regions, posttranscriptional control, and the importance of a "cysteine-rich" loop. *Exp Cell Res* **259**, 247-256 (2000).
194. Salvioli, R., *et al.* Glucosylceramidase mass and subcellular localization are modulated by cholesterol in Niemann-Pick disease type C. *J Biol Chem* **279**, 17674-17680 (2004).
195. Karten, B., Vance, D.E., Campenot, R.B. & Vance, J.E. Cholesterol accumulates in cell bodies, but is decreased in distal axons, of Niemann-Pick C1-deficient neurons. *J Neurochem* **83**, 1154-1163 (2002).
196. Zervas, M., Dobrenis, K. & Walkley, S.U. Neurons in Niemann-Pick disease type C accumulate gangliosides as well as unesterified cholesterol and undergo dendritic and axonal alterations. *J Neuropathol Exp Neurol* **60**, 49-64 (2001).
197. Bu, B., Li, J., Davies, P. & Vincent, I. Deregulation of cdk5, hyperphosphorylation, and cytoskeletal pathology in the Niemann-Pick type C murine model. *J Neurosci* **22**, 6515-6525 (2002).

198. Karten, B., Vance, D.E., Campenot, R.B. & Vance, J.E. Trafficking of cholesterol from cell bodies to distal axons in Niemann Pick C1-deficient neurons. *J Biol Chem* **278**, 4168-4175 (2003).
199. Sleat, D.E., *et al.* Genetic evidence for nonredundant functional cooperativity between NPC1 and NPC2 in lipid transport. *Proc Natl Acad Sci U S A* **101**, 5886-5891 (2004).
200. Sevin, M., *et al.* The adult form of Niemann-Pick disease type C. *Brain* **130**, 120-133 (2007).
201. Frohlich, E., Harzer, K., Heller, T. & Ruhl, U. [Ultrasound echogenic splenic tumors: nodular manifestation of type C Niemann-Pick disease]. *Ultraschall Med* **11**, 119-122 (1990).
202. Fensom, A.H., *et al.* An adult with a non-neuronopathic form of Niemann-Pick C disease. *J Inherit Metab Dis* **22**, 84-86 (1999).
203. Zervas, M., Somers, K.L., Thrall, M.A. & Walkley, S.U. Critical role for glycosphingolipids in Niemann-Pick disease type C. *Curr Biol* **11**, 1283-1287 (2001).
204. Bame, K.J. & Rome, L.H. Genetic evidence for transmembrane acetylation by lysosomes. *Science* **233**, 1087-1089 (1986).
205. Meikle, P.J., Whittle, A.M. & Hopwood, J.J. Human acetyl-coenzyme A:alpha-glucosaminide N-acetyltransferase. Kinetic characterization and mechanistic interpretation. *Biochem J* **308** (Pt 1), 327-333 (1995).
206. Jensen, L.J., *et al.* Prediction of human protein function from post-translational modifications and localization features. *J Mol Biol* **319**, 1257-1265 (2002).
207. Schwartz, S., *et al.* PipMaker--a web server for aligning two genomic DNA sequences. *Genome Res* **10**, 577-586 (2000).
208. Frazer, K.A., Pachter, L., Poliakov, A., Rubin, E.M. & Dubchak, I. VISTA: computational tools for comparative genomics. *Nucleic Acids Res* **32**, W273-279 (2004).
209. Kahsay, R.Y., Gao, G. & Liao, L. An improved hidden Markov model for transmembrane protein detection and topology prediction and its applications to complete genomes. *Bioinformatics* **21**, 1853-1858 (2005).
210. Blom, N., Sicheritz-Ponten, T., Gupta, R., Gammeltoft, S. & Brunak, S. Prediction of post-translational glycosylation and phosphorylation of proteins from the amino acid sequence. *Proteomics* 4, 1633-1649 (2004).
211. Ensembl Genome Browser - http://www.ensembl.org/
212. Thompson, J.D., Higgins, D.G. & Gibson, T.J. CLUSTAL W: improving the sensitivity of progressive multiple sequence alignment through sequence weighting, position-specific gap penalties and weight matrix choice. *Nucleic Acids Res* **22**, 4673-4680 (1994).
213. Caenorhabditis Elegans: Modern Biological Analysis of an Organism. in *Methods in Cell Biology*, Vol. 48 (eds. Wilson, L. & Matsudaira, P.) (1995).
214. Kuwabara, P.E. & O'Neil, N. The use of functional genomics in C. elegans for studying human development and disease. *J Inherit Metab Dis* **24**, 127-138. (2001).
215. Genome sequence of the nematode C. elegans: a platform for investigating biology. The C. elegans Sequencing Consortium. *Science* **282**, 2012-2018. (1998).
216. Kamath, R.S., Martinez-Campos, M., Zipperlen, P., Fraser, A.G. & Ahringer, J. Effectiveness of specific RNA-mediated interference through ingested double-stranded RNA in Caenorhabditis elegans. *Genome Biol* **2**(2000).
217. Fire, A., *et al.* Potent and specific genetic interference by double-stranded RNA in Caenorhabditis elegans. *Nature* **391**, 806-811. (1998).
218. Ruvkun, G. & Hobert, O. The taxonomy of developmental control in Caenorhabditis elegans. *Science* **282**, 2033-2041 (1998).
219. Brenner, S. The genetics of Caenorhabditis elegans. *Genetics* 77, 71-94. (1974).
220. Chalfie, M., Tu, Y., Euskirchen, G., Ward, W.W. & Prasher, D.C. Green fluorescent protein as a marker for gene expression. *Science* **263**, 802-805 (1994).
221. Wormbase - http://www.wormbase.org/
222. C.elegans Gene Knock-out Consortium - http://www.celeganskoconsortium.omrf.org/default.aspx
223. Mushegian, A.R., Garey, J.R., Martin, J. & Liu, L.X. Large-scale taxonomic profiling of eukaryotic model organisms: a comparison of orthologous proteins encoded by the human, fly, nematode, and yeast genomes. *Genome Res* **8**, 590-598. (1998).
224. Liu, G., Wong-Staal, F. & Li, Q.X. Development of new RNAi therapeutics. *Histol Histopathol* **22**, 211-217 (2007).
225. Grishok, A., Tabara, H. & Mello, C.C. Genetic requirements for inheritance of RNAi in C. elegans. *Science* **287**, 2494-2497. (2000).
226. Timmons, L., Court, D.L. & Fire, A. Ingestion of bacterially expressed dsRNAs can produce specific and potent genetic interference in Caenorhabditis elegans. *Gene* **263**, 103-112. (2001).
227. Jackson, A.L. & Linsley, P.S. Noise amidst the silence: off-target effects of siRNAs? *Trends Genet* **20**, 521-524 (2004).
228. Salcini, A.E., *et al.* The Eps15 C. elegans homologue EHS-1 is implicated in synaptic vesicle recycling. *Nat Cell Biol* **3**, 755-760. (2001).
229. Zhang, Y., Grant, B. & Hirsh, D. RME-8, a conserved J-domain protein, is required for endocytosis in Caenorhabditis elegans. *Mol Biol Cell* **12**, 2011-2021 (2001).
230. Grant, B., *et al.* Evidence that RME-1, a conserved C. elegans EH-domain protein, functions in endocytic recycling. *Nat Cell Biol* **3**, 573-579. (2001).
231. Clark, S.G., Shurland, D.L., Meyerowitz, E.M., Bargmann, C.I. & van der Bliek, A.M. A dynamin GTPase mutation causes a rapid and reversible temperature-inducible locomotion defect in C. elegans. *Proc Natl Acad Sci U S A* **94**, 10438-10443. (1997).

232. Grant, B. & Hirsh, D. Receptor-mediated endocytosis in the Caenorhabditis elegans oocyte. *Mol Biol Cell* **10**, 4311-4326. (1999).
233. Rugarli, E.I., *et al.* The Kallmann syndrome gene homolog in C. elegans is involved in epidermal morphogenesis and neurite branching. *Development* **129**, 1283-1294 (2002).
234. Sym, M., Basson, M. & Johnson, C. A model for niemann-pick type C disease in the nematode Caenorhabditis elegans. *Curr Biol* **10**, 527-530. (2000).
235. de Voer, G., *et al.* Deletion of the Caenorhabditis elegans homologues of the CLN3 gene, involved in human juvenile neuronal ceroid lipofuscinosis, causes a mild progeric phenotype. *J Inherit Metab Dis* **28**, 1065-1080 (2005).
236. Lin, X., Hengartner, M.O. & Kolesnick, R. Caenorhabditis elegans contains two distinct acid sphingomyelinases. *J Biol Chem* **273**, 14374-14379 (1998).
237. Jacobson, L.A., *et al.* Identification of a putative structural gene for cathepsin D in Caenorhabditis elegans. *Genetics* **119**, 355-363. (1988).
238. Kostich, M., Fire, A. & Fambrough, D.M. Identification and molecular-genetic characterization of a LAMP/CD68-like protein from Caenorhabditis elegans. *J Cell Sci* **113**, 2595-2606. (2000).
239. Treusch, S., *et al.* Caenorhabditis elegans functional orthologue of human protein h-mucolipin-1 is required for lysosome biogenesis. *Proc Natl Acad Sci U S A* **101**, 4483-4488 (2004).
240. Schaheen, L., Dang, H. & Fares, H. Basis of lethality in C. elegans lacking CUP-5, the Mucolipidosis Type IV orthologue. *Dev Biol* **293**, 382-391 (2006).
241. Fares, H. & Greenwald, I. Genetic analysis of endocytosis in Caenorhabditis elegans: coelomocyte uptake defective mutants. *Genetics* **159**, 133-145 (2001).
242. Fares, H. & Greenwald, I. Regulation of endocytosis by CUP-5, the Caenorhabditis elegans mucolipin-1 homolog. *Nat Genet* **28**, 64-68 (2001).
243. Hersh, B.M., Hartwieg, E. & Horvitz, H.R. The Caenorhabditis elegans mucolipin-like gene cup-5 is essential for viability and regulates lysosomes in multiple cell types. *Proc Natl Acad Sci U S A* 99, 4355-4360 (2002).
244. Protein families database of alignments and HMMs - http://www.sanger.ac.uk/cgi-bin/Pfam/
245. Desnick, R.J. & Schindler, D. α-N-Acetylgalactosaminidase Deficiency: Schindler Disease. in *The Metabolic & Molecular Bases of Inherited Disease*, Vol. 3 (eds. Scriver, C.R., Beaudet, A.L., Sly, W.S. & Valle, D.) 3483-3506 (McGraw-Hill Companies, Inc., New York, 2001).
246. Desnick, R.J., Ioannou, Y.A. & Eng, C.M. α-Galactosidase A Deficiency: Fabry Disease. in *The Metabolic & Molecular Bases of Inherited Disease*, Vol. 3 (eds. Scriver, C.R., Beaudet, A.L., Sly, W.S. & Valle, D.) 3733-3774 (McGraw-Hill Companies, Inc., New York, 2001).
247. Asfaw, B., *et al.* Defects in degradation of blood group A and B glycosphingolipids in Schindler and Fabry diseases. *J Lipid Res* **43**, 1096-1104 (2002).
248. Wormbase BLAST or BLAT Search - http://www.wormbase.org/db/searches/blat
249. Felsenstein, J. PHYLIP - Phylogeny Inference Package (Version 3.2). *Cladistics* **5**, 164-166 (1988).
250. Kneen, M., Farinas, J., Li, Y. & Verkman, A.S. Green fluorescent protein as a noninvasive intracellular pH indicator. *Biophys J* 74, 1591-1599 (1998).
251. Demaurex, N. pH Homeostasis of cellular organelles. *News Physiol Sci* **17**, 1-5 (2002).
252. Kaletta, T. & Hengartner, M.O. Finding function in novel targets: C. elegans as a model organism. *Nat Rev Drug Discov* **5**, 387-398 (2006).
253. Barr, M.M. & Sternberg, P.W. A polycystic kidney-disease gene homologue required for male mating behaviour in C. elegans. *Nature* **401**, 386-389 (1999).
254. Barr, M.M., *et al.* The Caenorhabditis elegans autosomal dominant polycystic kidney disease gene homologs lov-1 and pkd-2 act in the same pathway. *Curr Biol* **11**, 1341-1346 (2001).
255. Barr, M.M. Caenorhabditis elegans as a model to study renal development and disease: sexy cilia. *J Am Soc Nephrol* **16**, 305-312 (2005).

9 List of author's publications and presentations

9.1 *Appended publications related to the thesis (sorted chronologically, IF 2006):*

Sikora J, Pavlů-Pereira H, Elleder M, Roelofs H, Wevers RA (2003) Seven novel acid sphingomyelinase gene mutations in Niemann-Pick type A and B patients. *Ann Hum Genet.* 67:63-70
IF - 3.192
cited by:
Jensen JM, *et al. Exp Dermatol.* 2005; 14: 609-18
Seto M, *et al. Protein Sci.* 2004; 13:3172-86.
Ricci V, *et al. Hum Mutat.* 2004
Pittis MG, *et al. Hum Mutat.* 2004

Hujová J*, **Sikora J***, Dobrovolný R*, Poupětová H, Ledvinová J, Kostrouchová M, Hřebíček M (2005) Characterization of gana-1, a Caenorhabditis elegans gene encoding a single ortholog of vertebrate alpha-galactosidase and alpha-N-acetylgalactosaminidase. *BMC Cell Biol.* 6:5
*** contributed equally**
IF – 2.652
cited by:
Kaleta T, *et al. Nature Rev Drug Discov.* 2006

Pavlů-Pereira H, Asfaw B, Poupětová H, Ledvinová J, **Sikora J**, Vanier MT, Sandhoff K, Zeman J, Novotná Z, Chudoba D, Elleder M (2005) Acid sphingomyelinase deficiency. Phenotype variability with prevalence of intermediate phenotype in a series of twenty-five Czech and Slovak patients. A multi-approach study. *J Inherit Metab Dis.* 28:203-227
IF – 1.722
cited by:
van Diggelen OP, *et al. J Inherit Metab Dis.* 2005; 28: 733-41
Wasserstein MP, *et al. J Pediatrics.* 2006; 149: 554-59

Dvořáková L, **Sikora J**, Hřebíček M, Hůlková H, Boučková M, Stolnaja L, Elleder M (2006) Subclinical course of adult visceral Niemann-Pick type C1 disease. A rare or underdiagnosed disorder? *J Inherit Metab Dis.* 29:591
IF – 1.722
cited by:
Sevin M, *et al. Brain* 2007; 130: 120-33

Hřebíček M, Mrázová L, Seyrantepe V, Durand S, Roslin NM, Nosková L, Hartmannová H, Ivánek R, Čížková A, Poupětová H, **Sikora J**, Uřinovská J, Stránecký V, Zeman J, Lepage P, Roquis D, Verner A, Ausseil J, Beesley CE, Maire I, Poorthuis BJ, van de Kamp J, van Diggelen OP, Wevers RA, Hudson TJ, Fujiwara TM, Majewski J, Morgan K, Kmoch S, Pshezhetsky AV (2006) Mutations in TMEM76 Cause Mucopolysaccharidosis IIIC (Sanfilippo C Syndrome). *Am J Hum Genet.* 79:807-819
IF – 12.649

Sikora J, Harzer K, Elleder M (2007) Neurolysosomal pathology in human prosaposin deficiency suggests essential neurotrophic function of prosaposin. *Acta Neuropathol (Berl).* 113: 163-175
IF – 2.527

9.2 Other publications (sorted chronologically, IF 2006)

Franková V, Serbinová I, Matěj R, Koukolík F, **Sikora J**, Belšan T (2004) Creutzfeldtova-Jakobova nemoc, kazuistika familiární formy onemocnění. *Psychiatrie pro praxi* :317-321

Libý P, Kostrouchová M, Pohludka M, Yilma P, Hrabal P, **Sikora J**, Brožová E, Rall JE, Kostrouch Z (2006) Elevated and deregulated expression of HDAC3 in human astrocytic glial tumours. *Folia Biol (Praha).* 52:21-33
IF – 0.719

Vylet'al P, Kublová M, Kalbáčová M, Hodaňová K, Barešová V, Stibůrková B, **Sikora J**, Hůlková H, Živný J, Majewski J, Simmonds A, Fryns JP, Venkat-Raman G, Elleder M, Kmoch S (2006) Alterations of uromodulin biology: a common denominator of the genetically heterogeneous FJHN/MCKD syndrome. *Kidney Int.* 70:1155-1169
IF – 4.927
cited by:
Kumar S, 2007, *J Am Soc Nephrol.* 18:10-2

Sikora J, Srbová A, Koukolík F, Matěj R (2006) Retrospective sequence analysis of the human PRNP gene from the formaldehyde-fixed paraffin embedded tissues: report of two cases of Creutzfeldt-Jakob Disease. *Folia Microbiol.* 51:619-625
IF – 0.918

Sikora J, Dvořáková L, Vlášková H, Stolnaja L, Betlach J, Špaček J, Elleder M (2007) A case of excessive autophagocytosis with multiorgan involvement and low clinical penetrance. *Cesk Patol. (accepted to press)*

9.3 Published abstracts

Sikora J, Perereira H, Elleder M
Mutational analysis of six Niemann-Pick disease type A nad B patients of Dutch and Turkish origin.
XVII. International Congress of Czech Society for Biochemistry and Molecular Biology, September 2000, Prague, Czech Republic
Chem. listy 94, 543, (2000).

Sikora J, Perereira H, Elleder M, Wevers RA
Mutational analysis of 30 Niemann-Pick type A and B patients – 21 novel mutations.
10th International Congress of Human Genetics, May 2001, Vienna, Austria
Eur J Hum Genet. 2001, 9, Suppl.1.

Sikora J, Hujová J, Dobrovolný R, Holanová D, Asfaw B, Poupětová H, Ledvinová J, Kostrouchová M, Hřebíček M
Caenorhabditis elegans as a model for lysosomal glycosidase deficiencies.
European Human Genetics Conference 2003, May 2003, Birminhgham, UK
Eur J Hum Genet. 2003, 11, Suppl.1.

Hřebíček M, **Sikora J**, Hujová J, Holanová D, Poupětová H, Asfaw B, Ledvinová J, Kostrouchová M
Evaluation of *Caenorhabditis elegans* model for lysosomal diseases caused by deficits of glycosidases.
American Society of Human Genetics Conference 2003, November 2003, Los Angeles, USA
Am J Hum Genet. 2003, 73:348-348

9.4 Other selected presentations

Pavlů-Pereira H, **Sikora J** and Elleder M
Mutational analysis of Czech and Slovak patients with acid sphingomyelinase deficiency.
12th ESGLD workshop, September 1999, Vidago, Portugal

Elleder M, Pavlů-Perreira H, **Sikora J**, Asfaw B, Poupětová H, Berná L
Sphingomyelinase deficiency- genotype and multilevel phenotype study of 25 Czech and Slovak patients
13th ESGLD workshop, September 2001, Woudschoten, Netherlands

Sikora J, Hujová J, Dobrovolný R, Holanová D, Befekadu A, Poupětová H, Ledvinová J, Kostrouchová M, Hřebíček M
Caenorhabditis elegans as a model for lysosomal glycosidase deficiencies
18. pracovní dny Dědičné Metabolické Poruchy, May 2003, Slušovice, Czech Republic
First price for the scientists under 30 years of age

Sikora J, Hujová J, Dobrovolný R, Holanová D, Befekadu A, Poupětová H, Ledvinová J, Kostrouchová M, Hřebíček M
Caenorhabditis elegans as a model for acid α–glucosidase deficiency
14th ESGLD Workshop, September 2003, Poděbrady, Czech Republic

Hujová J, Dobrovolný R, **Sikora J**, Holanová D, Befekadu A, Poupětová H, Ledvinová J, Kostrouchová M, Hřebíček M
Caenorhabditis elegans as a model for Fabry and Schindler diseases
14th ESGLD Workshop, September 2003, Poděbrady, Czech Republic

Hujová J, Dobrovolný R, **Sikora J**, Holanová D, Befekadu.A, Poupětová H, Ledvinová J
Caenorhabditis elegans has only one alpha galactosidase and alpha N-acetylgalactosaminidase ortholog
5th students´ scientific conference 1.LF UK, April 2004, Prague, Czech Republic
1st price (PhD students´ section)

Elleder M, **Sikora J**, Harzer K
Neurolysosomes in human prosaposin deficiency

15th ESGLD Workshop, September 2005, Oslo, Norway

Sikora J, Elleder M
Vacuolar autophagic disorder with predominant involvement of liver, heart, and smooth muscle. Accidental autopsy finding in an elderly patient.
15th ESGLD Workshop, September 2005, Oslo, Norway

Sikora J, Dvořáková L, Hřebíček M, Boučková M, Stolnaja L, Matěj R, Srbová A, Koukolik F, Elleder M
Úskalí sekvenční analýzy DNA z formolem fixovanyýh tkání: praktické aplikace na příkladu familiálni formy Creutzfeldt-Jakobovy choroby a netypických forem Niemann-Pickovy choroby typu C.
Molekulární patologie začátku III. tisíciletí: využití bioptických vzorků pro molekulární analýzu, April 2005, Olomouc, Czech Republic

Sikora J, Elleder M
A case of excessive autophagy with multiorgan involvement and low clinical penetrance. A novel lysosomal disorder?
33rd Congress of the Czech Society of Pathologists and 2nd Satellite Symposium and Workshop on Molecular Pathology, May 2006, Olomouc, Czech Republic

10 Appended publications

Acta Neuropathol (2007) 113:163–175
DOI 10.1007/s00401-006-0148-7

ORIGINAL PAPER

Neurolysosomal pathology in human prosaposin deficiency suggests essential neurotrophic function of prosaposin

Jakub Sikora · Klaus Harzer · Milan Elleder

Received: 28 June 2006 / Revised: 15 August 2006 / Accepted: 29 August 2006 / Published online: 6 October 2006

Abstract A neuropathologic study of three cases of prosaposin (pSap) deficiency (ages at death 27, 89 and 119 days), carried out in the standard autopsy tissues, revealed a neurolysosomal pathology different from that in the non-neuronal cells. Non-neuronal storage is represented by massive lysosomal accumulation of glycosphingolipids (glucosyl-, galactosyl-, lactosyl-, globotriaosylceramides, sulphatide, and ceramide). The lysosomes in the central and peripheral neurons were distended by pleomorphic non-lipid aggregates lacking specific staining and autofluorescence. Lipid storage was borderline in case 1, and at a low level in the other cases. Neurolysosomal storage was associated with massive ubiquitination, which was absent in the non-neuronal cells and which did not display any immunohistochemical aggresomal properties. Confocal microscopy and cross-correlation function analyses revealed a positive correlation between the ubiquitin signal and the late endosomal/lysosomal markers. We suppose that the neuropathology most probably reflects excessive influx of non-lipid material (either in bulk or as individual molecules) into the neurolysosomes. The cortical neurons appeared to be uniquely vulnerable to pSap deficiency. Whereas in case 1 they populated the cortex, in cases 2 and 3 they had been replaced by dense populations of both phagocytic microglia and astrocytes. We suggest that this massive neuronal loss reflects a cortical neuronal survival crisis precipitated by the lack of pSap. The results of our study may extend the knowledge of the neurotrophic function of pSap, which should be considered essential for the survival and maintenance of human cortical neurons.

Keywords Prosaposin deficiency · Neurolysosomal disorder · Ubiquitination · Cross-correlation function · Cortical neuronal survival crisis

J. Sikora · M. Elleder (✉)
Institute of Inherited Metabolic Disorders,
1st Faculty of Medicine, Charles University and
General Teaching Hospital, Ke Karlovu 2,
Prague 2, 12808, Czech Republic
e-mail: melleder@beba.cesnet.cz

K. Harzer
Neurometabolic Laboratory,
Department of Pediatrics and Child Development
(Universitäts-Kinderklinik), University of Tubingen,
Tübingen, 72076, Germany

Introduction

Prosaposin (pSap) deficiency is a rapidly progressive fatal neurovisceral lysosomal storage disorder caused by mutations in the *PSAP* gene which leads to the blockage of pSap protein translation or to the premature (intranuclear) nonsense-mediated decay of pSap mRNA [13, 25, 43, 54]. The proven genotypes result in the absence of pSap and the products of pSap proteolytic processing. These polypeptide products, called saposins (Saps, sphingolipidhydrolase activating proteins), are essential for activating a set of lysosomal sphingolipid hydrolases [54]. In the absence of Saps, the sphingolipid substrates remain undegraded. The accumulated substrates, in visceral cell types, cause the lysosomes to become distended, giving them a foamy appearance and the process ultimately ends in organ failure, similar to full blown classic lipid storage disorders [3, 13, 25]. In this study, we show that in pSap deficiency the neurolysosomes of both the peripheral and

central neurons express a distinct pathology, which may indicate a process resembling autophagocytosis. Given the opportunity to compare the cortical structure at the earliest stage of the disease to that in the more advanced stages, we were able to describe a unique failure of cortical neurons to survive after reaching the cerebral cortex. We would like to characterize this destructive phenomenon, precipitated by the absence of pSap, as a cortical neuronal survival crisis, which seems to be a feature of human pSap deficiency. This fits well with the concept of pSap having fundamental neurotrophic functions [47].

Materials and methods

Formaldehyde fixed paraffin embedded (FFPE) tissue samples were available from three cases of verified pSap deficiency. The life spans of the cases were: 27 days (case 1 [14]), 89 days (case 2 [25]) and 119 days (case 3 [13]). In two of the three cases (27, 119 days) we were kindly provided by colleagues from the pathology departments unembedded routinely formaldehyde fixed samples of several cortical and subcortical brain areas. The tissue samples available were as follows: case 1 (27 days)–parts of the frontal and insular cortex, striatum, pallidum, thalamus, and adjacent parts of the white matter; case 2 (89 days)–several cortical samples, thalamus, and basal ganglia; and case 3 (119 days)–cerebral cortex from all lobes, cerebellum, pons, medulla oblongata and spinal cord.

Histology, immunohistochemistry, electron microscopy and lipid biochemistry

The tissue sections (5 μm) were dewaxed, hydrated and hematoxylin-eosin stained. The primary antibodies and their respective dilutions used for immunohistochemistry are listed in Table 1. The primary antibodies (incubated overnight at 4°C) were detected with

Table 1 Dilutions and sources of antibodies

Antigen (Antibody clone)	Source	Dilution	
		IH	*IF*
LAMP 1 (rabbit polyclonal)	kindly provided by Dr.S.Carlsson (University of Umea, Sweden)	1:200	
LAMP 2 (rabbit polyclonal)	kindly provided by Dr.S.Carlsson	1:200	1:100
Cathepsin D (rabbit polyclonal)	DAKO, Copenhagen, Denmark	1:4000	
Cathepsin D (MCA2068)	Serotec, Raleigh, NC, USA		1:50
Ubiquitin (rabbit polyclonal)	DAKO, Copenhagen, Denmark	1:1500	1:500
Ubiquitin (FPM1)	Novocastra, Newcastle upon Tyne, United Kingdom	1:100	1:100
Poly ubiquitinylated proteins (FK1) [16]	Biomol, Plymouth Meeting, PA, USA	1:500	
Mono- and poly ubiquitinylated proteins (FK2) [16]	Biomol, Plymouth Meeting, PA, USA	1:1000	
LC3 (rabbit polyclonal) [27]	MBL, Naka-ku Nagoya, Japan	1:500	
Glial fibrillary acidic protein - GFAP (6F2)	DAKO, Copenhagen, Denmark	1:200	
GFAP (rabbit polyclonal)	DAKO, Copenhagen, Denmark		1:500
CD68 (PGM1)	DAKO, Copenhagen, Denmark	1:200	1:200
Neuron specific nuclear protein – NeuN (A60)	Chemicon Int., Temecula, CA, USA	1:500	
Prohibitin (11-14–10)	Lab Vision, Westinghouse, CA, USA	1:500	
60 kDa antigen of human mitochondria (113–1)	Biogenex, San Ramon, CA, USA	1:100	1:50
Subunit c of mitochondrial ATP synthase - SCMAS	kindly provided by prof. E.Kominami (Juntendo University, Tokyo, Japan)	1:200	
p62 component of aggresome (guinea pig polyclonal) [67]	Progen, Heidelberg, Germany	1:4000	
Activated caspase 3 (rabbit monoclonal)	Epitomics, Burlingame, CA, USA	1:25	
Protein disulfide isomerase (PDI) (1D3)	Stressgen, Victoria, Canada		1:500

IH immunohistochemistry, *IF* immunofluorescence

appropriate Envision ™ kits (DAKO, Copenhagen, Denmark) or rabbit anti-guinea pig HRP labeled secondary antibody (DAKO).

In conjunction, various neurolysosomal storage disorders (previously defined biochemically at the Institute of Inherited Metabolic Disorders) were studied to follow neuronal ubiquitination (for the list, see Results). The FFPE tissue samples from various parts of the brain were examined together with the samples of storage affected visceral organs.

The sections of the formaldehyde fixed unembedded samples (cases 1 and 2) were processed for electron microscopy after osmification, using standard dehydration in ethanol and embedding in an Araldite–Epon mixture. The paraffin embedded samples of the pons (case 3) were processed for electron microscopy after deparaffination, hydration, and osmification.

The residual lipids extracted from the paraffin embedded brain samples were analyzed using a procedure recently described [13].

Immunofluorescence and laser scanning confocal microscopy

The FFPE paraffin embedded tissue sample from the spinal cord (case 3) was chosen for immunofluorescence multiple labeling colocalization analysis. The tissue sections were treated as described above. The primary antibodies and their dilutions used for immunofluorescence labeling are listed in Table 1.

The combinations of the primary antibodies were as follows: anti-LAMP2/anti-ubiquitin, anti-cathepsin D/anti-ubiquitin, anti-LAMP2/anti-60 kDa antigen of human mitochondria, anti-PDI/anti-ubiquitin, anti-60 kDa antigen of human mitochondria/anti-ubiquitin. The details of the tissue section processing and staining protocol for both immunohistochemistry and immunofluorescence labeling are available from the authors upon request.

Images (xy sampled at the maximum of z fluorescence intensity) were acquired using a Nikon Eclipse E800 microscope equipped with a C1 confocal head and 488, 543 and 633 nm laser lines and appropriate 515 ± 15 nm, 590 ± 15 nm and 650LP band pass filters. The sampling density was corrected to conform to the Nyquist criterion according to the objective lens used (Nikon Plan Apo 60 × 1.4 N.A.). The microscope settings including laser intensity, pinhole size, pixel dwell times; photomultiplier gains were kept constant for all image acquisitions and the images were checked for the presence of spectral cross-talk.

Point spread functions (PSF) at appropriate excitation/detection wavelengths were measured using PS-Speck Microscope Point Source Kit (Invitrogen- Molecular Probes, Carlsbad, CA).

The cerebral cortex sample from (case 2, day 89) was double-labeled with mouse monoclonal anti-CD 68 and rabbit polyclonal anti-GFAP antibodies. Secondary detections were performed using donkey anti-mouse IgG Alexa Fluor 555 and goat anti-rabbit IgG Alexa Fluor 488 antibodies (Invitrogen- Molecular Probes, Carlsbad, CA) diluted 1:500.

Image restoration, processing and cross-correlation function (CCF) analysis

Between 25 and 30 images of neurons of the spinal cord anterior columns were acquired and further processed for each of the double-labeling experiments. The images were restored based on deconvolution using an appropriately measured PSF with a classical maximum likelihood estimate algorithm (Huygens Professional software, SVI, Hilversum, Netherlands). Only pixels included in the neurons were further evaluated without any additional thresholding or pixel intensity manipulation. Cross-correlation function analysis [65] was performed using a Tcl/Tk script employing the Huygens Scripting modality in Huygens Professional software. Single pixel shifts with parallel Pearson's coefficient calculations were applied to the red channel of the images with respect to the green channel to the extent of −4 to +4 μm (only values −3 to +3 μm are shown, Fig. 5). The appropriate pixel shifted Pearson's coefficient values were calculated for each individual evaluated shifted image. The median values and 5/95 percentile values and first and third quartile values of Pearson's coefficient were plotted on the y axis for each single pixel shifted position (x axis) to get the final cross-correlation curves and to document the distribution of the values.

The Pearson's coefficient values range from −1 to +1. Positive Pearson's coefficient values at $\Delta x = 0$ demonstrate significant overlap (colocalization) of the signals, negative values demonstrate repulsion (anti-colocalization) of the signals, and values around zero demonstrate a random distribution of signals. The details of the Tcl/Tk script used to calculate CCF is available from the authors upon request. All the image manipulations and figure preparations were performed using Huygens Professional or ImageJ (NIH, http://www.rsb.info.nih.gov/ij/) software.

In order to avoid any ambiguity, the use of neurolysosomal in this paper refers to the lysosomal compartment of neurons.

Results

General neuropathology

The general neuropathologic findings in all the three cases have already been published [13, 14, 25]. However, to briefly summarize, the neuronal perikarya were variably distended by fine eosinophilic non-autofluorescent granules (Figs. 1a inset, 2a). Neuronal storage was present in all the regions available for examination: brain cortex (see below), basal ganglia, thalamus, pons, medulla oblongata, spinal cord, and cerebellum. The only exception was the subventricular zone (cases 1 and 2) which was cellular and devoid of histological and immunohistochemical abnormalities. There was a marked difference between the brain cortical pathology in case 1 as compared to cases 2 and 3 (see below). Storage was manifested in the peripheral nervous system in all samples available (gut, lung, liver, kidney, and urinary bladder).

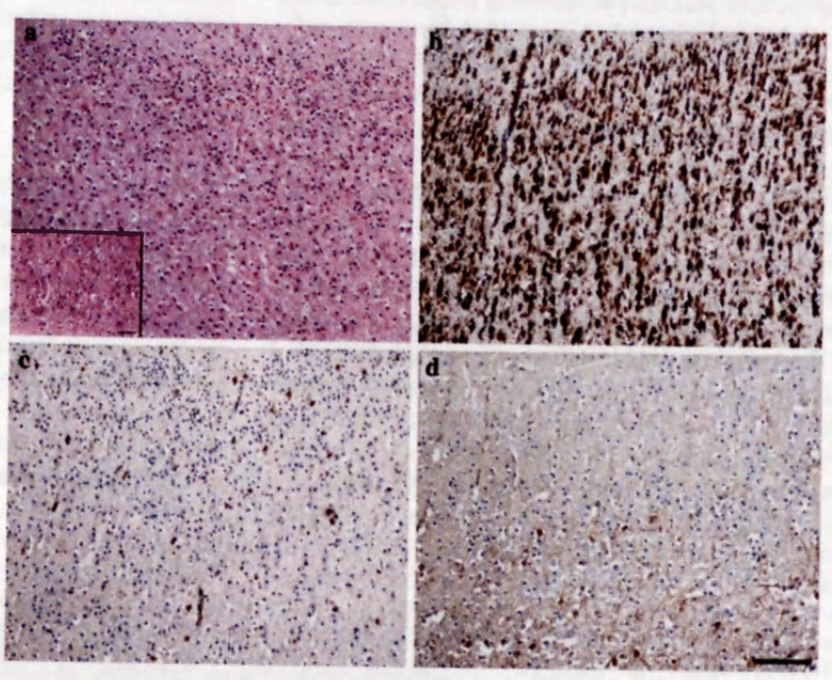

Fig. 1 Cortex in case 1 (day 27) in pSAP deficiency. **a** Numerous cortical neurons with a rather normal architecture. Discrete neuronal storage accented in basal layers (*inset*); H&E. **b** Strong neuronal perikaryal staining for cathepsin D. **c** Paucity of microglial phagocytes demonstrated by CD 68 antibody (clone PGM1), and **d** of astroglia stained with GFAP antibody. **a**–**d** correspond to the identical cortical area. Scale bar 200 μm **a**–**d**. Scale bar in inset in (a) 100 μm

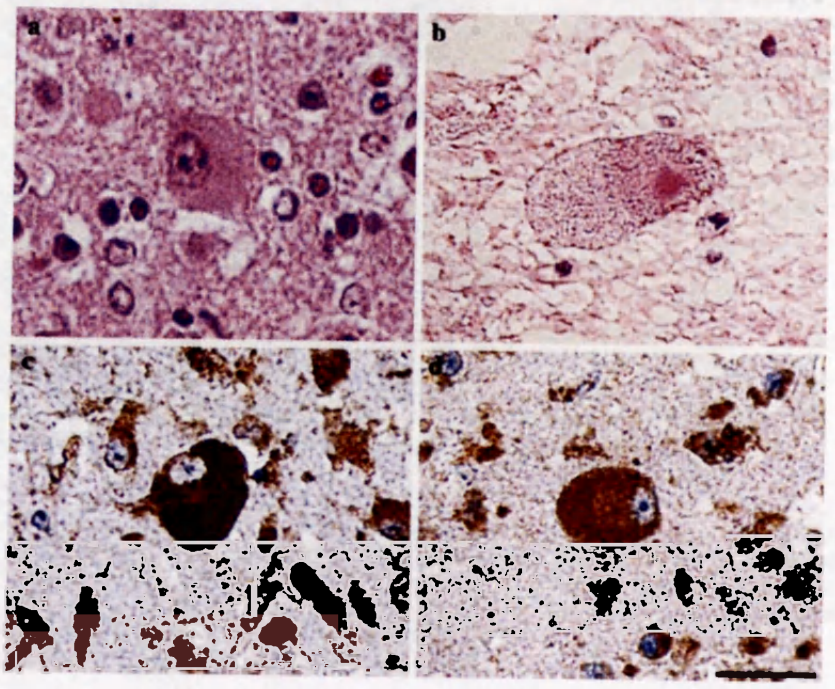

Fig. 2 Neuronal cytology and immunodetection of lysosomal markers in pSAP deficiency. **a** Case 1 (day 27): a subcortical storage neuron with the perikaryal region distended by fine granules; H&E. **b** Case 3 (day 119): storage in spinal motor neuron with a granulovacuolar appearance of the perikaryon. **c** Case 1 (day 27): strong staining of the perikaryal granules for cathepsin D and for LAMP 2 **d**. Scale bar 50 μm

The following data represent novel and previously unreported features of the neurolysosomal storage process in pSap deficiency.

Study on the nature of neurolysosomal processes

Cytology, electron microscopy and lipid biochemistry

Contrary to the foamy appearance of the storage cells in the visceral region, the neuronal perikarya were distended even ballooned by a uniform population of fine eosinophilic granules. In case 3, their appearance changed to granulovacuolar (Fig. 2b). The granules were not autofluorescent and did not exhibit any distinct staining in routine histological stainings. Lipid histochemistry showed an absence of birefringence and no significant detectable amounts of glycolipids and sphingolipids [14].

In contrast to the neurons the astrocytes displayed significantly milder storage changes [13, 25]. Regarding the oligodendroglia, the lysosomal storage has never been demonstrated [13, 17]. Changes of microglial phagocytes are discussed below.

Electron microscopy (cases 1 and 2) showed vacuoles approximately 0.5 μm in diameter containing numerous dense granules of various densities, 45–230 nm in diameter, sometimes with amorphous or coarse membranous substructure, occasionally resembling degraded mitochondria (Fig. 3). Identical structures were observed in the dystrophic axons. Other organelles (RER, Golgi aparatus), while reduced in number, were without substantial alteration. Electron microscopy of dewaxed pontine samples (case 3) showed similar structures. The only difference was an increase of electron lucent space in the storage compartment leading to granulovacuolar neuronal cytology and an increase in the size of individual storage lysosomes, up to 1 μm in diameter on average. The ultrastructure differed from the ultrastructure of the lysosomes in the visceral storage cells [25] and from the lysosomes of the other known neurolysosomal storage disorders featured by membranous lipid deposits.

Biochemical analysis of residual lipids in FFPE samples from the pons (case 3, day 119) which were rich in ballooned granulovacuolar neurons, revealed a threefold to sixfold elevation of gangliosides (G_{M1}, G_{M2}, G_{M3} types), lactosylceramide and globotriaosylceramide as compared to the controls (data not shown). At this point we must note some limitations of the analysis caused by previous dehydrations, as well as the potential contribution (although minor) to the overall lipid content of non-neuronal storage elements present in the tissue.

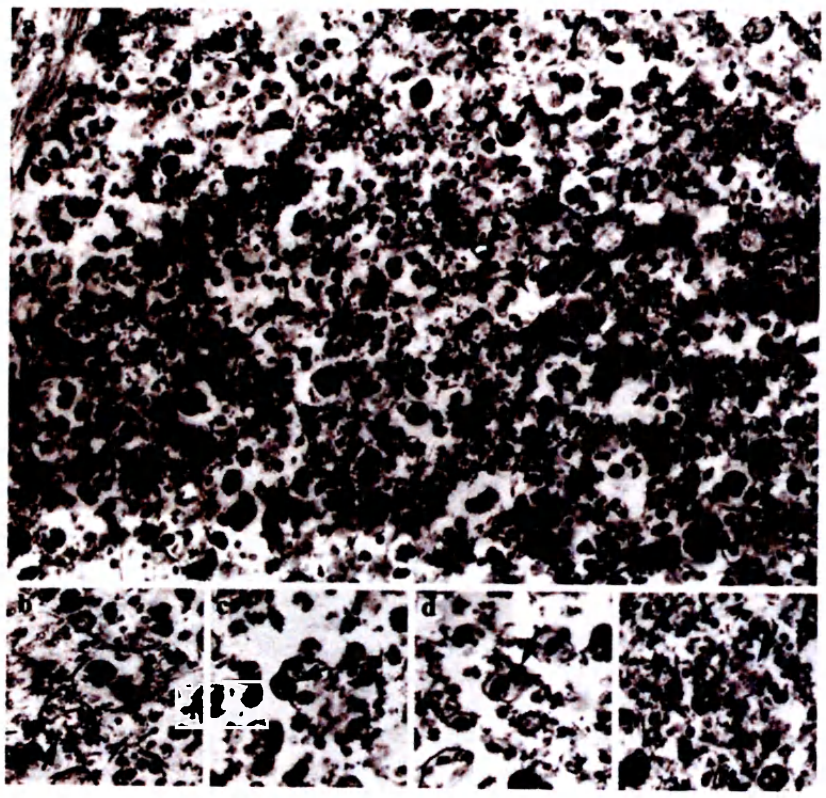

Fig. 3 Ultrastructure of a subcortical neuron in case 1 (day 27) of prosaposin deficiency. **a** A dense population of lysosomes containing pleiomorphic condensed deposits. **b–e** Some of the deposits resemble degenerated mitochondria (*arrows* **c–e**), for comparison refer to intact mitochondrion (**b**, *arrow*). Magnification ×28,000

Immunohistochemistry, immunofluorescence, laser scanning confocal microscopy (LSCM) and cross-correlation function (CCF) analysis

In all the three cases the neuronal perikaryal storage granules displayed a uniform lysosomal immunophenotype, featured by strong staining for cathepsin D (luminal marker) and for the late endosomal/lysosomal membrane markers LAMP1, 2 (Figs. 1b, 2c, d). In the majority of storage neurons the perikaryal granules displayed variable positivity for the subunit c of mitochondrial ATP synthase (SCMAS) with the respective antibody (data not shown).

A peculiar feature of the immunophenotype was the nearly uniform, strong, granular immunostaining of ubiquitin (Fig. 4a–c), present in all analyzed samples (cortical, subcortical and extra cerebral). The cortical neurons in case 1 were ubiquitinated almost without any substantial difference between the individual layers. Axonal spheroids were ubiquitinated as well. The neurons of the peripheral nervous system (gut, lung, liver, kidney, and urinary bladder) displayed an identical lysosomal immunophenotype, including the high extent of ubiquitination (Fig. 4d). The cellular pattern of ubiquitination, seen in bright-field microscopy, was suggestive of its association with storage lysosomes (for details, see below).

To evaluate the proportion of ubiquitin protein conjugates (mono- and polyubiquitinated) in the overall ubiquitin signal, the antibodies (clone FK1 and FK2, Table 1) against these types of epitopes [16] were used. We were able to detect significant amounts of mono- and polyubiquitinated moieties (FK2 antibody, data not shown) with the same staining patterns as the above-described ubiquitin staining. Unfortunately, the FK1 antibody (polyubiquitinated protein conjugates) did not provide reliable staining in the control samples (Mallory bodies rich liver biopsy) and as such was not included in the study. The cortical neurons in age-matched controls were immunonegative for ubiquitin. The immunophenotype of storage lysosomes in all the affected non-neuronal cells, from the brain (astrocytes, microglial phagocytes) and the visceral region was identical to the neurolysosomes, except for the absence of any detectable ubiquitination (Fig. 4e).

The immunohistochemical detection of cytoplasmic aggresomal sequestered proteins using p62 antibody did not show any positivity in any of the evaluated cortical and subcortical brain samples of all the three cases (data not shown).

In contrast to pSap deficiency, neurolysosomal ubiquitination was undetectable in the following neurolysosomal storage disorders: Niemann–Pick disease type CI, type A (Fig. 4f), infantile sialic storage disorder, mucolipidosis type I, aspartylglucosaminuria, alpha-mannosidosis, polysulphatase deficiency, and glycogen storage disease type II. Only the axonal spheroids and the neuronal tangles, particularly numerous in protracted

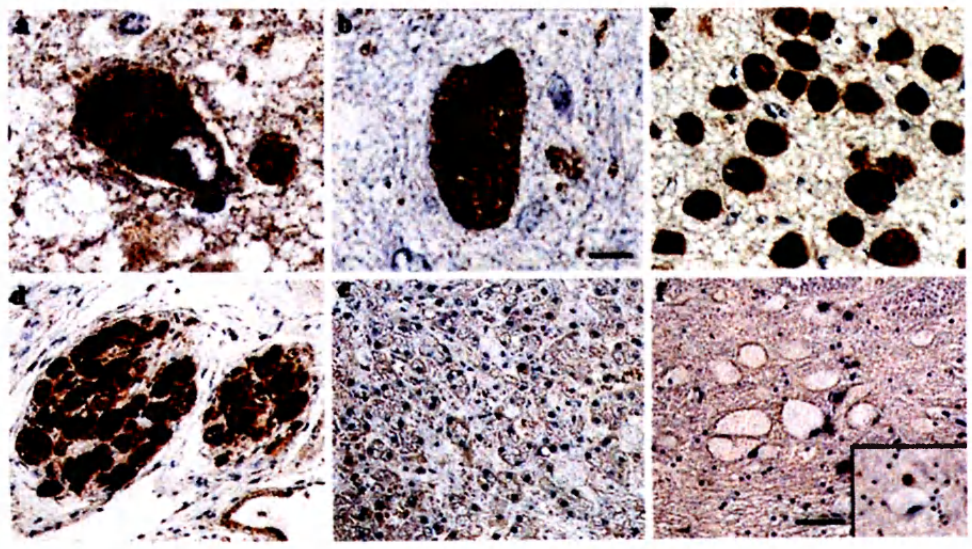

Fig. 4 Immunodetection of ubiquitin in prosaposin deficiency (except for panel **f**). **a** Strong granular staining in perikarya of subcortical storage neurons in case 1 (day 27), and **b** case 2 (day 89). **c** Uniform strong ubiquitination in pontine storage neurons in case 3 (day 119), and **d** in peripheral neurons of the kidney hilus in the same case. **e** Absence of detectable ubiquitination in the storage cells in the liver in pSap deficiency (case 2). **f** Absence of ubiquitination in storage neurons in Niemann–Pick-disease type A. Inset shows intense ubiquitination of the small dystrophic axon close to another negative neuronal perikaryon. Scale bar 25 μm (**a**,**b**) and 100 μm (**c**–**f**)

neuronopathic Niemann–Pick type C cases, displayed strong ubiquitination. In neuronal ceroid lipofuscinoses, types 2, 3, 4 and 8, the main population of storage granules was devoid of ubiquitination. The only exception was strong ubiquitination seen in a small population of transformed storage material present as globules or spheroids in the neuronal perikarya [12]. Moderate ubiquitination of storage neurons has been seen in the group of mucopolysaccharidoses (types I–III). Extra cerebral non-neuronal storage cells in all the above-mentioned disorders lacked any detectable ubiquitination. We could not confirm improved ubiquitin immunostaining with the recommended pretreatment [34].

Multiple indirect immunofluorescence labeling experiments were performed on sections of the spinal cord (case 3) in order to evaluate the relationship between the detectable ubiquitin signals and the potentially involved, cellular compartments. Prior to the evaluation of the signals in confocal images, we performed image restoration based on deconvolution using the microscope's measured PSF, a method known to increase the effective image resolution [35, 57, 64]. The characteristics of the signals in the evaluated images allowed us to apply the cross-correlation function (CCF) estimation [65] for the analysis of their spatial (colocalization) relationship. The CCF method of colocalization evaluation of complex staining patterns is advantageous because it does not require image segmentation and can discriminate positive, negative and non-correlating signals.

In general, the signals obtained by immunofluorescence labeling followed the patterns observed by immunohistochemical staining. The intensity of the ubiquitin signal was inversely correlated to the endoplasmic reticulum (ER) and mitochondrial signals among the evaluated neurons. This resulted in a population of neurons strongly positive for ubiquitin and almost negative for ER and mitochondrial signals. This feature could be documented by the distribution of Pearson's coefficient values in the CCF plots (Fig. 5c, d). While this loss of epitope detectability in the presence of strong ubiquitin positivity was clear for the ER and mitochondrial epitopes, a similar phenomenon was not observed for the two late endosomal/lysosomal markers (LAMP2, CatD).

In addition, the double labeling of the mitochondrial epitopes and of the late endosomal/lysosomal membrane epitope (LAMP2) in search for lysosomes with entrapped mitochondria or for mitochondrial remnants did not provide clear evidence of such events. This was, most probably, due to the combination of diffraction limited resolution of the microscope and/or advanced degradation of the mitochondrial epitopes.

Figure 5 shows images of the selected neurons with the corresponding CCFs and their distribution for the above-mentioned immunofluorescence labeling. From the five evaluated labeling combinations, only the signals of ubiquitin and LAMP 2/cathepsin D showed a non-random distribution (colocalization) according to the CCF in the population of evaluated neurons (Fig. 5a, b). The full-width of the half maximum (FWHM) of the CCF curves should correspond to the diameter of the evaluated objects [65]. This criterion stands for the median value of both the CCF curves representing the ubiquitin/LAMP2-CatD signals and corresponds to the diameter values obtained by electron microscopy. The characteristics of ubiquitin/LAMP2 and ubiquitin/cathepsin D CCF curves (FWHM or maximum Pearson's coefficient values) did not allow unambiguous discrimination between the prevalence of the two phenomena i.e. ubiquitination of the late endosomal/lysosomal membranes or ubiquitination of the late endosomal/lysosomal contents. Despite this ambiguity, which is most likely caused by the resolution limit of the microscope, we were able to demonstrate the colocalization of the ubiquitin signal with the late endosomal/lysosomal cellular compartment in pSap deficient neurons. Analysis of the other staining combinations (anti-ubiquitin/anti-PDI, anti-ubiquitin/anti-60 kDa antigen of human mitochondria and anti-60 kDa antigen of human mitochondria/anti-LAMP2) yielded a wide distribution of values, ranging from random distributions to mild exclusion of the signals (negative values of the Pearson's coefficient) (Fig. 5c–e). CCF found that for the anti-60 kDa antigen of human mitochondria/anti-LAMP2 (mitochondrial/lysosomal), staining could be regarded, in this case, as a positive control for a random/exclusion relationship of the signals.

Limited survival potential of cortical neurons

A comparison of brain cortical neuropathology showed pronounced differences between case 1 and cases 2 and 3. The histology in case 1 revealed a dense population of cortical neurons without substantial numerical and structural deviation from age-matched controls. The cortical neurons were moderately affected by storage, with a gradual increase toward the deeper layers (Fig. 1a). The neuronal nuclei were mostly vesicular with well-discernible nucleoli. The process culminated in the neurons of the subcortical regions (thalamus and basal ganglia). The degree of astrocytosis and the number of microglial phagocytes were proportional to the degree of neuronal storage, i.e. it was minimal in the cortex (Fig. 1c, d). In cases 2 and 3 the cortical areas

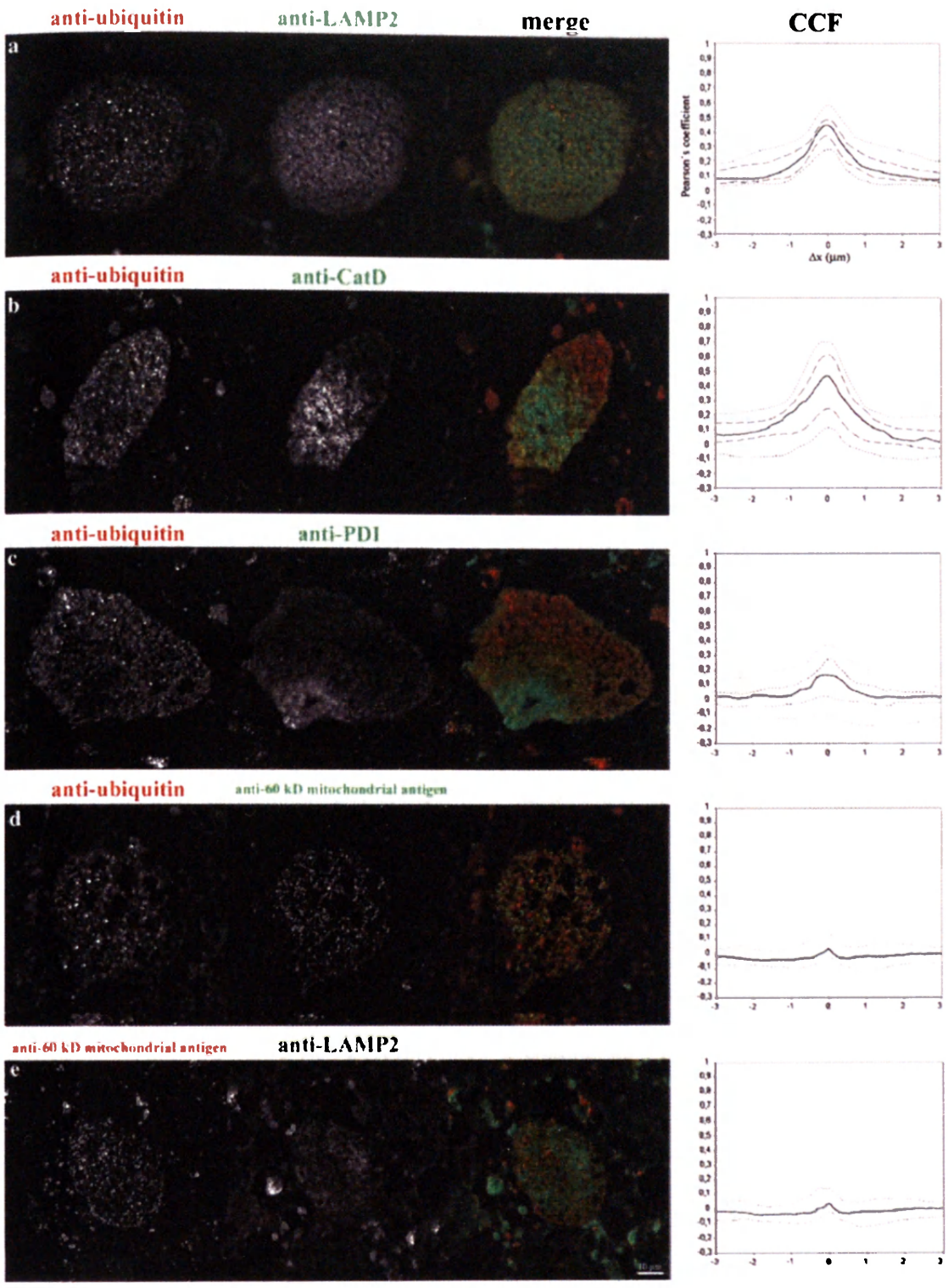

Fig. 5 Laser scanning confocal microscopy. Figure shows isolated gray scale single channel, and merged RGB images of the double-labeled neurons for appropriate indirect immunofluorescence labels (used antibodies given in panels **a**–**e**). On the right are the corresponding CCF curves: *Full line* median values, *dotted lines* 5/95 percentile values, *dashed lines* 1st and 3rd quartile (for details on graph construction see Methods). CCF values were determined only for the pixels located inside the neurons, the surrounding tissue was excluded from the CCF calculations. Positive Pearson's coefficient values demonstrate significant overlap (colocalization) of the signals, negative values demonstrate repulsion (anti-colocalization) of the signals, and values around zero demonstrate random distribution of the signals. For CCF calculation refer to Materials and methods. Scale bar (10 μm)

displayed a profound depletion of the neurons [13, 25] and the residual neurons were identified as finely granulated single cells or small groups of cells that were detectable by using the NeuN antibody. Instead of the normal neuronal architecture there was a dense cellular population composed of equal proportions of large, coarsely vacuolated, CD 68 positive phagocytic microglia and hyperplastic, GFAP positive astrocytes (Fig. 6). In the rest of the central nervous system, the neurons were not substantially reduced in amount. No signs of caspase 3 activation or other cytological features of apoptosis were present either in the cortical or the subcortical neurons in case 1 or in the neurons in cases 2 and 3 (data not shown).

Discussion

In all the three cases there was a complete absence of pSap protein caused either by the nonsense-mediated decay of the gene transcript [25] or by the failure of the mRNA translation [13, 54]. The discussion is focused on the nature of neurolysosomal storage and the remarkable sensitivity of the cortical neurons to pSap deficiency.

Nature of the neurolysosomal process

Whereas lysosomes in non-neuronal cells were distended by a massive accumulation of a set of sphingolipids due to multiple sphingolipid hydrolase insufficiency, due to pSap deficiency, leading to the foamy appearance of the affected cells, the neurons expressed an appreciably different pathology. The neuronal pathology featured finely granular lysosomes containing condensed pleiomorphic inclusions. Besides the standard membrane (LAMP 1 and LAMP 2) and luminal (cathepsin D) markers, their distinct feature was an association with strong ubiquitination including a significant proportion of ubiquitin protein conjugates detected by specific antibodies. They were devoid of ceroidlipofuscin and the lipid storage was borderline or of a low degree. We consider it important that ubiquitination has been proved to be absent in non-neuronal storage cells and even in numerous microglial phagocytes. It was also absent in the bulk of other neurolysosomal storage disorders featured by storage of defined lipid or glycoconjugate substrates due to deficient enzyme catalytic activity or due to altered lipid trafficking (see also [68]). Thus, in contrast to the non-neuronal cells, the absence of pSap leads to a different pathology in the neurolysosomes.

It should be compared to processes featured by the lysosomally associated ubiquitination. Ubiquitination associated with neurolysosomes has been described in the granulovacuolar lesions seen in Alzheimer's disease and in scrapie infected mice, both appear to be autophagic vacuoles [39]. The ultrastructure of neurolysosomes in neuronal perikarya (Fig. 3) and axons in our cases of pSap deficiency resembled ultrastructural changes in the neuroaxonal dystrophy classified as a macroautophagy process [46] that also featured a high degree of ubiquitination [11, 42] combined with lysosomal enzyme activities [63].

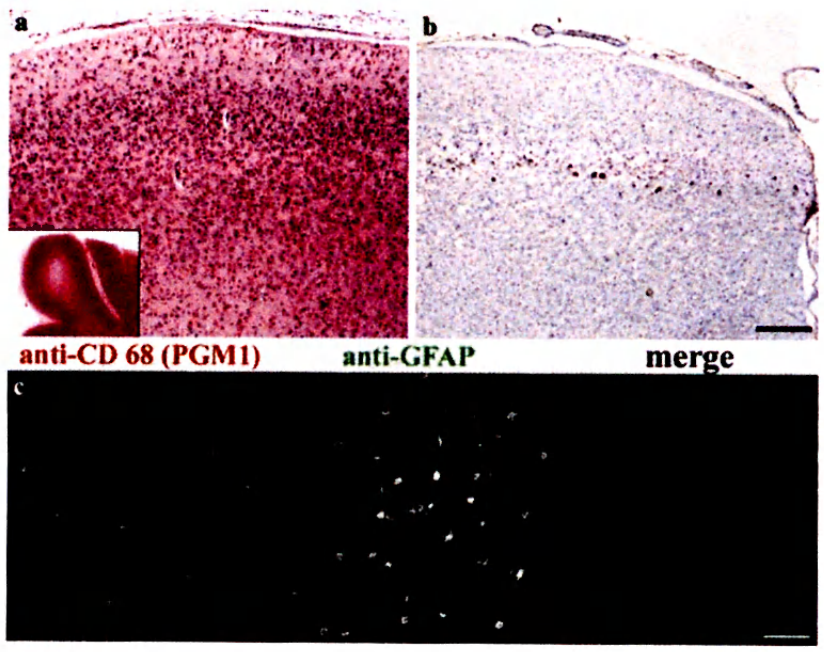

Fig. 6 Neuronal cortical crisis in prosaposin deficiency. Case 2 (day 89). **a** Low power magnification (H&E) showing cellular cortex with well preserved shape and well delineated from the white matter (inset). **b** Very few residual neurons stained with NeuN antibody. **c** Dense cellularity of cerebral cortex in case 2 (day 89) formed by two distinct cell populations (CD 68 positive microglial phagocytes and GFAP positive astrocytes), LSCM acquired image. Note the intimate contact of the two cell types. Scale bar 500 μm **a, b** and 50 μm **c**. Compare with Fig. 1

In the cases of pSap deficiency we were able to document a positive correlation (colocalization) to ubiquitination and late endosomal/lysosomal markers as well as signs attributable to mitochondrial degradation (SCMAS detectability).

Ubiquitination has also been described as a part of the protein conjugation system of autophagosomal compartment [18, 38, 58, 59], a process dominated, however, by the homologs of yeast Atg ubiquitin-like proteins including mammalian LC3 protein [27, 28]. Unfortunately, the antibody against the LC3 autophagosomal membrane component provided ambiguous results in our FFPE tissues, partly due to the lack of appropriate reference samples; therefore we decided not to include these results. Ubiquitination of lysosomal contents has been repeatedly described [10, 36, 37, 41, 58] and explained by lysosomal sequestration of ubiquitin-tagged proteins.

We thus propose the existence of a similar mechanism in pSap deficiency, i.e. excessive lysosomal sequestration of the ubiquitin-tagged proteins released most probably from damaged neuronal membranes or resulting from impaired downstream pSap signaling [2, 23]. The previously demonstrated relationship of the ubiquitin/proteasome pathway and cytoplasmic vacuoles with non-lysosomal characteristics [61] does not correspond with our findings in pSap deficiency. The absence of immunodetectable p62 does not support the aggresomal-based ubiquitination [67] in pSap deficiency neuropathology, nevertheless, ubiquitination has been suggested to trigger an autophagocytosis process under certain conditions [30]. In summary, our findings can be interpreted as an excessive influx of ubiquitinated biological material (either in bulk or as individual molecules) into the neurolysosomes. It represents features compatible with the process of autophagy, encompassing a range of both bulk (macro and micro types) and of its molecular variants, [8, 49, 53] which are difficult to distinguish in routinely processed FFPE samples. It is worth mentioning that the absence of neurotrophic factors was found to activate autophagocytosis, which may culminate in a specific type of programmed cell death (PCD II) [4, 59] or persist as an ongoing process [40]. This supports our hypothesis that the specific neurolysosomal pathology in human pSap deficiency may be closely related to the absence of pSap's trophic function.

Selective vulnerability of the cortical neurons–the cortical neuronal survival crisis

The vulnerability of the cortical neurons to cell death in pSap deficiency is immense. The findings in the three presented cases suggest a critical inability of nearly the whole cortical neuronal population to survive after a certain postnatal time point. The subependymal germinal zone as well as the neuronal migration does not seem to be affected. This massive, stage dependant neuronal loss, most probably triggered by pSap absence, occurs within a time period of 60–80 days. With respect to the extent and relative abruptness of this phenomenon we would like to designate it as a cortical neuronal survival crisis. A similar phenomenon has never been described in any of the known neurolysosomal storage disorders, with the exception of infantile NCL1 and the recently described congenital NCL [60]. In infantile NCL1, the profound neuronal cortical depopulation develops over several years [56], strongly contrasting with the early cortical neuronal survival crisis in pSap deficiency. The congenital NCL, caused by profound cathepsin D deficiency, is featured by extensive prenatal neuronal loss.

Unfortunately, brains from other cases of pSap deficiency [19, 66] were not available for study. The loss of neuronal survival capacity as described has been repeatedly reported as a consequence of neurotrophic factor deprivation leading to programmed cell death, mostly from the caspase independent (non-apoptopic) type [1, 9, 26, 29, 52]. The absence of detectable activated caspase 3 in our cases is in accord with it. It should be stressed that an amino acid sequence has been recognized in pSap [33, 48, 51] as being responsible for the neurotrophic activities in a variety of neural cells in vitro and in vivo, including differentiation, cell death prevention, regeneration [5, 24, 32, 33, 47, 55], and stimulation of myelin synthesis [7, 21, 22]. Cell death prevention by pSap has also been described in non-neuronal U937 monocytic cells [7, 44]. It has been postulated that unprocessed pSap, localized to both fetal and adult human neurons [15, 31], exerts its neurotrophic effect partly through a putative Go protein coupled receptor [20] and MAP kinase [6], and partly due to its unique affinity for glycosphingolipids, particularly gangliosides [45].

The above-mentioned data support the concept of pSap as having a crucial role in the survival of human cortical neurons and indicate that its absence may be critical for their survival in early postnatal life.

In this context it is worth noting that in the mouse pSap KO model [17, 50], the neurolysosomal storage starts around day 10 and 30 in spinal and cerebral neurons, respectively, and progresses rapidly to full blown glycolipid storage. As in human cases, storage is accompanied, by a high degree of neuronal ubiquitination. The neurological symptoms start on day 20. The animals do not survive beyond day 40. No signs of

neuronal cortical depopulation have been described. These findings might point to the absence of a significant trophic effect of pSap on normal mouse neurons despite the fact that there is a strong postnatal increase in its mRNA [62].

Conclusions and perspectives

Our results indicate that pSap deficiency in humans has different consequences with respect to the cell types affected. In non-neuronal cells, the disorder does not lead to any demonstrable trophic defect and is dominated by the biochemical sequels linked to the absence of Saps i.e. inactivation of multiple sphingolipid hydrolases. The resulting storage of undigested lipids markedly distends the lysosomal compartment. However, in the peripheral and central neurons, the consequences of pSap deficiency seem to be determined by the unique sensitivity of the neurons to the lack of a trophic effect of secreted unprocessed pSap. We speculate that the initial phase of the neurolysosomal process (in both brain and peripheral neurons) strongly resembles autophagocytosis, while lipid storage plays only a minor role. In the cortical neurons the process seems to be terminated after several weeks of life by massive cell death, which by exclusion corresponds most probably to the programmed cell death type II, followed by removal by microglial phagocytes. It appears likely that pSap is one of the trophic factors essential for survival, differentiation and maintenance of human neurons particularly in the early phases of brain development.

Acknowledgments This work was supported by the research project MSM 0021620806 of the Ministry of Education, Youth and Sports of the Czech Republic.

References

1. Acheson A, Conover JC, Fandl JP, DeChiara TM, Russell M, Thadani A, Squinto SP, Yancopoulos GD, Lindsay RM (1995) A BDNF autocrine loop in adult sensory neurons prevents cell death. Nature 374:450–453
2. Bonifacino JS, Weissman AM (1998) Ubiquitin and the control of protein fate in the secretory and endocytic pathways. Annu Rev Cell Dev Biol 14:19–57
3. Bradova V, Smid F, Ulrich-Bott B, Roggendorf W, Paton BC, Harzer K (1993) Prosaposin deficiency: further characterization of the sphingolipid activator protein-deficient sibs. Multiple glycolipid elevations (including lactosylceramidosis), partial enzyme deficiencies and ultrastructure of the skin in this generalized sphingolipid storage disease. Hum Genet 92:143–152
4. Bursch W (2001) The autophagosomal-lysosomal compartment in programmed cell death. Cell Death Differ 8:569–581
5. Calcutt NA, Campana WM, Eskeland NL, Mohiuddin L, Dines KC, Mizisin AP, O'Brien JS (1999) Prosaposin gene expression and the efficacy of a prosaposin-derived peptide in preventing structural and functional disorders of peripheral nerve in diabetic rats. J Neuropathol Exp Neurol 58:628–636
6. Campana WM, Hiraiwa M, Addison KC, O'Brien JS (1996) Induction of MAPK phosphorylation by prosaposin and prosaptide in PC12 cells. Biochem Biophys Res Commun 229:706–712
7. Campana WM, Hiraiwa M, O'Brien JS (1998) Prosaptide activates the MAPK pathway by a G-protein-dependent mechanism essential for enhanced sulfatide synthesis by Schwann cells. Faseb J 12:307–314
8. Cuervo AM, Dice JF (1998) Lysosomes, a meeting point of proteins, chaperones, and proteases. J Mol Med 76:6–12
9. Davies AM (1993) Promoting motor neuron survival. Curr Biol 3:879–881
10. Davis WL, Jacoby BH, Goodman DB (1994) Immunolocalization of ubiquitin in degenerating insect flight muscle. Histochem J 26:298–305
11. Dickson DW, Wertkin A, Kress Y, Ksiezak-Reding H, Yen SH (1990) Ubiquitin immunoreactive structures in normal human brains. Distribution and developmental aspects. Lab Invest 63:87–99
12. Elleder M (1978) A histochemical and ultrastructural study of stored material in neuronal ceroid lipofuscinosis. Virchows Arch B Cell Pathol 28:167–178
13. Elleder M, Jerabkova M, Befekadu A, Hrebicek M, Berna L, Ledvinova J, Hulkova H, Rosewich H, Schymik N, Paton BC, Harzer K (2005) Prosaposin deficiency–a rarely diagnosed, rapidly progressing, neonatal neurovisceral lipid storage disease. Report of a further patient. Neuropediatrics 36:171–180
14. Elleder M, Jirasek A, Smid F, Ledvinova J, Besley GT, Stopekova M (1984) Niemann–Pick disease type C with enhanced glycolipid storage. Report on further case of so-called lactosylceramidosis. Virchows Arch A Pathol Anat Histopathol 402:307–317
15. Fu Q, Carson GS, Hiraiwa M, Grafe M, Kishimoto Y, O'Brien JS (1994) Occurrence of prosaposin as a neuronal surface membrane component. J Mol Neurosci 5:59–67
16. Fujimuro M, Sawada H, Yokosawa H (1994) Production and characterization of monoclonal antibodies specific to multiubiquitin chains of polyubiquitinated proteins. FEBS Lett 349:173–180
17. Fujita N, Suzuki K, Vanier MT, Popko B, Maeda N, Klein A, Henseler M, Sandhoff K, Nakayasu H (1996) Targeted disruption of the mouse sphingolipid activator protein gene: a complex phenotype, including severe leukodystrophy and wide-spread storage of multiple sphingolipids. Hum Mol Genet 5:711–725
18. Gropper R, Brandt RA, Elias S, Bearer CF, Mayer A, Schwartz AL, Ciechanover A (1991) The ubiquitin-activating enzyme, E1, is required for stress-induced lysosomal degradation of cellular proteins. J Biol Chem 266:3602–3610
19. Harzer K, Paton BC, Poulos A, Kustermann-Kuhn B, Roggendorf W, Grisar T, Popp M (1989) Sphingolipid activator protein deficiency in a 16-week-old atypical Gaucher disease patient and his fetal sibling: biochemical signs of combined sphingolipidoses. Eur J Pediatr 149:31–39
20. Hiraiwa M, Campana WM, Martin BM, O'Brien JS (1997) Prosaposin receptor: evidence for a G-protein-associated receptor. Biochem Biophys Res Commun 240:415–418
21. Hiraiwa M, Campana WM, Mizisin AP, Mohiuddin L, O'Brien JS (1999) Prosaposin: a myelinotrophic protein that promotes expression of myelin constituents and is secreted after nerve injury. Glia 26:353–360
22. Hiraiwa M, Taylor EM, Campana WM, Darin SJ, O'Brien JS (1997) Cell death prevention, mitogen-activated protein

kinase stimulation, and increased sulfatide concentrations in Schwann cells and oligodendrocytes by prosaposin and prosaptides. Proc Natl Acad Sci U S A 94:4778–4781
23. Horak J (2003) The role of ubiquitin in down-regulation and intracellular sorting of membrane proteins: insights from yeast. Biochim Biophys Acta 1614:139–155
24. Hozumi I, Hiraiwa M, Inuzuka T, Yoneoka Y, Akiyama K, Tanaka R, Kikugawa K, Nakano R, Tsuji S, O'Brien JS (1999) Administration of prosaposin ameliorates spatial learning disturbance and reduces cavity formation following stab wounds in rat brain. Neurosci Lett 267:73–76
25. Hulkova H, Cervenkova M, Ledvinova J, Tochackova M, Hrebicek M, Poupetova H, Befekadu A, Berna L, Paton BC, Harzer K, Boor A, Smid F, Elleder M (2001) A novel mutation in the coding region of the prosaposin gene leads to a complete deficiency of prosaposin and saposins, and is associated with a complex sphingolipidosis dominated by lactosylceramide accumulation. Hum Mol Genet 10:927–940
26. Hutchins JB, Barger SW (1998) Why neurons die: cell death in the nervous system. Anat Rec 253:79–90
27. Kabeya Y, Mizushima N, Ueno T, Yamamoto A, Kirisako T, Noda T, Kominami E, Ohsumi Y, Yoshimori T (2000) LC3, a mammalian homologue of yeast Apg8p, is localized in autophagosome membranes after processing. Embo J 19:5720–5728
28. Kirisako T, Baba M, Ishihara N, Miyazawa K, Ohsumi M, Yoshimori T, Noda T, Ohsumi Y (1999) Formation process of autophagosome is traced with Apg8/Aut7p in yeast. J Cell Biol 147:435–446
29. Kirkland RA, Adibhatla RM, Hatcher JF, Franklin JL (2002) Loss of cardiolipin and mitochondria during programmed neuronal death: evidence of a role for lipid peroxidation and autophagy. Neuroscience 115:587–602
30. Komatsu M, Waguri S, Ueno T, Iwata J, Murata S, Tanida I, Ezaki J, Mizushima N, Ohsumi Y, Uchiyama Y, Kominami E, Tanaka K, Chiba T (2005) Impairment of starvation-induced and constitutive autophagy in Atg7-deficient mice. J Cell Biol 169:425–434
31. Kondoh K, Sano A, Kakimoto Y, Matsuda S, Sakanaka M (1993) Distribution of prosaposin-like immunoreactivity in rat brain. J Comp Neurol 334:590–602
32. Kotani Y, Matsuda S, Sakanaka M, Kondoh K, Ueno S, Sano A (1996) Prosaposin facilitates sciatic nerve regeneration in vivo. J Neurochem 66:2019–2025
33. Kotani Y, Matsuda S, Wen TC, Sakanaka M, Tanaka J, Maeda N, Kondoh K, Ueno S, Sano A (1996) A hydrophilic peptide comprising 18 amino acid residues of the prosaposin sequence has neurotrophic activity in vitro and in vivo. J Neurochem 66:2197–2200
34. Kovacs GG, Flicker H, Budka H (2003) Immunostaining for ubiquitin: efficient pretreatment. Neuropathol Appl Neurobiol 29:174–177
35. Landmann L (2002) Deconvolution improves colocalization analysis of multiple fluorochromes in 3D confocal data sets more than filtering techniques. J Microsc 208:134–147
36. Laszlo L, Doherty FJ, Osborn NU, Mayer RJ (1990) Ubiquitinated protein conjugates are specifically enriched in the lysosomal system of fibroblasts. FEBS Lett 261:365–368
37. Laszlo L, Doherty FJ, Watson A, Self T, Landon M, Lowe J, Mayer RJ (1991) Immunogold localisation of ubiquitin-protein conjugates in primary (azurophilic) granules of polymorphonuclear neutrophils. FEBS Lett 279:175–178
38. Lenk SE, Dunn WA Jr, Trausch JS, Ciechanover A, Schwartz AL (1992) Ubiquitin-activating enzyme, E1, is associated with maturation of autophagic vacuoles. J Cell Biol 118:301–308
39. Lowe J, McDermott H, Kenward N, Landon M, Mayer RJ, Bruce M, McBride P, Somerville RA, Hope J (1990) Ubiquitin conjugate immunoreactivity in the brains of scrapie infected mice. J Pathol 162:61–66
40. Lum JJ, Bauer DE, Kong M, Harris MH, Li C, Lindsten T, Thompson CB (2005) Growth factor regulation of autophagy and cell survival in the absence of apoptosis. Cell 120:237–248
41. Mayer RJ, Lowe J, Landon M, McDermott H, Laszlo L (1991) The role of protein ubiquitination in neurodegenerative disease. Acta Biol Hung 42:21–26
42. Migheli A, Attanasio A, Pezzulo T, Gullotta F, Giordana MT, Schiffer D (1992) Age-related ubiquitin deposits in dystrophic neurites: an immunoelectron microscopic study. Neuropathol Appl Neurobiol 18:3–11
43. Millat G, Verot L, Rodriguez-Lafrasse C, Di Marco JN, Rimet Y, Poujol A, Girard N, Monges G, Livet MO, Vanier MT (2003) Fourth reported family with prosaposin deficiency. 14th ESGLD Workshop (September 18th-21st, 2003). Podebrady/Prague, Czech Republic
44. Misasi R, Garofalo T, Di Marzio L, Mattei V, Gizzi C, Hiraiwa M, Pavan A, Grazia Cifone M, Sorice M (2004) Prosaposin: a new player in cell death prevention of U937 monocytic cells. Exp Cell Res 298:38–47
45. Misasi R, Sorice M, Garofalo T, Griggi T, Campana WM, Giammatteo M, Pavan A, Hiraiwa M, Pontieri GM, O'Brien JS (1998) Colocalization and complex formation between prosaposin and monosialoganglioside GM3 in neural cells. J Neurochem 71:2313–2321
46. Nixon RA, Wegiel J, Kumar A, Yu WH, Peterhoff C, Cataldo A, Cuervo AM (2005) Extensive involvement of autophagy in Alzheimer disease: an immuno-electron microscopy study. J Neuropathol Exp Neurol 64:113–122
47. O'Brien JS, Carson GS, Seo HC, Hiraiwa M, Kishimoto Y (1994) Identification of prosaposin as a neurotrophic factor. Proc Natl Acad Sci U S A 91:9593–9596
48. O'Brien JS, Carson GS, Seo HC, Hiraiwa M, Weiler S, Tomich JM, Barranger JA, Kahn M, Azuma N, Kishimoto Y (1995) Identification of the neurotrophic factor sequence of prosaposin. Faseb J 9:681–685
49. Ohsumi Y (2001) Molecular dissection of autophagy: two ubiquitin-like systems. Nat Rev Mol Cell Biol 2:211–216
50. Oya Y, Nakayasu H, Fujita N, Suzuki K (1998) Pathological study of mice with total deficiency of sphingolipid activator proteins (SAP knockout mice). Acta Neuropathol (Berl) 96:29–40
51. Qi X, Qin W, Sun Y, Kondoh K, Grabowski GA (1996) Functional organization of saposin C. Definition of the neurotrophic and acid beta-glucosidase activation regions. J Biol Chem 271:6874–6880
52. Rabizadeh S, Bredesen DE (2003) Ten years on: mediation of cell death by the common neurotrophin receptor p75(NTR). Cytokine Growth Factor Rev 14:225–239
53. Salvador N, Aguado C, Horst M, Knecht E (2000) Import of a cytosolic protein into lysosomes by chaperone-mediated autophagy depends on its folding state. J Biol Chem 275:27447–27456
54. Sandhoff K, Kolter T, Harzer K (2001) Sphingolipid activator proteins. In: Scriver CR, Beaudet AL, Sly WS, Valle D, Childs B, Kinzler KW, Vogelstein B (eds) The metabolic and molecular bases of inherited disease. McGraw-Hill, New York, pp 3371–3388
55. Sano A, Matsuda S, Wen TC, Kotani Y, Kondoh K, Ueno S, Kakimoto Y, Yoshimura H, Sakanaka M (1994) Protection by prosaposin against ischemia-induced learning disability and neuronal loss. Biochem Biophys Res Commun 204:994–1000

56. Santavuori P, Gottlob I, Haltia M, Rapola J, Lake BD, Tyynelä J, Peltonen L (1999) CLN1. Infantile and other types of NCL with GROD. In: Goebel HH, Mole SE, Lake BD (eds) The Neuronal Ceroid Lipofuscinoses (Batten Disease). IOS Press, Amsterdam, pp 16–36
57. Shaw PJ, Rawlins DJ (1991) Three-dimensional fluorescence microscopy. Prog Biophys Mol Biol 56:187–213
58. Schwartz AL, Ciechanover A, Brandt RA, Geuze HJ (1988) Immunoelectron microscopic localization of ubiquitin in hepatoma cells. Embo J 7:2961–2966
59. Schwartz LM, Smith SW, Jones ME, Osborne BA (1993) Do all programmed cell deaths occur via apoptosis? Proc Natl Acad Sci U S A 90:980–984
60. Siintola E, Partanen S, Stromme P, Haapanen A, Haltia M, Maehlen J, Lehesjoki AE, Tyynela J (2006) Cathepsin D deficiency underlies congenital human neuronal ceroid-lipofuscinosis. Brain 129:1438–1445
61. Skinner PJ, Vierra-Green CA, Clark HB, Zoghbi HY, Orr HT (2001) Altered trafficking of membrane proteins in purkinje cells of SCA1 transgenic mice. Am J Pathol 159:905–913
62. Sun Y, Witte DP, Grabowski GA (1994) Developmental and tissue-specific expression of prosaposin mRNA in murine tissues. Am J Pathol 145:1390–1398
63. Suzuki K, Terry RD (1967) Fine structural localization of acid phosphatase in senile plaques in Alzheimer's presenile dementia. Acta Neuropathol (Berl) 8:276–284
64. van der Voort HT, Strasters KC (1995) Restoration of Confocal Images for Quantitative Image Analysis. J Micr 178:165–181
65. van Steensel B, van Binnendijk EP, Hornsby CD, van der Voort HT, Krozowski ZS, de Kloet ER, van Driel R (1996) Partial colocalization of glucocorticoid and mineralocorticoid receptors in discrete compartments in nuclei of rat hippocampus neurons. J Cell Sci 109:787–792
66. Vanier MT, Millat G, Verot L, Di Marco JN, Rimet Y, Poujol A, Girard N, Monges G, Livet MO (2003) Fourth reported family with prosaposin deficiency. In: Proceedings of international symposium on lysosomal storage diseases, Santiago de Compostela, Spain
67. Zatloukal K, Stumptner C, Fuchsbichler A, Heid H, Schnoelzer M, Kenner L, Kleinert R, Prinz M, Aguzzi A, Denk H (2002) p62 is a common component of cytoplasmic inclusions in protein aggregation diseases. Am J Pathol 160:255–263
68. Zhan SS, Beyreuther K, Schmitt HP (1992) Neuronal ubiquitin and neurofilament expression in different lysosomal storage disorders. Clin Neuropathol 11:251–255

Seven Novel Acid Sphingomyelinase Gene Mutations in Niemann-Pick Type A and B Patients

J. Sikora[1]*, H. Pavlu-Pereira[1], M. Elleder[1], H. Roelofs[2] and R. A. Wevers[2]

[1] *Institute of Inherited Metabolic Disorders, Charles University, 1st Faculty of Medicine, Prague, Czech Republic*

[2] *Laboratory of Pediatrics and Neurology, University Medical Center Nijmegen, Nijmegen, The Netherlands*

Summary

We have analyzed acid sphingomyelinase (*SMPD1*; E.C. 3.1.4.12) gene mutations in four Niemann-Pick disease (NPD) type A and B patients of Turkish ancestry and in three patients of Dutch origin.

Among four NPD type A patients we found two homozygotes for the g.1421C > T (H319Y) and g.3714T > C (Y537H) mutations and two compound heterozygotes, one for the g.3337T > C (F463S) and g.3373C > T (P475L) mutations and the other for the g.84delC (G29fsX74) and g.1208A > C (S248R) mutations.

One of the type B patients was homozygous for the g.2629C>T (P371S) mutation. The last two type B patients were homozygotes for the common g.3927_3929delCGC (R608del) mutation.

The G29fsX74, S248R, H319Y, P371S, F463S, P475L and Y537H *SMPD1* mutations are all novel and were verified by PCR/RFLP and/or ARMS. All of the identified mutations are likely to be rare or private, with the exception of R608del which is prevalent among NPD type B patients from the North-African Maghreb region. Geographical and/or social isolation of the affected families are likely contributing factors for the high number of homozygotes in our group.

Introduction

Niemann-Pick disease is an autosomal recessive sphingolipidosis caused by the deficiency of lysosomal acid sphingomyelinase (ASM, E.C. 3.1.4.12) resulting in lysosomal accumulation of sphingomyelin. At the extremes of the phenotype spectrum lie two common presentations: infantile neurovisceral fatal type A, and type B, characterized by purely visceral involvement and by survival till adulthood (Elleder, 1989; Kolodny, 2000; Schuchman & Desnick, 2001; Vanier & Suzuki, 1996). Patients with intermediate phenotypes have been reported (Elleder & Cihula, 1983; Elleder *et al.* 1986; Sperl *et al.* 1994; Takada *et al.* 1987). Both type A and B variants have higher prevalence in the Ashkenazi Jewish population, reaching 1:40 000 for NPD type A (Goodman, 1979); NPD type B incidence is estimated to be significantly less than that of NPD type A (Schuchman & Desnick, 2001) in this population. Little is known about the frequency of NPD types A and B in non-Jewish populations. Individual reports on the number of NPD type A and B patients and estimated birth prevalence data are available from several European countries, and Australia (Czartoryska *et al.* 1994; Krasnopolskaya *et al.* 1993; Meikle *et al.* 1999; Ozand *et al.* 1990; Poorthuis *et al.* 1999).

The *SMPD1* gene is 5kb long, consists of six exons (Schuchman *et al.* 1992; Schuchman *et al.* 1991), and is located on chromosome 11p15.1–11p15.4 (Da Veiga Pereira *et al.* 1991). More than 20 mutations associated with both types of NPD in Ashkenazi and non-Ashkenazi patients have been published. Most of the mutations are single base substitutions and small deletions with or without a frameshift. Three mutations, g.3592G > T (R496L) (Levran *et al.* 1991a), g.1372T > C (L302P) (Levran *et al.* 1992) and a single nucleotide

*Correspondence: Dr. Jakub Sikora, Institute of Inherited Metabolic Disorders, Div. B, Ke Karlovu 2, 128 08, Praha 2, Czech Republic. Fax: + 420/2/2491 9392. E-mail: jakub.sikora@lf1.cuni.cz

deletion in a C rich region of exon 2 (fsP330) (Levran *et al.* 1993), are prevalent among Ashkenazi NPD type A patients, comprising 92% of all mutations in this population. A three base in-frame deletion in exon 6, g.3927_3929delCGC (R608del) (Levran *et al.* 1991b) is the most prevalent mutation in the population of NPD type B patients from the North-African region of Maghreb (87% of mutated alleles in this area) (Vanier *et al.* 1993). Another mutation with ethnic prevalence is the c.677delT among Israeli Arab NPD type A patients from the lower Galilee and Samaria region (Gluck *et al.* 1998). The remainder of the mutations are rare or private. The total number of NPD type A and B patients diagnosed in the Netherlands in the years 1970–1996 was 27 (14 NPD type A and 13 in whom the type was not determined). The calculated birth prevalence for both NPD variants in the Netherlands is 0.53/100000 newborns (Poorthuis *et al.* 1999). This is the first report on mutation profiles in a subset of NPD type A and B patients diagnosed in the Netherlands.

Materials and Methods

Subjects

The diagnosis of Niemann-Pick disease was based on the clinical data and biochemically measured ASM deficiency in peripheral white blood cells and/or in cultured skin fibroblasts (Table 1). Samples of parental DNA were not available for mutation analysis. The control group consisted of 25 healthy males and 25 healthy females of Czech origin. Participation in the project was based on informed consent.

ASM Activity Measurements

ASM activity was measured in homogenates of leukocytes and cultured skin fibroblasts (Table 1) using N-methyl-^{14}C sphingomyelin (Amersham) as a substrate (Vanier *et al.* 1980).

Chitotriosidase Activity Measurements

Chitotriosidase activity was measured in blood plasma with the artificial substrate 4-methylumbelliferyl β-D-N, N′, N″-triacetylchitotrioside hydrate (Sigma-Aldrich) according to Guo *et al.* (1995).

Genomic DNA Isolation and PCR Amplification of *SMPD1* Gene

Genomic DNA was isolated from cultured skin fibroblasts or leukocytes using the standard phenol/chlorophorm method (Strauss, 2000). PCR amplifications of the *SMPD1* coding region were performed in four fragments using five pairs of primers (Table 2). The final volume of PCR reactions was 50 μl. The reaction mixture contained 100 ng of genomic DNA, 0.2 mM dNTPs, 1× PCR buffer Sigma (protocol 1 and 3), 1× LA PCR buffer (protocols 2a, 2b, 4) (Barnes, 1994), DMSO 4–5% (protocols 1, 2a, 2b, 4), 10 μg/ml gelatine (protocol 1), 1.0–3.0 mM $MgCl_2$, 0.12–0.2 μM of each primer. Thermal conditions for all PCR amplifications were as follows: initial denaturation for 2 min (94°C), then 35 cycles, starting with denaturation for 55 s (94°C), followed by 1 min annealing at primer specific temperatures (Table 2), extension for 2 min 20 s (72°C). Protocol 3 included annealing and extension in one step at 72°C for 3 min; final extension lasted 10 min at 72°C for all protocols. *Taq* DNA polymerase 2.5U (Promega - protocol 1, Sigma - protocol 3), Klen *Taq* 1.5-3U (Ab Peptides, protocols 2a, 2b, 4) together with Deep Vent 0.1U (NEB, protocols 2a, 2b, 4) were used as well as Perfect Match 1U (Stratagene, protocol 3) PCR enhancer. PCR amplifications were carried out in GeneAmp 2400 (Perkin-Elmer) or PHC-3 (Techne) thermocyclers. PCR products were purified using High Pure™ PCR Product Purification Kit (Boehringer Manheim).

Sequencing of *SMPD1* Gene

Direct cycle sequencing reactions contained 100–200 fmol of purified PCR products, 1.0 μM of 5′Cy5 labeled primer (intragenic or universal, Table 2), 0.1 mM dNTP's, 0.1 mM deaza dGTP, 0.83 μM ddNTP's and 6.5 mM $MgCl_2$, 1 × LA PCR buffer (Barnes 1994) and AmpliTaqFS (Perkin-Elmer). Thermal conditions for all cycle sequencing reactions were as follows: initial denaturation for 2 min (94°C), then 35 cycles, starting with denaturation for 15 s (95°C), followed by 30 s (55°C) annealing, and extension 30 s (68°C). Sequence analysis was performed on the automated fluorescent sequencer Alfexpress (Pharmacia).

Table 1 Clinical, biochemical and genetic characteristics

Patient	NPD type	Sex	Ethnic origin	Age/age at death	Phenotype and notes	Leukocytes-ASM activ. (nmol mg^{-1} h^{-1})	Fibroblasts-ASM activ. (nmol mg^{-1} h^{-1})	Chitotriosidase activ. in plasma (nmol mg^{-1} h^{-1})	Genotype	Aminoacid character of the mutation	Intragenic position
1	A	male	Dutch	died at 20 months	Hepatosplenomegaly, growth and developmental retardation at time of death, cherry red macula	0,0	2,0	848	[g 3337T>C]+ [g 3373C>T]	F463S/P475L 463 Phe>Ser 475 Pro>Leu	exon 5, exon 5
2	A	male	Turkish	died at 3 years	Psychomotor retardation at one year of age, hepatosplenomegaly	0,0	0,6	515	[g.3714T>C]+ [g 3714T>C]	Y537H/Y537H 537 Tyr>His	exon 6
3	A	male	Turkish	died at 1 year	Hepatosplenomegaly at 2 months of age, consanguineous parents	0,6	1,0	1868	[g.1421C>T]+ [g.1421C>T]	H319Y/H319Y 319 His>Tyr	exon 2
4	A (mild)	male	Dutch	died at 5 years	Hepatosplenomegaly, psychomotor retardation, foam cells in bone marrow	1,0	3,0	data not available	[g.1208A>C]+ [g.84delC]	S248R/ G296X74 248 Ser>Arg Stop 74 Ile	exon 2, exon 1
5	B	female	Turkish	adult, > 20 years	Hepatosplenomegaly, no mental retardation at at 20 years of age	0,4	Fibroblasts not available	492	[g 2629C>T]+ [g 2629C>T]	P371S/P371S 371 Pro>Ser	exon 3
6	B	female	Turkish	adult, > 30 years	Hepatosplenomegaly, sea blue histiocytes in bone marrow, no neurological impairment	0,1	18,0	not expressed	[g 3927_3929delCGC]+ [g 3927_3929delCGC]	R608del/ R608del 608 del Arg	exon 6
7	B	male	Dutch	adult, > 20 years	Splenomegaly and hyperbilirubinemia, foam cells in bone marrow, no neurological impairment	1,1	35,0	194	[g 3927_3929delCGC]+ [g.3927_3929delCGC]	R608del/ R608del 608 del Arg	exon 6
					reference values (nmol mg^{-1} h^{-1})	2,2–6,8	260–700	10–103			

Table 2 PCR and sequencing primers

PCR primers	Nucleotide sequence	Orientation	Amplified exons	PCR product size (bp)	gDNA position	TANN (°C)	Protocol
NPD 307	5′-TGA CAG CCG CCC GCC ACC GAG AGA-3′	5′ → 3′	1	645	−211	60	1
OV-NP 2	*5′-*CAG GAA ACA GCT ATG ACC* TCC ATC AGG GAT GCA TT-3′	3′ → 5′	1		417	60	1
NPD 1249	5′-TC CTC TGC TCT GCC TCT GAT TTC TCA CCA T-3′	5′ → 3′	2	926	731	68	2a
OV-NPD 2157	*5′-*CAG GAA ACA GCT ATG ACA* ATC AGA GAC AAT GCC CCA GGT TCC CTT CT-3	3′ → 5′	2		1639	68	2a
OV-NPD 1249	*5′-*CAG GAA ACA GCT ATG ACT* CCT CTG CTC TGC CTC TGA TTT CTC ACC AT-3′	5′ → 3′	2	926	731	68	2b
NPD 2157	5′-AAT CAG AGA CAA TGC CCC AGG TTC CCT TCT-3′	3′ → 5′	2		1639	68	2b
NPD 3061	5′-CCC AGC ACA GGA GGA CCA GGA TTG GAA-3′	5′ → 3′	3,4	645	2543	72	3
OV-NPD 3688	*5′-*CAG GAA ACA GCT ATG ACG* GGA CAA CAG GGA TGG TGA GAT GCT CA-3′	3′ → 5′	3,4		3170	72	3
NPD 3658	5′-GCA TCT CAC CAT CCC TGT TGT CCC ATG-3′	5′ → 3′	5,6	920	3147	68	4
OV-NPD 4567	*5′-*CAG GAA ACA GCT ATG ACG* CTT TTT CAC CCT TTC CTA CAT CAA GAA CT-3′	3′ → 5′	5,6		4049	68	4
Sequencing primers							
SNP1Cy5	5′Cy5-GGA CGG GAC AGA CGA ACC-3′	5′ → 3′			−41	55	
SNP2Cy5	5′Cy5-CAC TGG GAC ATT TTC TC-3′	5′ → 3′			965	55	
SNPR2Cy5	5′Cy5-GGC TTC GGC ACA GTA GG-3′	3′ → 5′			1017	55	
SNP7Cy5	5′Cy5-CTC ACC ATC CCT GTT GTC C-3′	5′ → 3′			3151	55	
SNP6Cy5	5′Cy5-CCA GTC AGC CCC ACA TC-3′	5′ → 3′			3562	55	
CyNPD 3061	5′Cy5-CCC AGC ACA GGA GGA CCA GGA TTG GAA-3′	5′ → 3′			2543	55	
SNP8Cy5	5′Cy5-GAC CCA GGC AAA CAT AC-3′	5′ → 3′			3668	55	
UP	5′Cy5-CAG GAA ACA GCT ATG AC-3′				Universal primer	55	

*Primer contains at its 5′ end universal primer sequence (underlined), which does not anneal to the target sequence.

Confirmation of Novel Mutations

Five of the novel mutations altered the recognition site for one of the following restriction endonucleases: *Nla*III, *Apo*I, *Bsl*I, *Sfc*I and *Eag*I (all NEB). The patient and control PCR products were digested by the corresponding endonuclease (Table 3). The Amplification-Refractory Mutation System (ARMS) (Little, 1998) method was used for confirmation of the G29fsX74 and S248R mutations. ARMS reaction conditions were identical to that of PCR protocol 4, and ARMS primer sequences are listed in the Table 4.

Each of the novel mutations was assessed in 100 wild type *SMPD1* alleles to exclude the possibility of a common genetic polymorphism.

Mutation Nomenclature

All mutations and genes are described according to recent mutation nomenclature (Den Dunnen & Antonarakis 2000, 2001; Wain *et al.* 2002). Nucleotide change numbers and primer positions are derived from the genomic sequence of the *SMPD1* gene (GenBank accession no. X63600), nucleotide A from the methionine initiator codon (ATG) being nucleotide +1, both for mutation description and primer location.

Table 3 Restriction endonucleases and PCR products cleaved for mutation confirmation.

Mutation	Restriction endonuclease	Cleaved PCR product*
H319Y	*Nla*III	NPD1249/OV-NPD2157
P371S	*Bsl*I	NPD3061/OV-NPD3688
F463S	*Apo*I	NPD3658/OV-NPD 4567
P475L	*Eag*I	NPD3658/OV-NPD 4567
Y537H	*Sfc*I	NPD3658/OV-NPD 4567

*PCR products are described by primers used for amplification.

Table 4 ARMS primers

Mutation	ARMS primer	Orientation		gDNA position	Paired primer
G29fsX74	5′-GCC AGG CCC ATC CAA AGG AGT CCG GGA C-3′	3′ → 5′	mutated	106	NPD 307
	5′-GCC AGG CCC ATC CAA AGG AGT CCG GGA G-3′	3′ → 5′	normal	106	NPD 307
S248R	5′-AGG GTC CTC AGG GGC AGG TCA CAC TTG TG-3′	3′ → 5′	mutated	1236	NPD1249
	5′-AGG GTC CTC AGG GGC AGG TCA CAC TTG TT-3′	3′ → 5′	normal	1236	NPD1249

Table 5 Common polymorphisms in *SMPD1* gene

Patient	Exon 1 polymorphism no. of repeats	Exon 2 polymorphism Thr 322 (ACA/ATA)	Exon 6 polymorphism Gly 506(GGG/AGG)
1	six/six	ACA/ACA	GGG/GGG
2	five/five	ACA/ACA	AGG/AGG
3	five/five	ACA/ACA	AGG/AGG
4	six/six	ACA/ACA	GGG/GGG
5	five/five	ACA/ACA	AGG/AGG
6	six/six	ACA/ACA	GGG/GGG
7	six/six	ACA/ACA	GGG/GGG

Results

Fourteen mutant alleles were characterized (Table 1) as well as the presence of the three common polymorphisms in the *SMPD1* gene (Table 5). We found seven novel mutations (G29fsX74, S248R, H319Y, P371S, F463S, P475L, Y537H) and identified one previously known (R608del) mutation. Mutations were distributed throughout the whole gene (Table 1). Six of the novel mutations (S248R, H319Y, P371S, F463S, P475L, Y537H) are single base substitutions; the single nucleotide deletion (G29fsX74) is a frameshift mutation. Information on genotype/phenotype associations is summarized in Table 1. Mutation S248R was found in one patient from the cohort of Czech and Slovak NPD type A and B patients analysed in parallel by Hana Pavlu-Pereira at our institution (manuscript in preparation).

Significant elevations of plasma chitotriosidase activity in Niemann-Pick disease and some other lysosomal storage diseases have already been reported by Guo *et al.* (1995). This enzyme derives from activated macrophages and if elevated may be an indicator of lysosomal storage. Table 1 shows elevated activity of

blood plasma chitotriosidase in all cases where it was measured.

Discussion

The disease-causing character of the novel mutations was evaluated with respect to the accepted criteria for sequence variation discovery and reporting (Cotton & Horaitis, 2000):

1. there was no other nucleotide change in the *SMPD1* coding region, except for the previously described common polymorphisms.
2. all mutations, with the exception of P475L, result in non-conservative amino acid exchanges, the frameshift mutation G29fsX74 results in an early stop codon.
3. the affected amino acid residues are conserved in the human and murine (GenBank accession no. Z14132) *SMPD1* gene, with the exception of glycine 29 which is located in the signal part of the protein.
4. at least two (usually more) independent PCR products were used for DNA sequence analysis.
5. negative results in restriction analysis and ARMS of one hundred control alleles diminished the possibility that the sequence variations found are common genetic polymorphisms. However, in this regard we must note that the controls were of Czech origin because DNA samples of healthy subjects from Dutch and Turkish populations were not available.

The seven novel mutations are most probably private mutations. For these reasons sequencing is the most suitable method for mutation analysis in NPD families.

In patient 7 we found in addition to R608del a synonymous heterozygous mutation (g.54G > A) in exon 1 in one of the alleles. This single nucleotide substitution changes glutamic acid codon GAG, with a frequency of 40,2 per 1000 of codon usages, and to GAA with a frequency of 29,1 per 1000 of codon usages (data based on GenBank Release 129.0, 15th April 2002). A BLAST search set at default values (http://www.ncbi.nlm.nih.gov/BLAST/) using the *SMPD1* gene exon 1 as a query sequence did not reveal a single human EST with this pattern out of 174 BLAST hits. We thus regard this polymorphic change as relatively unimportant, for the above reasons.

Of considerable interest is the high number of homozygotes in our cohort of patients. All four patients of Turkish origin, and one patient of Dutch origin, were found to be homozygous for mutations H319Y, P371S, Y537H, and R608del, respectively. Geographical and/or social isolation (probably more important in our group) of the affected families together with a high rate of intra-ethnic marriages may explain these findings.

The results suggest that the mutations H319Y and Y537H are associated with a type A phenotype, as these two mutations were found homozygously in patients 3 and 2 respectively. Both patients presented with a progressive infantile course of the disease and with residual ASM activities in the range of commonly accepted criteria for type A NPD (Schuchman & Desnick, 2001).

We base association of mutation P371S with type B NPD on the phenotype of patient 5, whose clinical presentation includes only hepatosplenomegaly and no mental retardation in early adulthood.

The influence of mutations G29fsX74, S248R, F463S and P475L on phenotype cannot be derived from our data due to compound heterozygosity of patients 1 and 4. We assume that G29fsX74 is a null mutation as it results in a premature stop codon.

The R608del, found in patients 6 and 7, is the prevalent mutation (87% of mutated alleles) among North-African NPD type B patients from the region of Maghreb (Morocco, Algeria, Tunisia) (Vanier *et al.* 1993). Mutation R608del was always associated with milder type B NPD, even when identified heteroallelically with a severe type A mutation (Levran *et al.* 1991b). The in-frame character of this deletion, and the localisation at the end of the coding sequence of the *SMPD1* gene, may be the reason why the mutation associates exclusively with NPD type B. Both patients 6 and 7 suffer from a typical type B phenotype with corresponding higher residual ASM activities in cultured skin fibroblasts (Table1). At this point we should note that *in-situ* cell-loading assay provides better estimation of lysosomal sphingomyelin degradative capacity than plain *in-vitro* activity measurement (Graber *et al.* 1994). Despite this, genotype/phenotype correlation, as shown for R608del, may play an important role in future

decisions about enzyme replacement therapy of NPD patients.

Acknowledgements

This work was funded by the Research Project of the Czech Ministry of Education No.11110003. We would like to thank Dr. Martin Hrebicek, Dr. Lenka Dvorakova (both from Institute of Inherited Metabolic Disorders, Prague, Czech Republic) and Prof. Jan P. Kraus (Department of Pediatrics, University of Colorado School of Medicine, USA) for critical reading of the manuscript.

References

Barnes, W. M. (1994) PCR amplification of up to 35-kb DNA with high fidelity and high yield from lambda bacteriophage templates. *Proc Natl Acad Sci USA* **91**, 2216–2220.

Cotton, R. G. & Horaitis, O. (2000) Quality control in the discovery, reporting, and recording of genomic variation. *Hum Mutat* **15**, 16–21.

Czartoryska, B., Tylki-Szymanska, A., Gorska, D. *et al.* (1994) Lipidoses detected in Poland through 1993. *Pediatr Neurol* **11**, 295–297.

Da Veiga Pereira, L., Desnick, R. J., Adler, D. A. *et al.* (1991) Regional assignment of the human acid sphingomyelinase gene (SMPD1) by PCR analysis of somatic cell hybrids and in situ hybridization to 11p15.1–p15.4. *Genomics* **9**, 229–234.

Den Dunnen, J. T. & Antonarakis, S. E. (2000) Mutation nomenclature extensions and suggestions to describe complex mutations: a discussion. *Hum Mutat* **15**, 7–12.

Den Dunnen, J. T. & Antonarakis, S. E. (2001) Nomenclature for the description of human sequence variations. *Hum Genet* **109**, 121–124.

Elleder, M. (1989) Niemann-Pick disease. *Pathol Res Pract* **185**, 293–328.

Elleder, M. & Cihula, J. (1983) Niemann-Pick disease (variation in the sphingomyelinase deficient group). Neurovisceral phenotype (A) with an abnormally protracted clinical course and variable expression of neurological symptomatology in three siblings. *Eur J Pediatr* **140**, 323–328.

Elleder, M., Nevoral, J., Spicakova, V. *et al.* (1986) A new variant of sphingomyelinase deficiency (Niemann-Pick): visceromegaly, minimal neurological lesions and low in vivo degradation rate of sphingomyelin. *J Inherit Metab Dis* **9**, 357–366.

Gluck, I., Zeigler, M., Bargal, R. *et al.* (1998) Niemann Pick Disease type A in Israeli Arabs: 677delT, a common novel single mutation. Mutations in brief no. 161. Online. *Hum Mutat* **12**, 136.

Goodman, R. (1979) *Genetic Disorders Among Jewish People.* Baltimore: John Hopkins University Press.

Graber, D., Salvayre, R. & Levade, T. (1994) Accurate differentiation of neuronopathic and nonneuronopathic forms of Niemann-Pick disease by evaluation of the effective residual lysosomal sphingomyelinase activity in intact cells. *J Neurochem* **63**, 1060–1068.

Guo, Y., He, W., Boer, A. M. *et al.* (1995) Elevated plasma chitotriosidase activity in various lysosomal storage disorders. *J Inherit Metab Dis* **18**, 717–722.

Kolodny, E. H. (2000) Niemann-Pick disease. *Curr Opin Hematol* **7**, 48–52.

Krasnopolskaya, K. D., Mirenburg, T. V., Aronovich, E. L. *et al.* (1993) Diagnosis and prevention of lysosomal storage diseases in Russia. *J Inherit Metab Dis* **16**, 994–1002.

Levran, O., Desnick, R. J. & Schuchman, E. H. (1991a) Niemann-Pick disease: a frequent missense mutation in the acid sphingomyelinase gene of Ashkenazi Jewish type A and B patients. *Proc Natl Acad Sci USA* **88**, 3748–3752.

Levran, O., Desnick, R. J. & Schuchman, E. H. (1991b) Niemann-Pick type B disease. Identification of a single codon deletion in the acid sphingomyelinase gene and genotype/phenotype correlations in type A and B patients. *J Clin Invest* **88**, 806–810.

Levran, O., Desnick, R. J. & Schuchman, E. H. (1992) Identification and expression of a common missense mutation (L302P) in the acid sphingomyelinase gene of Ashkenazi Jewish type A Niemann-Pick disease patients. *Blood* **80**, 2081–2087.

Levran, O., Desnick, R. J. & Schuchman, E. H. (1993) Type A Niemann-Pick disease: a frameshift mutation in the acid sphingomyelinase gene (fsP330) occurs in Ashkenazi Jewish patients. *Hum Mutat* **2**, 317–319.

Little, S. (1998) Amplification-Refractory Mutation System (ARMS) Analysis of Point Mutations. In: *Current Protocols in Human Genetics* (eds. N. C. Dracopoli, J. L. Haines, B. R. Korf *et al.*), vol. 2 sec. 9.8. New York: John Wiley & Sons, Inc.

Meikle, P. J., Hopwood, J. J., Clague, A. E. *et al.* (1999) Prevalence of lysosomal storage disorders. *Jama* **281**, 249–254.

Ozand, P. T., Gascon, G., Al Aqeel, A. *et al.* (1990) Prevalence of different types of lysosomal storage diseases in Saudi Arabia. *J Inherit Metab Dis* **13**, 849–861.

Poorthuis, B. J., Wevers, R. A., Kleijer, W. J. *et al.* (1999) The frequency of lysosomal storage diseases in The Netherlands. *Hum Genet* **105**, 151–156.

Schuchman, E. H. & Desnick, R. J. (2001) Niemann-Pick Disease Types A and B: Acid Sphingomyelinase Deficiencies. In: *The Metabolic & Molecular Bases of Inherited Disease* 8th ed. (eds. C. R. Scriver, A. L. Beaudet, W. S. Sly *et al.*), vol. 3 pp. 3589–3610. New York: The McGraw-Hill Companies, Inc.

Schuchman, E. H., Levran, O., Pereira, L. V. *et al.* (1992) Structural organization and complete nucleotide sequence of the gene encoding human acid sphingomyelinase (SMPD1). *Genomics* **12**, 197–205.

Schuchman, E. H., Suchi, M., Takahashi, T. *et al.* (1991) Human acid sphingomyelinase. Isolation, nucleotide sequence and expression of the full-length and alternatively spliced cDNAs. *J Biol Chem* **266**, 8531–8539.

Sperl, W., Bart, G., Vanier, M. T. *et al.* (1994) A family with visceral course of Niemann-Pick disease, macular halo syndrome and low sphingomyelin degradation rate. *J Inherit Metab Dis* **17**, 93–103.

Strauss, W. M. (2000) Preparation of Genomic DNA from Mammalian Tissue. In: *Current Protocols in Molecular Biology* (eds. F. M. Ausubel, R. Brent, R. E. Kingston *et al.*), vol. 1 sec. 2.2. New York: John Wiley & Sons, Inc.

Takada, G., Satoh, W., Komatsu, K. *et al.* (1987) Transitory type of sphingomyelinase deficient Niemann-Pick disease: clinical and morphological studies and follow-up of two sisters. *Tohoku J Exp Med* **153**, 27–36.

Vanier, M. T., Ferlinz, K., Rousson, R. *et al.* (1993) Deletion of arginine (608) in acid sphingomyelinase is the prevalent mutation among Niemann-Pick disease type B patients from northern Africa. *Hum Genet* **92**, 325–330.

Vanier, M. T., Revol, A. & Fichet, M. (1980) Sphingomyelinase activities of various human tissues in control subjects and in Niemann-Pick disease - development and evaluation of a microprocedure. *Clin Chim Acta* **106**, 257–267.

Vanier, M. T. & Suzuki, K. (1996) Niemann-Pick diseases. In: *Neurodystrophies and Neurolipidoses* (ed. H. W. Moser), vol. 66 (22) pp. 133–162. Amsterdam: Elsevier Science.

Wain, H. M., Bruford, E. A., Lovering, R. C. *et al.* (2002) Guidelines for human gene nomenclature. *Genomics* **79**, 464–470.

Received: 11 June 2002
Accepted: 11 November 2002

Appended publication #3

J. Inherit. Metab. Dis. 28 (2005) 203–227

Acid sphingomyelinase deficiency. Phenotype variability with prevalence of intermediate phenotype in a series of twenty-five Czech and Slovak patients. A multi-approach study

H. PAVLŮ-PEREIRA[1], B. ASFAW[1], H. POUPĚTOVÁ[1], J. LEDVINOVÁ[1], J. SIKORA[1], M. T. VANIER[3], K. SANDHOFF[4], J. ZEMAN[2], Z. NOVOTNÁ[1], D. CHUDOBA[5] and M. ELLEDER[1*]

[1]*Institute of Inherited Metabolic Disorders;* [2]*Department of Pediatrics, Charles University 1st Faculty of Medicine and University Hospital, Prague, Czech Republic;* [3]*INSERM U189, Lyon-Sud Medical School, and Laboratoire Fondation Gillet Mérieux, Lyon-Sud Hospital, Pierre-Bénite, France;* [4]*Institute of Organic Chemistry and Biochemistry, University of Bonn, Germany;* [5]*Institute of Biology and Medical Genetics, Charles University 2nd Faculty of Medicine and University Hospital Motol, Prague, Czech Republic*

[*]*Correspondence: Institute of Inherited Metabolic Disorders, Division B, Bldg. D, Ke Karlovu 2, 128 08 Prague 2, Czech Republic. E-mail: melleder@beba.cesnet.cz*

Summary: A multi-approach study in a series of 25 Czech and Slovak patients with acid sphingomyelinase deficiency revealed a broad phenotypic variability within Niemann–Pick disease types A and B. The clinical manifestation of only 9 patients fulfilled the historical classification: 5 with the rapidly progressive neurovisceral infantile type A and 4 with a slowly progressive visceral type B. Sixteen patients (64%) represented a hitherto scarcely documented 'intermediate type' (IT). Twelve patients showed a protracted neurovisceral course with overt or mild neurological symptoms, three a rapidly progressing fatal visceral affection with rudimentary neurological lesion. One patient died early from a severe visceral disease. The genotype in our patients was represented by 4 frameshift and 14 missense mutations. Six were novel (G166R, R228H, A241V, D251E, D278A, A595fsX601). The Q292K mutation (homoallelic, heteroallelic) was strongly associated with a protracted neurovisceral phenotype (10 of 12 cases). The sphingomyelin loading test in living fibroblasts resulted in total degradation from less than 2% in classical type A to 70–80% in classical type B. In the IT group it ranged from 5% to 49% in a 24 h chase. The liver storage showed three patterns: diffuse, zonal (centrolobular), and discrete submicroscopic. Our series showed a notable variability in both the neurological and visceral lesions as well as in their proportionality and synchrony, and demonstrates a continuum between the historical 'A' and 'B' phenotypes of ASM deficiency. This points to a broad

phenotypic potential of ASM deficiency, suggesting the existence of still unknown factors independently controlling the storage level in the visceral and neuronal compartments. This report highlights the important position of the IT in the ASM deficiency phenotype classification. We define IT as a cluster of variants combining clinical features of both the classical types. The protracted neuronopathic variant with overt, borderline or subclinical neurology prevails and is important in view of future enzyme replacement therapy. It appears more common in central Europe. The visceral, rapidly progressing early fatal type has been recognized rarely so far.

Niemann–Pick (NP) disease is a biochemical disorder caused by mutations in the acid sphingomyelinase (ASM) gene (close to 100 published to date). The long history of the disorder, encompassing its separation from types C and D, is a subject of several review articles and monograph chapters (Elleder 1989; Schuchman and Desnick 2001; Vanier and Suzuki 1996). In short, acid sphingomyelinase (ASM; EC 3.1.4.12) deficiency, leading to lysosomal expansion by uncleaved sphingomyelin (SM), presents so far in two phenotypes distinguished by the presence or absence of nervous system involvement. The neurovisceral form, type A, is currently characterized as rapid and fatal within the first years of life. In type B, where storage of SM is restricted to the viscera, the course is considered to be slowly progressive, with patients usually living to adulthood. Atypical or 'intermediate' phenotypes are described as exceedingly rare (Schuchman and Desnick 2001; Vanier and Suzuki 1996). This communication points to an important position of the intermediate type in ASM deficiency in central Europe. It was identified in two-thirds of a series of 25 ASM-deficient patients from 21 families diagnosed during the past 25 years in the Czech and Slovak Republics. We discuss these cases with reference to genotype–phenotype correlation based on clinical data, biochemical findings and results of DNA analysis.

MATERIALS AND METHODS

Information about the patients was collected from clinical records. Diagnosis of ASM deficiency was carried out by the following well-established procedures. In cases clinically suspicious of lysosomal storage, bone marrow smears were examined cytologically (Giemsa staining) and histochemically to identify the ASM deficiency specific storage pattern represented by accumulation of SM liquid crystals (Elleder and Cihula 1983). In most cases ASM activity was examined in peripheral white blood cells (WBC), cultured fibroblasts or postmortem tissue samples using [^{14}C-choline] sphingomylin as substrate according to (Vanier et al 1980). In the liver samples, both bioptic and postmortem, phospholipids were studied quantitatively as well as *storage distribution* in hepatocytes throughout the lobule (Elleder 1989; Elleder et al 1980). Phenotype was determined according to the generally accepted criteria (Schuchman and Desnick 2001). See Figure 1.

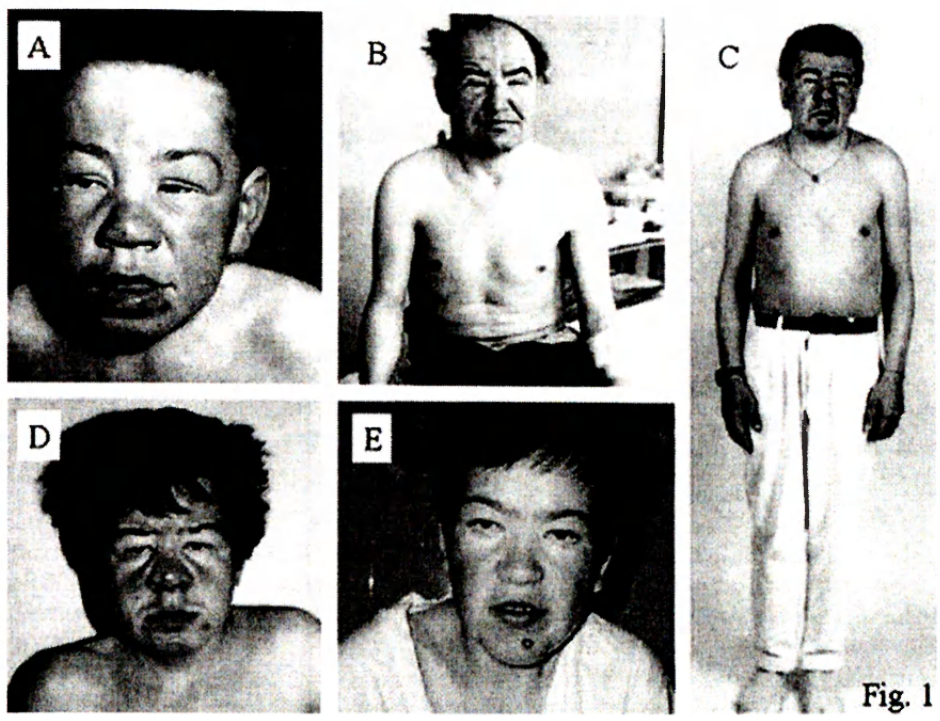

Figure 1 Patients. (A) patient 10 (age 15 years) (published with agreement of the editorial board of *Vnitni lékaství*); (B) patient 11 (age 26 years); (C) patient 14 (age 24 years); (D) patient 15 (age 17 years); (E) patient 9 (age 22 years)

Genomic DNA extraction: Genomic DNA of most of the patients was extracted from blood or from cultured skin fibroblasts. Genomic DNA of patients 3, 6, 21, 23 and 24 was extracted from frozen postmortem tissue samples (spleen, liver and brain). Genomic DNA isolation was carried out according to a standard proteinase K/phenol/chloroform method.

PCR amplifications: The complete ASM coding region, including exon/intron boundaries and parts of 5′ and 3′ untranslated regions, was amplified in four fragments (Table 1). The fragment 1 reaction contained 5% DMSO. Amplifications of fragments 2 and 4 included PCR additive Taq Extender (Stratagene, La Jolla, CA, USA). The yield of fragment 3 amplification was increased using Perfect Match DNA Polymerase Enhancer (Stratagene).

Sequencing: Initially, PCR products were sequenced directly on solid phase (Dynabeads M-280 Streptavidin, Dynal AS, Oslo, Norway) with T7 DNA polymerase and fluorescein-labelled primers or fluorescein-dATP internal label. Later, cycle sequencing protocol with AmpliTaqFS (Perkin Elmer, Boston, USA) and Cy-5-labelled primers was performed. Sequencing reactions were analysed on

Table 1 PCR amplifications

Fragment	*Amplified region*[a]	*Exons*	*Primer*	*Nucleotide sequence* (5′–3′)	*Reference*	T_{ANN} (°C)
1	−211→419	1	NP307	TGACAGCCGCCCGCCACCGAGAGA	Present study	60
			NP2	CTCCATCAGGGATGCATT	(Takahashi et al 1992)	
2	731→1639	2	NP1249	TCCTCTGCTCTGCCTCTGATTTCTCACCAT	Present study	68
			NP2157	AATCAGAGACAATGCCCCAGGTTCCCTTCT	Present study	
3	2543→3170	3,4	NP3061	CCCAGCACAGGAGGACCAGGATTGGAA	Present study	72
			NP3688	GGGACAACAGGGATGGTGAGATGCTCA	Present study	
4	3140→4039	5,6	NP3658	CCCTTGAGCATCTCACCATCCCTGTTG	Present study	68
			NP4567	GCTTTTTCACCCTTTCCTACATCAAGAACT	Present study	

[a] Nucleotides numbered at gDNA level starting with the first ATG

automated fluorescent sequencers ALFExpress (Amersham Biosciences, Uppsala, Sweden).

RFLP: To confirm and detect novel mutations, restriction analysis was carried out for each of the novel mutations changing a restriction endonuclease recognition site (Table 2).

ARMS: The amplification refractory mutation system was established for the detection of the rest of the novel mutations. PCR primers (Table 2) were designed to discriminate between the mutant and wild-type alleles. As an internal control for amplification, the reaction mixture contained a second pair of primers, amplifying a different part of the genome (not shown).

Site-directed mutagenesis: Six of 14 mutations found in our laboratory were introduced into the full-length ASM cDNA in the pSVSport1 cloning vector (Life Technologies, Paisley, UK) using Transformer Site-Directed Mutagenesis Kit (Clontech, Palo Alto, CA, USA) based on the method of Deng and Nickoloff (1992).

Transient expression in ASM-deficient skin fibroblasts: Skin fibroblasts of patient 3, carrier of the L178fsX190 mutation in homozygous state, were immortalized with pRNS-1 plasmid by a lipofection transfection (FuGene TM6, Boehringer, Mannheim, Germany) (Litzkas et al 1984). Transformed NP-A fibroblasts were cultured routinely in DMEM (Gibco, Paisley, UK) supplemented with antibiotics and 10% fetal calf serum (FCS). Cells were transfected in OptiMEM (Gibco) in the absence of serum by DOTAP Liposomal Transfection Reagent (Roche, Basel, Switzerland). Negative controls for the transfections contained either no plasmid or vector alone. After overnight transfection, cells were incubated in DMEM with antibiotics and 10% FCS and

Table 2 Methods for confirmation and detection of novel mutations

Mutation	*Restriction endonuclase*	*ARMS primer for mutant allele* (5′–3′)	*ARMS primer for wild-type allele* (5′–3′)	*5′-Primer*
G166R	*Sfc*I			
P184L	*Alu*I			
R228H	*Xcm*I			
A241V	*Ban*I			
S248R	–	AGGGTCCTCAGGGG CAGGTCACACTTGTG	AGGGTCCTCAGGGG CAGGTCACACTTGTT	NP1249
D251E	*Bsp*MI			
D278A	*Bsm*AI			
R289H	*Bcg*I			
Q292K	*Ava*II			
L341P	*Sau*96I			
R376H	*Aci*I			
R474W	*Alu*I, *Bsr*FI			
W533R	*Bsr*FI			
A595fsX601	–	CTGTCAGCACGGGCA GAGAGCTGGGCACTG	CTGTCAGCACGGGCA GAGAGCTGGGCACTA	NP3658

harvested after 53 h. ASM activities were determined using the micromethod of Vanier and colleagues (1980).

Mutation nomenclature: All new mutations are described according to recent recommendations (den Dunnen and Antonarakis 2001). The reference genomic sequence of the ASM gene is numbered from the first ATG translation-initiation codon.

SM loading test: Preparation of (methyl-^{14}C)sphingomyelin. Sphingomyelin isolated from human erythrocytes was demethylated with sodium thiophenolate and remethylated with (^{14}C)methyl iodide (Bowser and Gray 1978). The crude product was purified by preparative TLC. The specific radioactivity of purified (*methyl*-^{14}C)sphingomyelin was 53 mCi/mmol and purity ranged from 98% to 100%.

Cell culture. Skin fibroblasts derived from normal controls and from patients with NP disease were routinely grown in MEM containing 10% FCS in 25 cm^2 flasks.

Loading assays. Near-confluent monolayer cells were preincubated in MEM containing 10% lipoprotein-deficient serum prior to application of SM. After 2 days, the same fresh medium containing human serum LDL (75 μg/ml) and [^{14}C]-sphingomyelin (60 nmol, 300 000 dpm/flask) was applied to each flask in a total volume of 3 ml. After a 3 h pulse, the medium was replaced with fresh medium for 2 or 24 h chase. Lipoprotein-deficient serum and LDL were prepared from fresh human plasma in the laboratory by ultracentrifugation as described by Goldstein and colleagues (1983). Pre-incubation in the lipoprotein-free medium enhances expression of LDL-receptors and promotes apoB/E-receptor-mediated pathway of substrate cellular transportation, thus providing fast and specific lysosomal targeting of SM. This is a similar strategy to substrate application in liposomal form with integrated apolipoprotein E (Asfaw et al 1998, 2002).

Cell harvesting. Incubation was terminated by removing the medium; the fibroblasts were rinsed twice with 3 ml of PBS and then incubated with 0.6 ml of trypsin in PBS for 5 min at 37°C. After adding 4 ml of medium (MEM with 10% FCS), the suspension was transferred to centrifuge tubes, the culture flask was washed with PBS (2 ml) and the washing was added to the cell suspension. After centrifugation, the cell pellet was resuspended in 1.5 ml PBS and centrifuged. This procedure proved to be sufficient to remove adsorbed lipids from the cell surface.

Extraction and TLC analysis of lipids. The cell pellet was sonicated for 3 min in a cup-horn sonifier. Aliquots of cell homogenate, medium and trypsin-PBS were mixed with scintillation cocktail and radioactivity was measured in each fraction. Cell homogenate (400 μl) was extracted with chloroform–methanol 2:1 v/v (1.6 ml). After vigorous mixing, the mixture was centrifuged for 10 min at 1000*g*. Both the upper and the lower phases were aspirated and saved. The interphase was re-extracted with (1.6 ml) chloroform–methanol 2:1 v/v. The combined extracts were evaporated to dryness under N_2 (Asfaw et al 1998). The residues were redissolved in 50 μl chloroform–methanol 2:1 v/v and applied to the TLC plate (20×20 cm). Chromatograms were developed in chloroform–methanol–water 65:35:4 (by volume). Evaluation was performed either using a TLC-Linear Radioactivity Analyzer (Raytest, Straubenhardt, Germany) or spots were localized by exposure to iodine and scraped. After mixing with scintillation cocktail, radioactivity was measured.

Table 3 Rapidly progressing neurovisceral storage, classic type A

Patient no. *Sex* *Year of birth*	*Clinical history*	*Liver SM* (μm/g w.w.) [% of lip P] *storage pattern*	*ASM activity* (nmol/h per mg) [% of controls]	*ASM gene mutations*	*No. of alanine/leucine repeats in signal peptide*
1 M 1989	Infantile onset with PMR, prominent HSM, abnormal EEG, hypotonia and retinal cherry- red spot. Death at the age of $5\frac{1}{2}$ months. Brother of case 2.	(fixed sample) 74.3 [72%] Diffuse	ND	A595fsX601/ A595fsX601	6/6
2 F 1984	Infantile onset with prominent HSM, PMR, areflexia, hypotonia; abnormal EEG; retinal cherry-red spot. Death at the age of 2 years. Sister of case 1.	ND	Liver 0.48 [0.4%]	A595fsX601/ A595fsX601	6/6
3 M 1989	Infantile onset with massive HSM, progressive PMR and hypotonia; retinal cherry-red spot. Death at the age of 20 months.	A 90.1 [51%] Diffuse	Fibroblasts 0.0 (0%)	L178fsX190/ L178fsX190	6/6
4 M 1974	Infantile onset with prominent HSM, progressive PMR and fits; pulmonary infiltration; eye fundus not examined. Death at the age of 3 years 9 months. Brother of case 5.	ssA 1.7 [63%] Diffuse	Liver 0.065 [0.3%]	D278A/Q292K	4/6
5 F 1980	Infantile onset with prominent HSM and progressive PMR; diffuse pulmonary infiltration; eye fundus described as normal. Death at the age of 3 years 7 months. Sister of case 4.	A 142.7 [60%] Diffuse	Liver 0.046 [0.2%]	D278A/Q292K	4/6

M, male; F, female; A, autopsy sample; HSM, hepatosplenomegaly; PMR, psychomotor retardation; ND, not done
[a] Control values: liver SM lipid P 2.21 ± 0.94 (8 + 1.8%)
[b] Control ASM activities: fibroblasts 134 ± 33 (n = 10); peripheral WBC 3.68 ± 0.99 (n = 65), liver 19.6 ± 9.37 (n = 3)

Table 4 Intermediate type with protracted course and severe neurological symptomatology

Patient no *Sex* *Year of birth*	*Clinical history* (age at which the symptom was first recorded is given in parentheses)	*Liver SM* (μm/g ww) [% of lip.P.] *Storage pattern*	*ASM activity* (nmol/h per mg [% of controls]	*ASM gene mutations*	*No. of alanine/leucine repeats in signal peptide*
6[a] M 1963	Infantile onset with prominent HSM, spasticity, rigidity and ataxia; fits (3 years); eye fundus not examined. Death at the age of 8 years.	A 27.4 [54.9%] Diffuse	Liver 0.005 [0.3%][g]	D278A/Q292K	4/6
7[b] M 1974	Prominent HSM (2 years); progressive PMR, spasticity, rigidity, dyskinesis (3 years); eye fundus normal; decreased NCV. Death at the age of 9 years.	B Diffuse (revision)	Fibroblasts[h] 1.18 [0.9%]	P189fsX254/Q292K	4/6
8[c] F 1968	Moderate HSM (infancy); progressive PMR with dementia, hypertonia, hypokinesis (1 year); retinal cherry-red spot. Death at the age of 14 years.	B 36.6 [57.8%] Diffuse	Indirectly[i]	Q292K/P330fsX382	4/5
9 F 1978	Prominent HSM (2 years); PMR, hypotonia, fits, facial myoclonias (14 years); perimacular whitish halo with external ill-defined border; MRI (22 years): slightly decreased T2W and increased T1W signals in pallidum (increased Fe content?), slight periventricular atrophy; EEG grossly abnormal; decreased motor NCV (to 16.5 m/s), n.peroneus unresponsive; prolonged BAEP and SEP latencies; stabilized course. Present age 24 years. (Figure 1E).	B Diffuse (revision)	WBC[h] 0.02 [0.5%] Fibroblasts[h] 0.2 [0.15%]	Q292K/Q292K	4/4
10[d] M 1948	Prominent HSM and progressive PMR (since infancy); dementia, spasticity, contractures; pulmonary infiltration (Figure 1A); dysmorphia (urinary	A Unsuccessful for autolysis (revision)	ND[j]	paternal gDNA: Q292K	Paternal gDNA: 4/6

	GAG analyses normal); eye fundus physiological. Death at the age of 26 years.				
11[e] M 1961	Moderate HSM and lymphadenopathy (6 years); dementia, hypertonia, dystonia, rare fits (8 years); retinal cherry-red spot; premature aged appearance (Figure 1B). Death at the age of 32 years.	B 18.25 [40.1%] Diffuse with centrolobular accentuation	Fibroblasts[i] 1.15 [1.1%]	Q292K/Q292K	4/4
12[f] M 1960	HSM (6 years); extrapyramidal symptoms, followed by neo- and paleocerebellar symptoms (8 years); retinal perimacular halo; prominent cerebellar atrophy on MRI; stabilized course. Present age 43 years. Brother of patients 16 and 18.	B Medio/centrolobular	Fibroblasts[i] 2.27 [2.1%]	P330fsX382/L341P	5/6
13 M 1994	Moderate HSM (infancy); slowly progressive PMR, hypertonia, ataxia since infancy; EEG within normal limits; uniilateral (right eye) perimacular whitish ring (5 years); peripheral neuropathy (lower extremities); slowly progressive course. Present age 9 years.	Not biopsied	WBC[h] 0.0 [0%] Fibroblasts 1.04 [0.8%]	Q292K/W533R	4/6

B biopsy sample; NCV, nerve conduction velocity (normal value this age group is 40–60 m/s); BAEP, brainstem auditory evoked potentials; SEP, somatosensory evoked potentials. *For further abbreviations see Table 3*

[a] Published as Niemann–Pick type C (Elleder et al 1975) and subsequently in biochemically verified form (Elleder et al 1980)

[b] Two sisters died with similar symptomatology

[c] For further details see case 2 in (Elleder and Cihula 1983)

[d] Published as 'sea-blue histiocyte syndrome', case 1 in Hermansky et al (1971). Revision of the autopsy protocol and additional histochemical examination showed findings compatible with ASM deficiency (Elleder 1989). Heterozygous values of ASM could be proved in the only one living parent

[e] See case 1 in Elleder and Cihula (1983)

[f] Published as case 4 in Elleder and Cihula (1983). See also Obenberger et al (1999)

[g] Activity assayed by K. Harzer (Tübingen). Control values 2 ± 1.5 (n = 5)

[h] Activities assayed in Prague. Control values: fibroblasts 134 ± 33 (n = 10); WBC 3.68 ± 0.99 (n = 65)

[i] Activity assayed by M.T. Vanier (Lyon). Control range 108 ± 36 (n = 30)

[j] ASM values in parental WBC were in heterozygous range. Retrospective study after proband's death

The study was approved by the Ethics Committee of the University Hospital and First Faculty of Medicine, Charles University, Prague.

RESULTS

Only 9 of the 25 patients (36%) could be classified according to the established scheme dividing ASM deficiency into groups A and B. Five of the patients corresponded to the classical type A (Table 3) and four to the classical (protracted course) type B phenotype (patients 22–25, Table 7). The remaining 16 patients (64%) differed either by atypical course length (abnormally protracted in neuronopathic or abnormally accelerated in nonneuronopathic cases) or by an unusual proportion between the storage intensity in the visceral and neuronal cell pools: 12 patients displayed *protracted course* with neuronopathic features more (Table 4) or less (Table 5) apparent; in three other patients the course was dominated by prominent visceral affection of relatively rapid course associated with discrete neuronal storage disclosed mostly at autopsy (patients 18–20, Table 6). In one case with rapid course, the neuronal lesion was absent at both clinical and histological levels (patient 21, Table 7). Nine patients are living: two are of the classical type B; seven belong to one of the above-mentioned intermediate phenotypes.

Results of biochemical and molecular analyses (except those from the SM loading test) are presented together with clinical data in Tables 3–7.

Storage pattern in the liver lobule: Storage distribution differed (see Tables 3–7). There was diffuse uniform involvement of hepatocytes in patients with pronounced visceral storage and in neurologically affected patients, with the exception of patients 12, 16 and 18 in whom involvement was restricted to the inner half of the lobule. In patients with the protracted B type, with high residual ASM activity and high value of SM degradation in loading tests, the storage was either restricted to small groups of centrolobular hepatocytes (patients 23, 24 and 25) or histologically undetectable within the lobule except for the Kupffer cells (patient 22). Typical storage cells were identified in the bone marrow in all patients. The only exception was patient 19 with rudimentary vacuolized bone marrow macrophages.

Mutational analysis: Forty-one independent mutant alleles (49 mutant alleles for the whole series) were characterized. From proband 10, only paternal gDNA was available.

Four frameshift and 14 missense mutations were identified. Five mutations are new: P184L (g.1017C>T), R228H (g.1149G>A), A241V (g.1188C>T), D251E (g.1219C>A) and D278A (g.1299A>C). In addition, two further mutations were described in our previous communication (Q292K (g.1340C>A) and L341P (g.1488T>C) (Pavlu and Elleder 1997)) and seven (G166R, S248R, R289H, R376H, R474W, W533R and A595fsX601) were published during completion of the present work (Sikora et al 2003; Simonaro et al 2002). Other mutations (L178fsX190, P189fsX254, P330fsX382 and G577S) are known (Ferlinz et al 1991; Gluck et al 1997; Levran et al 1993; Takahashi et al 1992). In families of patients 4, 5, 9, 12, 14, 15, 16, 17 and 18, where it was possible to obtain gDNA samples, mutations were confirmed in both parents, always in heterozygous state.

Table 5 Intermediate type with chronic visceral storage and mitigated/subclinical neurological lesion

Patient no. *Sex* *Year of birth*	*Clinical history* (age at which the symptom was first recorded is given in parentheses)	*Liver SM* (μm/g ww) [% of lip.P] *Storage pattern*	*ASM activity* (nmol/h per mg) [% of controls]	*ASM gene mutations*	*No. of alanine/leucine repeats in signal peptide*
14[a] M 1976	Moderate HM and prominent SPM (1 year). Brownish-red macula surrounded by relatively sharply demarcated whitish-grey ring. Stabilized course. Since the second decade frust prefrontal and extrapyrimidal syndrome, mild prolongation of evoked potentials latencies (VEP, BAEP, SEP) and further decrease in both motor and sensitive NCVs (to 19.1 m/s, and 11.4 m/s, resp.); dysmorphic and premature age appearances. Present age 27 years. (Figure 1C).	B 16 2 [35.4%] Centrolobular	Fibroblasts[d] 1.04 [0.9%]	Q292K/Q292K	4/4
15[b] M 1983	Prominent HSM (4 months). Slowly progressing PMR. Retinal cherry- red spot with whitish perimacular unsharply demarcated infiltration. Mild pulmonary infiltration. Since the end of the first decade, dementia and occasional fits. EEG slightly abnormal (8 years); NCV decreased (last measurement 1996); peripheral neuropathy of mixed axonal and demyelization type; dysmorphic features. Present age 20 years. (Figure 1D).	B 21 3 [40.3%] Diffuse	Fibroblasts[d] 0 47 [0.4%]	Q292K/Q292K	4/4

Continued.

Table 5 Continued

Patient no *Sex* *Year of birth*	*Clinical history* (age at which the symptom was first recorded is given in parentheses)	*Liver SM* (μm/g w.w) [% of lip.P] *Storage pattern*	*ASM activity* (nmol/h per mg) [% of controls]	*ASM gene mutations*	*No. of alanine/leucine repeats in signal peptide*
16[c] M 1964	Moderate HSM (6 years); perimacular relatively sharply demarcated halo; neurology without any overt deficit. MRI: cerebellar atrophy. Present age 39 years. Brother of patients nos. 12 and 18.	B ND Medio/centroiobular	Fibroblasts[d] 2.2 [2.1%]	P330fsX382/L341P	5/6
17 F 1996	Moderate HSM (18 months); retinal perimacular whitish relatively sharply demarcated halo; normal neurology and BAEP, except for slight prolongation of N70 wave (VEP). MRI: slight frontotemporal atrophy. Present age 7 years.	Not biopsied	WBC[e] 0.05 [1.4%] Fibroblasts[e] 0.95 [0.7%]	Q292K/G577S	4/5

SPM, splenomegaly; ND, not done. *For further abbreviations see Tables 3 and 4*. NCV normal value this age group is 40–60 m/s
[a, b] Published as cases no. 3 and no. 1 respectively, in Elleder et al (1986)
[c] For further details see Elleder and Cihula (1983), Obenberger et al (1999)
[d] Activity assayed in Lyon (M T. Vanier). Control range 108 ± 36 (n = 30)
[e] Activities assayed in Prague. Control values: fibroblasts 134 ± 33 (n = 10), WBC 3.68 ± 0.99 (n = 65)

Table 6 Intermediate type with accelerated visceral course with rudimentary neurological lesion

Patient n.o. *Sex* *Year of birth*	*Clinical history* (age at which the symptom was first recorded is given in parentheses)	*Liver SM* (μm/g ww) [% of lip P] *Storage pattern*	*ASM activity* (nmol/h per mg) [% of controls]	*ASM gene mutations*	*No. of alanine/leucine repeats in signal peptide*
18[a] F 1955	Moderate HM with prominent SPM (2years); progressive diffuse pulmonary infiltration subsequently; whitish perimacular sharply demarcated halo; neurologically normal[b]. Died at the age of 7 years. Sister of patients 12 and 16.	A Medio/ centrolobular (revision)	ND	P330fsX382/L341P	5/6
19[c] M 1982	Massive rapidly progressive HSM since early infancy; retinal cherry-red spot; slight PMR, hyporeflexia (8 years); terminally fits[d] Rudimentary vacuolation of bone marrow storage cells.Died at the age of 9 years.	B 84.5 [63.5 %] Diffuse	Fibroblasts[e] 1.44 [1.3%]	D251E/D251E	6/6
20[d] M 1975	Massive HSM (2 months); PMR (24 months); cherry red spot (27 months); progressive diffuse pulmonary infiltration. Succumbed to liver and respiratory failure at the age of 31 months.	B 81.7 [80%] Diffuse	Fibroblasts 6.2 [4.6%][f]	S248R/D278A	6/6

For abbreviations see Tables 3–5

[a] Sibling of patients 12 and 16. Because of identity of the genotype in these two siblings, the same mutation pattern is presumed

[b] Mild neuronal storage identified at autopsy (Elleder and Ciutia 1983)

[c] Published as case no. 2 in Elleder et al (1986); autopsy disclosed mild neuronal storage and cerebellar cortical atrophy (unpublished)

[d] Published by Rosipal and Machalec (1982). Normal values of SM were reported for the brain

[e] Assayed in Lyon (for control range see Table 5)

[f] Assayed in Prague (control range 134 ± 33; $n = 10$). Assayed in London (E. Young) showed 2.6 nmol/h per mg (control range 38–161 nmol/h per mg; typical values for type A 0.47). Residual 20% ASM activity in WBCs was found by K. Harzer (Tübingen)

Table 7 Patients with purely visceral affection with various speed of clinical progression (patient no. 21 represents an intermediate type)

Patient no. Sex Year of birth	Clinical history and findings (age at which the symptom was first recorded)	Liver M (µg/g ww) Storage cells [% of cells]	M (nmol/mg) [% of controls]	Genotype	No. of alleles/leucine sites
21 M 1967	Massive HSM since infancy; neurologically normal[b]; normal eye fundus. Died at the age of 8 years in liver failure.	[69.4%]	[1%]	A241V/R474W	5/6
78	SPM (2 years); slowly progressive hypersplenism; no signs of neurological affection; normal eye fundus; slow course. Typical bone marrow storage cells. Present age 25 years.			R289 / 292K	4/5
23[d] M 1927	Cirrhosis with SPM and hypersplenism (36 years); normal eye fundus; slow progression with development of liver cirrhosis and liver cancer; terminally acute psychiatric symptomatology. Died at the age of 56 years from oesophageal varices bleeding.	5.		P184L/Q292K	4/5
24[e] f 31	SPM and mild HM (51 years) when examined and treated for multiple sclerosis; normal eye fundus; slow course influenced by the neurological disease[f]. Died at the age of 60 years (pulmonary embolism).	.8 [36.	4.4	R22 / 595t 601	5/6
25 M 1965	Moderate HSM (9 years); splenic storage identified in the spleen ruptured at motoring accident (21 years); normal eye fundus, no neurology; neurasthenic syndrome; stabilized course. Typical bone marrow storage cells. Present age 38 years.		20.2 [18.7%]	/R376H	5/5

tion ge 7 s

ities saye L (tro a 08 n = 30)

al st ge a aut s l re ls h en ual storage (Elleder 1989)

Tub gen (Hi 2 1 ( )

y He ansk al cyt d , c and al s a(eder an 3) a type The d

h lse e rim g ture (E Ben 19 (M Vanie 7 type 30

e y Rc et al (19 dati ngle h tes M. Vanier, c ad r type

e leros verified itho of M ie ela n l storage (M.)

The disease-causing character of the novel mutations was evaluated with respect to the accepted criteria for sequence variation discovery and reporting (Cotton and Horaitis 2000): (1) There was no other nucleotide change in the ASM coding region, except for the described common polymorphisms. (2) All affected amino acid residues are conserved between human and mouse (GenBank accession no. Z14132) ASM gene; the R228, A241, D251 and D278 amino acids between human, murine and also *C. elegans* potential ASM orthologous gene (GenBank accession no. NP495415). (3) At least two (usually more) independent PCR products were used for DNA sequence analysis. (4) Negative results in restriction analysis and ARMS of 100 control alleles diminished the possibility that the found sequence variations might be common genetic polymorphisms.

Polymorphisms within the ASM gene: All patients were homozygous for Thr in the polymorphic codon 322 (Schuchman et al 1991b). In Gly/Arg 506 polymorphism (Schuchman et al 1991a), most of the patients carried the Gly506 allele in the homozygous state, with the exception of patient 25, who was homozygous for the Arg506 allele and patients 17, 21, 22 and 23, who were mixed heterozygotes. Alleles with four to six hexanucleotide units were identified in the signal peptide polymorphic alanine/leucine repeat region (Wan and Schuchman 1995). Interestingly, in all the carriers of the Q292K mutation in the heterozygous or homozygous state, the four-unit allele was found in the heterozygous or homozygous state, respectively. One hundred control alleles were screened for the polymorphism in the signal peptide region. The four-hexanucleotide variant was found in eight of them, always in the heterozygous state. None of the controls carried the Q292K mutation as verified by RFLP.

Results of the transient expression in ASM-deficient human skin fibroblasts (Table 8): Six mutations were subjected to transient expression in ASM-deficient fibroblasts. Mutation D278A, identified in two patients with type A and in one patient with a protracted form of type A, did not express a catalytically active enzyme. Both expressed D251E and Q292K ASM mutations, identified in the homozygous state in patients

Table 8 Transient expression of ASM in NP A cells

Enzyme source	*ASM activity* (nmol/h per mg)
Untransfected NP A cells	0
NP A cells tranfected by:	
PSVSport1	0.26 ± 0.11
pSVSport1–ASM constructs:	
WT-ASM	13.12 ± 3.5
P184L	5.71 ± 0.45
D251E	0.36 ± 0.04
D278A	0.13 ± 0.08
Q292K	0.31 ± 0.06
L341P	0.88 ± 0.31
R376H	5.38 ± 1.31

The values from our patients represent an average of 2–3 experiments

with neurovisceral protracted forms, displayed very low catalytic activity. The L341P mutation, found together with a known frameshift P330fsX382 mutation in one family with three children, each with intermediate phenotype (patients 12, 16 and 18), produced about 5% of the levels obtained from expression of normal ASM. Activity of mutations R376H and P184L identified in NP-B patients in heterozygous state reached about 40% of the values from the expressed wild-type ASM.

Sphingomyelin ex vivo *hydrolysis* (Figure 2): Loading experiments showed two extreme groups with results corresponding to the data published to date and with clear-cut correlation to the phenotype: the *NPA group* with almost zero ASM activity and rapid fatal course (patients 2 and 3), and patients with the *classic B type* (patients

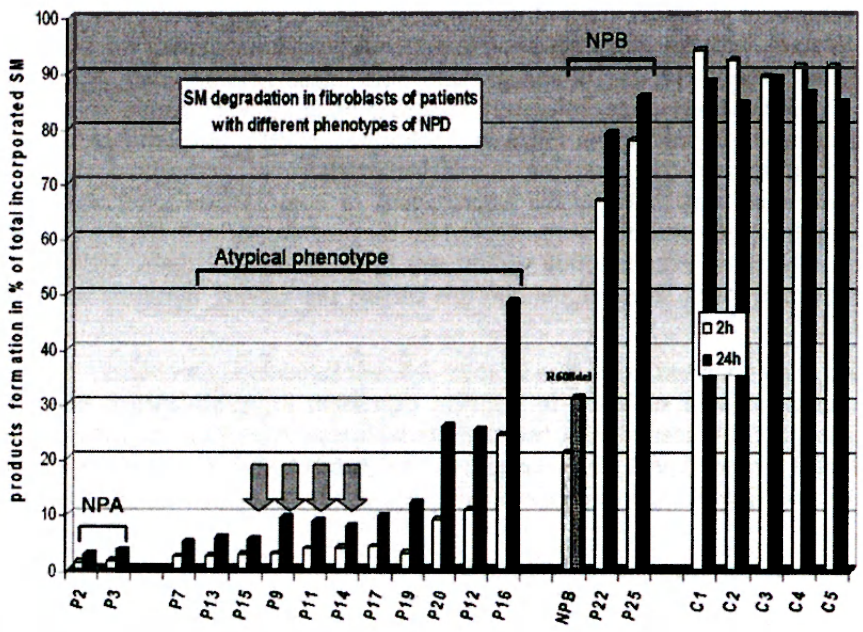

Figure 2 Degradation of LDL-targeted [^{14}C]sphingomyelin in cultures of skin fibroblasts of NP patients with different phenotypes (white columns 2 h chase, black columns 24 h chase). P2–P25 indicate patients. Numbers correspond with the description in Tables 3–7. NPA = classical NPA phenotype. Atypical phenotype = group of patients with atypical phenotypes. Arrows mark patients homozygous for Q292K mutation. NPB = NPB phenotype. R608del = mean values obtained with cells from NPB patients homozygous for R608del mutation (French patients from the M.T. Vanier series). R608del is considered the 'standard' NPB mutation (mild). Grey columns represent 2 h chase ($n = 5$, mean ± SD = 20.5 ± 8.7), hatched columns 24 h chase ($n = 5$, mean ± SD = 31.2 ± 7.4). Values are included for demonstration of a wide heterogeneity in NPB phenotypes. C1–C5 = controls ($n = 5$, 2 h chase mean ± SD = 90.3 ± 2.3; 24 h chase mean ± SD = 88.7.6 ± 2.9). Values are means from at least two experiments

22 and 25) with highest residual activities described so far (compare with Graber et al 1994; Schuchman and Desnick 2001; Vanier et al 1985).

The group with the intermediate phenotype proved to be heterogeneous in the loading test. It encompasses the subgroup of patients homozygous for the Q292K mutation (patients 9, 11, 14 and 15) with low but still significant residual degradative capacity, a condition that could explain the protracted course with neuronopathic features. In contrast, two patients with higher degradation capacity (patients 19 and especially 20) displayed mostly visceral relatively rapid progression of the disease contrasting with the slow progression in the Q292K homozygotes.

In three siblings showing diverse phenotypes in spite of similar genotypes, the values of sphingomylin hydrolysis measured in two of them (patients12 and 16) differed and reflected exactly the severity of the clinical phenotype. In accordance with the relatively efficient SM degradation, again close to the B range, the course of patient 12 is chronic and stabilized but with neurological participation.

DISCUSSION

The phenotype at the clinical level

The clinical course of the majority of our patients does not correspond to the standard phenotypes. The classical phenotypes A with rapid progression of proportionally severe neurovisceral storage (Table 3) and B with protracted purely visceral storage (Table 7) were seen in only 9 of the 25 cases (36%). The remaining 16 cases in the series (64%) displayed variable dynamics, intensity and timing of the storage process in the two basic compartments: neuronal and visceral.

Neuronopathic lesion – a continuous clinical spectrum: In 12 patients (Tables 4 and 5) the combination of visceral storage with a protracted course of neurological involvement (from subclinical to overt clinical) with a protracted course sharply contrasted with the rapid progression of the classical acute neurovisceral type A. In five of the patients with clinically overt neurology, the course was fatal, with age at death between 8 and 32 years. The remaining patients are alive with present ages ranging from 7 to 43 years. The neurological lesion was mostly progressive and its severity was indirectly proportional to the age of its onset. However, in three cases with borderline neurological symptoms (patients 12, 14 and 16), the course has been surprisingly stabilized, even over two to three decades. In two other cases the initial subclinical neurological affection deteriorated (patients 9 and 15). This finding also shows that there is no rigid demarcation between the two groups of patients presented in Tables 4 and 5. In three further cases (patients 18, 19 and 20) the delayed borderline neurological manifestation was disproportional to the rapidly progressive fatal visceral storage, which we consider to be an extreme in this group (see also below).

The relatively high proportion of protracted atypical neuronopathic forms in the present series contrasts with their paucity in published reports on ASM deficiency (Martin et al 1972; Vanier et al 1985). However, a recently published report fully supports fully our observation (Harzer et al 2003). Adult ASM-deficient patients have

been reported with psychiatric symptoms, the nature of which may have not been related to the enzymopathy (Dubois et al 1990; Sogawa et al 1978). In our series, combination of the typical B type with an unrelated neurological disorder has been described in patient 24 and terminal psychiatric symptoms developed in patient 23 (Table 7). In both cases brain storage was excluded *post mortem*. There are reports of a ' macula halo syndrome', which is considered to belong to the phenotype B with retinal involvement represented by a sharply demarcated perimacular halo. Despite the retinal lesion, which might signify neuronal affection (Walton et al 1978), the patients were free of neurological symptoms (Cogan et al 1983; Filling-Katz et al 1992; Hammersen et al 1979; Harzer et al 1978; Lipson et al 1986; Matthews et al 1986; Shah et al 1983; Sperl et al 1994; Takada et al 1987; Takahashi et al 1997). However, the result of the SM loading tests that was carried out in one of the families was in the A range (Sperl et al 1994). What is missing is knowledge about the nature of the affected retinal cell type. Affection of the retinal macrophagic system was suggested by Lowe and colleagues (1986). However, the perimacular retinal lesion seen in patients 9, 12 and 14–18 was always associated with neurological affection mostly of a progressive nature. This led us to the suggestion that the retinal lesion in our patients might be a variant of the classical cherry-red spot concentrated to the perimacular region most rich in neuronal cell bodies (Fawcett 1986). The features of the typical macula halo (i.e. a sharp demarcation of its borders and granular interior) never dominated, except for patients 12 and 16, who also displayed neurological affection. The neurological status of our patients with perimacular retinal lesions thus differs from that in the recently published cohort of type B patients (McGovern et al 2004)

Spectrum of clinically dominant visceral phenotype: Four patients with typical B type (patients 22–25, Table 7) displayed benign course with high residual enzyme activity and remarkably high SM degradation in the loading test (measured in patients 22 and 25). This correlates well with the restricted, albeit definite, visceral storage and higher residual ASM activity, sufficient to protect neurons from the storage in these patients (Graber et al 1994; Schuchman and Desnick 2001). Accelerated fatal B type has only been described in two unrelated patients (Labrune et al 1991) and identified in another one (M.T.V., unpublished). Otherwise, liver failure in adult B type patients was precipitated by additional factors (Wilson and Raufman 1986; Zhou et al 1995), including terminal stage of cirrhosis (Putterman et al 1992). In four patients of our series (Table 6 and patient 21 in Table 7) the clinical course, remarkably accelerated with massive visceral storage, was fatal within the first decade of life. The striking feature of these cases was a notable disproportion between the levels of visceral and neuronal storage. Whereas the visceral storage attained levels seen in classical A types (cf. values of SM storage in patients in Table 3), the neuronal storage (checked by neuropathology) was disproportionately low (patients 18, 19 and 20), pointing to variant type A (borderline or subclinical neurology). In patient 21 the rapidly progressive massive storage was restricted to the visceral organs, leaving neurons intact, even after an interval exceeding several times that of classical type A. Likewise, a fully normal lipid composition of brain tissue, with no abnormal sphingomylin or lysosphingomyelin storage, was also reported in

the above-mentioned acute type B patients deceased at 3 years of age (Labrune et al 1991; Rodriguez-Lafrasse and Vanier 1999). The unique phenotype of these patients represents an extreme in the B group and strongly suggests a continuum in the viscerally restricted storage.

In summary, the range of phenotypic diversity allows us to conclude that, besides the classical variants A and B, a broad 'intermediate' phenotype (IT) shares feature of both classic types. This IT constitutes a continuum ranging from protracted neurovisceral variants to accelerated visceral variants. The latter may be (but need not be) associated with delayed onset of manifest neurolysosomal storage, the first stage of which may be at the subclinical level

The remarkable disproportionality between the visceral and neuronal involvement suggests that these two tissue compartments may react in different ways to the same degree of ASM deficiency and indicates the presence of factors either influencing lysosomal SM turnover in these two pools in a differential manner or exerting relatively efficient protection, at least temporarily, against storage. This observation is in sharp contrast with the widely accepted view that massive visceral storage and low ASM residual activity are generally associated with a rapid course and severe neuronal damage (Graber et al 1994; Schuchman and Desnick 2001).

The existence of such additional factors is supported by phenotypic diversity within the intermediate type in three siblings (patients 12, 16 and 18), which may be interpreted as a neurovisceral phenotypic continuum featuring visceral storage, either rapidly progressive fatal with subclinical neurolysosomal storage (patient 18), or moderate with delayed onset of clinically borderline (patient 16) or overt (patient 12) neurological affection. Phenotypic variability in this family, albeit rather unusual, should be kept in mind in genetic counselling.

The molecular basis of the phenotype variability

Correlation with the genotype: The transient expression systems do not reflect possible accelerated degradation of the mutant enzyme *in vivo*. In the case of mutant alleles with high residual activity, R376H and P184L, either enzyme instability as already described (Ferlinz et al 1995) or interference with the second mutant allele (see below) may explain the very mild clinical phenotype of patients 23 and 25 (Table 7) with restricted storage pattern. The R376H mutation is listed among the B type-causing pathogenic alleles (Simonaro et al 2002). The Q292K mutation constituted 40% of the independent alleles in our cohort of NP patients. It is noteworthy that it was always bound to the four-repeat-unit variant of the signal peptide polymorphism, although there was no consanguinity declared. This mutation in homoallelic state clearly correlates with a protracted neuronopathic phenotype. From the four patients homozygous for the mutation, two (cases 9 and 11) were classified as variant type A with protracted course and two (cases 14 and 15) showed chronic visceral storage with mild neurological involvement. A similar phenotype was observed in an additional patient homozygous for the Q292K mutation with a different ethnic background (M.T.Vanier and C. Marçais, personal communication 2003) and in the series recently published (Harzer et al 2003). In patients bearing the Q292K mutation on one

allele, the clinical phenotype was, as expected, variable, depending on the nature of the second mutant allele. Association with D278A (patients 4, 5 and 6) or with P189fsX254 or P330fsX382 (patients 7 and 8) resulted in type A with a slower neurological course. However, its association with the less deleterious, high residual ASM activity alleles R289H or P184L resulted in a type B phenotype. Interestingly, the Q292K mutation was found to be associated with false normal or enhanced ASM activity using HNP artificial substrate (Harzer et al 2003).

Correlation with the results of the SM loading in cultured fibroblasts: The minimal residual activity of the cell lines with mutations leading either to truncated enzyme protein (patient 2) or to its absence (patient 3) most probably reflects non-lysosomal degradation or side activity of other hydrolases. Such minor values and small differences in residual activity are insignificant and are generally observed in loading experiments (Asfaw et al 2002). On the other hand, patients 22 and 25 may have an unusually high capacity for SM hydrolysis, reflecting their clinical status (Table 7). It is worthy of mention that five other patients homozygous for the most common type B R608del mutation (Vanier et al 1993), not belonging to the present series but studied under the same conditions, gave maximum values of about 31% and 41% after 2 h chase and 24 h chase, respectively. This finding points to the remarkable biochemical heterogeneity in the group B patients. We stress that the most reliable evaluation of the SM degradative capacity is based on a comparison of results achieved in individual patients within a series performed in the same experiment. In contrast to NP fibroblasts, the capacity of lysosomal enzymes in normal cells usually greatly exceeds substrate influx. This implies that the control values are generally underestimated, as was observed in similar experiments testing degradation capacity of different glycohydrolases in mutant and normal cells (Asfaw et al 2002). This effect is more obvious in longer chase experiments. In this study, therefore, we consider results from a 2 h chase as more accurate.

It can be concluded that the intermediate values in our series allow the prediction of a protracted course (the only exception being patient 20) but are associated with neuronopathic features (albeit mitigated), even in values attaining the B range (patients 12 and 16). Thus, the prediction for patient 17 is protracted course and highly possible neurological involvement.

The '*ex vivo*' loading test, even in combination with the chase stage procedure (Graber et al 1994), need not necessarily reflect entirely the situation *in vivo*. The problem is that we evaluate the degradative capacity of one cell type from the 'visceral pool' and then try to extrapolate the results to the rest of the body's cell population, including neurons. It may be argued, however, that the results in fibroblasts have been corroborated by results in transformed B lymphocytes (Graber et al 1994), albeit in typical A and B types. Comparative studies of the SM degradation capacity in more cell types may shed further light on this problem. Absence of the Q292K mutation in a large cohort of published (Pittis et al 2004; Ricci et al 2004) and unpublished ASM-deficient patients (M.T.V.) suggests its prevalence in central Europe.

Correlation with the liver storage pattern: There was no definite correlation of the storage pattern with the presence either of neurological manifestation or of

pronounced visceral storage. In these cases the pattern was diffuse, except for intensive sharp centrozonal expression of hepatocyte storage in patients 12, 16 and 18. Only in protracted B types in which SM hydrolysis in skin fibroblasts reached almost the normal range and represents the highest values ever observed in ASM deficiency, was the storage either restricted to centrolobular hepatocytes (patients 23, 24 and 25) or histologically detectable (along with ceroid) only in Kupffer cells and bone marrow macrophages (patients 22). This observation suggests that SM lysosomal turnover is highest in the latter cell type. The centrolobular gradient clearly shows that conditions for overt lysosomal SM storage may develop during the lifespan of ASM-deficient hepatocytes along the portocentral axis (MacSween et al 2002).

CONCLUSIONS AND REMARKS ON THE CURRENT CLASSIFICATION OF ASM DEFICIENCY

The spectrum of phenotypes in our patients led us to the conclusion that *both the speed of the clinical course and storage intensity are not classic type specific*. Therefore, presenting type A as an acute neuronopathic form is an oversimplification. The situation resembles the neuronopathic types II and III and their subtypes in Gaucher disease (Beutler and Grabowski 2001). It turned out that the varying degrees of brain storage, neurological severity and speed of the clinical course reveal a broad continuous phenotypic spectrum. It should be also stressed that the neurological involvement may be delayed.

The B type similarly may exist as a spectrum of visceral storage of various dynamics and intensity, with extremes represented by slowly progressing storage manifesting mainly in macrophages on one side and by fulminant generalized nonneuronopathic storage fatal within the first decade of life, the latter being rare.

In summary, there seems to be a sound basis to conclude that a phenotypic continuum exists within both basic neurovisceral and purely visceral types.

Our report highlights an important position of the so far scarcely mentioned intermediate type in ASM deficiency. We define IT as a cluster of variants combining clinical features of both the classical types. The protracted neuronopathic variant with overt, borderline or subclinical neurology clearly prevails and is important in view of future enzyme replacement therapy. Isolated retinopathy on the background of the B type symptoms (see above) may be considered as the most benign subvariant in this group. One of us (M.E.) suggests inclusion of the rare visceral, rapidly progressing early fatal B type in the IT as, similarly to the protracted neuronopathic variant, it does not fit to the predominant slow course of the B type lesion. The problem remains how to define limits between the classical and the intermediate types. For type A it should be death at the age of 2–3 years (Schuchman and Desnick 2001); for type B it might be life-threatening, rapidly progressing visceral storage within the first decade of life.

This approach respects both the existing classification scheme and the plasticity of the phenotype, preventing establishment of any rigid subgroups. Clinicians should be aware of the IT variability and also of the fact that it appears to be regionally restricted.

As for enzyme replacement therapy, it is clear that B types, irrespective of the severity of the lesion, should be treated effectively. However, as neurological lesions may accompany the visceral manifestation temporarily in subclinical form, *any B type patient, especially when showing rapid progression of visceral storage, should be carefully examined neurologically*. Recognition of such potentially neuronopathic B types will soon have a practical implication, as enzyme replacement therapy might allow the neurological lesion beyond the blood–brain barrier to progress to a clinically overt state.

Results of the SM loading tests point out that the broad range of intermediate values may be associated either with protracted neurovisceral manifestation or with accelerated course dominated by visceral storage. This and the apparent independence of the dynamics of storage in the two basic compartents suggests the existence of factors in the genetic background influencing the severity and diversity of symptoms (Dipple and McCabe 2000; Dipple et al 2001). This is a challenge for future exploration of the molecular biology of ASM deficiency.

Databases: ASM: OMIM 257200, 607616; GDB 128144; GenBank X63600 (gDNA).

ACKNOWLEDGEMENTS

The project was partly supported by the Grant Agency of the Czech Republic (No. 301/93/01854), by research projects of the Ministry of Education and Youth of the Czech Republic VS 96127, VZ 111100003 (to M.E). VZ 00000064203 (to D.Ch), and by Vaincre les Maladies Lysosomales (to M.T.V.).

REFERENCES

Asfaw B, Schindler D, Ledvinova J, Cerny B, Smid F, Conzelmann E (1998) Degradation of blood group A glycolipid A-6-2 by normal and mutant human skin fibroblasts. *J Lipid Res* **39:** 1768–1780.

Asfaw B, Ledvinova J, Dobrovolny R et al (2002) Defects in degradation of blood group A and B glycosphingolipids in Schindler and Fabry diseases. *J Lipid Res* **43:** 1096–1104.

Beutler E, Grabowski GA (2001) Gaucher disease. In: Scriver CR, Beaudet AL, Sly WS, Valle D, eds; Childs B, Kinzler KW, Vogelstein B, assoc. eds. *The Metabolic and Molecular Bases of Inherited Disease*, 8th edn. New York, McGraw-Hill.

Bowser PA, Gray GM (1978) Sphingomyelinase in pig and human epidermis. *J Invest Dermatol* **70:** 331–335.

Cogan DG, Chu FC, Barranger JA, Gregg RE (1983) Macula halo syndrome. Variant of Niemann–Pick disease. *Arch Ophthalmol* **101:** 1698–1700.

Cotton RG, Horaitis O (2000) Quality control in the discovery, reporting, and recording of genomic variation. *Hum Mutat* **15:** 16–21.

den Dunnen JT, Antonarakis SE (2001) Nomenclature for the description of human sequence variations. *Hum Genet* **109:** 121–124.

Deng WP, Nickoloff JA (1992) Site-directed mutagenesis of virtually any plasmid by eliminating a unique site. *Anal Biochem* **200:** 81–88.

Dipple KM, McCabe ER (2000) Modifier genes convert "simple" Mendelian disorders to complex traits. *Mol Genet Metab* **71:** 43–50.

Dipple KM, Phelan JK, McCabe ER (2001) Consequences of complexity within biological networks: robustness and health, or vulnerability and disease. *Mol Genet Metab* **74:** 45–50.
Dubois G, Mussini JM, Auclair M et al. (1990) Adult sphingomyelinase deficiency: report of 2 patients who initially presented with psychiatric disorders. *Neurology* **40:** 132–136.
Elleder M (1989) Niemann–Pick disease. *Pathol Res Pract* **185:** 293–328.
Elleder M, Benesova E (1986a) [An adult form of type B Niemann–Pick disease manifesting as blue histiocyte syndrome]. *Vnitr Lek* **32:** 1114–1120.
Elleder M, Cihula J (1983) Niemann–Pick disease (variation in the sphingomyelinase deficient group). Neurovisceral phenotype (A) with an abnormally protracted clinical course and variable expression of neurological symptomatology in three siblings. *Eur J Pediatr* **140:** 323–328.
Elleder M, Jirasek A, Smid F (1975) Niemann–Pick disease (Crocker's type C): a histological study of the distribution and qualitative differences of the storage process. *Acta Neuropathol (Berl)* **33:** 191–200.
Elleder M, Smid F, Harzer K, Cihula J (1980) Niemann–Pick disease. Analysis of liver tissue in sphingomyelinase-deficient patients. *Virchows Arch A Pathol Anat Histol* **385:** 215–231.
Elleder M, Nevoral J, Spicakova V et al (1986b) A new variant of sphingomyelinase deficiency (Niemann–Pick): visceromegaly, minimal neurological lesions and low *in vivo* degradation rate of sphingomyelin. *J Inherit Metab Dis* **9:** 357–366.
Fawcett DW (1986) The eye. In: Fawcett DW, ed. *A Textbook of Histology*. Philadelphia: Saunders, 913–959.
Ferlinz K, Hurwitz R, Sandhoff K (1991) Molecular basis of acid sphingomyelinase deficiency in a patient with Niemann–Pick disease type A. *Biochem Biophys Res Commun* **179:** 1187–1191.
Ferlinz K, Hurwitz R, Weiler M, Suzuki K, Sandhoff K, Vanier MT (1995) Molecular analysis of the acid sphingomyelinase deficiency in a family with an intermediate form of Niemann–Pick disease. *Am J Hum Genet* **56:** 1343–1349.
Filling-Katz MR, Fink LK, Gorin MB et al. (1992) Ophthalmologic manifestations of type B Niemann–Pick diseases. *Metab Pediatr Syst Ophthalmol* **15:** 16–20.
Gluck U, Zeigler M, Bargal R, Schiff E, Bach G (1997) Niemann Pick disease type A in Israeli Arabs: 677delT, a common novel single mutation. *Hum Mutat Mut in Brief.*
Goldstein JL, Basu SK, Brown MS (1983) Receptor-mediated endocytosis of low-density lipoprotein in cultured cells. *Methods Enzymol* **98:** 241–260.
Graber D, Salvayre R, Levade T (1994) Accurate differentiation of neuronopathic and non-neuronopathic forms of Niemann–Pick disease by evaluation of the effective residual lysosomal sphingomyelinase activity in intact cells. *J Neurochem* **63:** 1060–1068.
Hammersen G, Oppermann HC, Harms E, Blassmann K, Harzer K (1979) Oculo-neural involvement in an enzymatically proven case of Niemann–Pick disease type B. *Eur J Pediatr* **132:** 77–84.
Harzer K, Ruprecht KW, Seuffer-Schulze D, Jans U (1978) [Niemann–Pick disease type B: An enzymatically confirmed case with unexpected retinal involvement (author's transl)]. *Albrecht Von Graefes Arch Klin Exp Ophthalmol* **206:** 79–88.
Harzer K, Rolfs A, Bauer P et al. (2003) Niemann–Pick disease type A and B are clinically but also enzymatically heterogeneous: pitfall in the laboratory diagnosis of sphingomyelinase deficiency associated with the mutation Q292K. *Neuropediatrics* **34:** 301–306.
Hermansky F, Janele J, Smetana K (1971) [Syndrome of the so-called blue pigmentophages]. *Vnitr Lek* **17:** 857–862.
Labrune P, Bedossa P, Huguet P, Roset F, Vanier MT, Odievre M (1991) Fatal liver failure in two children with Niemann–Pick disease type B. *J Pediatr Gastroenterol Nutr* **13:** 104–109.
Levran O, Desnick RJ, Schuchman EH (1993) Type A Niemann–Pick disease: a frameshift mutation in the acid sphingomyelinase gene (fsP330) occurs in Ashkenazi Jewish patients. *Hum Mutat* **2:** 317–319.
Lipson MH, O'Donnell J, Callahan JW, Wenger DA, Packman S (1986) Ocular involvement in Niemann–Pick disease type B. *J Pediatr* **108:** 582–584.

Litzkas P, Jha KK, Ozer HL (1984) Efficient transfer of cloned DNA into human diploid cells: protoplast fusion in suspension. *Mol Cell Biol* **4:** 2549–2552.
Lowe D, Martin F, Sarks J (1986) Ocular manifestations of adult Niemann–Pick disease: a case report. *Aust N Z J Ophthalmol* **14:** 41–47.
MacSween R, Desmet VJ, Roskams T, Scothorne RJ (2002) Developmental anatomy and normal structure. In: Portman BC, ed. *Pathology of the Liver*. London: Churchill Livingston, 2–66.
Martin JJ, Philippart M, Van Hauwaert J, Callahan JW, Deberdt R (1972) Niemann–Pick disease (Crocker's group A). Late onset and pigmentary degeneration resembling Hallervorden–Spatz syndrome. *Arch Neurol* **27:** 45–51.
Matthews JD, Weiter JJ, Kolodny EH (1986) Macular halos associated with Niemann–Pick type B disease. *Ophthalmology* **93:** 933–937.
McGovern MM, Wasserstein MP, Aron A, Desnick RJ, Schuchman EH, Brodie SE (2004) Ocular manifestations of Niemann–Pick disease type B. *Ophthalmology* **111:** 1424–1427.
Obenberger J, Seidl Z, Pavlu H, Elleder M (1999) MRI in an unusually protracted neuronopathic variant of acid sphingomyelinase deficiency. *Neuroradiology* **41:** 182–184.
Pavlu H, Elleder M (1997). "Two novel mutations in patients with atypical phenotypes of acid sphingomyelinase deficiency." *J Inherit Metab Dis* **20:** 615–616.
Pittis MG, Ricci V, Guerci VI et al. (2004) Acid sphingomyelinase: identification of nine novel mutations among Italian Niemann Pick type B patients and characterization of in vivo functional in-frame start codon. *Hum Mutat* **24:** 186–187.
Putterman C, Zelingher J, Shouval D (1992) Liver failure and the sea-blue histiocyte/adult Niemann–Pick disease. Case report and review of the literature. *J Clin Gastroenterol* **15:** 146–149.
Ricci V, Stroppiano M, Corsolini F et al. (2004) Screening of 25 Italian patients with Niemann–Pick A reveals fourteen new mutations, one common and thirteen private, in SMPD1. *Hum Mutat* **24:** 105.
Rodriguez-Lafrasse C, Vanier MT (1999) Sphingosylphosphorylcholine in Niemann–Pick disease brain: accumulation in type A but not in type B. *Neurochem Res* **24:** 199–205.
Rosa L, Elleder M, Beránek J (1990) Simultaneous occurence of multiple sclerosis and Niemann–Pick disease type B [in Czech]. *Prakt lék* **70:** 18–20.
Rosipal S, Michalec C (1982) [Niemann–Pick disease]. *Cesk Pediatr* **37:** 646–648.
Shah MD, Desai AP, Jain MK et al. (1983) Niemann Pick disease type B with oculoneural involvement. *Indian Pediatr* **20:** 521–522.
Schuchman EH, Desnick RJ (2001) Niemann–Pick disease types A and B: acid sphingomyelinase deficiencies. In: Scriver CR, Beaudet AL, Sly WS, Valle D, eds; Childs B, Kinzler KW, Vogelstein B, assoc. eds. *The Metabolic and Molecular Bases of Inherited Disease*, 8th edn, Vol. 3. New York, McGraw-Hill, 3589–3610.
Schuchman EH, Levran O, Suchi M, Desnick RJ (1991a) An MspI polymorphism in the human acid sphingomyelinase gene (SMPD1). *Nucleic Acids Res* **19:** 3160.
Schuchman EH, Suchi M, Takahashi T, Sandhoff K, Desnick RJ (1991b) Human acid sphingomyelinase. Isolation, nucleotide sequence and expression of the full-length and alternatively spliced cDNAs. *J Biol Chem* **266:** 8531–8539.
Sikora J, Pavlu-Pereira H, Elleder M, Roelofs H, Wevers RA (2003) Seven novel acid sphingomyelinase gene mutations in Niemann–Pick type A and B patients. *Ann Hum Genet* **67:** 63–70.
Simonaro CM, Desnick RJ, McGovern MM, Wasserstein MP, Schuchman EH (2002) The demographics and distribution of type B Niemann–Pick disease: novel mutations lead to new genotype/phenotype correlations. *Am J Hum Genet* **71:** 1413–1419.
Sogawa H, Horino K, Nakamura F et al. (1978) Chronic Niemann–Pick disease with sphingomyelinase deficiency in two brothers with mental retardation. *Eur J Pediatr* **128:** 235–240.

Sperl W, Bart G, Vanier MT et al. (1994) A family with visceral course of Niemann–Pick disease, macular halo syndrome and low sphingomyelin degradation rate. *J Inherit Metab Dis* **17:** 93–103.

Takada G, Satoh W, Komatsu K, Konn Y, Miura Y, Uesaka Y (1987) Transitory type of sphingomyelinase deficient Niemann–Pick disease: clinical and morphological studies and follow-up of two sisters. *Tohoku J Exp Med* **153:** 27–36.

Takahashi T, Suchi M, Desnick RJ, Takada G, Schuchman EH (1992) Identification and expression of five mutations in the human acid sphingomyelinase gene causing types A and B Niemann–Pick disease. Molecular evidence for genetic heterogeneity in the neuronopathic and non-neuronopathic forms. *J Biol Chem* **267:** 12552–12558.

Takahashi T, Akiyama K, Tomihara M et al. (1997) Heterogeneity of liver disorder in type B Niemann–Pick disease. *Hum Pathol* **28:** 385–388.

Vanier MT, Suzuki K (1996). Niemann–Pick diseases. In: Moser HW ed. *Neurodystrophies and Neurolipidoses*. Amsterdam: Elsevier Science, pp 133–162.

Vanier MT, Revol A, Fichet M (1980) Sphingomyelinase activities of various human tissues in control subjects and in Niemann–Pick disease—development and evaluation of a microprocedure. *Clin Chim Acta* **106:** 257–267.

Vanier MT, Rousson R, Garcia I et al (1985) Biochemical studies in Niemann–Pick disease. III. In vitro and in vivo assays of sphingomyelin degradation in cultured skin fibroblasts and amniotic fluid cells for the diagnosis of the various forms of the disease. *Clin Genet* **27:** 20–32.

Vanier MT, Ferlinz K, Rousson R et al. (1993) Deletion of arginine (608) in acid sphingomyelinase is the prevalent mutation among Niemann–Pick disease type B patients from northern Africa. *Hum Genet* **92:** 325–330.

Walton DS, Robb RM, Crocker AC (1978) Ocular manifestations of group A Niemann–Pick disease. *Am J Ophthalmol* **85:** 174–180.

Wan Q, Schuchman EH (1995) A novel polymorphism in the human acid sphingomyelinase gene due to size variation of the signal peptide region. *Biochim Biophys Acta* **1270:** 207–210.

Wilson JA, Raufman JP (1986) Hepatic failure in adult Niemann–Pick disease. *Am J Med Sci* **292:** 168–172.

Zhou H, Linke RP, Schaefer HE, Mobius W, Pfeifer U (1995) Progressive liver failure in a patient with adult Niemann–Pick disease associated with generalized AL amyloidosis. *Virchows Arch* **426:** 635–639.

Appended publication #4

JIMD Short Report #009 (2006) Online
DOI 10.1007/s10545-006-0330-z

SHORT REPORT

Subclinical course of adult visceral Niemann–Pick type C1 disease. A rare or underdiagnosed disorder?

L. Dvorakova · J. Sikora · M. Hrebicek · H. Hulkova · M. Bouckova · L. Stolnaja · M. Elleder

Received: 13 January 2006 / Accepted: 8 May 2006

Summary We present the third case of Niemann–Pick disease type C without neurological symptoms. The patient was a 53-year-old woman without significant prior health problems who died of acute pulmonary embolism. Autopsy findings of hepatosplenomegaly, lymphadenopathy and ceroid-rich foam cells raised the suspicion of the visceral form of acid sphingomyelinase deficiency (Niemann–Pick disease type B; NPB) or a much rarer disorder, variant adult visceral form of Niemann–Pick disease type C (NPC). To verify the histopathological findings, *SMPD1*, *NPC1* and *NPC2* genes were analysed. Two novel sequence variants, c.1997G > A (S666N) and c.2882A > G (N961S) were detected in the *NPC1* gene. No pathogenic sequence variants were found either in the *SMPD1* gene mutated in NPB or in *NPC2* gene. The pathogenicity of both *NPC1* variants was supported by their location in regions important for the protein function. Both variations were not found in more than 300 control alleles. Identified sequence variations confirm the diagnosis of the extremely rare adult visceral form of Niemann–Pick disease type C, which is otherwise dominated by neurovisceral symptoms. Although only three patients have been reported, this (most probably underdiagnosed) form of NPC should be considered in differential diagnosis of isolated hepatosplenomegaly with foam cells in adulthood.

Communicating Editor: Robert Steiner

Competing interests: None declared

References to electronic databases: OMIM (http://www.ncbi.nlm.nih.gov/): Niemann–Pick disease, type C1 #257220; Niemann–Pick disease, type C2 #607625; Niemann Pick disease type A/B #257200, #607616; Gaucher disease, type I #230800. GenBank reference sequences (http://www.ncbi.nlm.nih.gov/), accession numbers: *SMPD1*, NC_000011.8 REGION: 6368302..6372783; *NPC1*, NC_000018.8, REGION: complement (19365461..19420426); *NPC2 (HE1)*, NC_000014.7, REGION: complement(74016397..74029837). Uniprot database (http://www.expasy.uniprot.org/). The National Center for Biotechnology Information (http://www.ncbi.nlm.nih.gov/). Databases used for SNP analysis: GenBank (http://www.ncbi.nlm.nih.gov/), Ensembl (http://www.ensembl.org/), HGVD (http://hgvbase.cgb.ki.se/).

Enzymes: SMPD1 (EC 3.1.4.12), HMG CoA reductase (EC 1.1.1.88)

L. Dvorakova · J. Sikora · M. Hrebicek · H. Hulkova · M. Bouckova · L. Stolnaja · M. Elleder (✉)
Institute of Inherited Metabolic Disorders, Charles University, First Faculty of Medicine and University Hospital, Prague, Czech Republic.
e-mail: melleder@beba.cesnet.cz

Abbreviations

FFPE	formalin fixed paraffin-embedded
LDL	low-density lipoprotein
NP A/B	Niemann–Pick disease type A/B
NPB	Niemann–Pick disease type B
NPC	Niemann–Pick disease type C
PCR	polymerase chain reaction
RFLP	restriction fragment length polymorphism
SSD	sterol sensing domain

Introduction

Niemann–Pick disease type C (NPC; OMIM 257220, 607625) is an autosomal recessive lysosomal disorder caused by deregulation of the cellular lipid trafficking due to the molecular defects in either of the two late endosomal/lysosomal proteins (NPC1 and NPC2). NPC1, a transmembrane protein localized in a subset of late endosomes, is endowed with a sterol sensing domain exerting control of cholesterol content of late endosomal membranes (Liscum and Sturley 2004). Excess cholesterol is translocated for

esterification to other cellular membranes, including Golgi apparatus. When mutated (as it is in the majority of NPC patients), NPC1 protein impairs control of cholesterol membrane content and leads to a cascade of events, not yet fully defined, resulting in an accumulation of a variable set of lipids (e.g. glucosyl and lactosylceramide, GM_2 ganglioside, and sphingomyelin) in late endosomes/lysosomes. This process resembling classical lysosomal storage progresses despite unhindered degradative capacity of lysosomal enzymes. The cellular changes described are found mainly in neurons and macrophages, and to a lesser extent in other cell types (Mukherjee and Maxfield 2004).

The second protein (NPC2) engaged in intracellular cholesterol trafficking is localized in the lysosomal lumen and functions in close association with NPC1 (Vanier et al 2004; Zhang et al 2003). Its dysfunction leads to the phenotype that is clinically and/or biochemically indistinguishable from NPC1 phenotype with the exception of a tendency to more severe lung involvement (Vanier and Millat 2003).

Clinical presentation of NPC is highly variable. An acute form presents usually at birth and is associated with severe hepatopathy and splenomegaly. Surviving patients develop psychomotor retardation during infancy and slowly progressive neurodegeneration with vertical supranuclear gaze palsy, seizures and spasticity later in childhood. Patients with the juvenile-onset form develop slowly progressive ataxia, spasticity, seizures and supranuclear gaze palsy during childhood and dementia later in the teenage years. NPC individuals with later-onset forms have similar clinical symptoms appearing in adolescence or adulthood. Adult-onset NPC patients can be especially difficult to diagnose, as only about 50% of them have palpable hepatosplenomegaly and the dominant symptoms can be psychiatric (psychosis or bipolar disorder) (Vanier and Millat 2003).

The proof of lysosomal storage of free cholesterol, detected in cultured skin fibroblasts by filipin staining and reduced rate of LDL-derived cholesterol esterification, is diagnostic for NPC. The residual rates of cholesterol esterification tend to some extent to correlate inversely with the severity of the phenotype.

Some patients do not fulfil the clinical criteria of the three common phenotypes described above (Klunemann et al 2002). It is not unusual for the patients to present initially with isolated splenomegaly. The majority of the patients develop the neurological symptoms later during the course of the disease. Only two of the reported cases were free of neurological symptoms in their fourth and sixth decades, respectively, suggesting that most likely they would never develop them (Fensom et al 1999; Frohlich et al 1990).

In this report we present the third case of this rare purely visceral NPC1 variant, evaluated at both the tissue and molecular levels, and argue that a substantial number of these patients can easily escape diagnosis.

Clinical report

The clinical history of the patient was unremarkable. She was employed as a clerk. She had varicose veins of the lower extremities and from 48 years of age she had been treated for arterial hypertension. She never complained of neurological symptoms and spleen enlargement was not noted. During the 6 months before her admission to hospital she became easily fatigued and developed occasional mild dyspnoea. Shortly after arrival from a prolonged coach trip she suffered acute pulmonary embolism, and after admission to the hospital she suffered acute myocardial infarction. In spite of early and adequate hospital care she died the next day due to cardiac failure at the age of 53 years. Splenomegaly was noted on examination and laboratory work-up showed unexplained moderately severe microcytic anaemia (haemoglobin 87 g/L, reference range 116–183; red blood cells 4.25×10^{12}/L, reference range 3.54–5.18; mean cell volume 64 fl, reference range 82.3–100) with normal counts of white blood cells and platelets.

Her mother and two sons are without any clinical abnormalities; family history was uneventful and was not suggestive of a hereditary disorder. Informed consents were obtained from the living relatives of the patient.

Methods

Histology and immunohistology

An autopsy and a histopathological examination were performed according to the standard protocols including immunohistochemical detection of cathepsin D with rabbit polyclonal antibody (DAKO Cytomation, Copenhagen, Denmark), and of CD68 (PGM1) and Tau protein with mouse monoclonal antibodies purchased from DAKO and Novocastra (Newcastle Upon Tyne, UK), respectively. The primaries (after overnight incubation at 4°C) were detected with appropriate Envision systems (DAKO).

DNA analysis

Sequence analysis of the *SMPD1* gene and the acid sphingomyelinase activity measurements were performed as described previously (Pavlu-Pereira et al 2005; Sikora et al 2003).

Genomic DNA of the proband was extracted from the formalin fixed paraffin embedded (FFPE) tissues (spleen and lymph node) using heat deparaffinization, Proteinase K

digestion and phenol–chloroform extraction as no other biological materials were available. Genomic DNA from the proband's living relatives (her mother and two sons) was isolated from peripheral blood leukocytes using standard phenol–chloroform extraction procedure. The entire gene-coding region as well as 5′ and 3′ untranslated regions and exon–intron boundaries of *NPC1* and *NPC2* genes were examined by direct sequencing of PCR products. Primers for both genes, *NPC1* and *NPC2 (HE1)*, were designed according to GenBank reference sequences (NC_000018.8 and NC_000014.7). PCR product sizes, primers and PCR reaction conditions are available from the authors upon request. The substitution c.1997G > A was verified by PCR/RFLP using restriction endonuclease *Dde*I (NEB, Ipswich, MA, USA). As the c.2882A > G did not alter a restriction site, we designed a modified primer (5′ GCATTGCAGAACTGGTCAGGGATA 3′) that produced a new recognition site for *Bfu*I (Fermentas, Burlington, ONT, Canada) in the variant allele. This PCR/RFLP protocol was used for patients' samples and control samples.

Protein sequences mentioned in the Discussion were retrieved from the Uniprot database (http://www.expasy.uniprot.org/) and from The National Center for Biotechnology Information (http://www.ncbi. nlm.nih.gov/). Multiple alignments were performed using ClustalW in Blosum61 matrix (Thompson et al 1994).

Results

Autopsy findings of hepatosplenomegaly (spleen weight 1230 g, liver 3000 g) and lymphadenopathy together with histopathological signs of visceral lysosomal storage raised the pathologist's initial suspicion of Gaucher disease (OMIM 230800). Verification of the diagnosis required by the clinical geneticist was carried out using the paraffin-embedded autopsy samples. This showed spleen and bone marrow infiltration with histiocytic foam cells, many of them containing ceroid admixture (typical yellowish autofluorescence and sudanophilia in paraffin sections). Storage histiocytes were numerous in some of the lymph nodes and scarce in the liver. A large number of histiocytes (CD68 PGM1 positive) in mediastinal lymph nodes and liver sinusoids (Fig. 1, A–C) did not show any histologically detectable storage or ceroid accumulation. Hepatocytes were without vacuolization but displayed increased granular immunostaining for cathepsin D disproportional to lipofuscin pigmentation. There was extramedullary trilineage haematopoiesis in the liver and spleen. Neurons in the brain samples (basal ganglia) were remarkably distended, with numerous lipofuscin granules (Fig. 1D) that were in excess compared with the age-matched controls. Neither definite neuronal vacuolization nor neurofibrillary tangles were detectable by immunostaining.

The revision excluded Gaucher disease and suggested Niemann–Pick disease type B (OMIM 607616) as the most probable diagnosis with regard to the relatively high incidence of this disorder and to the visceral foam cell storage pattern.

In order to verify the histopathological findings, we analysed the acid sphingomyelinase gene (*SMPD1*), which is mutated in Niemann–Pick disease type A/B (NP A/B). As only FFPE tissues were available from the proband, we began the analyses using genomic DNA isolated from the peripheral blood leukocytes from the proband's living relatives, who were obligatory heterozygotes (the mother and two sons of the proband).

Direct sequencing of the *SMPD1* gene did not reveal any pathogenic sequence variations. Also, acid sphingomyelinase (EC 3.1.4.12) activity in leukocytes was in the normal range in all three relatives examined, while in NP A/B heterozygotes the activities are characteristically about 50% of control values.

Since neither biochemical assays nor mutation analyses supported the diagnosis of Niemann–Pick disease type B, we focused on the much less common disorder, variant adult visceral form of Niemann Pick disease type C. As noted in the introduction, NPC patients belong to either of the two complementation groups associated with pathogenic variations in *NPC1* or *NPC2* genes.

While no variations were detected in *NPC2*, the previously undescribed substitution c.1997G > A (S666N) was identified in exon 13 of the *NPC1* gene in all three living relatives and later in the DNA isolated from FFPE tissues from the proband.

In addition to common polymorphisms (Y129Y, H215R, I858V, N931N and IVS19 + 28T > C) and the c.1997G > A (S666N) variation, another novel nucleotide substitution was found in the *NPC1* gene of the proband: c.2882A > G (N961S) in exon 19. In order to minimize the artefacts due to previous formalin fixation (Williams et al 1999; Wong et al 1998) or translesion PCR synthesis from the low-quality DNA template (Quach et al 2004), we verified the c.2882A > G using an additional short PCR product. Direct sequencing of these 162 bp PCR products, obtained from DNA isolated from both tissues in a 35-cycle PCR reaction, confirmed the presence of c.2882A > G.

To exclude the possibility that c.1997G > A and c.2882A > G are common polymorphisms, we examined 318 control alleles from the Czech population by PCR/RFLP technique. Restriction analysis confirmed the substitution c.1997G > A in the proband and other three family members but in none of control alleles. Variation c.2882A > G was found only in the proband's samples.

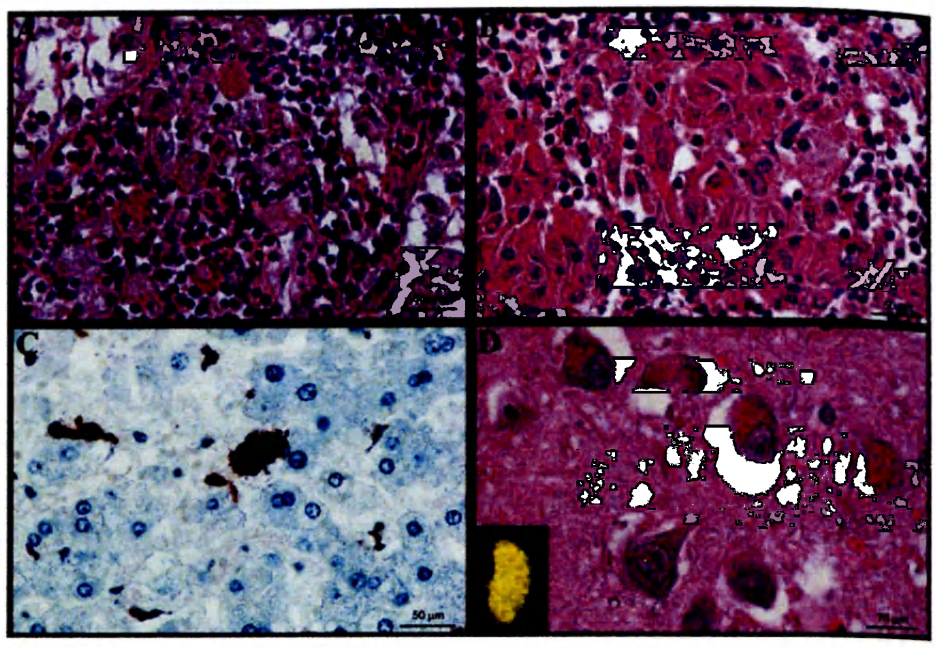

Fig. 1 Features of the storage process in the patient. (A) Lymph node infiltrated with ceroid-rich foam histiocytes (HE stain). (B) Mediastinal lymph node. Nonstorage histiocytes with compact (epitheloid) cytoplasm superficially resembling Gaucher cells (HE stain). (C) Liver sinusoidal histiocytes. Significant storage is present only in one of them (CD68 – clone PGM1). (D) Neurons in basal ganglia distended with an excess of lipopigment (HE stain). *Insert:* typical autofluorescence of the accumulated lipopigment

Fig. 2 Alignment of the amino acid sequence for the human NPC1 regions containing the mutation loci (S666N and N961S) with the corresponding regions from NPC1-related sequences of seven mammalian species. Arrow heads indicate the position of the found sequence variations.

Discussion

We feel fully justified in concluding, on the basis of the results of the analyses, that the patient presented here suffered from the visceral variant of Niemann–Pick disease type C1, although the filipin test could not be performed. The storage pattern with foamy ceroid-rich histiocytes was similar to that in Niemann–Pick disease type B (Elleder 1989). We consider the novel missense nucleotide changes found in the *NPC1* gene of the patient to be disease-causing for the following reasons:

1. The variations found do not occur commonly in the population, as we did not find them in any of 318 examined control alleles. In addition, SNP searches in the GenBank, Ensembl and HGVD databases did not reveal the substitutions.
2. The substitutions found are located in two out of the three functionally critical NPC1 domains (Vanier and Millat 2003). The S666N variant is situated in the highly hydrophobic and evolutionarily conserved region homologous to the sterol sensing domain (SSD) of the two key regulators of cholesterol homeostasis, HMG CoA reductase

(3-hydroxy-3-methylglutaryl coenzyme A reductase, EC 1.1.1.88) and SCAP protein (sterol regulatory element binding protein cleavage-activating protein). The serine residue at position 666 of NPC1 is conserved in the SSD of all three proteins. All mutations found so far in the SSD in the homozygous state, resulted in the lack of mature NPC1 protein and were associated with very severe biochemical and clinical phenotype (Millat et al 2001; Yamamoto et al 2000).The second variation, N961S, is situated in the cysteine-rich luminal loop between transmembrane domains VIII and IX. All but two mutations associated with the biochemical variant phenotype (mild alterations of cellular cholesterol trafficking) were located in the cysteine-rich loop (Vanier and Millat 2003).

3. The functional importance of both amino acid residues (S666 and N961) is supported by their conservation in seven other mammalian NPC1 homologous proteins.

As the NPC1 phenotype, despite its variability, is characterized by neurological involvement either closely associated with visceral symptoms or delayed (see Introduction), our case clearly belongs to the extremely rare visceral variant described so far only in two cases. The first described patient was a 63-year-old woman with a nonneuronopathic form homozygous for G992R localized in cysteine-rich domain (Millat et al 2001). The second patient came to attention at the age of 46 years because of splenomegaly found during splenectomy after a road traffic injury. The diagnosis of NPC1 was confirmed by biochemical analysis (Fensom et al 1999) and later by mutation analysis, when two heterozygous mutations were found (I1061T and V378A) (Millat et al 2001). Both patients were free of neurological symptoms at 66 and 50 years of age, respectively, suggesting that they may never develop neurological disease.

Dysfunction of the mutant NPC1 in the case described in this report became manifest within the lifespan of 53 years in the fraction of the histiocytic population with borderline involvement of hepatocytes and neurons. The patient had no neurological symptoms compatible with NPC during her life; moreover, the histological examination of her brain showed only increased amount of neurolipofuscin and none of the plethora of neuropathological signs that are abundant in NPC patients with neurological involvement (Vanier and Millat 2004). That allows us to assume that the patient had a visceral-only form of NPC1. The cause of microcytic anaemia in the patient remains unclear; no source of chronic bleeding was discovered at postmortem examination. It was apparently unrelated to the symptoms of NPC.

Although NPC1 patients as a group apparently represent a continuum of phenotypes with a wide range of severities, we feel that it is justified to distinguish the visceral-only adult phenotype as a separate form of the disease. This variant appears to be extremely rare, but its main clinical symptom, splenomegaly without neurological symptoms in adulthood, is nonspecific enough to raise suspicion for NPC only late if at all. At the tissue level, the presence of foam cells in an adult should alert the pathologist to this diagnosis. However, uneven expression of the storage in the histiocytic population may seriously complicate the diagnosis *in vivo*. We presume that the visceral variant of NPC may pass routine diagnosis undetected and therefore remain underdiagnosed. Whether these patients have subtle psychological or neurological symptoms remains to be established by repeated neuropsychological and neurophysiological evaluations. As patients with adult forms of NPC may benefit from future therapies—as suggested by preliminary results of a trial evaluating the effect of miglustat (Zavesca) in NPC patients (Patterson et al 2005)—adult physicians should be alert to the possibility of NPC in the absence of apparent neurological symptomatology.

Acknowledgements This work was supported by grant no. 8351–3 from the Ministry of Health of the Czech Republic and the research project no. 0021620806 from the Ministry of Education, Youth and Sports of the Czech republic. We would like to acknowledge Pavel Noll, MD for providing autopsy tissue samples, Helena Stepankova, MD for patient data, Lenka Vepřeková, MD for expertise in haematology, and Mrs Eva Richterova for technical assistance.

References

Elleder M (1989) Niemann–Pick disease. *Pathol Res Pract* **185**(3): 293–328.

Fensom AH, Grant AR, Steinberg SJ, et al (1999) An adult with a non-neuronopathic form of Niemann–Pick C disease. *J Inherit Metab Dis* **22**(1): 84–86.

Frohlich E, Harzer K, Heller T, et al (1990) [Ultrasound echogenic splenic tumors: nodular manifestation of type C Niemann–Pick disease]. *Ultraschall Med* **11**(3): 119–122.

Klunemann HH, Elleder M, Kaminski WE, et al (2002) Frontal lobe atrophy due to a mutation in the cholesterol binding protein HE1/NPC2. *Ann Neurol* **52**(6): 743–749.

Liscum L, Sturley SL (2004) Intracellular trafficking of Niemann–Pick C proteins 1 and 2: obligate components of subcellular lipid transport. *Biochim Biophys Acta* **1685**(1–3): 22–27.

Millat G, Marcais C, Tomasetto C, et al (2001) Niemann–Pick C1 disease: correlations between NPC1 mutations, levels of NPC1 protein, and phenotypes emphasize the functional significance of the putative sterol-sensing domain and of the cysteine-rich luminal loop. *Am J Hum Genet* **68**(6): 1373–1385.

Mukherjee S, Maxfield FR (2004) Lipid and cholesterol trafficking in NPC. *Biochim Biophys Acta* **1685**(1–3): 28–37.

Patterson M, Vecchio D, Prady H, Ait-Aissa N, Abel L, Wraith E (2005) Oral miglustat in adult and pediatric patients with Niemann–Pick type C (NPC) disease: rationale, methodology and interim analyses of a clinical study. Poster 2505/T, ASHG 2005 (Salt Lake City).

Pavlu-Pereira H, Asfaw B, Poupetova H, et al (2005) Acid sphingomyelinase deficiency. Phenotype variability with prevalence of intermediate phenotype in a series of twenty-five Czech and Slovak patients. A multi-approach study. *J Inherit Metab Dis* **28**(2): 203–227.

Quach N, Goodman MF, Shibata D (2004) In vitro mutation artifacts after formalin fixation and error prone translesion synthesis during PCR. *BMC Clin Pathol* **4**(1): 1.

Sikora J, Pavlu-Pereira H, Elleder M, et al (2003) Seven novel acid sphingomyelinase gene mutations in Niemann–Pick type A and B patients. *Ann Hum Genet* **67**(Pt 1): 63–70.

Thompson JD, Higgins DG, Gibson TJ (1994) CLUSTAL W: improving the sensitivity of progressive multiple sequence alignment through sequence weighting, position-specific gap penalties and weight matrix choice. *Nucleic Acids Res* **22**(22): 4673–4680.

Vanier MT, Millat G (2003) Niemann–Pick disease type C. *Clin Genet* **64**(4): 269–281.

Vanier MT, Millat G (2004) Structure and function of the NPC2 protein. *Biochim Biophys Acta* **1685**(1–3): 14–21.

Vanier MT, Saito Y, Murayma S, et al (2004) Niemann–Pick type C disease. In: Golden JA, Harding BN, eds. *Developmental Neuropathology*. Basel: ISN Neuropath Press, 283–286.

Williams C, Ponten F, Moberg C, et al (1999) A high frequency of sequence alterations is due to formalin fixation of archival specimens. *Am J Pathol* **155**(5): 1467–1471.

Wong C, DiCioccio RA, Allen HJ, et al (1998) Mutations in BRCA1 from fixed, paraffin-embedded tissue can be artifacts of preservation. *Cancer Genet Cytogenet* **107**(1): 21–27.

Yamamoto T, Ninomiya H, Matsumoto M, et al (2000) Genotype–phenotype relationship of Niemann–Pick disease type C: a possible correlation between clinical onset and levels of NPC1 protein in isolated skin fibroblasts. *J Med Genet* **37**(9): 707–712.

Zhang M, Sun M, Dwyer NK, et al (2003) Differential trafficking of the Niemann–Pick C1 and 2 proteins highlights distinct roles in late endocytic lipid trafficking. *Acta Paediatr Suppl* **92**(443): 63–73; discussion 45.

ARTICLE

Mutations in *TMEM76** Cause Mucopolysaccharidosis IIIC (Sanfilippo C Syndrome)

Martin Hřebíček, Lenka Mrázová, Volkan Seyrantepe, Stéphanie Durand, Nicole M. Roslin, Lenka Nosková, Hana Hartmannová, Robert Ivánek, Alena Čížková, Helena Poupětová, Jakub Sikora, Jana Uřinovská, Viktor Stránecký, Jiří Zeman, Pierre Lepage, David Roquis, Andrei Verner, Jérôme Ausseil, Clare E. Beesley, Irène Maire, Ben J. H. M. Poorthuis, Jiddeke van de Kamp, Otto P. van Diggelen, Ron A. Wevers, Thomas J. Hudson, T. Mary Fujiwara, Jacek Majewski, Kenneth Morgan, Stanislav Kmoch,† and Alexey V. Pshezhetsky

Mucopolysaccharidosis IIIC (MPS IIIC, or Sanfilippo C syndrome) is a lysosomal storage disorder caused by the inherited deficiency of the lysosomal membrane enzyme acetyl–coenzyme A:α-glucosaminide *N*-acetyltransferase (*N*-acetyltransferase), which leads to impaired degradation of heparan sulfate. We report the narrowing of the candidate region to a 2.6-cM interval between *D8S1051* and *D8S1831* and the identification of the transmembrane protein 76 gene (*TMEM76*), which encodes a 73-kDa protein with predicted multiple transmembrane domains and glycosylation sites, as the gene that causes MPS IIIC when it is mutated. Four nonsense mutations, 3 frameshift mutations due to deletions or a duplication, 6 splice-site mutations, and 14 missense mutations were identified among 30 probands with MPS IIIC. Functional expression of human *TMEM76* and the mouse ortholog demonstrates that it is the gene that encodes the lysosomal *N*-acetyltransferase and suggests that this enzyme belongs to a new structural class of proteins that transport the activated acetyl residues across the cell membrane.

Heparan sulfate is a polysaccharide found in proteoglycans associated with the cell membrane in nearly all cells. The lysosomal membrane enzyme, acetyl–coenzyme A (CoA):α-glucosaminide *N*-acetyltransferase (*N*-acetyltransferase) is required to *N*-acetylate the terminal glucosamine residues of heparan sulfate before hydrolysis by the α-*N*-acetyl glucosaminidase. Since the acetyl-CoA substrate would be rapidly degraded in the lysosome,[1] *N*-acetyltransferase employs a unique mechanism, acting both as an enzyme and a membrane channel, and catalyzes the transmembrane acetylation of heparan sulfate.[2] The mechanism by which this is achieved has been the topic of considerable investigation, but, for many years, the isolation and cloning of *N*-acetyltransferase has been hampered by its low tissue content, instability, and hydrophobic nature.[3–5]

Genetic deficiency of *N*-acetyltransferase causes mucopolysaccharidosis IIIC (MPS IIIC [MIM 252930], or Sanfilippo syndrome C), a rare autosomal recessive lysosomal disorder of mucopolysaccharide catabolism.[6–8] MPS IIIC is clinically similar to other subtypes of Sanfilippo syndrome.[9] Patients manifest symptoms during childhood with progressive and severe neurological deterioration causing hyperactivity, sleep disorders, and loss of speech accompanied by behavioral abnormalities, neuropsychiatric problems, mental retardation, hearing loss, and relatively minor visceral manifestations, such as mild hepatomegaly, mild dwarfism with joint stiffness and biconvex dorsolumbar vertebral bodies, mild coarse faces, and hypertrichosis.[7] Most patients die before adulthood, but some survive to the 4th decade and show progressive dementia and retinitis pigmentosa. Soon after the first 3 patients with MPS IIIC were described by Kresse et al.,[6] Klein et al.[8,10] reported a similar deficiency in 11 patients who had received the diagnosis of Sanfilippo syndrome, therefore suggesting that the disease is a relatively frequent subtype. The birth prevalence of MPS IIIC in Australia,[11] Portugal,[12] and the Netherlands[13] has been estimated to be 0.07, 0.12, and 0.21 per 100,000, respectively.

The putative chromosomal locus of the MPS IIIC gene was first reported in 1992. By studying two siblings who received the diagnosis of MPS IIIC and had an apparently

From the Institute for Inherited Metabolic Disorders (M.H.; L.M.; L.N.; H.H.; R.I.; A.Č.; H.P.; J.S.; J.U.; V. Stránecký; J.Z.; S.K.) and Center for Applied Genomics (R.I.; A.Č.; V. Stránecký; J.Z.; S.K.), Charles University 1st School of Medicine, and Institute of Molecular Genetics, Academy of Sciences of the Czech Republic (R.I.), Prague; Hopital Sainte-Justine and Départements de Pédiatrie (V. Seyrantepe; S.D.; J.A.; A.V.P) and Biochimie (A.V.P), Université de Montréal, and Research Institute of the McGill University Health Centre (N.M.R.; T.J.H.; T.M.F.; K.M.), McGill University and Genome Quebec Innovation Centre (P.L.; D.R.; A.V.; T.J.H.; J.M.), and Departments of Human Genetics (T.J.H.; T.M.F.; J.M.; K.M.), Medicine (T.J.H.; T.M.F.; K.M.), and Anatomy and Cell Biology (A.V.P.), McGill University, Montreal; Biochemistry, Endocrinology & Metabolism Unit, UCL Institute of Child Health, London (C.E.B.); Hôpital Debrousse, Lyon, France (I.M.); Department of Medical Biochemistry, Academic Medical Center UVA (B.J.H.M.P.), and Department of Clinical Genetics, VU University Medical Center (J.v.d.K.), Amsterdam; Department of Clinical Genetics, Erasmus University Medical Center, Rotterdam, The Netherlands (O.P.v.D.); and Laboratory of Pediatrics and Neurology, University Medical Center, Nijmegen, The Netherlands (R.A.W.)

Received June 8, 2006; accepted for publication August 8, 2006; electronically published September 8, 2006.

Address for correspondence and reprints: Dr. Alexey V. Pshezhetsky, Service de Génétique Médicale, Hôpital Sainte-Justine, 3175 Côte Sainte-Catherine, Montreal, Quebec H3T 1C5, Canada. E-mail: alexei.pchejetski@umontreal.ca

* Footnote added in proof: the gene name has been changed to *HGSNAT*.

† S.K. has led the Prague team.

Am. J. Hum. Genet. 2006;79:000–000. 0002-9297/2006/7905-00XX$15.00

balanced Robertsonian translocation, Zaremba et al.[14] suggested that the mutant gene may be located in the pericentric region of either chromosome 14 or chromosome 21, but no further confirmation of this finding was provided. Previously, we performed a genomewide scan on 27 patients with MPS IIIC and 17 unaffected family members, using 392 highly informative microsatellite markers with an average interspacing of 10 cM. For chromosome 8, the scan showed an apparent excess of homozygosity in patients compared with their unaffected relatives.[15] Additional genotyping of 38 patients with MPS IIIC for 22 markers on chromosome 8 identified 15 consecutive markers (from *D8S1051* to *D8S2332*) in an 8.3-cM interval for which the genotypes of affected siblings were identical in state. A maximum multipoint LOD score of 10.6 was found at marker *D8S519*, suggesting that this region includes the locus for MPS IIIC.[15] Recently, localization of the MPS IIIC causative gene on chromosome 8 was confirmed by microcell-mediated chromosome transfer in cultured skin fibroblasts of patients with MPS IIIC.[16]

Here, we report the results of linkage analyses that narrowed the candidate region for MPC IIIC to a 2.6-cM interval between *D8S1051* and *D8S1831* and the identification of the *TMEM76* gene, located within the candidate region, as the gene that codes for the lysosomal *N*-acetyltransferase and, when mutated, is responsible for MPS IIIC.

Material and Methods

Families

In Montreal, 33 affected individuals and 35 unaffected relatives comprising 15 families informative for linkage were genotyped. The families came from Europe, North Africa, and North America. An additional 27 affected individuals and 9 unaffected relatives in uninformative pedigrees, as well as 40 controls, were also genotyped. Eleven of these families and the controls have been reported elsewhere.[15] In addition, 54 individuals from four MPS IIIC–affected families from the Czech Republic were studied in Prague (fig. 1). One family had two affected brothers, whereas the remaining three families each had one affected individual. The families came from various regions of the Czech Republic and were not related within the four most-recent generations. The diagnosis for affected individuals was confirmed by the measurement of *N*-acetyltransferase activity in cultured skin fibroblasts or white blood cells.

Genotyping

The samples in Montreal were genotyped for 22 microsatellite markers in the pericentromeric region of chromosome 8 spanning 8.9 cM on the Rutgers map, version 2.0.[17] The genotyping was performed as described by Mira et al.[18] at the McGill University and Genome Quebec Innovation Centre on an ABI 3730xl DNA Analyzer platform (Applied Biosystems). Alleles were assigned using Genotyper, version 3.6 (Applied Biosystems). The random-error model of SimWalk2, version 2.91,[19,20] was used to detect potential genotyping errors, with an overall error rate of 0.025. Nine genotypes for which the posterior probability of being incorrect was >0.5 were removed before subsequent analyses. In addition, nine genotypes for one marker in one family were removed because of a suspected microsatellite mutation. The samples from the Czech Republic were genotyped in Prague for 18 microsatellite markers in an 18.7-cM region that includes the 8.9-cM region mentioned above. The genotyping was performed on an LI-COR IR2 sequencer by use of Saga genotyping software (Li-Cor) as described elsewhere.[21] Genotypes were screened for errors by use of the PedCheck program.[22]

Linkage Analysis

For the families genotyped in Montreal, multipoint linkage analysis was performed using the Markov chain–Monte Carlo (MCMC) method implemented in SimWalk2, version 2.91,[19] since one pedigree was too large to be analyzed by exact computation. A fully penetrant autosomal recessive parametric model was used with a disease-allele frequency of 0.0045. Marker-allele frequencies were estimated by counting alleles in the available parents of patients with MPS IIIC and in control individuals. To check the consistency of the results, the MCMC analysis was repeated four times.

N-acetyltransferase activity was measured in all participants of the four families from the Czech Republic.[23] Individuals were classified as affected, carriers, or unaffected on the basis of the results of this assay. Mean affected and carrier activities were determined from the five affected individuals and their seven obligate heterozygote parents, respectively, whereas the mean control activity was determined from a sample of 89 unrelated individuals. Four individuals were unable to be classified because their values were within 2 SDs of the means of both the control and carrier groups. Multipoint linkage analysis was performed using a codominant model with a penetrance of 0.99 and a phenocopy rate of 0.01, to account for the possibility of misclassification or genotyping errors. The same disease-allele frequency of 0.0045 was used. Marker-allele frequencies were estimated by counting all genotyped individuals. Exact multipoint linkage analysis was run on 18 microsatellite markers by use of Allegro 1.2c,[24] which was also used to infer haplotypes.

Gene-Expression Analysis

For each of 32 genes located in the candidate interval, a single 5′-amino–modified 40-mer oligonucleotide probe (Illumina) was spotted in quadruplicate on aminosilane-modified microscopic slides and was immobilized using a combination of baking and UV cross-linking. Total RNA (250–1,000 ng) from white blood cells of two patients with MPS IIIC (patients AIV.8 and BIII.5) and four healthy individuals were amplified using the SenseAmp plus RNA Amplification Kit (Genisphere) and were reverse transcribed using 300 ng of poly(A)-tailed mRNA. Reverse transcription and microarray detection were done using the Array 900 Expression Detection Kit (Genisphere) according to the manufacturer's protocol. The two patient samples and four control samples were analyzed in dye-swap mode, in two replicates of each mode. The hybridized slides were scanned with a GenePix 4200A scanner (Molecular Devices), with photomultiplier gains adjusted to obtain the highest-intensity unsaturated images. Data analysis was performed in the R statistical environment (The R Project for Statistical Computing, version 2.2.1) by use of the Linear Models for Microarray Data package (Limma, version 2.2.0).[25] Raw data were processed using loess normalization and a moving minimum background correction on individual arrays and quantile

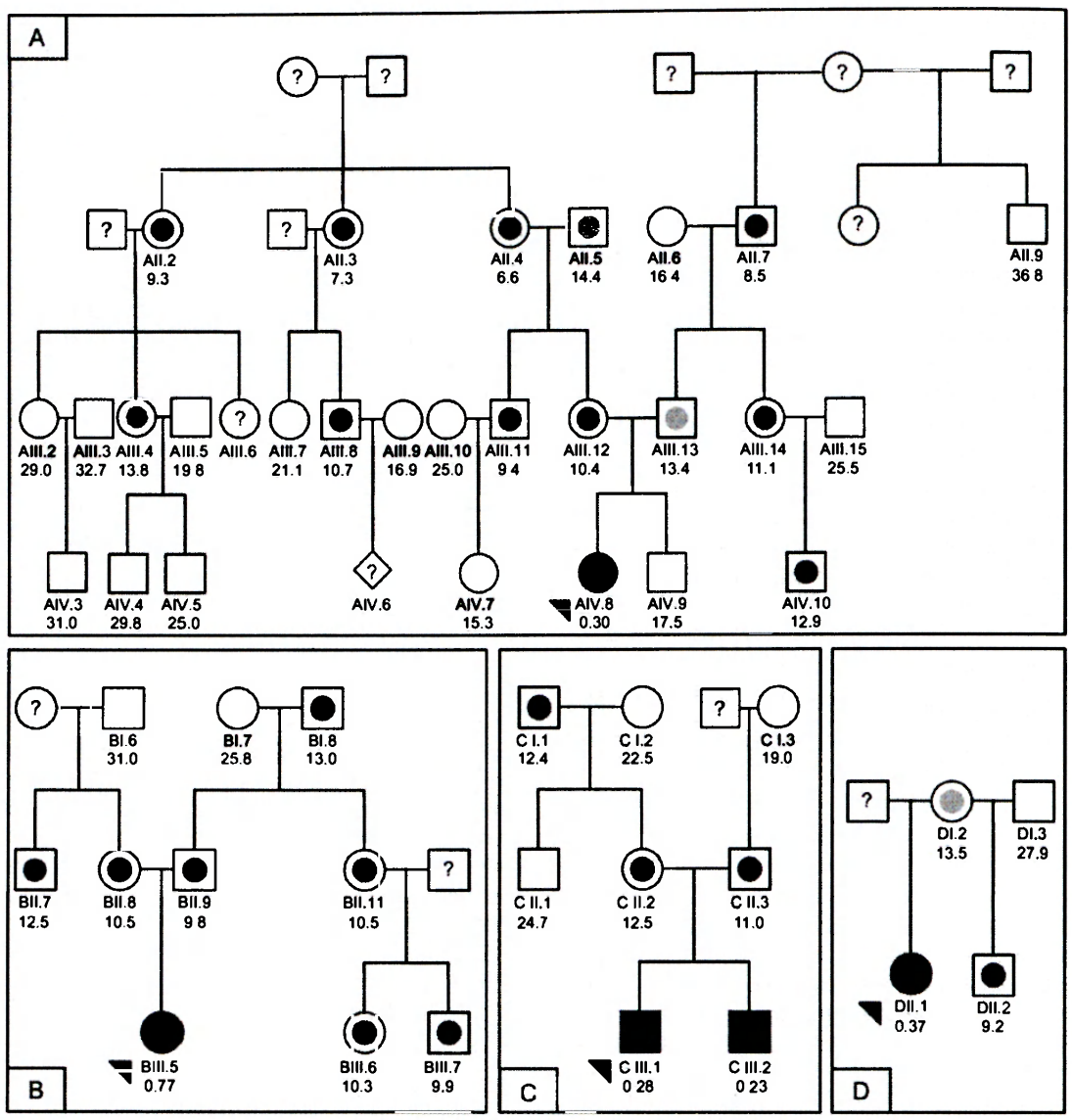

Figure 1. Four families from the Czech Republic used in the linkage and mutation analyses. Fully blackened symbols indicate individuals with MPS IIIC; arrowheads indicate probands. Measurements in seven obligate heterozygotes from these pedigrees (mean ± SD 11.6 ± 1.5 nmol/h/mg) and 89 controls not known to be related to members of the pedigree (mean ± SD 24.4 ± 5.7 nmol/h/mg) were used to establish *N*-acetyltransferase activity ranges for heterozygotes (symbols with blackened inner circle) and normal homozygotes (open symbols). An individual was assigned to a class if his or her enzyme activity was within 2 SDs of the class, unless the value was within the overlap of the upper end of the obligate heterozygotes and the lower end of the controls. Individuals with values within the open interval 13.0–14.6 nmol/h/mg were classified as unknown (symbols with gray inner circle). A symbol with a question mark (?) indicates that no material was available for the enzyme assay. DNA was available for individuals with ID numbers, and *N*-acetyltransferase activity measurements in white blood cells are shown below the ID numbers.

normalization between arrays. The correlation between four duplicate spots per gene on each array was used to increase the robustness. A linear model was fitted for each gene given a series of arrays by use of the lmFit function. The empirical Bayes method[26] was used to rank the differential expression of genes by use of the eBayes function. Correction for multiple testing was performed using the Benjamini and Hochberg false-discovery-rate method.[27] We considered genes to be differentially expressed if the adjusted *P* value was <.01.

DNA and RNA Isolation and Sequencing

Cultured skin fibroblasts from patients with MPS IIIC and normal controls were obtained from cell depositories (Hôpital Debrousse,

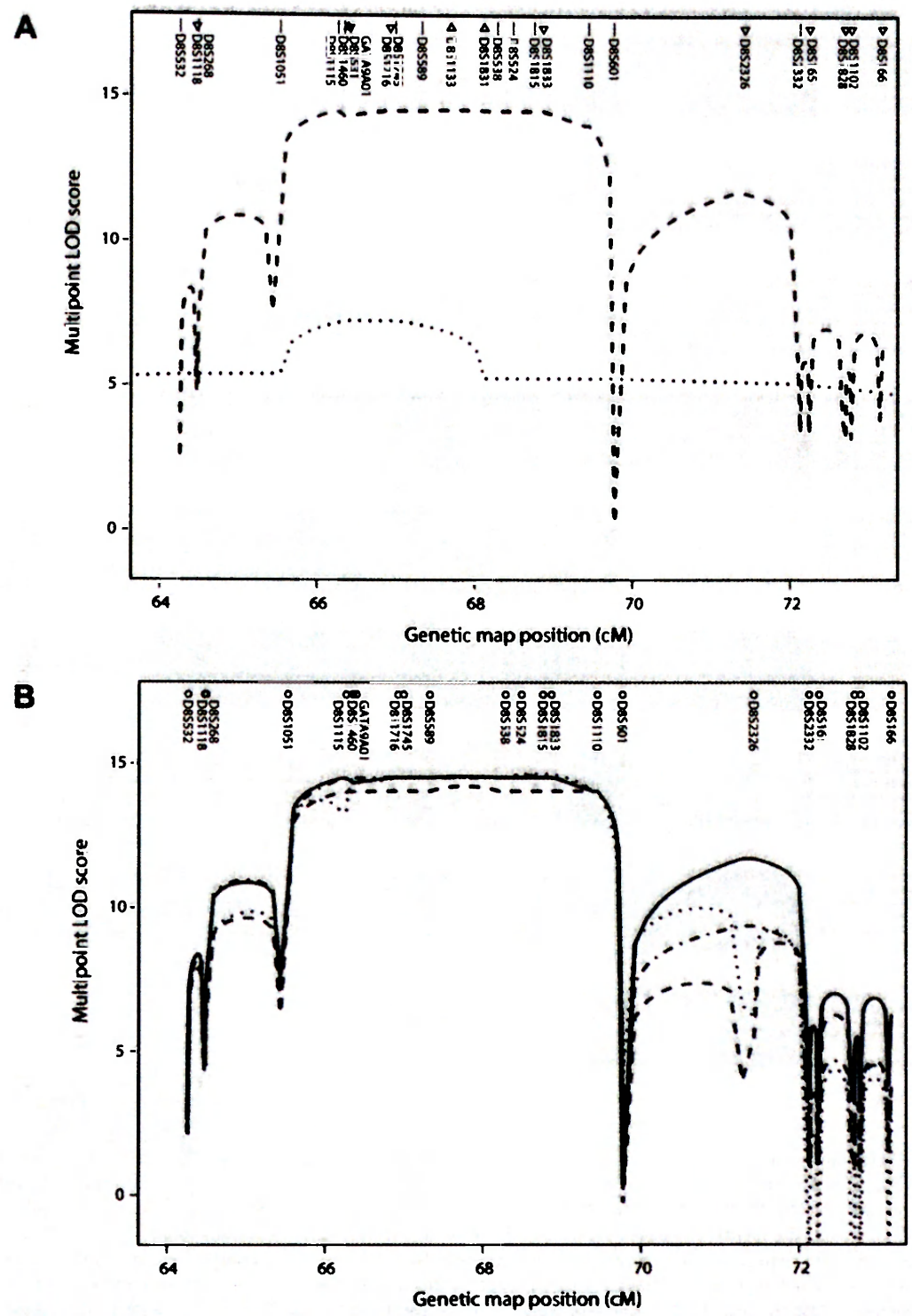

Figure 2. Multipoint linkage analysis of MPS IIIC on chromosome 8. *A,* Multipoint LOD scores in an 8.9-cM interval from two sets of families. Symbols above the marker names indicate the map position. Marker names are listed in the correct order but may be displaced from the symbols for visibility. The dashed line is based on families genotyped in Montreal, and the dotted line on families genotyped in Prague. Straight lines next to marker names indicate that the markers were typed in both data sets. Triangles pointing down indicate markers typed only in the Montreal data set, and triangles pointing up indicate markers typed only in the Prague data set. For the Montreal data, the SimWalk2 run with the highest likelihood is shown. *TMEM76* lies between *D8S1115* and *D8S1460*, and, according to the March 2006 freeze of the human genome sequence from the University of California–Santa Cruz Genome Browser,[30] the order is *D8S1115*–(500 kb)–*TMEM76*–(800 kb)–centromere–(200 kb)–*D8S1460*. *B,* Multipoint LOD scores from the Montreal data from four runs of SimWalk2, version 2.91,[19] showing the variation between runs.

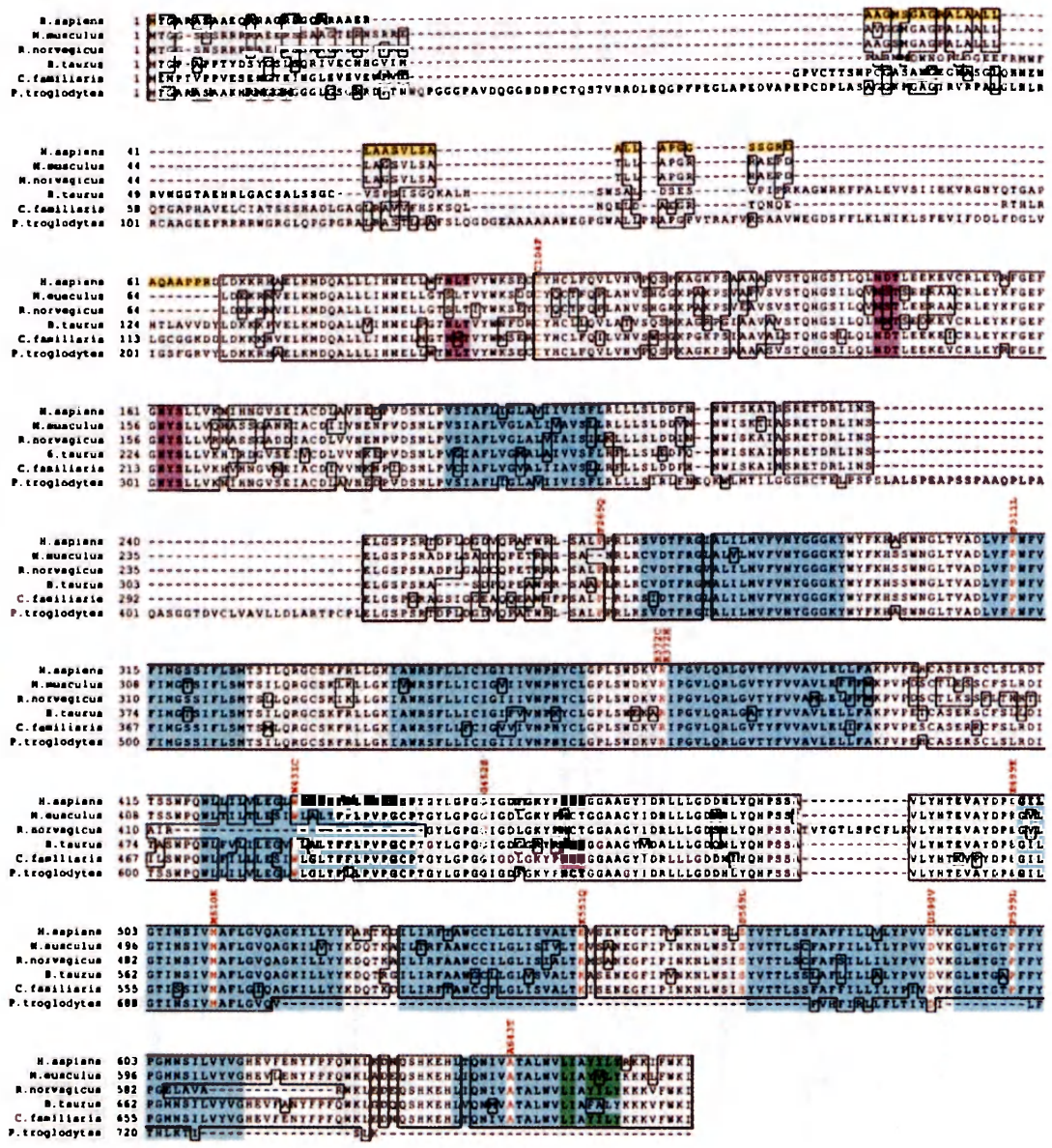

Figure 3. Predicted amino acid sequence of the TMEM76 protein. Amino acid sequence alignment of *Homo sapiens* TMEM76 with orthologs from *Mus musculus* (cloned sequence), *Canis familiaris* (GenBank accession number XP_539948.2), *Bos taurus* (XP_588978.2), *Rattus norvegicus* (XP_341451.2), and *Pan troglodytes* (XP_519741.1) by use of BLAST. All cDNA sequences are predicted except the sequence for *M. musculus*. The identical residues are boxed, the residues with missense mutations in patients with MPS IIIC are shown in red, and the amino acid changes are indicated above the sequence. The first 67 aa of the human sequence shown as black on yellow comprise the predicted signal peptide. The predicted transmembrane domains in the human sequence are shown as black on turquoise. The topology model[5–7] strongly predicts that the N-terminus is inside the lysosome and the C-terminus is outside. Four predicted *N*-glycosylation sites are shown as black on pink, and the predicted motifs for the lysosomal targeting, as black on green.

France; NIGMS Human Genetic Mutant Cell Repository; Montreal Children's Hospital, Canada; and Department of Clinical Genetics, Erasmus Medical Center, The Netherlands). Blood samples from patients with MPS IIIC, their relatives, and controls were collected with ethics approval from the appropriate institutional review boards. DNA from blood or cultured skin fibroblasts was extracted using the PureGene kit (Gentra Systems). Total RNA from cultured skin fibroblasts and pooled tissues (spleen, liver, kidney, heart, lung, and brain) of a C57BL/6J mouse was isolated using Trizol (Invitrogen), and first-strand cDNA synthesis was prepared with SuperScript II (Invitrogen). DNA fragments containing *TMEM76* exons and adjacent regions (~40 bp from each side; primer sequences are shown in appendix A) were amplified by PCR from genomic DNA and were purified with Montage PCR96

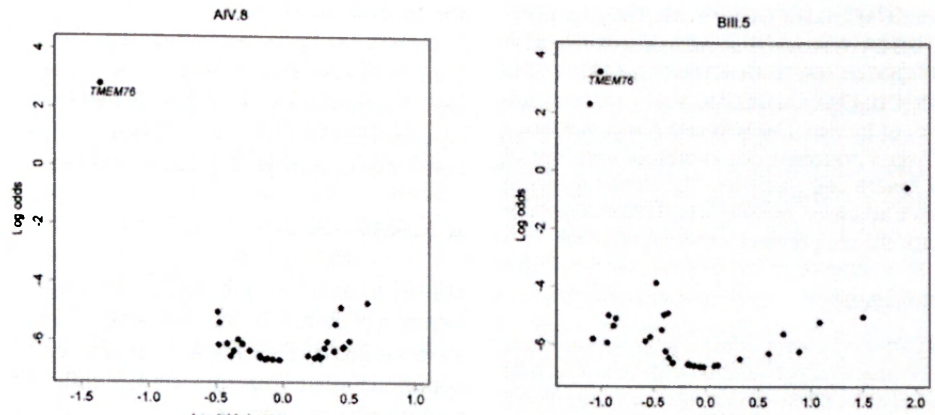

Figure 4. Volcano plot of genes located within the MPS IIIC candidate region, showing significantly reduced expression of the *TMEM76* gene in white blood cells of two patients with MPS IIIC: AIV.8 and BIII.5. The natural logarithm of the probability that the gene is differentially expressed (Log odds) is plotted as a function of the logarithm of the gene-expression $\log_2$ fold change (Log fold change) between the patient and control samples.

filter plates (Millipore). Each sequencing reaction contained 2 μl of purified PCR product, 5.25 μl of H_2O, 1.75 μl of 5 × sequencing buffer, 0.5 μl of 20 μM primer, and 0.5 μl of Big Dye Terminator v3.1 (all from Applied Biosystems). In Montreal, PCR products were analyzed using an ABI 3730x1 DNA Analyzer (Applied Biosystems). In Prague, PCR products were analyzed on an ALFexpress DNA sequencer (Pharmacia), as described elsewhere.[28] Included in the sequencing analysis were 30 probands with MPS IIIC who were considered unrelated and 105 controls. The controls were unrelated CEPH individuals, and amplified DNAs were combined in pools of two before sequencing.

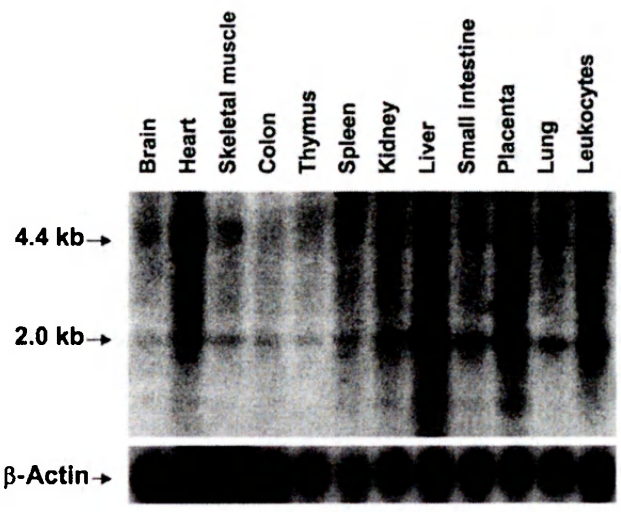

Figure 5. Northern-blot analysis of *TMEM76* mRNA in human tissues. A 12-lane blot containing 1 μg of poly A+ RNA per lane from various adult human tissues was hybridized with a [^{32}P]-labeled 220-bp cDNA fragment corresponding to exons 8–10 of the *TMEM76* gene or β-actin, as described in the Material and Methods section.

Northern Blotting

A 12-lane multiple-tissue northern blot containing 1 μg of poly A+ RNA per lane from various human tissues (BD Biosciences Clontech) was hybridized with the 220-bp cDNA fragment corresponding to exons 8–10 of the human *TMEM76* gene or the entire cDNA of human β-actin labeled with [^{32}P]-dCTP by random priming with the MegaPrime labeling kit (Amersham). Prehybridization of the blot was performed at 68°C for 30 min in ExpressHyb (Clontech). The denatured probes were added directly to the prehybridization solution and were incubated at 68°C for 1 h. The blots were washed twice for 30 min at room temperature with 2 × sodium chloride–sodium citrate (SSC) solution and 0.05% SDS and once for 40 min at 50°C with 0.1 × SSC and 0.1% SDS and were exposed to a BioMax film for 48 h.

Mouse and Human TMEM76 *cDNA Cloning*

Mouse coding sequence was amplified by PCR (forward primer 5′-GAATTCATGACGGGCGGGTCGAGC-3′; reverse primer 5′-ATATGTCGACGATTTTCCAAAACAGCTTC-3′) and was cloned into pCMV-Script, pCMV-Tag4A (Stratagene), and pEGFP-N3 (BD Biosciences Clontech) vectors by use of the *Eco*RI and *Sal*I restriction sites of the primers. The cloned sequence was identical to GenBank accession number AK152926.1, except that an "AT" was needed to complete an alternate ATG initiation codon. GenBank accession number AK149883.1 provides what we consider to be the complete clone and encodes a 656-aa protein. The GenBank sequences differ by 1 aa and three silent substitutions.

A 1,907-bp fragment of the human *TMEM76* cDNA (nt +75 to +1992) was amplified using Platinum High Fidelity *Taq* DNA polymerase (Invitrogen), a sense primer with an *Hin*dIII site (5′-AAGCTTGGCGGCGGGCATGAG-3′), and an antisense primer with an *Sal*I site (5′-GTCGACCTCAGTGGGAGCCATCAGATTTT-3′) and was cloned into pCMV-Script expression vector (Stratagene). Since high GC content (85%) of the 5′ region of human *TMEM76* cDNA prevented its amplification by PCR, a synthetic 186-bp codon-optimized double-stranded oligonucleotide fragment (5′-AAGCTTATGACCGGAGCGAGGGCAAGCGCCGCCG-

AACAAAGAAGAGCCGGACGGTCCGGCCAGGCTAGGGCCGC-AGAGCGAGCTGCTGGCATGTCAGGTGCAGGGCGCGCACTTG-CCGCCTTGCTGCTCGCCGCGAGTGTGCTGAGCGCTGCCCTC-CTGGCTCCCGGAGGCTCTTCCGGGCGGGAC-3′) corresponding to nt +1 to +186 of human *TMEM76* cDNA was purchased from BioS&T. A 177-bp 5′ fragment was combined with rest of the cDNA by use of *Hin*dIII and *Sap*I sites. The cloned sequence is identical to GenBank accession number XM_372038.4 from nt 131 to nt 1946, except for the presence of SNP *rs1126058*.

Cell Culture and Transfection

Skin fibroblasts and COS-7 cells were cultured in Eagle's minimal essential medium (Invitrogen) supplemented with 10% (v/v) fetal bovine serum (Invitrogen) and were transfected with the full-size mouse *Tmem76* (*Hgsnat*) coding sequence subcloned into pCMV-Script, pCMV-Tag4A, and pEGFP-N3 vectors or with the full-size human *TMEM76* coding sequence subcloned into pCMV-Script vector by use of Lipofectamine Plus (Invitrogen) according to the manufacturer's protocol. The cells were harvested 48 h after transfection, and *N*-acetyltransferase activity was measured in the homogenates of *TMEM76*-transfected and mock-transfected cells (i.e., transfected with only the cloning vector).

Enzyme Assay

N-acetyltransferase enzymatic activity was measured using the fluorogenic substrate 4-methylumbelliferyl β-D-glucosaminide (Moscerdam) as described elsewhere.[23] Protein concentration was measured according to the method of Bradford.[29] This assay was used for the activity measurements in cultured skin fibroblasts or white blood cells from patients and all participating members of the Czech families and for the functional expression experiments.

Confocal Microscopy

To establish colocalization of the tagged protein with the lysosomal compartment, the skin fibroblasts expressing mouse TMEM76-EGFP were treated with 50 nM LysoTracker Red DND-99 dye (Molecular Probes), were washed twice with ice-cold PBS, and were fixed with 4% paraformaldehyde in PBS for 30 min. Slides were studied on an LMS 510 Meta inverted confocal microscope (Zeiss).

Results

Linkage Analysis

Previously, we performed a genomewide linkage study that indicated that the locus for MPS IIIC is mapped to an 8.3-cM interval in the pericentromeric region of chromosome 8.[15] To reduce this interval, we genotyped the families from that study as well as newly obtained MPS IIIC–affected families for 22 microsatellite markers (Montreal data). Linkage analysis under an autosomal recessive model resulted in LOD scores >14 in the 4.2-cM region spanning *D8S1051* to *D8S601*, which included the centromere (fig. 2). The results of multiple MCMC runs showed consistent trends. Linkage was also performed in four families from the Czech Republic by use of an autosomal codominant model (Prague data). For these data, linkage analysis produced a maximum LOD score of 7.8 at 66.4 cM at *D8S531* and reduced the linked region for the Montreal data to a 2.6-cM interval between *D8S1051* and *D8S1831*. This region was defined by inferred recombinants at *D8S1051* in one family in each of the Montreal and Prague data sets, and a recombinant at *D8S1831* in an additional family in the Prague data set. This interval contains 32 known or predicted genes and ORFs.

Identification of a Candidate Gene

On the basis of our previous studies that defined the molecular properties of the lysosomal *N*-acetyltransferase,[31] we searched the candidate region for a gene encoding a protein with multiple transmembrane domains and a molecular weight of ~100 kDa, which allowed us to exclude the majority of the genes in the region. In contrast, the predicted protein product of the *TMEM76* gene has multiple putative transmembrane domains. The predicted coding region in GenBank accession number XM_372038.4 was extended by 28 residues at the 5′ end on the basis of the transcript in GenBank accession number DR000652.1 (which includes 14 of the 28 residues), examination of the genomic sequence in NT_007995.14, and comparison with mouse sequence AK149883.1. We predict that the modified *TMEM76* contains 18 exons, corresponding to an ORF of 1,992 bp, and codes for a 73-kDa protein. A comparison of human TMEM76 with five vertebrate orthologs is shown in figure 3. Furthermore, of all the genes present in the candidate interval, only *TMEM76* showed a statistically significant reduction of the transcript level in the cells of two patients with MPS IIIC (AIV.8 and BIII.5; adjusted P values < .001) in the custom oligonucleotide-based microarray assay (fig. 4). Further, we showed that both patients carried nonsense mutations presumably causing mRNA decay (R534X and L349X; see table 2).

Analysis of the TMEM76 *Transcript by Northern Blot and RT-PCR*

Northern-blot analysis identified two major *TMEM76* transcripts of 4.5 and 2.1 kb ubiquitously expressed in various human tissues (fig. 5). The highest expression was detected in leukocytes, heart, lung, placenta, and liver, whereas the gene was expressed at a much lower level in the thymus, colon, and brain, which is consistent with the expression patterns of lysosomal proteins. Consistent with the northern-blot results, a full-length 4.5-kb cDNA containing 1,992 bp of coding sequence and two polyadenylation signals as well as two shorter transcripts were amplified by RT-PCR from the total RNA of normal human skin fibroblasts, white blood cells, and skeletal muscle. In one transcript, exons 9 and 10 were spliced out, leading to an in-frame deletion of 64 aa, which contains the predicted transmembrane domains III and IV. Most likely, this transcript does not encode an active enzyme, since it was also detected in the RNA of two patients with MPS IIIC (patients CIII.1 and CIII.2) who had almost complete loss of

N-acetyltransferase activity. Another transcript lacked exons 3, 9, and 10.

The deduced amino acid sequence predicts 11 transmembrane domains and four potential *N*-glycosylation sites (fig. 3), consistent with the molecular properties of lysosomal *N*-acetyltransferase.[31] The first 67 aa may comprise the signal peptide, with length and composition resembling those of lysosomal proteins. According to the predictions made by empirical computer algorithms,[32–34] the C-terminus of the TMEM76 protein is exposed to the cytoplasm and contains conserved Tyr-X-X-Θ and Leu-Leu sequence motifs involved in the interaction with the adaptor proteins responsible for the lysosomal targeting of membrane proteins.[35]

Mutation Analysis

We identified 27 *TMEM76* mutations in the DNA of 30 MPS IIIC–affected families (table 1) that were not found in DNA from 105 controls. Among the identified mutations, there were 4 nonsense mutations, 14 missense mutations, 3 predicted frameshift mutations due to deletions or duplications, and 6 splice-site mutations. All the missense mutations occur at residues conserved among five species with the most homologous TMEM76 sequences (fig. 3), except for P265Q, which is not conserved in the mouse, and W431C, which is not conserved in the rat. There were three instances of two mutations on the same allele that were found in patients who were homozygous, and these are designated as complex mutations in table 1. cDNA sequencing of one of the patients homozygous for the splice-site mutation in intron 2 and a missense mutation (P265Q) demonstrated that the splice-site mutation disrupts the consensus splice-site sequence between exon 2 and intron 2 and causes exon 2 skipping and a frameshift (not shown).

Consanguinity was reported in 4 of the 13 families in which the patients were homozygous for *TMEM76* mutations: the two Moroccan families, the French family with two missense mutations (W431C and A643T), and the Turkish family with the splice-site mutation in intron

Table 1. Mutations in *TMEM76* Identified in Patients from 30 Families with MPS IIIC

Mutation Group and Mutation[a]	Predicted Effect on Protein	No. of Alleles	Location in *TMEM76*
Nonsense mutations:			
c.1031G→A	p.W344X	2	Exon 10
c.1046T→G	p.L349X	1	Exon 10
c.1234C→T	p.R412X	8	Exon 12
c.1600C→T	p.R534X	1	Exon 15
Missense mutations:			
c.311G→T	p.C104F	1	Exon 2
c.932C→T	p.P311L	3	Exon 9
c.1114C→T	p.R372C	3	Exon 11
c.1115G→A	p.R372H	1	Exon 11
c.1354G→A	p.G452S	2	Exon 13
c.1495G→A	p.E499K	3	Exon 14
c.1529T→A	p.M510K	1	Exon 14
c.1706C→T	p.S569L	4	Exon 17
c.1769A→T	p.D590V	1	Exon 17
c.1796C→T	p.P599L	1	Exon 17
Frameshift mutations:			
c.1118_1133del	p.I373SfsX3	1	Exon 11
c.1420_1456dup	p.V488GfsX22	1	Exon 13
c.1834delG	p.V612SfsX16	1	Exon 18
Splice-site mutations:			
c.202+1G→A	p.L69EfsX32[b]	1	Intron 1
c.577+1G→A	p.P193HfsX20[b]	1	Intron 4
c.935+5G→A	p.F313X	1	Intron 9
c.1334+1G→A	p.G446X[b]	1	Intron 12
c.1810+1G→A	p.S567NfsX14	2	Intron 17
Complex mutations:			
c.[318+1G→A; 794C→A]	p.[D68VfsX19; P265Q]	6	Intron 2; exon 7
c.[577+1G→A; 1650A→C]	p.[P193HfsX20; K551Q]	2	Intron 4; exon 16
c.[1293G→T; 1927G→A]	p.[W431C; A643T]	2	Exon 12; exon 18

[a] Mutation names were assigned according to the guidelines of the Human Genome Variation Society and on the basis of the cDNA sequence from GenBank accession number NT_007995.14, except that the first exon includes 84 nt 5′ of the stated ATG initiation codon. Thus, +1 corresponds to the A of the ATG at nt 13315945 (instead of nt 13316029).

[b] The mutations were named under the assumption that no exon skipping takes place; cDNA sequencing was not done.

17. The two Moroccan families were not known to be related to each other or to the Spanish patient homozygous for the same mutations (table 2). The parents of the French patient are second cousins in two ways (see family F1 in the work of Ausseil et al.[15]).

The splice-site mutation in the above-mentioned Turkish family disrupts the consensus splice-site sequence between exon 17 and intron 17 and causes exon 17 skipping and a frameshift in all transcripts, as detected by sequencing of multiple RT-PCR clones (not shown). The two affected siblings in this family (family F8 in the work of Ausseil et al.[15]) had a severe form of MPS IIIC and showed almost complete loss of *N*-acetyltransferase activity in cultured skin fibroblasts. Among other severely affected patients with MPS IIIC, a patient of French origin was homozygous for a nonsense mutation (W344X) in exon 10, which may result in the synthesis of a truncated protein or RNA decay. A patient of Polish origin was a compound heterozygote for a 37-bp duplication in exon 13 and a missense mutation (S569L) in exon 17 (table 2). The duplication results in a frameshift, whereas the substitution of a strictly conserved small polar Ser for a bulky hydrophobic Leu may have a significant structural impact (fig. 3).

The five patients from four Czech families are all compound heterozygotes for eight different mutations (table 2). Five of the eight mutations are predicted to result in truncated products (three nonsense mutations, one 16-bp deletion, and one splice-site mutation leading to the inclusion of 89 bases from the 5′ end of intron 9 and the splicing out of exon 10 in the transcript, and the remaining three are missense mutations affecting residues conserved among multiple species and located either in the predicted transmembrane regions (fig. 3) or in their close vicinity, suggesting that they may have a serious structural impact. In the Czech families, the mutations completely segregated with reduced enzyme activity. That is, all individuals assigned to be heterozygotes on the basis of the enzyme assay as well as the four individuals who were within 2 SD of the lower end of the controls (symbols with gray inner circle in fig. 1) were found to carry *TMEM76* mutations.

Functional Expression Studies

The fibroblast cell line from a patient homozygous for a splice-site mutation in intron 17 with negligible *N*-acetyltransferase activity was transfected with plasmids containing human *TMEM76* cDNA or cDNA of the mouse ortholog of TMEM76 carrying a FLAG tag on the C-terminus or of a fusion protein of mouse TMEM76 with enhanced green fluorescent protein (EGFP). All constructs increased the *N*-acetyltransferase activity in the mutant fibroblast cells to approximately normal level (fig. 6*A*). Significant increase in activity was also observed in transfected COS-7 cells, confirming that the TMEM76 protein

Table 2. TMEM76 Predicted Mutations in Probands from 30 Families with MPS IIIC

Patient Group and Mutation 1	Mutation 2	No. of Patients	Geographic Origin of Patient(s)
Patients from Czech families:			
p.I373SfsX3	p.R534X	1	Czech Republic
p.L349X	p.M510K	1	Czech Republic
p.F313X	p.R412X	1	Czech Republic
p.R372H	p.P599L	1	Czech Republic
Patients homozygous for *TMEM76* mutations:			
p.[D68VfsX19; P265Q]	p.[D68VfsX19; P265Q]	3	Morocco, Morocco, and Spain
p.[P193HfsX20; K551Q]	p.[P193HfsX20; K551Q]	1	France
p.P311L	p.P311L	1	United Kingdom
p.W344X	p.W344X	1	France
p.R372C	p.R372C	1	United Kingdom
p.R412X	p.R412X	2	Turkey and Poland
p.[W431C; A643T]	p.[W431C; A643T]	1	France
p.G452S	p.G452S	1	Canada
p.E499K	p.E499K	1	Canada
p.S567NfsX14	p.S567NfsX14	1	Turkey
Patients compound heterozygous for *TMEM76* mutations:			
p.C104F	...	1	Belarus
p.E499K	p.D590V	1	France
p.P193HfsX20	p.R412X	1	Canada
p.P311L	p.R372C	1	France
p.R412X	...	1	Poland
p.R412X	p.G446X	1	Poland
p.S569L	...	2	France and Portugal
p.S569L	p.L69EfsX32	1	United States
p.V488GfsX22	p.S569L	1	Poland
p.V612SfsX16	...	1	Finland
Families with no mutations identified to date	...	2	North Africa and Portugal

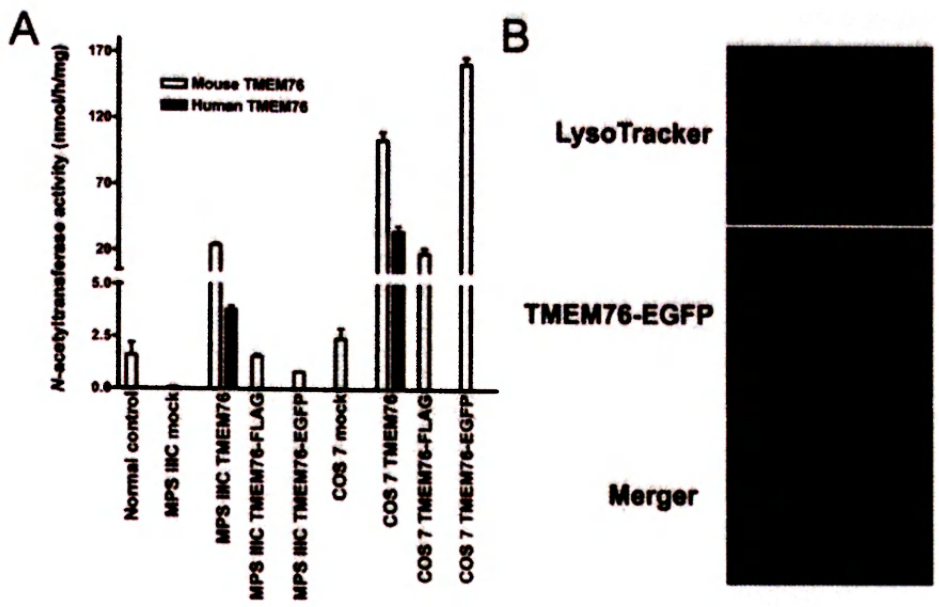

Figure 6. Functional expression of human and mouse TMEM76 protein. *A,* The full-size human and mouse *TMEM76* coding sequences subcloned into pCMV-Script, pCMV-Tag4A, and pEGFP-N3 vectors were expressed in COS-7 cells and in cultured skin fibroblasts from a patient with MPS IIIC. The cells were harvested 48 h after transfection, and *N*-acetyltransferase activity was measured in the homogenates of TMEM76-transfected and mock-transfected fibroblast or COS-7 cells by use of the artificial fluorometric substrate 4-methylumbelliferyl-β-D-glucosaminide.[23] Values represent means ± SD of four independent experiments. *B,* The intracellular localization of TMEM76 was studied by expressing the fusion protein of the mouse TMEM76 with EGFP. Before fixation, the cells were treated for 45 min with 50 nM lysosomal marker, LysoTracker Red DND-99 dye. Slides were analyzed on an LMS 510 Meta confocal microscope (Zeiss). Magnification × 1000. The image was randomly selected from 30 studied panels, all of which showed a similar localization of TMEM76-EGFP. The fluorescence of EGFP was not quenched as it would have been if the fluorophore had been exposed to the acidic lysosomal microenvironment, confirming that the C-terminus of TMEM76 faces the cytoplasmic side of the lysosomal membrane.

by itself has *N*-acetyltransferase activity. Confocal fluorescent microscopy shows that TMEM76-EGFP (fig. 6*B*) or TMEM-FLAG (not shown) peptides are targeted in human fibroblasts to cytoplasmic organelles, colocalizing with the lysosomal-endosomal marker LysoTracker Red.

Discussion

Degradation of heparan sulfate occurs within the lysosomes by the concerted action of a group of at least eight enzymes: four sulfatases, three exo-glycosydases, and one *N*-acetyltransferase, which work sequentially at the terminus of heparan sulfate chains, producing free sulfate and monosaccharides. The inherited deficiencies of four enzymes involved in the degradation of heparan sulfate cause four subtypes of MPS III: MPS IIIA (heparan *N*-sulfatase deficiency [MIM 252900]), MPS IIIB (α-*N*-acetylglucosaminidase deficiency [MIM 252920]), MPS IIIC (acetyl-CoA:α-glucosaminide acetyltransferase deficiency), and MPS IIID (*N*-acetylglucosamine 6-sulfatase deficiency [MIM 252940]). Since the clinical phenotypes of all these disorders are similar, precise diagnosis relies on the determination of enzymatic activities in patients' cultured skin fibroblasts or leukocytes. The biochemical defect in MPS IIIC was identified 30 years ago as a deficiency of an enzyme that transfers an acetyl group from cytoplasmically derived acetyl-CoA to terminal α-glucosamine residues of heparan sulfate within the lysosomes, resulting in the accumulation of heparan sulfate. Therefore, for identification of the molecular basis of this disorder, we used two complementary approaches. First, we performed a partial purification of human and mouse lysosomal *N*-acetyltransferase, which suggested that the enzyme has properties of an oligomeric transmembrane glycoprotein, with an ~100-kDa polypeptide containing the enzyme active site.[31] Second, by linkage analysis, we narrowed the locus for MPC IIIC to a 2.6 cM-interval (*D8S1051–D8S1831*) and, third, compared the level of transcripts of the genes present in the candidate region between normal control cells and those from patients with MPS IIIC. Thus, an Integrated bioinformatic search and gene-expression analysis both pinpointed a single gene, *TMEM76,* which encodes a 73-kDa protein with predicted multiple transmembrane domains and glycosylation sites. DNA mutation analysis showed that patients with MPS IIIC harbor *TMEM76* mutations incompatible with the normal function of the predicted protein, whereas expression of human *TMEM76* and the mouse ortholog proved that the protein has *N*-acetyltransferase activity and lysosomal lo-

calization, providing evidence that *TMEM76* is the gene that codes for the lysosomal *N*-acetyltransferase.

The TMEM76 protein does not show a structural similarity to any known prokaryotic or eukaryotic *N*-acetyltransferases or to other lysosomal proteins, on the basis of sequence homology searches. Thus, we think that it belongs to a new structural class of proteins capable of transporting the activated acetyl residues across the cell membrane. Moreover, TMEM76 shares homology with a conserved family of bacterial proteins COG4299 (uncharacterized protein conserved in bacteria) (Entrez Gene GeneID 138050). All 146 members of this family are predicted proteins from diverse bacterial species, including Proteobacteria, Cyanobacteria, and Deinococci. Since many of these bacteria are capable of synthesizing heparan sulfate and other structurally related glycosaminoglycans and perform reactions of transmembrane acetylation, it is tempting to speculate that this activity may also be performed by the proteins of the COG4299 family. Previous studies suggested two contradictory mechanisms of transmembrane acetylation. Bame and Rome[2,36,37] proposed that it is performed via a ping-pong mechanism. First, the acetyl group of acetyl-CoA is transferred to an His residue in the active site of the enzyme. This induces a conformational change that results in the translocation of the protein domain containing the acetylated residue to the lysosome, where the acetyl residue is transferred to the glucosamine residue of heparan sulfate. In contrast, Meikle et al.[38] were unable to demonstrate any specific acetylation of the lysosomal membranes and proposed an alternative mechanism that involved the formation of a tertiary complex of the enzyme, acetyl-CoA, and heparan sufate. Identification of *N*-acetyltransferase as a 73-kDa protein with multiple transmembrane domains, together with our previous data that showed that *N*-acetyltransferase is acetylated by [^{14}C]acetyl-CoA in the absence of glucosamine,[31] strongly supports the ping-pong mechanism of transmembrane acetylation.

For 23 of the 30 probands included in this study for mutation analysis, *TMEM76* mutations were identified in both alleles. Five probands were heterozygous for a missense mutation, with a second mutation yet to be identified. In two probands from North Africa and Portugal, we did not identify any mutations in the coding regions or immediate flanking regions. These patients are homozygous for the microsatellite markers throughout the entire MPS IIIC locus and may be homozygous for a yet-to-be-identified *TMEM76* mutation; however, we cannot formally exclude defects in other genes. Additional studies have been initiated to search for mutations in the introns and promoter regions. The patients with MPS IIIC with the identified frameshift and nonsense mutations all have a clinically severe early-onset form. The almost complete deficiency of *N*-acetyltransferase activity in cultured skin fibroblasts from these patients is consistent with the predicted protein truncations and/or nonsense-mediated mRNA decay. Further expression studies are necessary to confirm the impact of the identified substitutions of the conserved amino acids on enzyme activity. Nevertheless, the identification of the lysosomal *N*-acetyltransferase gene which, when mutated, accounts for the molecular defect in patients with MPS IIIC sets the stage for DNA-based diagnosis and genotype-phenotype correlation studies and marks the end of the gene-discovery phase for lysosomal genetic enzymopathies.

Acknowledgments

We thank the patients, their families, and the Czech Society for Mucopolysaccharidosis, for participating in our study, and members of the sequencing and genotyping facilities at the McGill University and Genome Quebec Innovation Centre, for their technical support. We also acknowledge Nina Gusina, Joe Clarke, and Tony Rupar, for providing cell lines from patients with MPS IIIC; Mila Ashmarina, Milan Elleder, J. Loredo-Osti, and Johanna Rommens, for helpful discussions; Karine Landry, for technical support; and Maryssa Canuel, for help with confocal microscopy. The Montreal study was supported by operating grants from the Sanfilippo Children's Research Foundation (to A.V.P.) and by the Canadian Networks of Centres of Excellence Program—the Mathematics of Information Technology and Complex System network (to K.M.). The Prague study was supported by grants NR8069-1 and 1A/8239-3 from the Grant Agency of the Ministry of Health of the Czech Republic. Institutional support was provided by Ministry of Education of the Czech Republic grant MSM0021620806. A.V.P. is a National Investigator of the Fonds de la Recherche en Santé du Québec.

Appendix A

Table A1. Exon-Flanking Primers Used for PCR Amplification and Sequencing of the Exons in the Human *TMEM76* Gene

Primer	Sequence (5′→3′)
TMEM76_Exon1_F	CTCCCGAAGACAAACACTCC
TMEM76_Exon1_R	GCGAAGTCGCAGCAACAGC
TMEM76_Exon2_F	AAGCTTTTGAGAAGCACTACTGG
TMEM76_Exon2_R	GAAGGGCTTTAGACATGAGAGC
TMEM76_Exon3_F	GGAAAAGTCATGTCAGGATCTCC
TMEM76_Exon3_R	GAATAATACATGTTCCTGGGTACG
TMEM76_Exon4_F	TTATTCTGCCTCCATGATATTAGC
TMEM76_Exon4_R	CTACAGAAAGCGTCATGGACTGC
TMEM76_Exon5_F	GGAAATTCAGCATGAGAATATAGG
TMEM76_Exon5_R	GCCACTTGAGGGTGACAGC
TMEM76_Exon6_F	GAATATGAGCTTTAATTTTATTTCC
TMEM76_Exon6_R	TTAGGAATACGGGAGCTACAACC
TMEM76_Exon7_F	CAAAATGAAATTTACCCCTTAGC
TMEM76_Exon7_R	ACATCCAAGAAATCCTTCCTAGC
TMEM76_Exon8_F	CCTTCCTTTTCACATAGCAAACC
TMEM76_Exon8_R	GCTCTGTGAAGGACGTATATAAGC
TMEM76_Exon9_F	CCCCTGGGTTTACTTTCTATACC
TMEM76_Exon9_R	CCAGCATCATCTGAAAAACAGG
TMEM76_Exon10_F	GGGGCTATATTCTGAACTCTTCC
TMEM76_Exon10_R	ACCTGAGATGGAGGAATTGC
TMEM76_Exon11_F	CTGGGATGAGAGGAGAAGTCC
TMEM76_Exon11_R	ACTTGAAGCCAGGAGTGAGG
TMEM76_Exon12_F	CCTTCTATTTGCATTTAGTTCACC
TMEM76_Exon12_R	GAGAATTCCTCTGACTCGAGACC
TMEM76_Exon13_F	TTTTATTCTTGTCCCTCTGTTCG
TMEM76_Exon13_R	CACTTCTGAAAGCCTGAGTTCC
TMEM76_Exon14_F	TTGGTCTAGGAGCTGTTTGTACG
TMEM76_Exon14_R	CCATAGCACAAGAGAGAATATGC
TMEM76_Exon15_F	TCTTTGTCAGGTAGTTAAGACAGTGG
TMEM76_Exon15_R	GTGAAGGAAAGGAATTTTAGC
TMEM76_Exon16_F	ACAAGTTTCAGCCCTCTCTACG
TMEM76_Exon16_R	GTGGAGGAGACGTTTCAGTGC
TMEM76_Exon17_F	ATGCTGAAATTGGATTTGTTCC
TMEM76_Exon17_R	ACCAAGGATGCTCCAGAGG
TMEM76_Exon18_F	AGTAGCCAACAATGGAAGTGC
TMEM76_Exon18_R	GAGCCGTGTCACAGTTAACC

NOTE.—For bidirectional sequencing on the ALFexpress DNA sequencer, all primers have the universal overhang synthesized on the 5′ end (AATACGACTCACTATAG for forward [F] primers and CAGGAAACAGCTATGAC for reverse [R] primers).

Web Resources

Accession numbers and URLs for data presented herein are as follows:

BLAST, http://www.ncbi.nlm.nih.gov/blast/ (used to identify ortholog protein sequences)

Entrez Gene, http://www.ncbi.nlm.nih.gov/entrez/query.fcgi?db=gene (for GeneID 138050)

GenBank, http://www.ncbi.nih.gov/Genbank/ (for accession numbers AK152926.1, AK149883.1, DR000652.1, XM_372038.4, NT_007995.14, XP_539948.2, XP_588978.2, XP_341451.2, and XP_519741.1)

Human Genome Variation Society, http://www.hgvs.org/

Online Mendelian Inheritance in Man (OMIM), http://www.ncbi.nlm.nih.gov/Omim/ (for MPS IIIA, IIIB, IIIC, and IID)

The R Project for Statistical Computing, http://www.r-project.org/

References

1. Rome LH, Hill DF, Bame KJ, Crain LR (1983) Utilization of exogenously added acetyl coenzyme A by intact isolated lysosomes. J Biol Chem 258:3006–3011
2. Bame KJ, Rome LH (1985) Acetyl-coenzyme A:α-glucosaminide *N*-acetyltransferase: evidence for a transmembrane acetylation mechanism. J Biol Chem 260:11293–11299
3. Pohlmann R, Klein U, Fromme HG, von Figura K (1981) Localisation of acetyl-CoA: α-glucosaminide *N*-acetyltransferase in microsomes and lysosomes of rat liver. Hoppe Seylers Z Physiol Chem 362:1199–1207
4. Hopwood JJ, Freeman C, Clements PR, Stein R, Miller AL (1983) Cellular location of N-acetyltransferase activities toward glucosamine and glucosamine-6-phosphate in cultured human skin fibroblasts. Biochem Int 6:823–830
5. Meikle PJ, Whittle AM, Hopwood JJ (1995) Human acetyl-coenzyme A:α-glucosaminide *N*-acetyltransferase: kinetic characterization and mechanistic interpretation. Biochem J 308:327–333
6. Kresse H, von Figura K, Bartsocas C (1976) Clinical and biochemical findings in a family with Sanfilippo disease, type C. Clin Genet 10:364
7. Bartsocas C, Grobe H, van de Kamp JJ, von Figura K, Kresse H, Klein U, Giesberts MA (1979) Sanfilippo type C disease: clinical findings in four patients with a new variant of mucopolysaccharidosis III. Eur J Pediatr 130:251–258
8. Klein U, Kresse H, von Figura K (1978) Sanfilippo syndrome type C: deficiency of acetyl-CoA:α-glucosaminide *N*-acetyltransferase in skin fibroblasts. Proc Natl Acad Sci USA 75: 5185–5189
9. Sanfilippo SJ, Podosin R, Langer LO Jr, Good RA (1963) Mental retardation associated with acid mucopolysaccharidiuria (heparitin sulfate type). J Pediatr 63:837–838
10. Klein U, van de Kamp JJP, von Figura K, Pohlmann R (1981) Sanfilippo syndrome type C: assay for acetyl-CoA:α-glucosaminide *N*-acetyltransferase in leukocytes for detection of homozygous and heterozygous individuals. Clin Genet 20:55–59
11. Meikle PJ, Hopwood JJ, Clague AE, Carey WF (1999) Prevalence of lysosomal storage disorders. JAMA 281:249–254
12. Pinto R, Caseiro C, Lemos M, Lopes L, Fontes A, Ribeiro H, Pinto E, Silva E, Rocha S, Marcao A, Ribeiro I, Lacerda L, Ribeiro G, Amaral O, Sa Miranda MC (2004) Prevalence of lysosomal storage diseases in Portugal. Eur J Hum Genet 12: 87–92
13. Poorthuis BJ, Wevers RA, Kleijer WJ, Groener JE, de Jong JG, van Weely S, Niezen-Koning KE, van Diggelen OP (1999) The frequency of lysosomal storage diseases in The Netherlands. Hum Genet 105:151–156
14. Zaremba J, Kleijer WJ, Juijmans JG, Poorthuis B, Fidzianska E, Glogowska I (1992) Chromosomes 14 and 21 as possible candidates for mapping the gene for Sanfilippo disease type IIIC. J Med Genet 29:514
15. Ausseil J, Loredo-Osti JC, Verner A, Darmond-Zwaig C, Maire I, Poorthuis B, van Diggelen OP, Hudson TJ, Fujiwara TM, Morgan K, Pshezhetsky AV (2004) Localization of a gene for mucopolysaccharidosis IIIC to chromosome region 8p11-8q11. J Med Genet 41:941–945

16. Seyrantepe V, Tihy F, Pshezhetsky AV (2006) The microcell-mediated transfer of human chromosome 8 restores the deficient *N*-acetylytransferase activity in skin fibroblasts of mucopolysaccharidosis type IIIC patients. Hum Genet 120:293–296
17. Kong X, Murphy K, Raj T, He C, White PS, Matise TC (2004) A combined linkage-physical map of the human genome. Am J Hum Genet 75:1143–1148
18. Mira MT, Alcais A, Nguyen VT, Moraes MO, Di Flumeri C, Vu HT, Mai CP, Nguyen TH, Nguyen NB, Pham XK, Sarno EN, Alter A, Montpetit A, Moraes ME, Moraes JR, Dore C, Gallant CJ, Lepage P, Verner A, Van De Vosse E, Hudson TJ, Abel L, Schurr E (2004) Susceptibility to leprosy is associated with PARK2 and PACRG. Nature 427:636–640
19. Sobel E, Lange K (1996) Descent graphs in pedigree analysis: applications to haplotyping, location scores, and marker sharing statistics. Am J Hum Genet 58:1323–1337
20. Sobel E, Papp JC, Lange K (2002) Detection and integration of genotyping errors in statistical genetics. Am J Hum Genet 70:496–508
21. Hodanova K, Majewski J, Kublova M, Vyletal P, Kalbacova M, Stiburkova B, Hulkova H, Chagnon YC, Lanouette CM, Marinaki A, Fryns JP, Venkat-Raman G, Kmoch S (2005) Mapping of a new candidate locus for uromodulin-associated kidney disease (UAKD) to chromosome 1q41. Kidney Int 68:1472–1482
22. O'Connell JR, Weeks DE (1998) PedCheck: a program for identifying genotype incompatibilities in linkage analysis. Am J Hum Genet 63:259–266
23. Voznyi YV, Karpova EA, Dudukina TV, Tsvetkova IV, Boer AM, Janse HC, van Diggelen OP (1993). A fluorimetric enzyme assay for the diagnosis of Sanfilippo disease C (MPS III C). J Inher Metab Dis 16:465–472
24. Gudbjartsson DF, Jonasson K, Frigge M, Kong A (2000) Allegro, a new computer program for multipoint linkage analysis. Nat Genet 25:12–13
25. Smyth GK (2005) Limma: linear models for microarray data. In: Gentleman R, Carey V, Dudoit S, Irizarry R, Huber W (eds) Bioinformatics and computational biology solutions using R and Bioconductor. Springer, New York, pp 397–420
26. Smyth GK (2004) Linear models and empirical Bayes methods for assessing differential expression in microarray experiments. Stat Appl Genet Mol Biol 3:article 3
27. Benjamini Y, Hochberg Y (1995) Controlling the false discovery rate: a practical and powerful approach to multiple testing. J R Stat Soc B 57:289–300
28. Kmoch S, Hartmannova H, Stiburkova B, Krijt J, Zikanova M, Sebesta I (2000) Human adenylosuccinate lyase (ADSL), cloning and characterization of full-length cDNA and its isoform, gene structure and molecular basis for ADSL deficiency in six patients. Hum Mol Genet 9:1501–1513
29. Bradford MM (1976) A rapid and sensitive method for the quantitation of microgram quantities of protein utilizing the principle of protein-dye binding. Anal Biochem 72:248–254
30. Hinrichs AS, Karolchik D, Baertsch R, Barber GP, Bejerano G, Clawson H, Diekhans M, et al (2006) The UCSC Genome Browser Database: update 2006. Nucleic Acids Res 34:D590–D598
31. Ausseil J, Landry K, Seyrantepe V, Trudel S, Mazur A, Lapointe F, Pshezhetsky AV (2006) An acetylated 120-kDa lysosomal transmembrane protein is absent from mucopolysaccharidosis IIIC fibroblasts: a candidate molecule for MPS IIIC. Mol Genet Metab 87:22–31
32. Kahsay RY, Gao G, Liao L (2005) An improved hidden Markov model for transmembrane protein detection and topology prediction and its applications to complete genomes. Bioinformatics 21:1853–1858
33. Jensen LJ, Gupta R, Blom N, Devos D, Tamames J, Kesmir C, Nielsen H, Staerfeldt HH, Rapacki K, Workman C, Andersen CA, Knudsen S, Krogh A, Valencia A, Brunak S (2002) Prediction of human protein function from post-translational modifications and localization features. J Mol Biol 319:1257–1265
34. Blom N, Sicheritz-Ponten T, Gupta R, Gammeltoft S, Brunak S (2004) Prediction of post-translational glycosylation and phosphorylation of proteins from the amino acid sequence. Proteomics 4:1633–1649
35. Bonifacino JS, Traub LM (2003) Signals for sorting of transmembrane proteins to endosomes and lysosomes. Annu Rev Biochem 72:395–447
36. Bame KJ, Rome LH (1986a) Acetyl-coenzyme A:α-glucosaminide *N*-acetyltransferase: evidence for an active site histidine residue. J Biol Chem 261:10127–10132
37. Bame KJ, Rome LH (1986b) Genetic evidence for transmembrane acetylation by lysosomes. Science 233:1087–1089
38. Meikle PJ, Whittle AM, Hopwood JJ (1995) Human acetyl-coenzyme A:α-glucosaminide *N*-acetyltransferase: kinetic characterization and mechanistic interpretation. Biochem J 308:327–333

Appended publication

BioMed Central

BMC Cell Biology

Research article

Open Access

Characterization of *gana-1*, a Caenorhabditis elegans gene encoding a single ortholog of vertebrate α-galactosidase and α-N-acetylgalactosaminidase

Jana Hujová†, Jakub Sikora†, Robert Dobrovolný†, Helena Poupětová, Jana Ledvinová, Marta Kostrouchová and Martin Hřebíček*

Address: Institute of Inherited Metabolic Disorders, Charles University, 1st Medical Faculty, Prague, Czech Republic

Email: Jana Hujová - jhujo@lf1.cuni.cz; Jakub Sikora - jakub.sikora@lf1.cuni.cz; Robert Dobrovolný - rdobr@lf1.cuni.cz; Helena Poupětová - helena.poupetova@lf1.cuni.cz; Jana Ledvinová - jledvin@beba.cesnet.cz; Marta Kostrouchová - marta.kostrouchova@lf1.cuni.cz; Martin Hřebíček* - mhreb@lf1.cuni.cz

* Corresponding author †Equal contributors

Published: 27 January 2005

BMC Cell Biology 2005, **6**:5 doi:10.1186/1471-2121-6-5

Received: 13 September 2004
Accepted: 27 January 2005

This article is available from: http://www.biomedcentral.com/1471-2121/6/5

Abstract

Background: Human α-galactosidase A (α-GAL) and α-N-acetylgalactosaminidase (α-NAGA) are presumed to share a common ancestor. Deficiencies of these enzymes cause two well-characterized human lysosomal storage disorders (LSD) – Fabry (α-GAL deficiency) and Schindler (α-NAGA deficiency) diseases. *Caenorhabditis elegans* was previously shown to be a relevant model organism for several late endosomal/lysosomal membrane proteins associated with LSDs. The aim of this study was to identify and characterize *C. elegans* orthologs to both human lysosomal luminal proteins α-GAL and α-NAGA.

Results: BlastP searches for orthologs of human α-GAL and α-NAGA revealed a single *C. elegans* gene (R07B7.11) with homology to both human genes (α-galactosidase and α-N-acetylgalactosaminidase) – *gana-1*. We cloned and sequenced the complete *gana-1* cDNA and elucidated the gene organization.

Phylogenetic analyses and homology modeling of GANA-1 based on the 3D structure of chicken α-NAGA, rice α-GAL and human α-GAL suggest a close evolutionary relationship of GANA-1 to both human α-GAL and α-NAGA.

Both α-GAL and α-NAGA enzymatic activities were detected in *C. elegans* mixed culture homogenates. However, α-GAL activity on an artificial substrate was completely inhibited by the α-NAGA inhibitor, N-acetyl-D-galactosamine.

A GANA-1::GFP fusion protein expressed from a transgene, containing the complete *gana-1* coding region and 3 kb of its hypothetical promoter, was not detectable under the standard laboratory conditions. The GFP signal was observed solely in a vesicular compartment of coelomocytes of the animals treated with Concanamycin A (CON A) or NH_4Cl, agents that increase the pH of the cellular acidic compartment.

Immunofluorescence detection of the fusion protein using polyclonal anti-GFP antibody showed a broader and coarsely granular cytoplasmic expression pattern in body wall muscle cells, intestinal cells, and a vesicular compartment of coelomocytes.

Inhibition of *gana-1* by RNA interference resulted in a decrease of both α-GAL and α-NAGA activities measured in mixed stage culture homogenates but did not cause any obvious phenotype.

Conclusions: GANA-1 is a single *C. elegans* ortholog of both human α-GAL and α-NAGA proteins. Phylogenetic, homology modeling, biochemical and GFP expression analyses support the hypothesis that GANA-1 has dual enzymatic activity and is localized in an acidic cellular compartment.

Background

Humans have two enzymes with α-galactosidase activity and an acidic pH optimum, α-N-acetylgalactosaminidase (α-NAGA) (previously called α-galactosidase B) and α-galactosidase A (α-GAL). Hereditary deficiency of each of the hydrolases causes a distinct lysosomal storage disorder in humans, Schindler and Fabry diseases, respectively [1,2].

Early studies suggested that both human enzymes were glycoforms with similar substrate specifities. Purified enzymes had similar physical properties, including subunit molecular mass (~46 kDa), homodimeric structure, and amino acid sequences. However, additional studies showed kinetic, structural, and immunologic differences proving that α-GAL and α-NAGA were products of two different genes [3,4]. The two genes differed in the number of exons (7 and 9, respectively) and also in the number, placement, and orientation of Alu repeats. Exons 2 – 7 of the α-NAGA gene showed high similarity to the first six exons of α-GAL gene. Because of the remarkable amino acid identity (49%) and similarity (63%) between the two genes and the similar intron placement, Wang [5] and co-workers suggested that a duplication event occurred during the evolution of both enzymes.

Both enzymes belong to the glycoside hydrolase family 27 clan D [6]. Glycoside hydrolase family 27 clan D orthologs have been identified in a broad spectrum of prokaryotes and eukaryotes, including plants. Members of the family have a highly similar active site and share the same reaction mechanism. The structures of chicken α-NAGA, human α-GAL and rice α-GAL have been determined by X-ray crystallography [7-9]. Chicken and human enzymes have a homodimeric quarternary structure whereas rice α-GAL acts as a monomer. The monomer units are composed of two distinct domains. Domain I contains the active site and adopts a $(\beta/\alpha)_8$ barrel structure, a domain fold observed commonly in glycosidases. Domain II has eight antiparallel β strands, packed into two β sheets in a β sandwich fold containing a Greek key motif [8].

The physiological importance of both enzymes is evidenced by the severe presentation of α-NAGA and α-GAL deficiencies in humans [1,2].

Our recent study on degradation of blood group A and B glycolipids in Fabry cells indicated a high residual activity in Fabry cells toward natural substrate glycolipid B-6-2 [10] although α-galactosidase activity was completely absent when measured in vitro by routine procedures using artificial substrates. We proposed that another enzyme, different from α-GAL, contributes in vivo to hydrolysis of α-galactosides. We suggested α-NAGA as the most likely candidate. Human α-NAGA is known to accept α-galactosides albeit with a high K_m [11,12]. Its activity must be inhibited when measuring α-GAL in tissues with high α-NAGA activity [13].

We investigated the phylogenesis of a single *C. elegans* α-GAL and α-NAGA ortholog (*gana-1*) to both human genes. We present evidence suggesting that this gene has indeed evolved from the α-GAL/α-NAGA ancestral gene before the duplication event which resulted in separate α-NAGA and α-GAL genes in higher metazoans. We further performed structural analysis of the GANA-1 3D model acquired by homology modeling. We determined the spatial and temporal expression of the gene in transgenic worms using a translational reporter and examined the effect of RNA interference (RNAi) as a first step in the possible use of *C. elegans* as a model organism for Schindler and Fabry diseases.

Results and discussion

cDNA amplification and sequencing

The complete *C. elegans* genome [14,15] contains only one open reading frame, designated *gana-1* (R07B7.11) that has sequence similar to human genes encoding α-GAL and α-NAGA. Similar results were obtained from searching the available *C. briggsae* genome sequence [15]. The *gana-1* gene consists of 5 exons and 4 introns and is annotated as an ortholog of human α-NAGA. Several EST clones for this open reading frame (ORF) have been reported and open-reading-frame sequence tag (OST) is present in the Worfdb database [16]. Available public database data are in agreement with our findings.

We verified the gene structure by sequencing the PCR products from genomic DNA and cDNA (Figure 1). The analyzed region spanned the entire coding region and the 3' and 5' untranslated regions (UTR). The 5' UTR SL1 element suggests that the gene is either the only gene transcribed from the promoter or is the first gene in an operon including *gana-1* and the two predicted downstream genes R07B7.12 and R07B7.13. Although this region has not been reported as an operon, the physical distances between this cluster of three genes are suggestive of an operon [17-19]. No alternative splicing was found using RT/PCR, a feature similar to both human and mouse orthologs. RNA editing was reported in the 3' UTR of human α-GAL, a finding that another group was unable to confirm [20]. We noted no signs of RNA editing in clones derived from the *gana-1* cDNA.

Phylogenetic studies

We aligned GANA-1 protein sequence with other melibiase family members (Figure 2) and constructed a phylogenetic tree (Figure 3). The alignment showed a striking similarity of GANA-1 to all other included sequences.

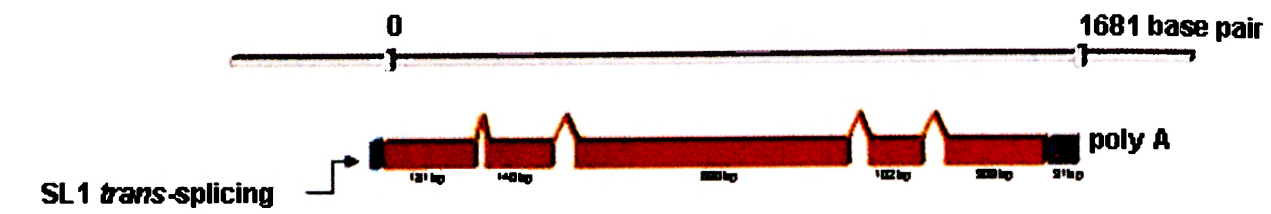

Figure 1
***gana-1* gene structure.** Schematic representation of *gana-1* gene structure. The length of genomic DNA from start to stop codons is 1681 bp. The spliced cDNA consists of 1356 bp + 91 bp of 3' UTR.

GANA-1 had the highest sequence similarity with *Anopheles gambiae* GAL (46%), the lowest similarity was observed with *Streptomyces avertimilis* GAL (22%). The results of our phylogenetic analysis are in accordance with generally accepted evolutionary concepts. The analysis identified four main clades: animal NAGAs, animal GALs, plant/lower organisms GALs and the clade containing sequences of *Drosophila melanogaster*, *Anopheles gambiae* and *Caenorhabditis elegans*. The branch including *C. elegans* is positioned between higher animal GALs and NAGAs and plant/lower organisms GALs. This position in the tree infers the evolutionary ancestrality of *gana-1* gene to both animal GALs and animal NAGAs. However, this conclusion is not in complete agreement with the presence of pairs of genes in *Drosophila* and *Anopheles* genomes annotated as α-GALs and α-NAGAs. The presence of these genes in the *Caenorhabditis/Drosophila/Anopheles* branch (and not in the GAL and NAGA clades) could be due to low divergence of these sequences from a common ancestral gene or to independent gene duplication in the *Drosophila/Anopheles* ancestral organism. It is also important to note that the phylogenetic analysis by maximum parsimony algorithm placed the *Caenorhabditis/Drosophila/Anopheles* branch into the neighborhood of the animal NAGAs branch [8]. In this case the computational algorithm probably favored the lower number of necessary sequence changes (parsimony) between GANA-1 and NAGA clade sequences.

In our opinion, the phylogenetic analysis provides evidence that the GANA-1 evolved from a common ancestor of α-GAL and α-NAGA enzymes. However, the topology of the tree could also be explained by a loss of the second gene during the evolution of *C. elegans*. In this case the enzyme found in *C. elegans* would probably be the ortholog of human α-NAGA and the lost gene would likely be the ortholog of human α-GAL. The likelihood of these two hypotheses depends on functional divergence of duplicated gene products and their dispensability for organism's metabolic pathways [21].

Homology modeling

The best Squared Root of Mean Square Deviations value (RMSD), found between GANA-1 backbone atoms and the chicken α-NAGA template [7], was 0.52 Å. The structural model of the enzyme molecule has a two-domain structure (Figure 4A). Domain I, which contains the predicted active site, adopts a $(\beta/\alpha)_8$ barrel structure which represents a common motif in many glycoside hydrolases. Less conserved is domain II that has a β domain with β sandwich structure containing a Greek key motif. The active site pocket of GANA-1 is formed by the same twelve amino acids (W31, D76, D77, Y118, C126, K152, D154, C156, S186, A189, Y190 and R211) (Figure 4B) as in chicken α-NAGA. This finding infers their identical function in catalytic reactions as described for chicken α-NAGA [7]. D134 carboxyl starts the initial nucleophilic attack and D215 carboxylic oxygen serves as a subsequent donor and acceptor of the proton during the reaction cycle.

Residues forming the "N-acetyl recognition loop" in the chicken α-NAGA [8] (S172, A175, Y176) have the closest contact with the N-acetyl moiety of the ligand. These residues are completely conserved between human and chicken NAGAs, but in human α-GAL serin 172 is replaced by glutamine and alanine 175 is replaced by leucine. The replacements with bulkier residues apparently discriminate between α-GAL and α-NAGA substrates. While NAGAs can accommodate α-galactose and can have some α-GAL activity, GALs do not have α-NAGA activity

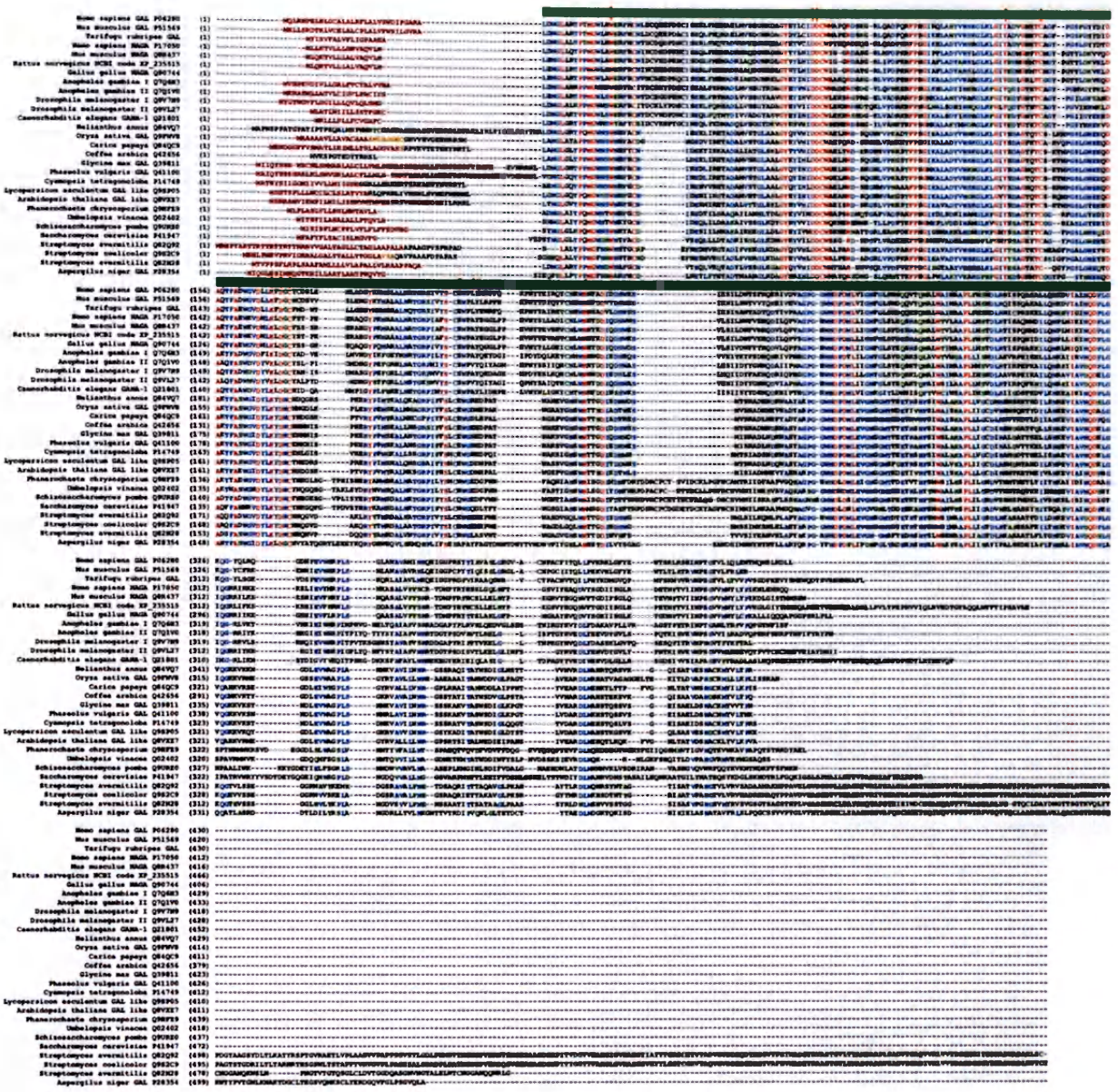

Figure 2
Multiple alignment. Multiple alignment of 29 sequences homologous with GANA-1. These sequences represent animal, plant and protozoan kingdoms. The SwissProt/TrEMBL codes are part of the sequence names. Predicted signal peptides are shown in brown letters. In cases where two signal sequence prediction algorithms gave different results the difference is marked by amber color. The residues forming active site pocket of GANA-1 are indicated by arrowheads above the alignment. The catalytic domain I is indicated by green band above the alignment.

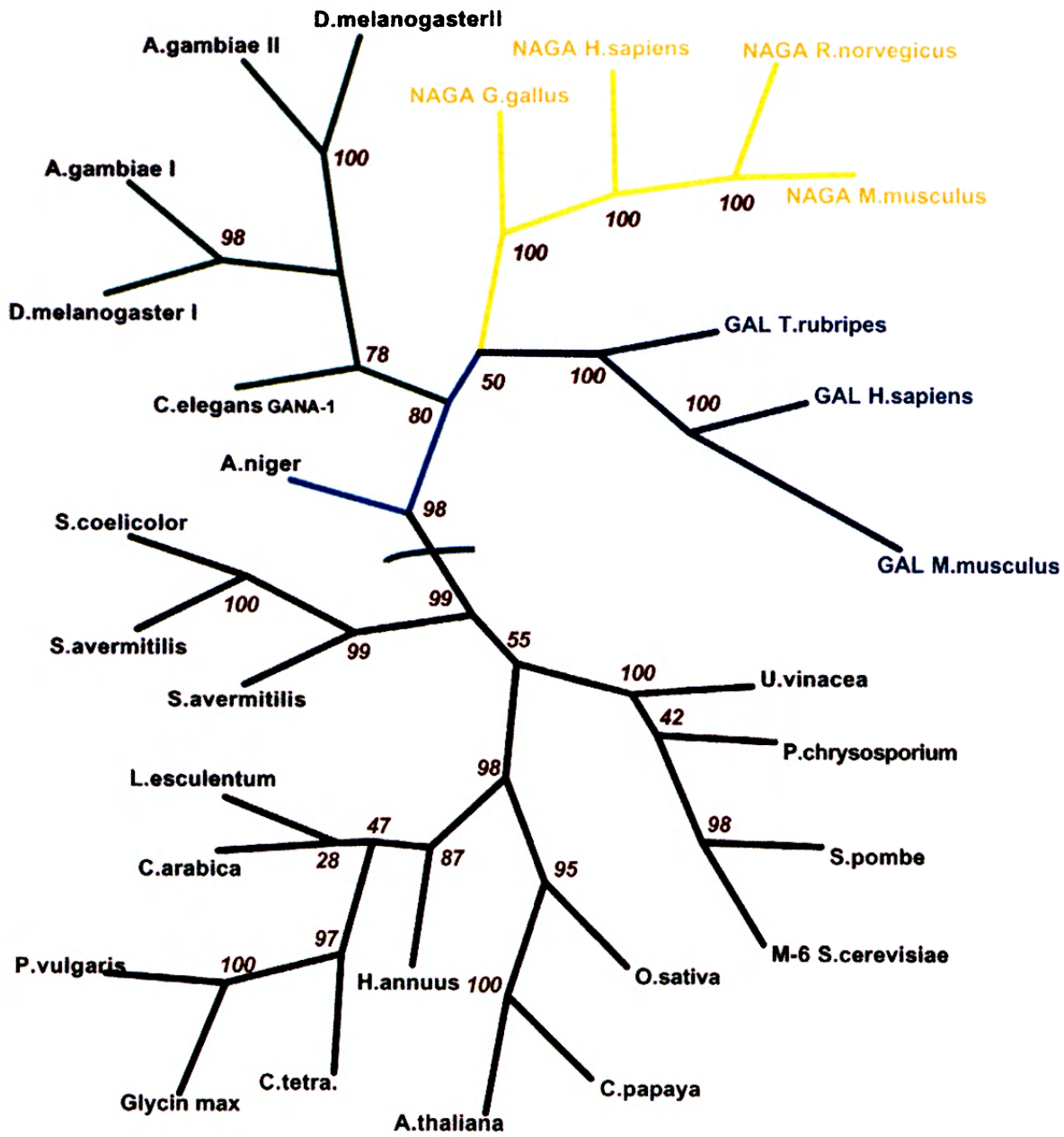

Figure 3
Cladogram of GANA-1 orthologs. Cladogram of GANA-1 orthologs. The numbers at the branch nodes represent bootstrap values.

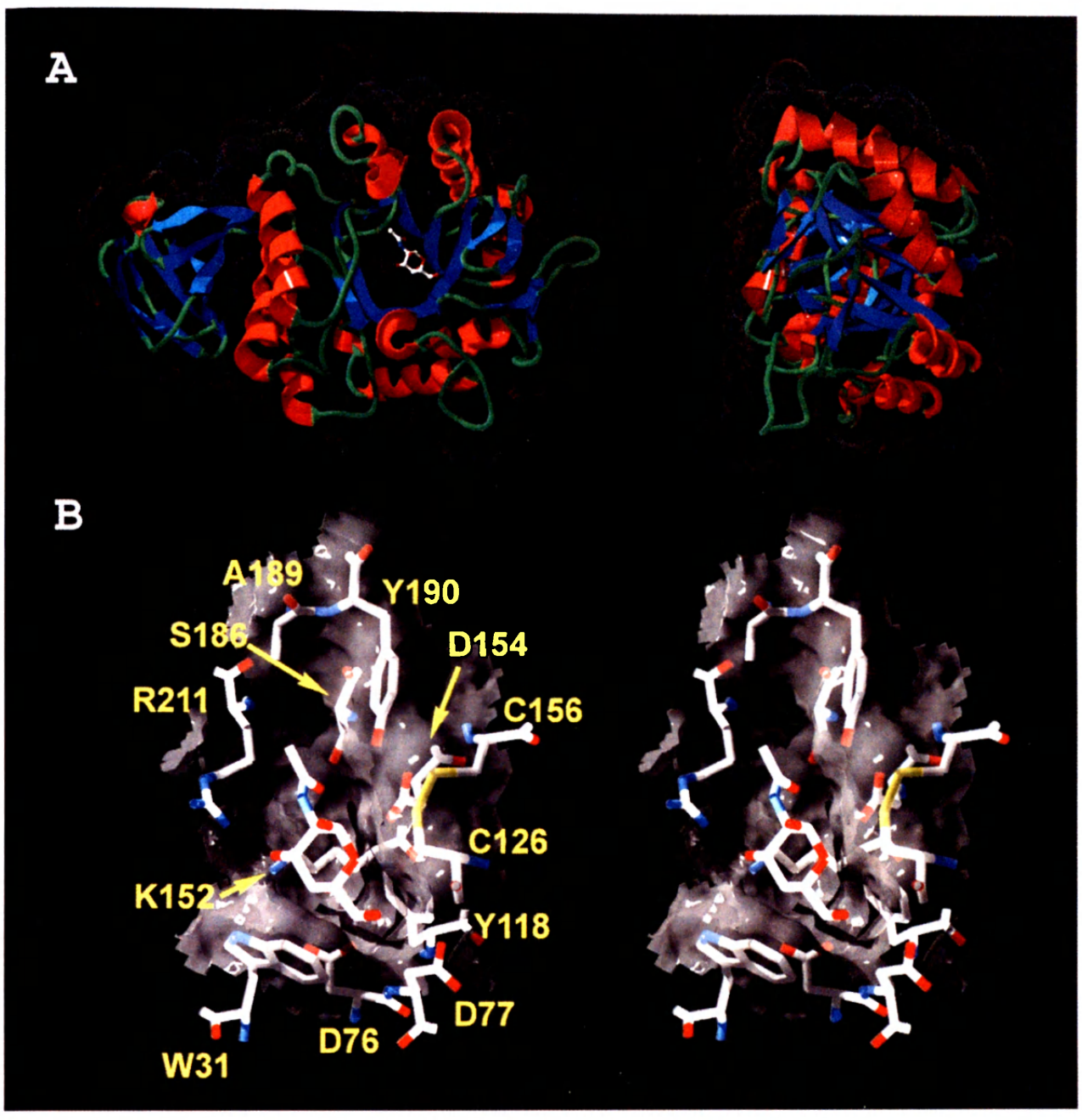

Figure 4

GANA-1 protein model. A) Ribbon representation of GANA-1 monomer model. A two-domain structure is apparent in the left picture. The N-acetyl-D-galactosamine (inhibitor) is placed into the active site. Dots represent VdW radii of surface atoms. B) Stereo picture of the active site pocket with N-acetyl-D-galactosamine (inhibitor) and amino acid labels. The viewing angles for stereo representation of the protein structure are ±2 degrees from the central axis.

and are not inhibited by N-acetylgalactosamine. The corresponding residues of GANA-1 in the NAGA recognition loop are S186 and A189 and are characteristic for NAGAs.

According to Garman [8] the key residue in the dimer interface in human α-GAL is F273. Residues corresponding to this position in other orthologs can serve as predictive markers of the protein quartenary structure. Phenylalanine or tyrosine is present in enzymes that act as homodimers while glycin indicates a monomeric structure [8]. The equivalent residue to human α-GAL F273 in GANA-1 is lysine at position 257 which is suggestive of homodimeric structure due to its sterical properties. The homology modeling showed that a groove opposing K257 is formed by residues T260, L261, D262, M263, I389, V390 and V391 of the other monomer unit of GANA-1. In the case of chicken α-NAGA these residues are equivalent to S246, Y247, E248, Q249, N375, P376 and S377 (for details see Additional file 1).

Biochemical studies

Standard bacteria/nematode separation protocol previously used by other authors [22,23] while evaluating lysosomal enzyme activites is based on sucrose flotation approach. We avoided standard sucrose flotation of worms because we could not exclude unpredictable artifacts caused by this compound, which is known to induce artificial lysosomal storage in eukaryotic cells and to alter lysosomal gene expression at concentrations significantly lower [24] than those used in flotation protocols.

We found both α-GAL and α-NAGA enzymatic activities in the homogenates from *C. elegans* N2 strain using 4-methylumbelliferyl (MU) substrates. The α-NAGA activity was dominant over the α-GAL activity. The activity of α-NAGA measured at 37°C was 430 $nmol.mg^{-1}.h^{-1}$ with MU-α-N-acetylgalactosaminide compared to the activity of α-GAL with MU-α-galactopyranoside of 43 $nmol.mg^{-1}.h^{-1}$ (about 10% of that of α-NAGA).

In the assay of α-GAL, the degradation of the MU-α-galactopyranoside was inhibited up to 95% in the presence of N-acetyl-D-galactosamine (D-GalNAc), whereas in the presence of D-galactose (D-Gal) the degradation of the same substrate was inhibited up to 75%. In the assay of α-NAGA, the degradation of the MU-α-N-acetylgalactosaminide was inhibited up to 97% by D-GalNAc and up to 90% by D-Gal. No inhibition of α-NAGA and α-GAL activity by D-glucose was observed.

According to published observations in human enzymes, D-GalNAc has no inhibitory effect on α-GAL activity. On the other hand, human α-NAGA activity is inhibited by both, D-GalNAc and D-Gal [25]. The model of GANA-1 predicts only one active site per monomer of the enzyme. If the enzyme had activity toward both substrates, MU-α-D-galactopyranoside and MU-α-N-acetylgalactosaminide, it is to be expected that D-GalNAc and D-Gal would inhibit both activities. The strong inhibitory effect of D-GalNAc on the α-GAL activity, which is not present in human α-GAL, supports the hypothesis that *C. elegans* has only one enzyme with both α-GAL and α-NAGA activities. Nevertheless, these experiments were not conducted with the pure enzyme and thus do not provide absolute proof of this hypothesis.

RNA interference

RNA interference assays directed against the whole coding region of *gana-1*, employing combination of microinjection and feeding approaches, did not reveal any abnormal morphological phenotypes. Nevertheless, measurement of α-GAL and α-NAGA activities in four different experiments showed a simultaneous decrease of both enzymatic activities in RNAi-treated worms (Table 1) as compared with control animals. In all RNAi experiments, both α-GAL and α-NAGA activities decreased proportionally, usually by tens of percent of activity of appropriate controls. The activity of the control enzyme (β-hexosaminidase) did not differ between the RNAi-treated nematodes and controls (data not shown). This finding supports the specificity of *gana-1* RNAi. The differences between individual experiments are not surprising due to the well-known variability in the efficiency of RNAi [26]. The results of RNAi experiments further support the hypothesis that GANA-1 has both enzymatic activities.

Both enzymatic activities were lower in RNAi-treated and control worms cultured on the bacterial strain HT115 [26] compared to a N2 strain cultured on the OP50 strain.

RNAi previously provided sufficient level of inhibition of structural lysosomal proteins for development of abnormal phenotypes in the worm [27,28]; however, it is apparently not efficient enough for lysosomal catalytic proteins.

Expression of gana-1

To study the expression of *gana-1* in *C. elegans*, we created transgenic worms with a reporter gene containing the entire coding region of *gana-1* C-terminally tagged with green fluorescent protein (GFP) under the control of a 3 kb region of the *gana-1* hypothetical promoter. The presence of the *gana-1::GFP* transgene in the worms was confirmed on the level of genomic DNA, cDNA and protein. However, no GFP signal was observed by fluorescence microscopy under the standard laboratory conditions. As Western blotting showed the presence of fusion protein of the expected size (data not shown), we assumed that the absence of the GFP signal was caused by a pH-dependent

Table 1: α-GAL and α-NAGA activities after *gana-1* RNAi. The table shows a proportional parallel decrease of both enzymatic activities (α-GAL and α-NAGA) after *gana-1* RNAi compared to controls.

experiment	sample	α-GAL	α-GAL (% of control)	α-NAGA	α-NAGA (% of control)	α-NAGA/α-GAL (% of control)
		nmol $mg^{-1}h^{-1}$		nmol $mg^{-1}h^{-1}$		
1	control	1.78	100	53.13	100	
	gana-1 RNAi	1.19	67	26.63	50	0.75
2	control	13.26	100	221.68	100	
	gana-1 RNAi	11.1	84	195.13	88	1.05
3	control	3.43	100	61.68	100	
	gana-1 RNAi	1.02	30	11.75	19	0.63
4	control	9.6	100	212.1	100	
	gana-1 RNAi	2.9	30	50.69	24	0.80

quenching of GFP fluorescence, which has neutral to alkaline optimum (pH 5.5–12) [29].

To study the tissue and intracellular distribution of the fusion protein, we resorted to immunofluorescence detection of the transgene product. Immunofluorescence detection of GFP fusion protein showed a specific and coarsely granular cytoplasmic pattern of fusion protein expression. This transgene product was limited to body wall muscle cells (30% of population) (Figure 5A, Additional file 2) or found in a broader tissue distribution that included body wall muscle cells, intestinal cells and coelomocytes (3–5% of population) (Figure 5B, Additional file 3).

This latter staining pattern is consistent with the GFP detection in NH_4Cl and concanamycin A (CON A) experiments (Figure 6) discussed below. The expression of the transgene was observed in about 30% of the population which corresponded to usual expression efficiency of extrachromosomal array transgenes [30,31]. The immunofluorescence staining protocol resulted in a significant decrease of inherent intestinal granular autofluorescence previously assigned to secondary lysosomes [32]. The decrease of autofluorescence intensity together with its poorly defined emission spectra hampered co-localization study.

To confirm that the absence of the GFP signal was due to the quenching of fluorescence by low pH in the acidic cellular compartment, we used two agents specifically alkalizing acidic cellular compartment [33,34] to enhance the GFP emission. Soaking of *gana-1::GFP* transgenic animals in NH_4Cl or CON A resulted in a distinct GFP signal in a vesicular compartment of endocytically active coelomocytes in a small proportion of worms (3–5% of population). The GFP signal intensity was dependent on the time of incubation and the concentration of the alkalizing agent used. The first visible GFP signal was observed after 8 hour incubation in 100 mM NH_4Cl and within 2 hours of incubation in 50 nM CON A. Lower concentrations of both NH_4Cl and CON A did not result in visible GFP signal even after prolonged incubation of up to 24 hours. The reappearance of the GFP signal after treatment of the worms with compounds increasing the acidic compartment pH indirectly confirms lysosomal localization of the fusion protein. The GFP signal in coelomocytes had the same coarsely granular pattern as that observed after immunostaining.

Limited access of alkalizing agents to the tissues can explain the differences between the results of immunofluorescence and alkalization studies.

Conclusions

Our findings showed that *gana-1* is the only ortholog of human α-NAGA and α-GAL in *C. elegans*. Based on phylogenetic and homology modeling analyses we speculate that GANA-1 most probably developed from a hypothetical ancestral gene before the duplication event which gave rise to separate α-NAGA and α-GAL genes.

We also speculate that *gana-1* gene product has both α-NAGA and α-GAL activities as detected in *C. elegans* homogenates. Importantly, both activities in the worm were inhibited by D-galactose and N-acetyl-D-galactosamine, which is a specific inhibitor of human α-NAGA and does not inhibit α-GAL.

The GANA-1::GFP fusion protein had a pattern of distribution that is compatible with lysosomal subcellular localization. The lysosomal localization of the fusion protein was also supported by pH sensitive fluorescence of GFP that was detectable only after alkalization of the acidic cellular compartment.

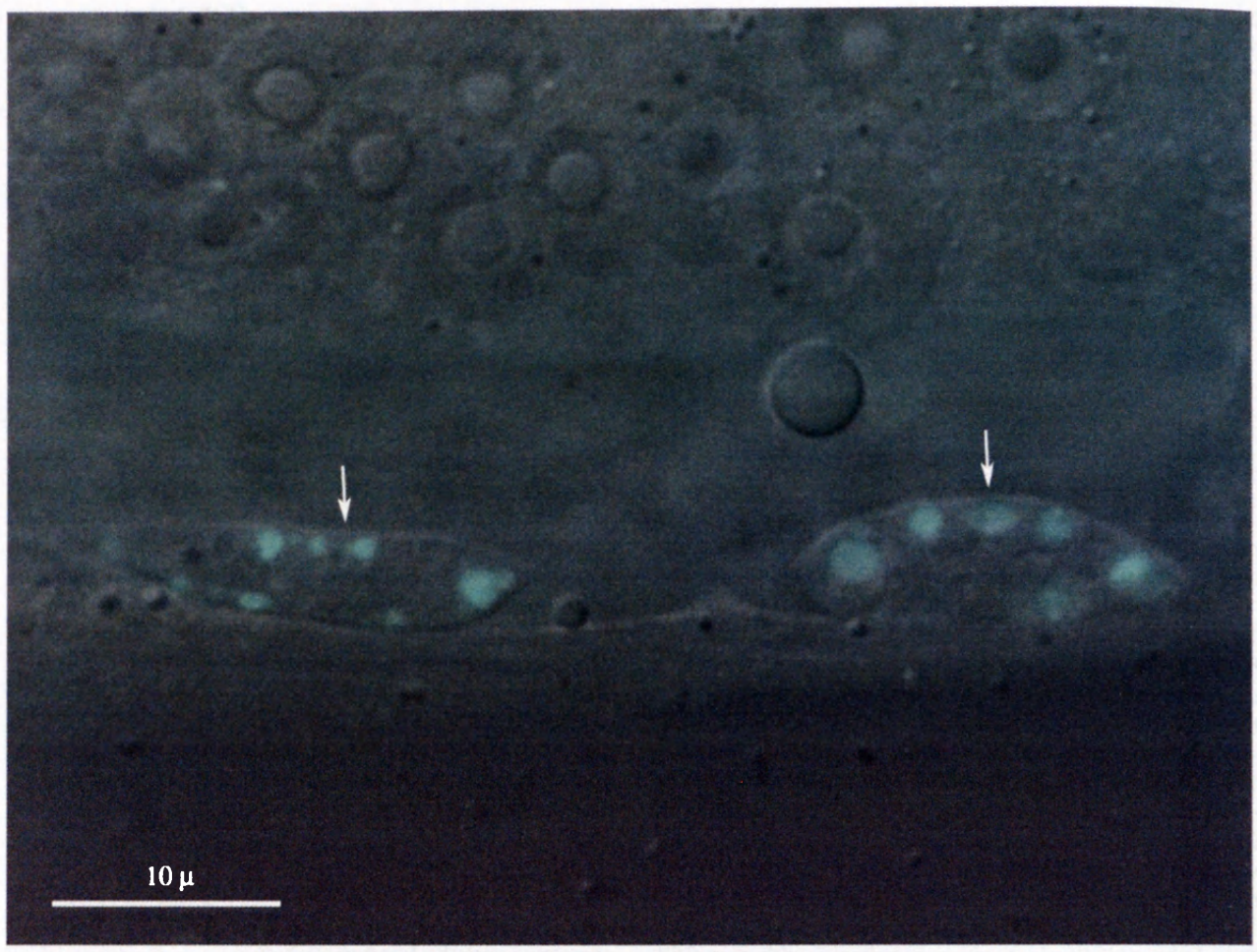

Figure 6
Alkalization of transgenic worms using CON A. Two coelomocytes showing a GFP signal in a membrane bound vesicular compartment (arrowheads) after 24 hour incubation in 50 nM CON A. DIC/fluorescence merged image.

Not suprisingly, RNAi of *gana-1* yielded no abnormal morphological phenotypes, most likely because it did not provide sufficient knockdown of enzymatic activities, necessary for development of lysosomal storage as observed in human pathology states. Nevertheless, *gana-1* RNAi resulted in a partial decrease of both enzymatic activities supporting the notion that this gene encodes both of them.

It is possible that a deletion allele of *gana-1* may provide more insight into the function of *gana-1* and efforts are underway to isolate such alleles. Deletion alleles of lysosomal hydrolases may serve as valuable models of human lysosomal storage disorders.

Methods

C. elegans methods, strains and nomeclature

The wild type Bristol N2 strain was used for all experiments and was handled under standard laboratory conditions as described previously [35]. Standard methods were used for DNA microinjection [36] and dsRNA synthesis and microinjection [37]. Nomenclature is in agreement with available Genetic Nomenclature for *Caenorhabditis elegans* [15] and has been approved prior to manuscript submission.

BLAST search

Wormbase (2002–2004 versions and freeze versions [15,38,39]) databases were repeatedly searched for

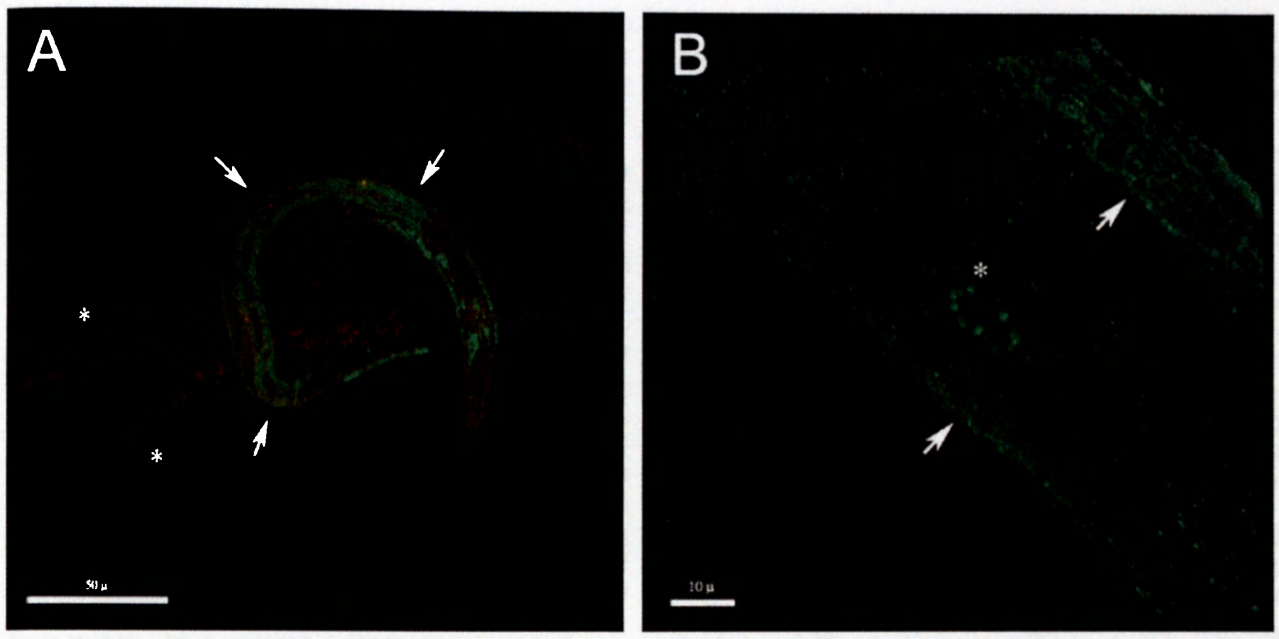

Figure 5
Immunofluorescence detection of GANA-1::GFP. A) A coarsely granular cytoplasmic distribution of immunopositivity (green) in body-wall muscle cells (arrowheads). Two non-transgenic worms are shown in the background (asterisks) for comparison. Nuclei are counterstained in red. B) Detailed view of two body wall muscle cells with coarsely granular cytoplasmic distribution of immunopositivity (arrowheads) and a coelomocyte (asterisk), both pictures were acquired by 3D rendering of initial confocal Z-stacks. Note: compare with figure 6.

human α-GAL and α-NAGA orthologs using the BLASTP [40] program set at default values. Amino acid sequences of human lysosomal α-GAL and α-NAGA (acc. no. NP_000160 and acc. no. NP_000253 [41]) were used as query sequences.

cDNA amplification and sequencing

Total RNA was isolated from mixed stages of N2 cultures [42] and reverse transcribed with an oligodT-T7 (5'-AATACGACTCACTATAG) primer and Superscript reverse transcriptase (Invitrogen). The entire coding region of R07B7.11 was PCR amplified in two overlapping PCR products, with intragenic primers designed according to available Wormbase [15] and Worfdb [16] data. SL1 primer (5'GGTTTAATTACCCAAGTTTGAG) and SL2 primer (5'GGTTTTAACCCAGTTACTCAAG) [17] together with gene specific primer (5'ATCCTGATTAATTTTAATTGC) were used to amplify 942 bp of the 5' part of the cDNA and to evaluate the mode of *trans* splicing; the 1142 bp fragment of the 3' end of cDNA was amplified with T7 primer and a gene specific primer (5'CTTAAGTTTGGAATTTATGAA). The dominant PCR products were cloned with TOPO TA cloning kit (Invitrogen) into the pCR 2.1 vector. Positive clones were sequenced using the Li-Cor automated fluorescent sequencer and sequences were aligned with R07B7 reference cosmid sequence in the AlignIR software (Li-Cor) to evaluate splicing boundaries and overall gene organization.

Multiple alignment and phylogenetic analyses

Confirmed or predicted amino acid sequences of melibiase family members [43] representing plant, unicellular, and animal kingdoms were aligned using ClustalW algorithm [44] and Blosum62 matrix. The SwissProt/TrEMBL [45] accesion code and source organism of the sequences are depicted in Figure 2. The sequence alignment was used for phylogenetic analysis with the software package PHYLIP [46]. The phylogenetic tree is based on 100 bootstraped input alignments and was constructed by maximum likelihood method with Jones-Taylor-Thornton matrix model [47]. Sequence identities between species were calculated without signal sequence in EMBOSS by Needleman-Wunsch global alignment algorithm with Blosum62 matrix, gap penalty - 10 and gap extension

penalty - 0.5 [8,48,49]. Signal peptides were predicted at the SignalP server [50] both by algorithms using neural networks and Hidden Markov Models. The results were compared to known signal sequences. The differences between signal peptides predicted by the algorithms are depicted in Figure 2.

The 3D model of GANA-1 is based on the X-ray structure of chicken α-NAGA, rice α-GAL and human α-GAL (PDB codes 1ktcA, 1uas and 1r47, respectively) [7-9,51]. The model was created using the automated homology modeling server SwissModel with structure refinement and model evaluation in the DeepView program [52]. The print quality figures (Figure 4) and animations (Additional file 1) were ray traced using PovRay software package [53].

Transgenic GFP expression

The entire coding region of the *gana-1* gene, including 3 kb of its 5'upstream sequence, was amplified from N2 genomic DNA through a nested PCR reaction using DyNAzyme EXT™ PCR system (Finnzymes) and two pairs of primers: the external pair (5'GTGAGAGTGGGGAGATAGAA and 5'TCAATTTGCTTGAGGTACATA) and the internal primers, with overhangs containing SphI and SalI restriction sites respectively (5'ACATGCATGCAACTTTCACAGGAACACAAC and 5'CGACGTCGACAATTGAACTCTATTGGTTCTCAA). The amplified DNA fragment (4709 bp) was cloned using TOPO-XL cloning kit (Invitrogen) into the pCR-XL-TOPO vector. The SphI and SalI *gana-1* restriction fragment was recloned into the GFP reporter vector pPD95.67 (supplied by A. Fire, Stanford University). The in-frame nature of the insert was confirmed by sequencing. The green fluorescent protein (GFP) fusion construct pJH3 (50 ng/μl) and pRF4 plasmid (50 ng/μl) used as the dominant marker were co-injected into the gonads of young adult N2 worms. Transgenic animals were screened for GFP signal. Nikon Eclipse E800 with C1 confocal module and 488 nm and 543 nm lasers and differential interference contrast (DIC) optics was used for specimen examination. EZ-C1 software (Nikon) was used for picture analysis and 3D rendering (Additional Files 1, 3).

Alkalization of acidic cell compartment

Mixed stage pJH3 and N2 (control) cultures were harvested from NGM OP50 plates and washed with water. Worms were pelleted by centrifugation (max. 1000 RPM, 2 min.) between the washes. Worms were treated with either one of two agents (NH_4Cl, concanamycin A - CON A) [33,34], that are known to specifically increase pH in the cellular acidic compartment. For the NH_4Cl method, animals were suspended in 0, 10, 25, 50, 75 and 100 mM aqueous solutions of NH_4Cl. Small aliquots of worms were examined after 30 min, 2, 4, 6, 8 and 24 hours. For CON A, animals were suspended in 0, 10, 20, 50, 100, 150, 200 nM solutions of CON A in aqueous media. Small aliquots of worms were examined after 1, 3, 6 and 24 hours.

Microscopical examination was performed as described above.

Immunofluorescence

The fixation and immunofluorescence staining procedures were based on the approaches of Nonet et al. [54]. Mixed stage N2 cultures were harvested from NGM OP50 plates and washed thoroughly in M9 buffer to remove intestinal bacteria. Worms were pelleted by centrifugation (1000 RPM, 2 min.) between the washes. Worms were fixed overnight in 4% paraformaldehyde in 100 mM sodium/potassium phosphate buffer. Afterwards the pellets were washed three times in 1 × PBS, and incubated in 1% Triton X-100, 100 mM Tris (pH 7.0), 1% β-Mercaptoethanol overnight at 37°C to reduce the cuticle. After 5 washes in 1 × PBS, the worms were incubated for 5 hours in 900 U/ml collagenase type IV (Sigma) diluted in Krebs-Ringer solution (119 mM NaCl, 25 mM $NaHCO_3$, 11.1 mM glucose, 1.6 mM $CaCl_2 \cdot H_2O$, 4.7 mM KCl, 1.2 mM KH_2PO_4, 1.2 mM $MgSO_4 \cdot 7H_2O$, pH 7.4). The reduction/digestion step was performed twice. Pellets were washed 3 times with 1 × PBS and stored for further processing in AbA buffer (1 × PBS, 0.1% Triton X-100, 1% BSA, 0.05% NaN_3). AbA buffer was used for antibody dilution. Primary antibody (polyclonal rabbit anti-GFP IgG (Abcam)) was diluted 1:500. Secondary antibody (goat anti-rabbit IgG Alexa Fluor 488 labeled (Molecular Probes)) was diluted 1:1000. Both incubations were performed overnight at room temperature, with AbB buffer (1 × PBS, 0.1% Triton X-100, 0.1% BSA, 0.05% NaN_3) washes in between.

Nuclei were counterstained with SYTOX orange (Molecular Probes) and the microscopic evaluation was performed as described above.

Western Blotting

Mixed stage pJH3 and N2 cultures were harvested from NGM OP50 plates. Worms were homogenized by sonication and the concentration of protein was measured by the Hartree method [55]. The proteins (equivalent of 25–50 μg of protein per lane) were separated by SDS-PAGE gradient gel (4% to 20% polyacrylamide) and transferred onto nitrocellulose membrane by semi-dry blotting. The membrane was treated according to a common Western blotting protocol with chemiluminiscence detection (SuperSignal, West Pico) [56]. Rabbit polyclonal anti-GFP IgG (Abcam, dilution 1:5000) was used as the primary antibody, the secondary antibody was goat anti-rabbit IgG/Px (Pierce, diluted 1:20 000).

RNA mediated Interference

The PCR product containing the entire *gana-1* cDNA was cloned into pCRII-TOPO vector (Invitrogen) and L4440 double promoter vector for microinjection and feeding RNAi respectively. In-vitro transcription employing T7 and SP6 RNA polymerases (Promega) was used to generate antisense single stranded RNA molecules, which were annealed to generate double stranded RNA (dsRNA). dsRNA was microinjected into N2 worms which were fed on HT115 [26]*E. coli* strain carrying L4440 plasmid with *gana-1* insert. The F_1 and early F_2 progeny was screened for morphological phenotypes. N2 worms microinjected with water and fed on HT115 *E. coli* transformed with L4440 vector without insert were used as a control. 5–7 worms were microinjected both with dsRNA and water in each of 4 separate experiments, single worm progeny reaching 110–150 individuals.

Determination of α-GAL and α-NAGA and β-hexosaminidase activities

Prior to all activity measurements worms were washed from culture plates and repeatedly (6 times) washed and centrifuged in M9 buffer and finally pelleted by centrifugation. 4-methylumbelliferyl (MU)-α-D-N-acetylgalactosaminide (1 mM), 4-MU-α-D-galactopyranoside and 4-MU-β-D-glucopyranoside in theMcIlvaine buffer (0.1 M citrate/0.2 M phosphate buffer at acidic pH) were used as enzyme substrates. Reaction mixtures (sample and enzyme substrate) were incubated at 37°C and reactions were stopped by 600 μl of 0.2 M glycine/ NaOH buffer (pH 10.6) [13,57]. Fluorescence signal of the 4-methylumbelliferone was measured on the luminiscence spectrofotometer LS 50B (Perkin Elmer) (emission 365 nm and excitation 448 nm). Inhibitors (N-acetyl-D-galactosamine, D-galactose and D-glucose) were used in 0.1 M final concentration. All measurements were performed in doublets.

Authors' contributions

JH carried out molecular, RNAi, expression and biochemical analyses and wrote the first draft of the manuscript. JS participated in the design of all experiments and participated on the bioinformatic, molecular, RNAi and expression analyses and wrote the final version of the manuscript. RD performed phylogenetic analyses including homology modeling. HP participated on the biochemical analyses. MK and JL participated on the coordination of the project. MH conceived the project and provided fundraising. All authors read and approved the final version of the manuscript.

Additional material

Additional File 1

Structure of GANA-1 dimer. The color of the backbone represents differences of amino acids between GANA-1 and chicken NAGA. Blue color represents identical residues and orange stands for non-conservative changes. The colors from cyan to green represent different degrees of conservation. The surface of one monomer unit at the interface area is rendered with colors representing electrostatic potential. N-acetyl-D-galactosamine (inhibitor) is placed in the active site pocket of both monomer units (D-GalNAc arrowhead). K257 arrowhead depicts predicted dimerisation residue.

Click here for file

[http://www.biomedcentral.com/content/supplementary/1471-2121-6-5-S1.mpg]

Additional File 2

Immunofluorescence detection of GANA-1::GFP in muscle cells. 3D volume rendered and animated image corresponding to Figure 5A

Click here for file

[http://www.biomedcentral.com/content/supplementary/1471-2121-6-5-S2.mpg]

Additional File 3

Immunofluorescence detection of GANA-1::GFP in muscle cells and coelomocytes. 3D volume rendered and animated image corresponding to Figure 5B

Click here for file

[http://www.biomedcentral.com/content/supplementary/1471-2121-6-5-S3.mpg]

Acknowledgements

This work was supported by a grant 303/02/1324 from the Czech Science Foundation and partially also from grant VZ111100003 from Ministry of Education of the Czech Republic (institutional support).

We would like to thank Michael Krause, Ph.D. (NIDDK) and Zdeněk Kostrouch, Ph.D. (Institute of Inherited Metabolic Disorders) for critical reading of the manuscript and Eva Brožová, Kateřina Šimečková, Hana Prouzová and Lenka Brtvová (Institute of Inherited Metabolic Disorders) for technical advice and assistance.

References

1. Desnick RJ, Schindler D: **α-N-Acetylgalactosaminidase Deficiency: Schindler Disease.** In *The Metabolic & Molecular Bases of Inherited Disease Volume 3*. 8th edition. Edited by: Scriver CR, Beaudet AL, Sly WS and Valle D. New York, McGraw-Hill Companies, Inc.; 2001:3483-3506.
2. Desnick RJ, Ioannou YA, Eng CM: **α-Galactosidase A Deficiency: Fabry Disease.** In *The Metabolic & Molecular Bases of Inherited Disease Volume 3*. 8th edition. Edited by: Scriver CR, Beaudet AL, Sly WS and Valle D. New York, McGraw-Hill Companies, Inc.; 2001:3733-3774.
3. Dean KJ, Sung SS, Sweeley CC: **The identification of alpha-galactosidase B from human liver as an alpha-N-acetylgalactosaminidase.** *Biochem Biophys Res Commun* 1977, **77:**1411-1417.
4. Schram AW, Hamers MN, Brouwer-Kelder B, Donker-Koopman WE, Tager JM: **Enzymological properties and immunological characterization of alpha-galactosidase isoenzymes from normal and Fabry human liver.** *Biochim Biophys Acta* 1977, **482:**125-137.
5. Wang AM, Desnick RJ: **Structural organization and complete sequence of the human alpha-N-acetylgalactosaminidase**

gene: homology with the alpha-galactosidase A gene provides evidence for evolution from a common ancestral gene. *Genomics* 1991, **10**:133-142.
6. Henrissat B, Davies G: **Structural and sequence-based classification of glycoside hydrolases.** *Curr Opin Struct Biol* 1997, **7**:637-644.
7. Garman SC, Hannick L, Zhu A, Garboczi DN: **The 1.9 A structure of alpha-N-acetylgalactosaminidase: molecular basis of glycosidase deficiency diseases.** *Structure (Camb)* 2002, **10**:425-434.
8. Garman SC, Garboczi DN: **The molecular defect leading to Fabry disease: structure of human alpha-galactosidase.** *J Mol Biol* 2004, **337**:319-335.
9. Fujimoto Z, Kaneko S, Momma M, Kobayashi H, Mizuno H: **Crystal structure of rice alpha-galactosidase complexed with D-galactose.** *J Biol Chem* 2003, **278**:20313-20318.
10. Asfaw B, Ledvinova J, Dobrovolny R, Bakker HD, Desnick RJ, van Diggelen OP, de Jong JG, Kanzaki T, Chabas A, Maire I, Conzelmann E, Schindler D: **Defects in degradation of blood group A and B glycosphingolipids in Schindler and Fabry diseases.** *J Lipid Res* 2002, **43**:1096-1104.
11. Dean KJ, Sweeley CC: **Studies on human liver alpha-galactosidases. II. Purification and enzymatic properties of alpha-galactosidase B (alpha-N-acetylgalactosaminidase).** *J Biol Chem* 1979, **254**:10001-10005.
12. Schram AW, Hamers MN, Tager JM: **The identity of alpha-galactosidase B from liver.** *Adv Exp Med Biol* 1978, **101**:525-529.
13. Mayes JS, Scheerer JB, Sifers RN, Donaldson ML: **Differential assay for lysosomal alpha-galactosidases in human tissues and its application to Fabry's disease.** *Clin Chim Acta* 1981, **112**:247-251.
14. **Genome sequence of the nematode C. elegans: a platform for investigating biology. The C. elegans Sequencing Consortium.** *Science* 1998, **282**:2012-2018.
15. **Wormbase** [http://www.wormbase.org/]
16. **The C. elegans ORFeome cloning project** [http://worfdb.dfci.harvard.edu/]
17. Krause M: **Transcription and Translation.** In *Caenorhabditis elegans: Modern Biological Analysis of an Organism Volume 48*. 1st edition. Edited by: Epstein HF and Shakes DC. San Diego, Academic Press, Inc.; 1995:483-512.
18. Nimmo R, Woollard A: **Widespread organisation of C. elegans genes into operons: fact or function?** *Bioessays* 2002, **24**:983-987.
19. Blumenthal T, Gleason KS: **Caenorhabditis elegans operons: form and function.** *Nat Rev Genet* 2003, **4**:112-120.
20. Blom D, Speijer D, Linthorst GE, Donker-Koopman WG, Strijland A, Aerts JM: **Recombinant enzyme therapy for Fabry disease: absence of editing of human alpha-galactosidase A mRNA.** *Am J Hum Genet* 2003, **72**:23-31.
21. Nadeau JH, Sankoff D: **Comparable rates of gene loss and functional divergence after genome duplications early in vertebrate evolution.** *Genetics* 1997, **147**:1259-1266.
22. Sarkis GJ, Kurpiewski MR, Ashcom JD, Jen-Jacobson L, Jacobson LA: **Proteases of the nematode Caenorhabditis elegans.** *Arch Biochem Biophys* 1988, **261**:80-90.
23. Sebastiano M, D'Alessio M, Bazzicalupo P: **Beta-glucuronidase mutants of the nematode Caenorhabditis elegans.** *Genetics* 1986, **112**:459-468.
24. Karageorgos LE, Isaac EL, Brooks DA, Ravenscroft EM, Davey R, Hopwood JJ, Meikle PJ: **Lysosomal biogenesis in lysosomal storage disorders.** *Exp Cell Res* 1997, **234**:85-97.
25. Conzelmann E, Sandhoff K: **Glycolipid and glycoprotein degradation.** *Adv Enzymol Relat Areas Mol Biol* 1987, **60**:89-216.
26. Kamath RS, Martinez-Campos M, Zipperlen P, Fraser AG, Ahringer J: **Effectiveness of specific RNA-mediated interference through ingested double-stranded RNA in Caenorhabditis elegans.** *Genome Biol* 2000, **2**:.
27. Kostich M, Fire A, Fambrough DM: **Identification and molecular-genetic characterization of a LAMP/CD68-like protein from Caenorhabditis elegans.** *J Cell Sci* 2000, **113**:2595-2606.
28. Fares H, Greenwald I: **Regulation of endocytosis by CUP-5, the Caenorhabditis elegans mucolipin-1 homolog.** *Nat Genet* 2001, **28**:64-68.
29. Kneen M, Farinas J, Li Y, Verkman AS: **Green fluorescent protein as a noninvasive intracellular pH indicator.** *Biophys J* 1998, **74**:1591-1599.
30. Mello C, Fire A: **DNA transformation.** In *Caenorhabditis elegans: Modern Biological Analysis of an Organism Volume 48*. 1st edition. Edited by: Epstein HF and Shakes DC. San Diego, Academic Press; 1995:451-481.
31. Stinchcomb DT, Shaw JE, Carr SH, Hirsh D: **Extrachromosomal DNA transformation of Caenorhabditis elegans.** *Mol Cell Biol* 1985, **5**:3484-3496.
32. Clokey GV, Jacobson LA: **The autofluorescent "lipofuscin granules" in the intestinal cells of Caenorhabditis elegans are secondary lysosomes.** *Mech Ageing Dev* 1986, **35**:79-94.
33. Poole B, Ohkuma S: **Effect of weak bases on the intralysosomal pH in mouse peritoneal macrophages.** *J Cell Biol* 1981, **90**:665-669.
34. Demaurex N: **pH Homeostasis of cellular organelles.** *News Physiol Sci* 2002, **17**:1-5.
35. Brenner S: **The genetics of Caenorhabditis elegans.** *Genetics* 1974, **77**:71-94.
36. Mello CC, Kramer JM, Stinchcomb D, Ambros V: **Efficient gene transfer in C.elegans: extrachromosomal maintenance and integration of transforming sequences.** *Embo J* 1991, **10**:3959-3970.
37. Fire A, Xu S, Montgomery MK, Kostas SA, Driver SE, Mello CC: **Potent and specific genetic interference by double-stranded RNA in Caenorhabditis elegans.** *Nature* 1998, **391**:806-811.
38. **WormBase Release WS100** [http://ws100.wormbase.org]
39. **WormBase Release WS110** [http://ws110.wormbase.org]
40. **Wormbase BLAST or BLAT Search** [http://www.wormbase.org/db/searches/blat]
41. **GenBank** [http://www.ncbi.nlm.nih.gov/Genbank/index.html]
42. Chomczynski P, Sacchi N: **Single-step method of RNA isolation by acid guanidinium thiocyanate-phenol-chloroform extraction.** *Anal Biochem* 1987, **162**:156-159.
43. **Protein families database of alignments and HMMs** [http://www.sanger.ac.uk/Software/Pfam]
44. Thompson JD, Higgins DG, Gibson TJ: **CLUSTAL W: improving the sensitivity of progressive multiple sequence alignment through sequence weighting, position-specific gap penalties and weight matrix choice.** *Nucleic Acids Res* 1994, **22**:4673-4680.
45. **Swiss-Prot / TrEMBL database** [http://www.expasy.org/sprot/]
46. Felsenstein J: **PHYLIP - Phylogeny Inference Package (Version 3.2).** *Cladistics* 1988, **5**:164-166.
47. Felsenstein J: **Confidence-Limits on Phylogenies - an Approach Using the Bootstrap.** *Evolution* 1985, **39**:783-791.
48. Needleman SB, Wunsch CD: **A general method applicable to the search for similarities in the amino acid sequence of two proteins.** *J Mol Biol* 1970, **48**:443-453.
49. Rice P, Longden I, Bleasby A: **EMBOSS: The European molecular biology open software suite.** *Trends in Genetics* 2000, **16**:276-277.
50. Bendtsen JD, Nielsen H, von Heijne G, Brunak S: **Improved prediction of signal peptides: SignalP 3.0.** *J Mol Biol* 2004, **340**:783-795.
51. **PDB - Protein Data Bank** [http://www.rcsb.org/pdb/]
52. Guex N, Peitsch MC: **SWISS-MODEL and the Swiss-Pdb-Viewer: an environment for comparative protein modeling.** *Electrophoresis* 1997, **18**:2714-2723.
53. **PovRay software** [http://www.povray.org/]
54. Nonet ML, Grundahl K, Meyer BJ, Rand JB: **Synaptic function is impaired but not eliminated in C. elegans mutants lacking synaptotagmin.** *Cell* 1993, **73**:1291-1305.
55. Hartree EF: **Determination of protein: a modification of the Lowry method that gives a linear photometric response.** *Anal Biochem* 1972, **48**:422-427.
56. Gallagher S, Winston SE, Fuller SA, Hurrell JGR: **Analysis of Proteins.** In *Current Protocols in Molecular Biology Volume 2*. 1st edition. Edited by: Ausubel FM, Brent R, Kingston RE, Moore DD, Seidman JG, Smith JA and Struhl K. Hoboken, John Wiley & Sons, Inc.; 1997:10.8.
57. Wenger DA, Williams C: **Screening for Lysosomal Disorders.** In *Techniques in Diagnostic Human Biochemical Genetics: A Laboratory Manual* 1st edition. Edited by: Hommes FA. New York, Wiley-Liss, Inc.; 1991:587-617.